University of Sussex

A University of Sussex PhD thesis

Available online via Sussex Research Online:

http://sro.sussex.ac.uk/

This thesis is protected by copyright which belongs to the author.

This thesis cannot be reproduced or quoted extensively from without first obtaining permission in writing from the Author

The content must not be changed in any way or sold commercially in any format or medium without the formal permission of the Author

When referring to this work, full bibliographic details including the author, title, awarding institution and date of the thesis must be given

Please visit Sussex Research Online for more information and further details

Synthesis of novel trypanosome alternative oxidase inhibitors for the treatment of African trypanosomiasis

Oran Gilliland O'Doherty

May 2015

This thesis is submitted to the University of Sussex

for the degree of Doctor of Philosophy

Declaration

This thesis, whether in the same or different form, has not been previously submitted to this or any other University for a degree.

This thesis is the result of my own investigations, except where otherwise stated. Other sources are acknowledged by footnotes giving explicit references. A bibliography is appended

Abstract

African trypanosomiasis is a protozoan infection affecting tens of thousands of people and millions of livestock animals across sub-Saharan Africa. In humans the disease is fatal without chemotherapeutic intervention and in animals it causes a severe anaemia that greatly impairs productivity. Available drug compounds are difficult to administer and unacceptably toxic.

A natural product, ascofuranone, inhibits a key trypanosome specific respiratory enzyme, trypanosome alternative oxidase, and was shown over a decade ago to be trypanocidal using both *in vitro* and *in vivo* experiments. The compound suffers from rapid metabolism and contains several functionalities undesirable in a drug compound. Despite the promising activity the lack of applicable synthetic methods available hampered the development of chemotherapeutics from ascofuranone.

In this work, novel synthetic routes were completed to explore the lead compound. New synthetic methods were successfully developed using palladium catalysed Suzuki couplings and Lewis acid catalysed rearrangements.

Ortho-lithiation approaches also afforded potent novel inhibitors. Of particular note is a benzisoxazole, which is expected to alleviate many of the metabolic issues associated with ascofuranone. Alternate heterocycle analogues were explored and an interesting indazole analogue obtained.

Finally, chemical methods were developed towards the benzisoxazole and indazole motifs with carboxylic acids, amenable to diversification by amide coupling. A preliminary range of novel amide containing 5, 6-heterocycles were synthesized to begin SAR exploration of these structures.

Acknowledgements

An incredible thank you to Professor Simon Ward for taking me on to do a PhD in what was a brand new group when I joined. Your guidance and understanding across the years has been invaluable and deeply appreciated.

Thank you to Dr. Trevor Askwith and Gareth Williams for their help on the biological side of this work. From chemistry, thank you to Dr. Paul Beswick, Michael Paradowski and particularly to Dr. Lewis Pennicott for the mentorship in the early years. Thank you to the Ward group as a whole, it has been a pleasure working with such engaging and lovely people.

It is by the good graces of the analytical chemists Dr. Ian Day and Dr. Alaa Abdul-Sada that any chemistry could be done and a great thank you to them for their work.

Thank you to my group mates and adoptive family Thomas Oliver Moore and Katie Duffell for being both incredibly smart and incredibly great people.

A special thank you to Katie Duffell for help in reviewing this thesis. I simply could not have done this without you. Thank you!

To all the people who have made the challenges of a PhD pale in comparison to the fun, and who made coming to work enjoyable even in the most difficult of times: Adam Close, Dan Guest, Dave Neill-Hall, Jessica Dwyer, Chris Gallop, Rhiannon Jones, Jess Higgins, Sandy Kilpatrick, Nikki Trathen, Laura Nicholls, Hayley Rand, Irene McLuenda, Jamie Laverick and Joseph Newcombe.

Finally, thank you to my girlfriend Caoileann Appleby who's love and support has been unwavering from the very start.

Abbreviations

AAT	animal African trypanosomiasis
ADME	absorption, distribution, metabolism, excretion
ADP	adenosine diphosphate
AF	ascofuranone
AMP	adenosine monophosphate
AOX	alterative oxidase
APO	apolipoprotein
AQP	aquaglyceroporin
ATP	adenosine triphosphate
BBB	blood-brain barrier
BBN	9-borabicyclo(3.3.1)nonane
BTMA	benzyltrimethylammonium
CAT	citric acid cycle
CCB	colletochlorin B
CNS	central nervous system
COX	cyclooxygenase
CSF	cerebro-spinal fluid
CYP	cytochrome P450
DA	diminazene aceturate
DALY	disability-adjusted life years
DCC	N,N'-dicyclohexylcarbodiimide
DCM	dichloromethane
DDQ	2,3-dichloro-5,6-dicyano-1,4-benzoquinone
DHAP	dihydroxyacetone phosphate
DMA	dimethylacetimide
DMF	dimethyl formaldehyde
DMG	directing metal protecting group
DMS	dimethylsulfate
DMSO	dimethylsulfoxide
DNA	deoxyribonucleic acid
DoM	Directed *ortho*-metalation
dppf	1,1'-Bis(diphenylphosphino)ferrocene
DRC	The Democratic Republic of the Congo
EDAC	1-ethyl-3-(3-dimethylaminopropyl)carbodiimide
EGFR	epidermal growth factor receptor
EPR	electron paramagnetic resonance spectroscopy
EtBr	ethidium bromide
EXXH	glutamic acid-X-X-histidine
G3P	glycerol 3 phosphate
GDP	gross domestic product
GPI	glycophosphatidylinositol

HAT	human African trypanosomiasis
HATU	1-[bis(dimethylamino)methylene]-1H-1,2,3-triazolo[4,5-b]pyridinium 3-oxid hexafluorophosphate
HBTU	N,N,N',N'-tetramethyl-O-(1H-benzotriazol-1-yl)uronium hexafluorophosphate
HDL	high density lipoprotein
hERG	the human Ether-à-go-go-Related Gene
HMBC	heteronuclear multiple-bond correlation spectroscopy
HMPA	hexamethylphosphoramide
HMPT	phosphine hexamethylphosphorous triamide
HPLC	high pressure liquid chromatography
HPR	haptoglobin-related protein
HRMS	high resolution mass spectrometry
IF-γ	gamma-interferon
ISM	isometamidium chloride
IM	intramuscular
IV	intravenous
LCMS	liquid chromatography–mass spectrometry
LDA	lithium diisopropylamide
Mel-T	melarsen oxide-trypanothione adduct
MFS	major facilitator superfamily
MIDA	N-methyliminodiacetic
MMP-9	matrix metallopeptidase 9
mp	melting point
MOM	methoxymethyl
MPXR	melarsoprol-pentamidine cross resistance
NAD^+	nicotinamide adenine dinucleotide oxidised form
NADH	nicotinamide adenine dinucleotide reduced form
n-BuLi	n-butyl lithium
NCS	N-chlorosuccinamide
NECT	nifurtimox-eflornithine combination therapy
NMR	nuclear magnetic resonance
NTD	neglected tropical disease
NTR	nitroreductase
OAc	acetate
ODC	ornithine decarboxylase
PdNP	Palladium nanoparticles
PG	protecting group
PK	pharmacokinetics
PSA	polar surface area
PVP	polyvinylpyrrolidone
rds	rate determining step

R$_f$	retention factor
RNA	ribonucleic acid
RNAi	ribonucleic acid interference
s-BuLi	*sec*-butyllithium
SAR	structure-activity relationship
SEM	2-(trimethylsilyl)ethoxymethyl
SHAM	salicylhydroxamic acid
SRA	serum resistance-associated
T3P	propylphosphonic anhydride
TAO	trypanosome alternative oxidase
TbAT1	trypanosoma brucei adenosine transporter 1
TbCatB	Trypanosoma brucei cathepsin B
TBDMS	*tert*butyldimethylsilyl
TbHpHbR	trypanosoma brucei haptoglobin-hemoglobin receptor
TFA	trifluoroacetic acid
TgsGP	*T. brucei gambiense*-specific glycoprotein
THF	tetrahydrofuran
TIPS	triisopropylsilyl
TLC	thin layer chromatography
TLF	trypanosome lytic factors
TMEDA	N,N,N',N'-tetramethylethylenediamine
TMSI	trimethyl silyl iodide
VSG	variant surface glycoprotein
WHO	World Health Organisation
XAS	X-ray absorption spectroscopy

Contents

Chapter 1 - Literature Review

Introduction

African trypanosomiasis is a disease caused by specific members of the genus *trypanosoma.* There are a diverse range of trypanosome species, and all are unicellular parasites that have developed elaborate mechanisms for survival within their hosts. An essential feature of these adaptations is the ability to continuously alter the expression of the antigens exposed on the cell's surface. This constant antigenic variation effectively conceals the parasitic infection from the host immune response, and this capacity to evade host immune systems has allowed trypanosomes to propagate in many species across the world. In Africa, some organisms have developed trypanosomal lytic factors (TLF) to combat these parasites. They are proteins specific to humans, apes and some monkeys that circulate in the blood and lyse trypanosomal cells on contact.

Two species of trypanosomes, *Trypanosoma brucei rhodesiense* and *Trypanosoma brucei gambiense*, have developed separate novel adaptations that negate the effect of the lytic factors and these species cause human African trypanosomiasis (HAT). In contrast, animal African trypanosomiasis (AAT), which affects important livestock species lacking lytic factors, is caused by different trypanosome species: *T. Congolese*, *T. vivax, and T. b. brucei.*

Trypanosomal diseases greatly impact Africa in terms of lives lost, suffering endured and livelihoods compromised. In animals, the major detrimental effect is chronic anaemia: however in humans, the disease is debilitating and fatal without chemotherapeutic intervention.

HAT has two distinct stages. In phase 1 it infects the blood and lymph; in phase 2 it penetrates the central nervous system (CNS), leading to neurodegeneration, coma and death. Drug treatments available for HAT are limited to five compounds, none of which are ideal: apart from their varying effectiveness, many are also overly toxic and difficult to administer. The development of novel therapeutics are underway, and an excellent candidate for drug development is trypanosomal alternative oxidase (TAO).

TAO is a parasite-specific respiratory enzyme: inhibiting this with a natural product, ascofuranone (AF), has been shown to be trypanocidal both *in vitro* and in murine models. AF inhibits TAO in picomolar concentrations and is a lead compound from which drug development can commence. With inhibition proven, AF represents an exciting opportunity for HAT treatment: however, there are several functionalities present on AF that are metabolically undesirable and require alteration. To date, the limited synthetic methods available to access AF-like compounds have impeded exploration of this lead compound. The development of novel methods and synthesis of drug-like AF analogues is the subject of this thesis.

Trypanosomes

Trypanosoma are a genus of kinetoplastids, a unicellular eukaryotic class of protozoa.[1,2] There are dozens of species of trypanosomes, all of which are obligate parasites in nature, requiring a host organism for survival.

The genus has several characteristic features. All trypanosomes have misshapen or modified mitochondria[3] that contain kinetoplastid deoxyribonucleic acid (DNA) loops in a combination of minicircle and maxicircle structures.[4] These unique circular DNA agglomerations encode the mitochondrial respiratory enzymes on their maxicircles and the regulation of maxicircle gene expression appears to be controlled in part by the minicircles, *via* guiding RNA.[5] They are monoflagellate[6] and have a cytoskeleton[7] primarily composed of microtubules and distinctly lacking in the other major eukaryotic cytoskeletal protein, actin.[7] Finally, flagellar rotation and cytoskeletal undulation contribute to permit them a distinctive corkscrew-like motility, which is observable by confocal microscopy.

The obligate parasitic life cycle of trypanosomes makes them the cause of many serious diseases. They are ubiquitous across the majority of vertebrate life forms including mammals,[8] amphibians,[9] birds[10], fish[11] and are likewise observed in various insects[12] and flora.[13]

Trypanosomes have evolved sophisticated immune-evasion mechanisms that allow them to perpetually reside alongside host immune systems and therefore become highly pervasive parasites. These adaptations are multifarious[14–18]but the trypanosomes' variant surface glycoprotein (VSG) is pre-eminent, easily surpassing its other virulent adaptations.[19,20] VSG is an example of antigenic variation, a changing of the proteins expressed on the cell's surface. It is a 58-kDa glycophosphatidylinositol (GPI)-anchored glycoprotein, predominantly α-helical in secondary structure, which has its C-terminus embedded in the membrane and sequentially varied N-terminus exposed to the extracellular medium of the host.[19]

VSG represents a huge proportion of the overall protein synthesized by the cell. There are an estimated 10^7 copies[21] comprising approximately 90% of cell surface polypeptides,[22] requiring 20,000 VSGs to be formed, modified and distributed to the cell surface every minute.[23] The VSG changes at a rate of up to 10^{-3} switches/cell/division[24] with each cell cycle taking 8 hours[19] and peak parasitic load being 10^6/mL (in murine models).[25]

Such frequent modification of the VSG during infection is enabled by various genetic and epigenetic mechanisms. VSG genes are >1600 in number,[26] existing internally on the 11 diploid chromosomes,[27] in non-expressed genes at the telomeres[28] and on hundreds of aneuploid mini-chromosomal units.[29] At any one time however only 5-10% of these VSG genes are expressed[26] and there are several ways in which a VSG gene present at an expression site can be transformed into another. Most commonly, after DNA damage upstream of the VSG expression site, one of several DNA damage repair mechanisms is utilized to replace the initial gene with the that of the recombinant VSG.[30] By this method, which accounts for about 80% of VSG replacement, the whole gene is exchanged. [31]

A less observed method also exists which consists of mixing various parts of several VSG genes and pseudogenes to create completely new VSGs.[32] This creates many non-viable proteins but importantly also a viable minority that are novel and affords the VSG a virtually inexhaustible variability.[32] This is further enhanced by the potential for post-

translational modification of the N-terminus by oligosaccharide glycan formation in the endoplasmic reticulum and Golgi apparatus.[33,34]

In combination, the variation and profligate production of VSGs outpaces the immune system's ability to identify and match the antigens on these pathogens. Consequently, even the adaptive immune system is permanently lagging and only ever able to act on parasites with the oldest antigens that it has had time to recognize and mobilize a response against. Meanwhile it remains continuously "blind" to the new antigen-expressing parasites, allowing sufficient time for this subset to further replicate and diverge, *ad infinitum*.

With their exceptional immune evasion capabilities, trypanosomes have successfully colonized much of the world, with specific species of the genus having adapted to particular hosts. This specification is true too for human hosts. There are two particularly striking examples of human infection. The first is Chagas Disease, which is native to South America and caused by *Trypanosoma cruzi,*[35] and the second, which is the main focus of this doctoral research, is Human African Trypanosomiasis (HAT) or sleeping sickness, caused by *Trypanosoma brucei*.[36]

Epidemiology and History of African Trypanosomiasis

The first unequivocal display of trypanosomes in human blood was made by the British Colonial surgeon Robert Michael Forde in 1901 when examining a steamboat captain in The Gambia.[37] Forde initially mistook the trypanosomes as worms[38] but was corrected a few months later by the English physician Joseph Everett Dutton, who also gave the species its name, *Trypanosoma gambiense* (now *T. b. gambiense*).[39] In the same year, the Italian physician and pathologist Aldo Castellani suggested that trypanosomes cause sleeping sickness, having identified them in the cerebrospinal fluid of patients.[38,40]

HAT is a debilitating disease with a severe social and economic impact across Africa (**Figure 1**). The parasite's transmission vector is the tsetse fly, as observed by Scottish pathologist and microbiologist David Bruce in 1903.[38,41] As such it is exclusively found in sub-Saharan Africa between 14°N and 20°S in the so-called "tsetse belt" where the

insect is endemic. Across the 36 affected countries an estimated 60 million people are at risk of contracting HAT.[42] About 70,000 people are thought to be currently infected, with approximately 30,000 new infections a year[43] and 10,000 deaths.[44]

The burden of the disease is measured not only in mortalities but also as the impact on community life and the contribution of individuals to food production and community support. This morbidity function is regularly measured in terms of disability-adjusted life years (DALYs),[45,46] where one DALY can be thought of as one lost year of "healthy" life. HAT exhibits high morbidity, currently resulting in 1.78 million DALYS with the 60 million at risk.[47] This magnitude is better understood when compared with the related trypanosomal disease leishmaniasis, which causes only slightly more DALYs, 2.06 million, despite being more widespread and affecting significantly more people, 350 million at risk in 88 countries.[47]
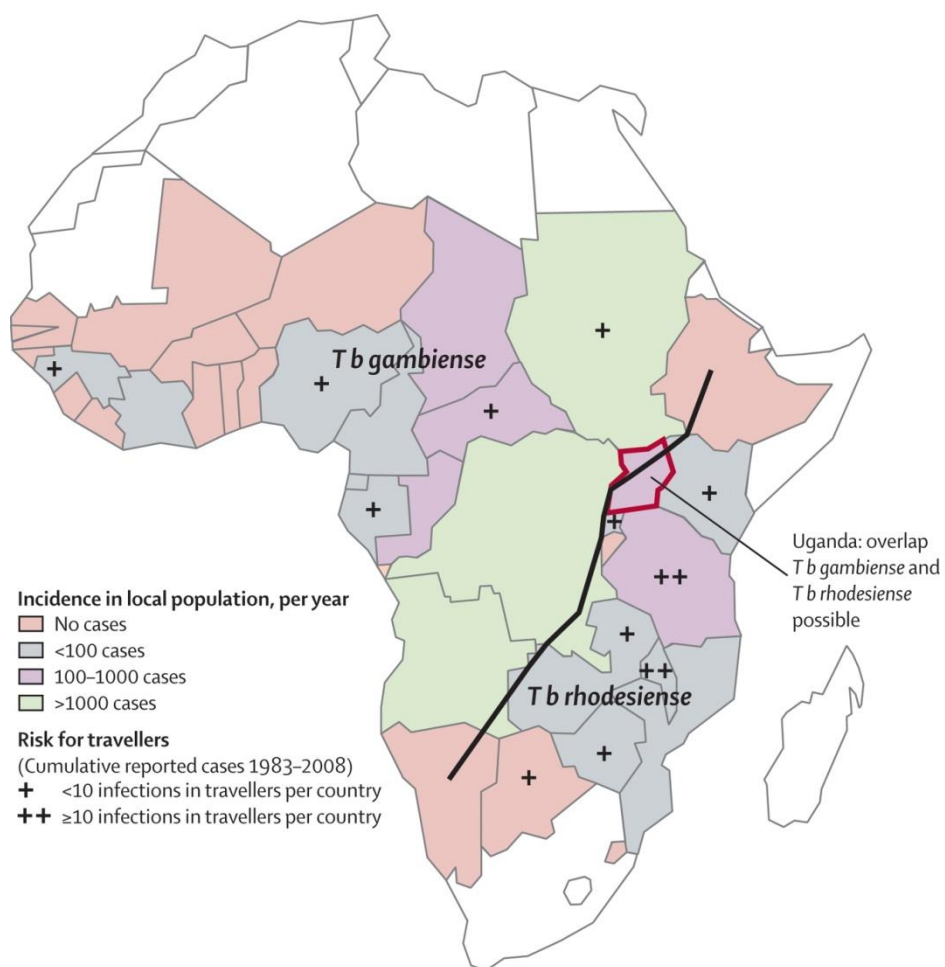
Figure 1 – Distribution of HAT with incidences and risk for travelers. The black line divides the areas in which *Trypanosoma brucei gambiense* prevails and those in which *Trypanosoma brucei rhodesiense* predominates.[36]

The history of human sleeping sickness has been characterized by the interspersion of disease epidemics with long periods of endemicity. Three major epidemics have been recorded in the 20th century: 1900-20, 1940-50 and 1970-80. Positively, HAT is currently experiencing a trend towards reduction of incidences and is in one of its endemic phases, but a resurgence is all but inevitable, especially as the co-ordinated national and pan-national monitoring and treatment can easily collapse when stressed: be it by governmental collapse, financial collapse, civil war or large-scale population migrations, which have been unfortunately common across sub-Saharan Africa over the decades.

Trypanosomes also cause sleeping sickness in animals, and in animals it is called 'nagana', or Animal African Trypanosomiasis (AAT). The disease affects animals in a similar way to humans, which is discussed at length below, however animals also suffer an onerous anemia[48] which has a major impact on livestock productivity be it in meat, dairy or breeding.[48]

Wild mammal species endemic to sub-Saharan Africa have largely developed a resistance to trypanosomiasis, termed trypanotolerance.[49] This ability allows the animals to remain healthy, active and gain weight whilst enduring parasitemia.[49] Native cattle species also display some trypanotolerance and substantial work has been done to identify its genetic origin.[50–53] Genes affording resistance have been identified across several quantitative trait loci in the trypanotolerant African N'dama (*Bos taurus*) and even in some breeds more recently arrived to Africa like the trypanosuceptible Boran (*Bos indicus*).[52]

Two phenotypes have been linked to possession of these trypanotolerant genes. The first is a better capacity to control parasitemia and is mediated by haemopoietic cells (T lymphocytes or antibodies). The second is a better capacity to limit anaemia development and is mediated by haemopoietic cells, but not by T lymphocytes or antibodies.[53] Weight gain has been linked to the latter mechanism, implying that anaemia control is more important for survival and productivity than parasite control.[53] The majority of cattle reared across sub-Saharan Africa are not trypanotolerant and work continues to see if selective breeding of these traits can be coupled to the

economically necessary traits of livestock and if successful this could represent a low-cost method to battle AAT.[52]

As it stands, however, AAT is a widespread problem, causing about three million deaths in cattle and requiring approximately 35 million doses of trypanocidal drugs to be administered[54] every year. The economic losses in cattle production alone are in the range of US$1-1.2 billion per annum and AAT is the single largest infectious disease of cattle in Africa.[54,55] This is a particularly high relative cost when the current states of sub-Saharan economies, which are largely primary economies with low GDPs, are taken into consideration. The full cost can be assumed to be higher as this figure doesn't take into account less measurable impacts such as the effect of reduced nutrition and income from meat and dairy loss, or the effect of increased manual labour, decreased area farmed and yield of crops due to unhealthy draught animals.

For example, the Democratic Republic of Congo (DRC) has accounted for roughly 70% of total HAT cases in the last ten years.[42] It also has 70% of citizens living below the international poverty line. A one billion dollar loss would represent a substantial portion of the national economy, lowering household incomes and retarding socio-economic development. Taking these figures in context further demonstrates the devastating impact African trypanosomiasis is having on the sub-Saharan region and the DRC in particular.

Trypanosomal lytic factor

Four species of trypanosomes cause the majority of trypanosomal disease in mammals and these have distinct infection profiles across Africa (**Figure 1**). There is a clear distinction in infective capabilities of different species due to the evolution of trypanosome lytic factors (TLFs) unique to humans, gorillas and Old World monkeys, which afford an innate immunity to a subset of trypanosomes.[56]

Two different serum complexes have been identified as TLFs.[57] TLF1 is the densest fraction of high density lipoprotein (HDL) particles. It contains a lipid core with an outer hydrophilic layer of phospholipids, cholesterol and several apolipoproteins (APO),

including APOA1, the major component of HDL in serum.[58] TLF2 is a distinct complex that has few lipids, instead comprising mostly of natural immunoglobulin Ms, together with APOA1 amongst other proteins.[59] Common to both complexes are the haptoglobin-related protein (HPR) and APOL1, which has been shown to be trypanocidal.[57]

As a result of the different compositions of the TLF1 and TLF2 complexes, the methods by which the two interact with trypanosomes are understandably divergent. In human serum, the TLF1-HPR complex binds to hemoglobin[60] and only then does it have a high affinity for the trypanosomal receptor TbHpHbR.[61] The ligand-bound complex undergoes receptor-mediated endocytosis[62] at a region known as the flagellar pocket, which is responsible for concentrating cell surface receptors, including TbHpHbR, around the base of the flagellum. This flagellar pocket is an ingenious parasitic evasion strategy, restricting most endo/excocytosis and exposed receptors to 0.5% of the cell surface.[63] This drastically limits the area of cell surface displaying foreign antigens, which if recognised would induce an immune response, and thus decreases the parasite's risk of detection. The mechanism of action of TLF2 is currently unknown, but is known to occur independent of the trypanosomal receptor TbHpHbR.[64]

APOL1's N-terminal domain is an analogue of bacterial pore proteins, colecins.[65] The exact molecular mechanism requires further elucidation but irrespective of the origin it appears APOL1 dissociates from the HDL complex and mediates trypanolysis *via* the transmembrane flux of chloride anions, osmotic swelling and rupture of the lysosome.[66,65]

APOL1 is also known to cause kidney damage and is well studied in African-American people,[67] whose inherited trypanosomal immunity from increased APOL1 levels in HDL conferred a 35-60% risk of impaired renal filtration, particularly in late stage chronic nephropathy.[68] Clearly trypanosomes exerted a powerful selective pressure on our hominid ancestors to afford evolution of this specific resistance in spite of the associated renal detriment.

Causative species of trypanosomiasis

T. congolese, *T. vivax and T. b. brucei* are the main causative species of AAT, all of which are susceptible to TLFs and, as such, not pathogenic in humans. Just two subspecies of trypanosomes can infect humans, *T. brucei gambiense* and *T. brucei rhodesiense*. These have distinct epidemiologies and pathologies, and have evolved different solutions to negate the human TLFs. These strategies are an excellent example of a host-parasite molecular "arms-race", where each party develops consecutively more complex methods to overcome any advance made by the other.[69] Domestic and wild animals can also become infected with *T.b. gambiense* and *T.b. rhodesiense*. Although they do not fall ill, they have an epidemiological role as carriers or reservoir animals from which tsetse flies can acquire an infection.[70]

3% of HAT infections are caused by *T. brucei rhodesiense*.[71] Particularly aggressive, this causes fast-onset acute trypanosomiasis in humans with infection periods measured in weeks, or at most months, and >80% mortality at six months.[72] It is most common in southern and eastern Africa where wild game animals and livestock are thought to be the primary reservoir[73,74,75]. Interestingly, a progressive increase in severity of infection is observed moving from south to north Africa,[76] however extrapolating the cause from genetic variation in host or parasite populations has proven difficult. *T. b. rhodesiense* has been the causative species of the three trypanosome epidemics in the 20th century.[77,78]

Investigations into the genetic differences in APOL1-sensitive and -tolerant *T. b. rhodesiense* clones have established the means by which the parasite has evolved to survive in normal human serum.[69] The trypanosome employs a version of its VSG to create an expression site-associated gene known as serum resistance-associated (SRA) which is able to neutralize the effects of APOL1.[79] SRA protein is a truncated form of VSG, lacking the antigenic loops exposed to the extracellular media.[80,81] Whereas correctly formed VSG is trafficked at a great rate to the cell surface, malformed proteins are shuttled to the endolysosomal system for degradation by proteases[82,83]. It is likely

that it is in this endolysosomal system that SRA co-locates with APOL1 given that a range of shortened VSGs were all shown to result in endocytic processing.[84]

The truncated SRA protein has two associating alpha helices, A and B, which ordinarily form a hairpin structure. However, when SRA and APOL1 are in close proximity the N-terminal A helix of the SRA interacts more strongly with the C-terminal helix of APOL1, thereby displacing the native helix B.[57,85] This SRA-APOL1 binding neutralizes the pore-forming ability of the TLF agent and without the lysosome's swelling and subsequent rupture the SRA-APOL1 proteins are degraded by proteases *via* normal lysosomal activity (**Figure 2**). In agreement, APOL1 C-terminus mutants that disrupt this coiled-coil SRA-APOL1 interaction were shown to restore the trypanocidal activity of APOL1 to *T. b. rhodesiense*.[85]
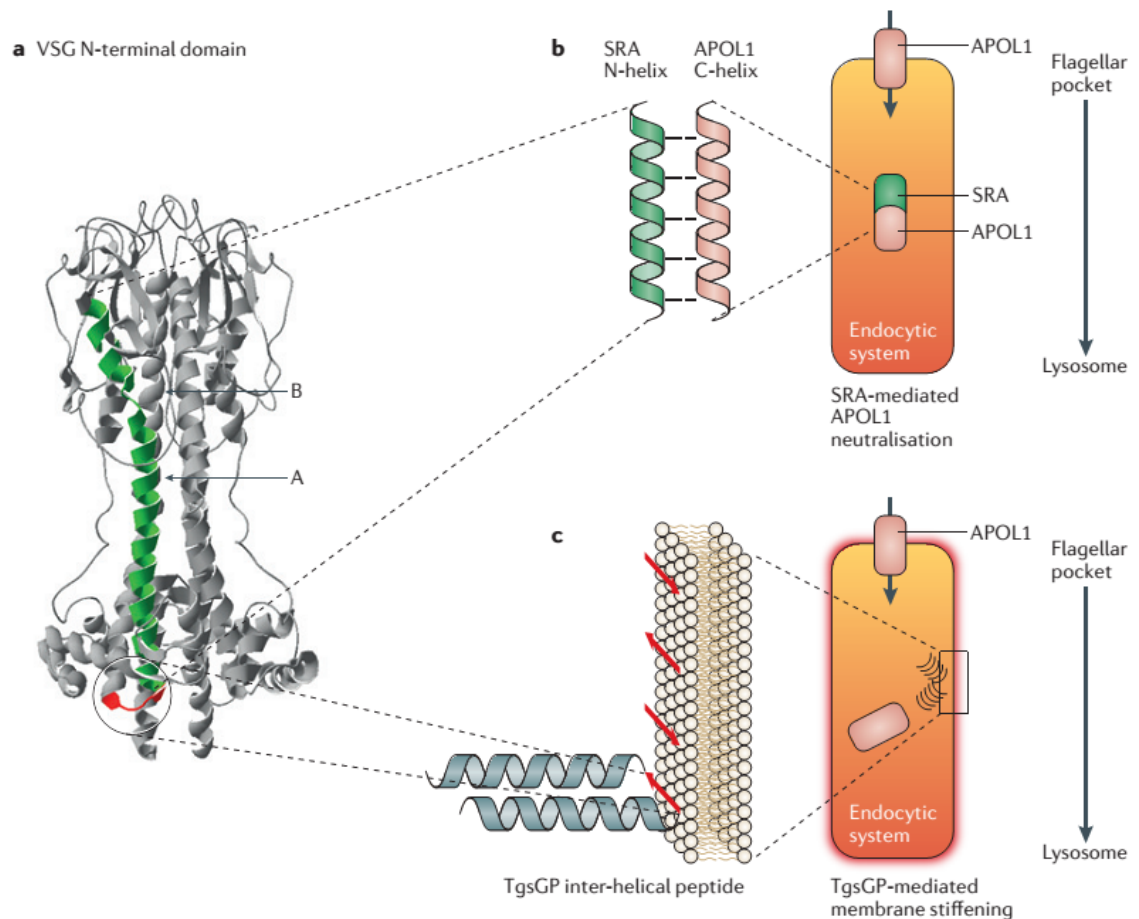
Figure 2 - VSG-derived adaptive proteins in human-infective Trypanosoma brucei subspecies. **a|** The structure of the variant surface glycoprotein (VSG) amino-terminal domain highlights the two long amphipathic helices, helix A (in green) and helix B (in grey), which form a hairpin structure with the inter-helical peptide (in red) that is located at the bottom. **b|** Helix A of the VSG-derived serum resistance-associated (SRA) protein of Trypanosoma brucei rhodesiense neutralizes apolipoprotein L1 (APOL1) by a coiled-coil interaction; SRA is targeted to the endocytic compartment instead of being anchored to the cell surface, probably as a result of the absence of surface-exposed loops. **c|** In Trypanosoma brucei gambiense, the inter-helical peptide of the VSG-derived protein T. b. gambiense-specific glycoprotein (TgsGP) protects trypanosomes from APOL1 toxicity in a process that is associated with membrane lipid stiffening involving antiparallel peptide organization; as TgsGP lacks a carboxy-terminal domain, the inter-helical peptide is expected to be located close to the membrane. The boxes represent the endocytic compartments, and a colour gradient illustrates the endosomal acidification that takes place between the beginning (that is, the flagellar pocket) and the end (that is, the lysosome) of the endocytic pathway.[69] (Image and caption from reference)

These laboratory-developed C-terminal mutants have posed the question as to whether these changes may have also developed in nature. Indeed, they have since been observed in baboons,[86] which are known to be resistant to *T. b. rhodesiense*, and most fascinatingly, in subpopulations of western African people.[67] Unfortunately however even a single allele of this mutant gene not only affords resistance but greatly increases the likelihood of end-stage kidney disease.[67] This is not completely dissimilar to other parasite-associated conditions in Africa, particularly sickle cell anaemia and malaria, whereby the negative impact on the sufferer is overcome by the resistance to the

parasite,[87] such that the disease allele represents a net gain in fitness and remains pervasive in sub-Saharan African gene pools.

The remaining 97% of HAT infections[71] are by *T. brucei gambiense*, which causes a slow-onset chronic trypanosomiasis in humans with infection averaging around three years[88] but some recorded persisting over three decades.[89] It is most common in central and western Africa, where humans are thought to be the primary reservoir,[90] with only small pockets residing in livestock.[90,91] .

Identification of the SRA VSGs in *T. b. rhodesiense* inspired a search for unique truncated VSGs that might mediate the resistance of *T. brucei gambiense* to TLFs. A screen identified the *T. brucei gambiense*-specific glycoprotein (TgsGP).[92] Deletion of this gene re-establishes vulnerability to APOL1 in *T. brucei gambiense* and exposure to normal human serum is trypanocidal.[92,93] TgsGP is located in the endocytic system,[94] much like SAR, but does not interact with APOL1 directly. Rather it induces membrane stiffening *via* a hydrophobic β-sheet interaction that is thought to hamper APOL1 membrane insertion and thus pore lytic formation.[94] This TgsGP is one of three changes that combine to confer resistance (**Figure 2**). In addition, more rapid acidification of endosomes results in increased degradation of APOL1 [94] and a point mutation of the TbHpHbR[95–97] inactivates it to TLF1 binding. Both of these serve to lower the volume of active APOL1 which reaches the lysosome. These factors in concert with TgsGp allow the lysosomal proteases time to disassemble the APOL1 before it acts.

VSGs are truly remarkable and have proven to be highly multifunctional tools. Not only do they afford immunological evasion but here have been repurposed in divergent manners to address an evolved trypanotolerance factor in normal human sera, HDL-TGFs. The power of pathogenic highly recombinant DNA motifs is also clearly evidenced. The VSG expression sites allow for the generation of completely novel adaptive solutions for the trypanosomes and are clearly a critical factor in the evolutionary success of the genus.

T. Brucei lifecycle

T. brucei is heteroxenous, requiring both mammalian and tsetse fly (*Glossina*) hosts at different stages of its lifecycle (**Figure 3**). The trypanosome has distinct developmental forms in each of these hosts. The stumpy bloodstream trypomastigote is ingested by the blood-sucking tsetse fly and develops in the fly's midgut into the procyclic trypomastigote before reproducing asexually by binary fission. The parasite then migrates to the salivary gland of the fly where it develops into the metacyclic epimastigote and waits to be injected into the next mammalian host. The full process in the fly takes three weeks.[98] The bloodstream trypomastigote develops in the mammalian extracellular fluid again reproducing by binary fission where it waits to infect another tsetse fly.
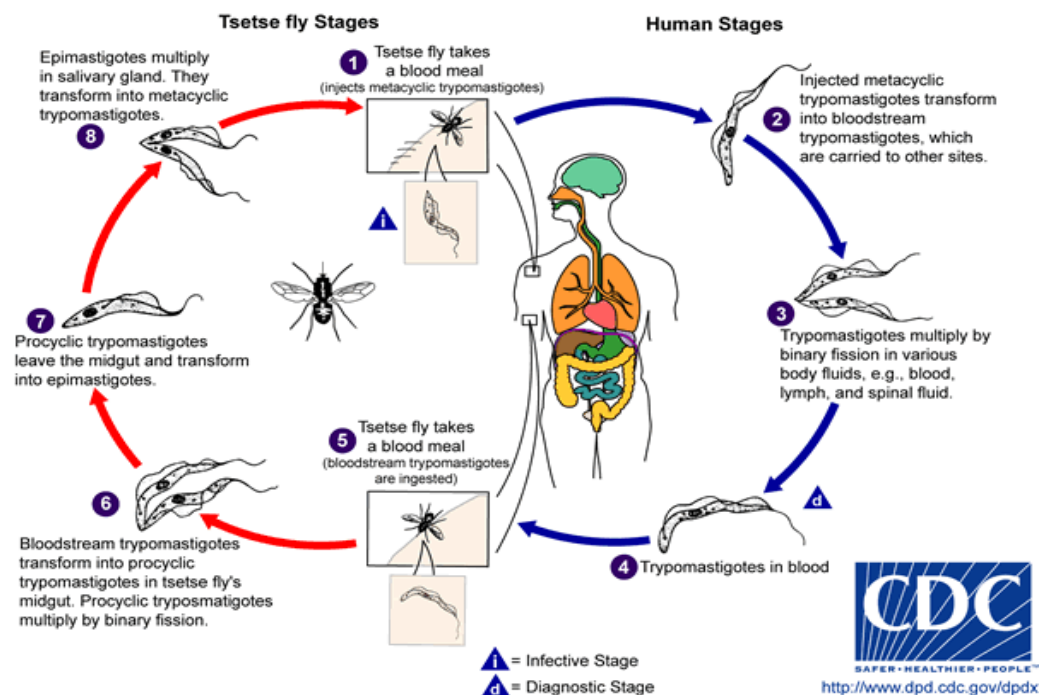
Figure 3 - Complete heteroxenous trypanosomal lifecycle[98]

Human African trypanosomiasis pathology

Haemolymphatic Phase 1

In haemolymphatic Phase 1, immediately after a bite from an infected tsetse fly, the parasite infects all intracellular fluids of the body with the exception of cerebrospinal fluid. Initial symptoms include fever, headaches, joint pains, and characteristic swollen lymph nodes on the back of the neck, termed Winterbottom's sign.[99] Usually a painful red sore called a chancre will develop at the location of the tsetse fly bite five to 15 days after the incident. Pathogen attacks come in waves and can fall into remission for periods of days or months in between each episode.

The symptoms of acute HAT caused by *T. brucei rhodesiense* naturally reoccur with much greater frequency than those in the chronic *T. brucei gambiense* infection.[99] If left untreated the pathogen can cause damage to any or all organ systems. Patients might develop various features including: lymphadenopathy; enlargement of the spleen and/or liver; cardiac features such as myocarditis, pericarditis, and congestive cardiac failure; ophthalmological features such as iritis, keratitis, and conjunctivitis; endocrine dysfunction including menstrual abnormalities, impotence, alopecia, and gynaecomastia; and fertility problems including sterility, prematurity and abortion.[36,100–102] However, it is also possible that patients present with only basic flu-like symptoms, giving the disease a whole spectrum of possible symptoms and severities.[103]

Neurological Phase 2

In neurological Phase 2, which can be several weeks to several months after infection, the parasite penetrates the blood brain barrier (BBB). Pathologically, the late stage is characterized by a meningoencephalitis, with extensive cerebral white matter infiltration by lymphocytes, macrophages, and plasma cells.[100,104] A multitude of symptoms result from this encephalitic degeneration of the central nervous system. Those clinically observed include: motor disturbances, with motor weakness reported in 35% of cases; gait disturbance in 22%; tremor in 21%; abnormal movements in 11%; speech disturbances in 14%;[105] myelitis, myelopathy, muscle fasciculation, and

peripheral motor neuropathy;[106] psychiatric disorders, with 25% of patients displaying behavioural disturbances, lassitude, hallucinations, delirium, anxiety, irritability, and excessive sexual impulses;[105] headache, which occurs in 79% of patients in one study;[105] sensory disturbances such as deep hyperaesthesia, pruritus, anaesthesia and paraesthesia and seizures; and finally visual problems such as optic neuritis, double vision, optic atrophy, and papilloedema.[100,106]

Characteristically, patients experience severe lethargy, insomnia and disruption to their diurnal cycle as the disease progresses. According to an extensive study on 2,541 patients with late-stage HAT, sleep disturbances occur in 74% of patients,[105] which, without treatment, invariably progress to coma and death. It is these typical sleep disturbances that give rise to the name 'sleeping sickness'. Sleep abnormalities consist of a reversal of the normal sleep/wake cycle, with nocturnal insomnia and daytime somnolence, uncontrollable episodes of sleep, and an alteration of the structure of sleep itself, with the early onset of rapid eye movement sleep rather than this occurring at the end of Stage 4 sleep.[107]

The vast scale of potential maladies highlights how profoundly debilitating HAT is for its sufferers, at 1.5 million DALYs per year[108] across sub-Saharan Africa. Coupled with the near 100% mortality[109] without medical intervention, this emphasizes the need for new effective treatments.

The blood-brain barrier

The central nervous system (CNS) and the brain are regarded as an immuno-privileged space, removed from the regular leukocyte mediated inflammation and immune response.[110] This is achieved *via* tight regulation of permeability across the blood-brain barrier (BBB), blood-cerebrospinal fluid barrier and arachnoid barrier. The BBB is particularly tightly regulated and investigations are ongoing to determine how trypanosomes are able to traverse it, though some key factors have been elucidated.

The BBB is complex, but essentially it is comprised of a barrier of tightly functioned endothelial cells with a protective basal membrane, perivascular space, parenchymal basement membrane and a large number of supporting structures and cells, particularly astrocytes and neurons.[111,112] The initial tight junctions of the endothelial barrier are

weakest and often fenestrated[113] in circumventricular organ regions of the brain. This improved contact allows rapid and accurate assessment of the composition of the sera, which can then be adjusted as necessary by the osmoregulation,[114] cardiovascular regulation,[115] and energy homeostasis[115] mechanisms. It is also at this region that important endocrine regulators such as oxytocin,[116] vasopressin[117] and melatonin[118] are secreted into the sera.

It remains unclear whether the parasites are better able to breach the BBB at these positions or whether this is still prevented by the remaining post endothelial barriers.[119] The constituents of these barriers appear to be of relevance. The endothelial and parenchymal membranes are composed of the protein laminin in association with type IV collagen networks *via* entactin, fibronectin, and perlecan.[120] Laminin comprises an α, β, γ trimer of proteins, where α, β and γ are variable. Trypanosomal CNS translocation of the endothelial basement membrane was found to be laminin alpha dependent. This membrane contains either α4 or α5. α5 has been shown to restrict parasite movement whilst α4 is permeable to CNS infection.[121]

γ-Interferon (IF-γ) has been shown to mediate trypanosomal crossing of the BBB. In mouse models with IF-γ knocked down or inhibited by RNAi, trypanosome translocation to the CNS was greatly diminished.[122] This is in interesting contradiction with the normal role of IF-γ as a potent activator of cell-mediated protective immunity against intracellular infections, where it activates different microbicidal effector mechanisms of macrophages and non-professional phagocytes.[123] In these experiments, the control mice with native IF-γ levels experienced reduced severity of parasitaemia but at the cost of greater parasite penetrance.[122] Further investigation is required to explain this effect.

Lacking its own immune response, the CNS must recruit leukocytes from the blood to fight infection. It does this by displaying cytokines on the BBB surface that are recognized by white blood cells, which initiates a translocation process.[124] Recombination-activating gene 1 (RAG-1) deficient mice lack B and T cells and are also largely resistant to trypanosome CNS phase 2 infection.[122] This suggests that trypanosomes utilize mechanisms similar to that of leukocytes to penetrate the BBB and invade the CNS or,

more likely, that translocation of the leukocytes could alter the structural integrity of the basement membranes paving way for subsequent penetration by the parasites.[121]

The trypanosome constantly secretes proteins and chemicals to manage its immediate environment. Two that have been shown to be of particular import are cysteine proteases cathepsin B and cathepsin L (brucipain). In one study, doxycycline induction of RNAi targeting cathepsin B led to parasite clearance from the bloodstream and prevented a lethal infection in the mice,[125] while all mice infected with *T. brucei* containing the uninduced Trypanosoma brucei cathepsin B (TbCatB) RNA construct died by day 13. The mechanism mediating this virulence is still under investigation. Brucipain has been shown and confirmed to mediate the translocation of trypanosomes across BBB models *in vitro*. It does this in a calcium dependent manner. Both calcium scavengers and brucipain RNAi removed penetrance in the BBB model[126] and although brucipain RNAi induced in murine models did not cure mice from infection, 50% of these mice survived 60 days longer than uninduced controls.[125]

It is now understood that in HAT infections the tight junctions of the brain-endothelial barrier are not disrupted and damage to the barrier is minimal, making it difficult to correlate CNS invasion with parasite-endothelium interactions. The exact mechanism of parasite CNS migration therefore remains uncertain. The factors outlined above demonstrate clearly that BBB penetrance in HAT is likely a multifactorial process which requires substantial further investigation.

Current Treatments for HAT

Due to the biphasic nature of HAT, chemotherapeutic treatments can be separated into two categories. The first aims to treat the haemolymphatic phase prior to BBB penetrance and involves intravenous or intramuscular injections of one of two drugs. Pentamidine is used to treat against *T.b. gambiense* infections and suramin against *T.b. rhodesiense.* The second is used at the neurological phase and therefore must overcome the challenge of BBB penetrance, ruling out the trypanocidals used at Phase 1. Three drugs are available: melarsoprol; eflornithine; and nifurtimox.

Despite HAT having been known since the turn of the 20th century, there are only these five drugs available to treat it, all of which have major limitations. The disease has affected millions of people and tens of millions of animals over decades but has received little attention until recently. As such it has been designated a neglected tropical disease (NTD) by the World Health Organization and will likely remain as such until new treatments make the current therapeutics redundant.
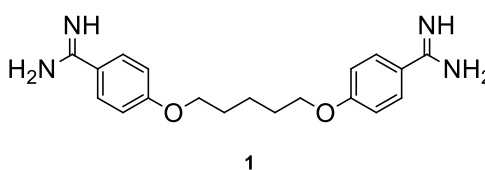
Phase 1 treatments

1

Figure 4 - Pentamidine

Pentamidine (**1**) (**Figure 4**) has been in use since the 1960s for Phase 1 infection in *T.b. gambiense*. The two phenyl amidine motifs make the molecule dicationic at both intestinal and plasma pH, restricting migration across the intestinal membranes as well as the CNS barriers. As a result, oral administration and Phase 2 HAT administration are impossible and the seven-day, once daily 4 mg/kg dosing must typically be given by intramuscular injection.[127] Pentamidine is trypanocidal and highly active at IC_{50} 1-10 nM.

Its exact mechanism is still debated, but interestingly its localisation to the mitochondria has been observed to precede mitochondrial kinetoplastid DNA degradation.[128] Pentamidine has specific transporters that act to increase its cellular concentrations to µM levels and the mutation of these transporters confers melarsoprol-pentamidine cross resistance (MPXR) which is detailed below. In addition, there are particular toxicity issues, with severe pain at the site of injection, nephrotoxicity, leukopenia and liver enzyme abnormalities, as well as the risk of hypoglycemia.[129]
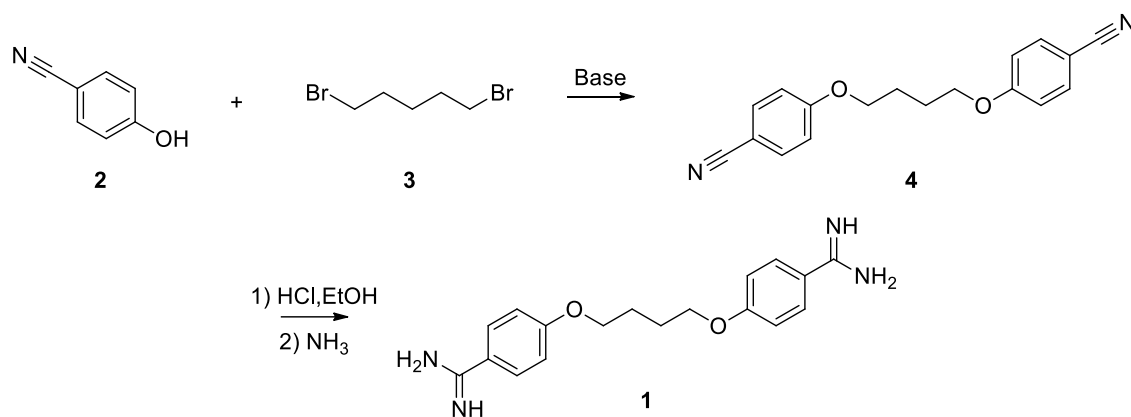
Scheme 1 - Synthesis of Pentamidine

The synthesis of pentamidine (**1**) is straightforward (**Scheme 1**); it involves the double S_N2 displacement of bromide on 1,5 dibromopentane (**3**) by two *para*-hydroxybenzonitriles[130] (**2**) followed by a Pinner amidine synthesis where the nitriles are converted first to ethyl benzimidates and then to amidines by the addition of ammonia.[131]
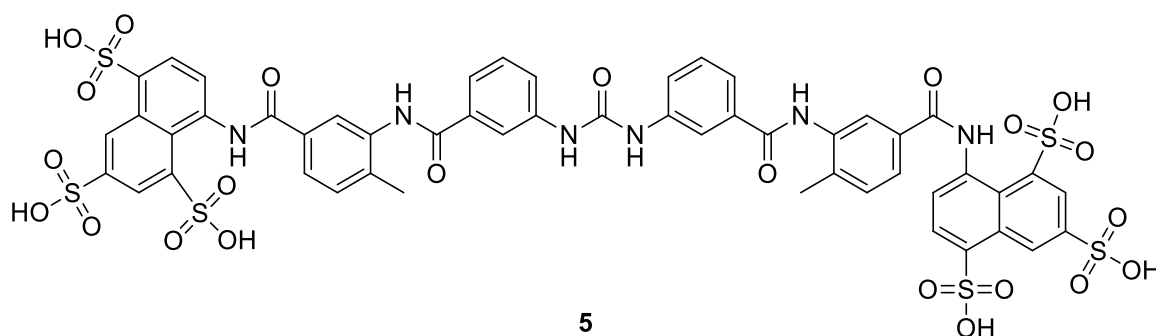

Figure 5 - Suramin

Suramin (**5**) (**Figure 5**) has been utilized as a trypanocidal since 1922 and is now the only Phase 1 treatment for *T.b. rhodesiense*. It is a very large molecule, with poor membrane permeability and high (>99%) serum protein binding. The serum binding extends the half-life of the drug to an extremely high 44-54 days.[132] The normal treatment course comprises intravenous (IV) injection of 20 mg/kg (no more than 1 g per injection) in a series of five injections at five-to-seven day intervals.[133] Suramin is also effective against *T. b. gambiense* infections, but due to the risk of sudden shock in case of infection by

Onchocerca volvulus, treatment with pentamidine is preferred.[129] Again the mechanism of action is not well understood but is linked to inhibition of glycolysis enzymes.[134]

Suramin resistance has been characterized by genome wide RNAi studies.[135] Links have been drawn to eight genes with the strongest suggestive of suramin uptake *via* a major facilitator superfamily (MFS) transporter. Suramin resistance is rarely seen in patients despite long-term use and is therefore not considered a threat to its continued application.[132] The main side-effects are fever, mucocutaneous eruptions, nausea, vomiting, polyneuropathy and haematological toxicity.[133]
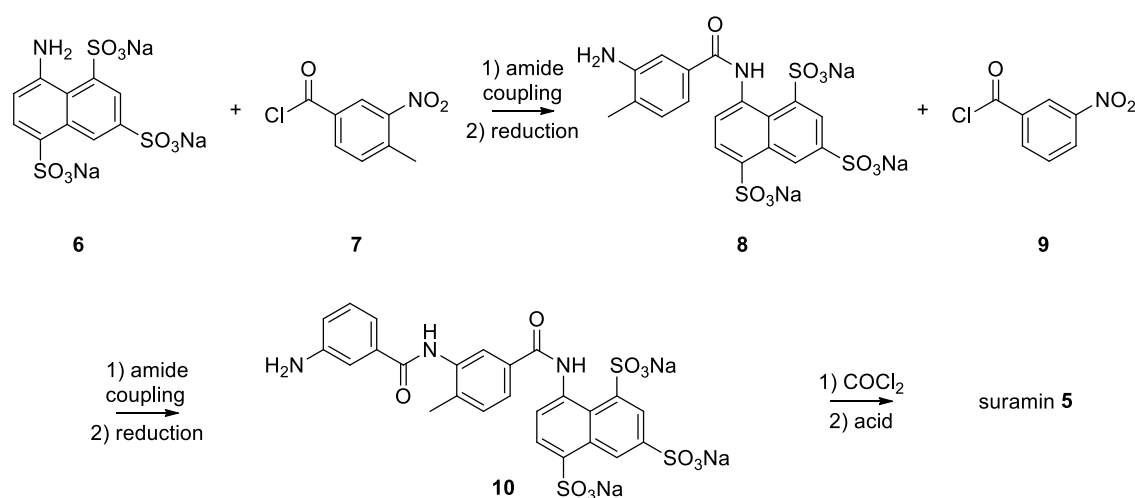
Scheme 2 - Synthesis of suramin

The synthesis of suramin[136] (**Scheme 2**) involves two consecutive amide couplings and nitro reductions. The nitro groups serve to both activate the acid chlorides for aniline attack and as a masked amine equivalent that is liberated by reduction. Two equivalents of compound (**10**) are then reacted with phosgene to form the symmetrical urea and this is acidified to give the neutral compound suramin (**5**).

Phase 2 treatments

11
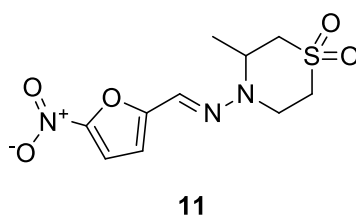
Nifurtimox (**11**) (**Figure 6**), a 5-nitrofuran pro-drug, was initially used in small-scale last-resort trials in the 1980s and 1990s to treat melarsoprol refractory patients.[137] It was only in 2009, with its implementation in nifurtimox-eflornithine combination therapy NECT, that it came into common use. Before this it existed as a monotherapy administered thrice daily at a dose of 15 mg/kg for two-three weeks.[138] It is readily metabolized at the liver resulting in a short half-life of two hours,[139] but as it remains the only orally available drug for HAT it is the most commonly prescribed.
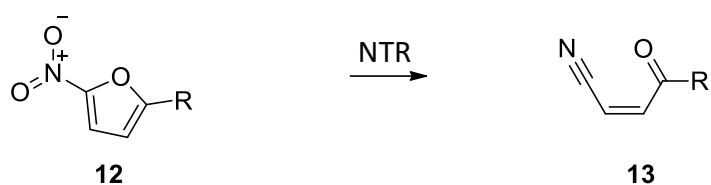
Figure 7 - Conversion of nitrofuran pro-drug to the active Michael acceptor nitrile compound

Trypanosomatids are unusual in that they possess a bacterial-like type I nitroreductase (NTR)[140] which is absent in the mammalian genome. This type 1 NTR can reduce nifurtimox to the nitrile compound **13** by introducing four electrons (**Figure 7**).[141] This nitrile has been synthesized and unfortunately is equally as toxic in mammalian cells.[142] The mechanism of toxicity is unknown but hypothesized to result from its Michael acceptor capabilities (**Figure 7**).[141] The IC_{50} of nifurtimox is 1.5 µM for both *T.b. rhodesiense* and *T.b. gambiense* forms of HAT,[143,144] and is below the maximum achievable concentration of 2.6 µM measured in healthy subjects. It appears to perfuse easily into the CNS, independent of BBB breakdown.[145] In fact, in mouse models [^{35}S]nifurtimox appears to concentrate in the CNS, with higher levels observed in both the frontal cortex (6.0 µM) and CSF (12 µM).[145]

Resistance to nifurtimox has been observed particularly in the treatment of *T. cruzi* for Chagas Disease where 20-25% of cases are refractory.[146] In both *T. brucei* and *T. cruzi* resistance is easily developed by reducing the expression of the type 1 NTR.[147] This reduced expression does however have a negative impact on rate of trypanosome proliferation and null Tbntr mutants were shown to be non-viable.[147] If the tenfold

decrease in drug sensitivity seen *in vitro* is reflective of the *in vivo* effect in *T. brucei*, this would result in an IC$_{50}$ above the achievable CNS concentration. Nifurtimox also suffers toxicity problems. Due to its ability to penetrate the CNS and its susceptibility to redox reactions, administration is associated with a range of neurological side effects and gastrointestinal issues that end upon cessation of treatment.[148,149]
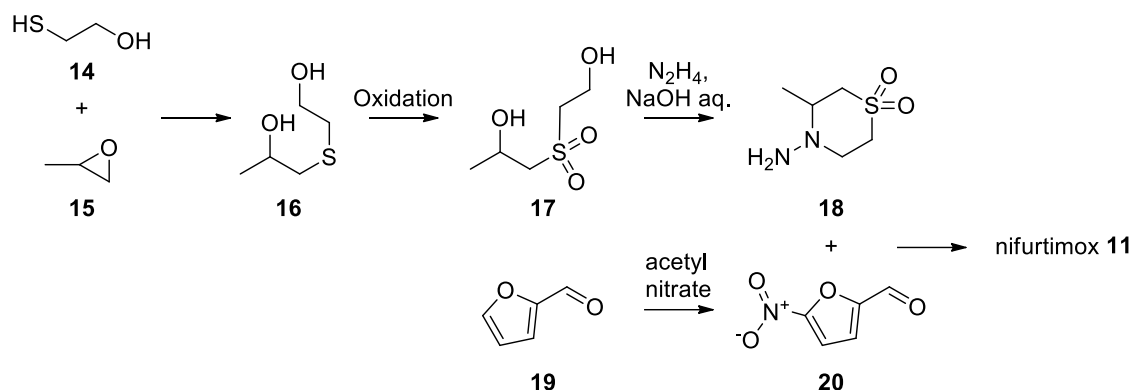
Scheme 3 - Synthesis of nifurtimox

There are several ways with which the components **18** and **20** that combine to form nifurtimox (**11**) can be synthesized and a possible route is illustrated (**Scheme 3**). The dihydroxy sulfide (**16**) is formed by epoxide opening[150] and is then oxidized to the sulfone (**17**).[151] Interestingly the formation of compound **18** requires catalytic sodium hydroxide, the mechanism is not discussed but presumably formation of the desired 6 membered ring (**18**) is kinetically favored over the available 7 membered diazepane. Compound **19** is achievable by direct nitration of furfural.[152] The drug is synthesized by the chemical company Bayer and they have patented the synthetic methods only for the formation of the cyclic hydrazine (**18**) from the 1-((2-hydroxyethyl)sulfonyl)propan-2-ol[153] (**17**) starting material and for the final hydrazone formation to arrive at nifurtimox (**11**).[154]
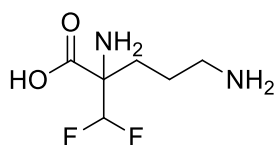
21

Figure 8 - Eflornithine

Eflornithine (**21**) (**Figure 8**), an analogue of ornithine, is a suicide inhibitor of the enzyme ornithine decarboxylase (ODC). ODC is the first biosynthetic step in production of polyamines such as putrescine, spermidine and spermine.[155] These polyamines are involved in the repair of DNA damage but they also play a key role in maintaining a normal cell cycle.[156] Cyclin dependent kinases are considered the drivers of cell cycle processes and changes.[157] Key signal molecules, cyclins, are reduced during polyamine inhibition,[158] resulting in cessation or retardation of cell growth. Both mammalian and parasitic ODC are inhibited but selectivity is achieved from the divergent enzyme turnover rates. Rates in the parasite are very slow compared to mammals thus the human cells only experience ODC inhibition for a short time whereas the parasite must endure the detrimental ODC inhibition for longer.[159]

Eflornithine does not kill trypanosomes but induces a shift from the reproductively active, long slender form to the non-profligate stumpy form.[160] As it is not a trypanocidal drug, the host's innate immune system is still necessary to clear the static infection throughout the body.[161] Eflornithine monotherapy regimen usually involved 100 mg/kg IV infusions at six-hour intervals for 14 days. Adverse effects include fever, headache, hypertension, macular rash, peripheral neuropathy, tremor, gastrointestinal problems and bone marrow suppression but these all recover post-treatment.[129,132]

Unfortunately eflornithine resistance is easily generated *in vitro*, with resistant cells reported in the 1980s.[162] The mechanism of this resistance is thought to result from the deletion of the TbAAT6 gene that encodes an amino acid transporter.[163] Much like that of MPXR, eflornithine resistance results from diminished cell uptake as opposed to any specific intracellular target protein.[163] Resistance leaves the cell 40 times less sensitive to the drug.[163] It is important to note that use of eflornithine was limited until NECT was introduced[164] so the fact that resistant infections have yet to be observed is somewhat

unsurprising and it remains to be seen if this mutation will impact fitness in wild trypanosomes. Eflornithine IC_{50} growth inhibitory values are 81–693 μM[165] *in vitro*, with average plasma levels of 234–528 μM and CSF levels at 22.3–64.7 μM in patients receiving standard doses of 100 or 125 mg/kg. C

Clearly there is a disconnect between these values – and perhaps the *in vivo* inhibitory reality is different – but the situation is complex, especially considering eflornithine is trypanostatic not trypanocidal and therefore requires CNS recruitment of leucocytes. At present eflornithine remains curative but could easily fall victim to a mutation that would confer a 40-times reduction in efficacy, which could have a particularly dramatic impact given that laboratory studies have shown it already to be at its upper limit of efficacy at achievable CNS concentrations.

Eflornithine and melarsoprol monotherapies were for decades the clinical standard for *T.b. gambiense* but since 2009 these have been rejected in favor of NECT.[166] By 2010 NECT was utilized in 59% of treatments because although it doesn't improve patient outcomes compared to eflornithine, it allows for reduced dosing, resulting in greater patient compliance.[167] Additionally, a NECT kit costs one-third as much as an eflornithine monotherapy kit and that is without accounting for cost of longer treatment times. Indeed, a multi-centre, randomized, Phase III trial found the best course of treatment to be intravenous eflornithine (400 mg/kg per day, every 12 hours) for seven days with oral nifurtimox (15 mg/kg per day, every eight hours) for ten days.[167] Toxicity is also reduced by half when compared to the severe and very severe reactions of eflornithine monotherapy.

NECT is now the highest standard of care and is an important improvement for HAT treatment. Combination therapies are also less likely to enable the development of resistance. It is very important that resistance to eflornithine and nifurtimox is limited whilst new trypanocidals are developed, especially in light of melarsoprol refractory trypanosome strains *vide infra* and the ease of developing resistant trypanosome strains *in vitro*.
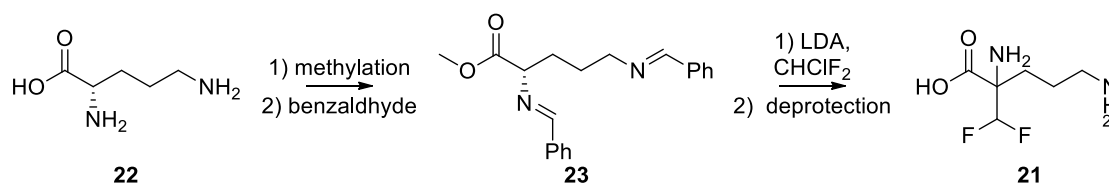
Scheme 4 - Synthesis of eflornithine

The synthesis of eflornithine[168] (**21**) (**Scheme 4**) unsurprisingly starts from the biologically-available ornithine (**22**). The protection of the carboxylic acid as a methyl ester and of the amines as benzylidines (**23**) facilitates the deprotination of the alpha carbon and allows for the addition of the difluoro group. Deprotection of both the ester and imines gives the desired product eflornithine (**21**).
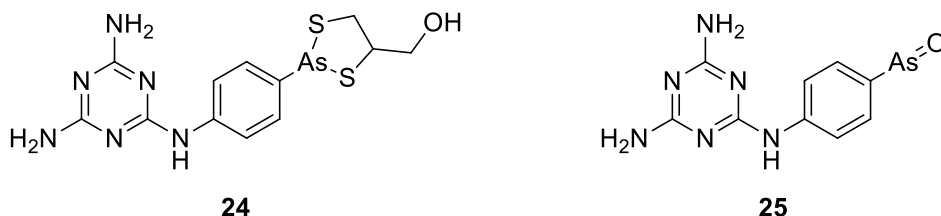

Figure 9 - Melarsoprol pro-drug and the active malrsen oxide

Melarsoprol (**24**) (**Figure 9**) is a melaminophenyl based organo arsenide pro-drug, introduced as a treatment for HAT in 1949. It is administered by IV injection, 2.2 mg/kg for ten days, as a 3.6% solution in propylene glycol, as it is immiscible with water.[169] Cellular metabolism produces the melarsen oxide, compound **25**, which has < 10 nM activity[170] and acts by sequestering trypanothione (N1,N8-bis(glutathionyl)spermidine) to form a melarsen oxide-trypanothione adduct (Mel-T).[171]

Mel-T both directly removes trypanothione and inhibits trypanothione reductase (K_i = 9.0 µM) such that trypanothione is removed from use in its normal role of mediating cellular response to reactive oxygen species (ROS).[172] The trypanocidal affect is thought to be mediated through increased ROS but Mel-T could itself be toxic and complement the ROS increase.[172] Melarsoprol is not only toxic to trypanosomes, it is extremely toxic in humans, resulting in severe reactive encephalopathies in 10% of patients and 5% fatality.[132] Other adverse events include convulsions, pyrexia, headache, pruritus, thrombocytopenia and heart failure.[129] It is incredibly painful to administer and it so

badly damages the veins that consecutive treatment requires new sites for administration.[132] The fact that this drug was accepted as the best treatment for Phase 2 HAT between 1950 and 1990, when eflornithine was introduced, and even then was only really replaced in 2009 by NECT, serves to emphasize how severely this disease has been neglected.
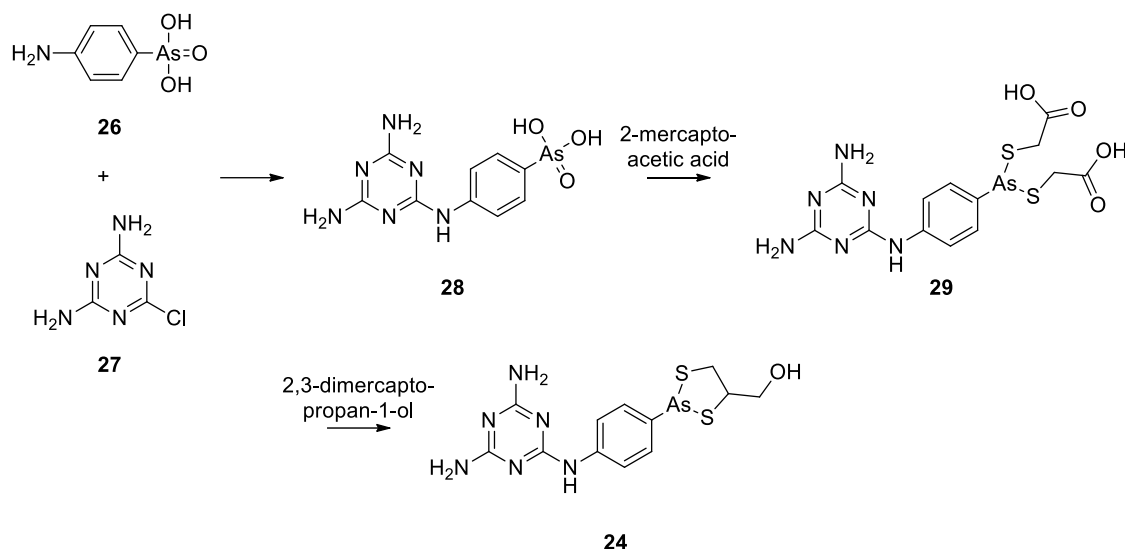
Scheme 5 - Synthesis of melarsoprol

The synthesis of melarsoprol (**24**) involves the substitution of the aniline (**26**) in place of the chlorine of the triazine (**27**).[173] 2-Mercaptoacetic acid is then utilized to reduce the arsenic from Ar(V) to Ar(III) and also forms compound **29** which easily undergoes displacement with 2,3 dimercaptopropan-1-ol to give melarsoprol (**24**).[174]

Interestingly, the first observed example of drug resistance was of trypanosomes with arsenical compounds by Paul Ehrlich. Subsequently arsenical–diamidine cross-resistance was first observed over 60 years ago.[175] Despite its toxicity melarsoprol is the least harmful of the arsenical drugs for HAT, and it and pentamidine have been in use since the 1940s and 1930s respectively.[176] It was not until the 1990s that the mechanism of resistance for both pentamidine and melarsoprol began to be elucidated and linked to the membrane protein P2 (purine transporter 2), encoded by the TbAT1 gene.[176]

Expression of TbAT1 in *Saccharomyces cerevisiae* enabled adenosine uptake and also conferred susceptibility to arsenicals.[177] TbAT1 gene deletion and loss-of-function mutations were then identified in drug-resistant trypanosomes generated in the

laboratory[178] and these mutations were also found in "wild" *T. brucei* field samples[179] including in cases of melarsoprol treatment failure.[180,181] Loss of the P2 transporter cannot explain melarsoprol-pentamidine cross resistance (MPXR) in its entirety. Laboratory generated resistance was substantially higher than observed for the mutated TbAT1 and the existence of a high-affinity pentamidine transporter (HAPT1) was postulated.

Recently, two closely related aquaglyceroporins, AQP2 and AQP3, were linked to MPXR in a high-throughput loss-of-function screen.[135] aq2-aq3 null strains were created and the AQ2 absent mutants were insensitive to melarsoprol and pentamidine, while restoring AQ2 re-established wild type sensitivities.[182] This is a particularly worrying scenario for HAT as detailed examination showed no fitness cost in aq2-aq3 null strains in cells at neither the developmentally distinct bloodstream stage or insect stage,[135] nor the transition between them.

Specific mutations in AQPs have been identified that correlate to reduced drug sensitivity in field-isolated trypanosomes: particularly common in the cited study was a completely novel AQP2/AQP3 chimera.[183] AQP2 alteration in melarsoprol insensitive and relapsed HAT patients was first reported in 2014. 45 *T.b. gambiense* strains were obtained from patients with 41 arising from relapse post-melarsoprol. In all these strains, irrespective of the patient treatment outcome, AQP 2 and 3 genes are replaced by chimeric AQP2/3 genes.

MPXR has been shown to arise from two specific transporter proteins, with the greatest resistance conferred by their concomitant expression, and worryingly (though as expected) these mutants bear no cost to fitness.[184] Both resistant alleles have been observed independently in patient population field isolates, so it can be assumed that these genes are now present in the parasite reservoirs and that genetic exchange in parasite populations could result in a trypanosome becoming almost completely resistant to melarsoprol. Even though uptake is reduced for pentamidine, the potency is so high (IC_{50} ~1 nM) that it remains lethal at patient blood concentrations, which peak at one-hour post injection at around 0.42-13 µM, even in the most resistant varieties observed in laboratories (IC_{50} ~100 nM).[183]

Melarsoprol however is already poorly CNS-penetrant, with the maximum obtainable CNS concentration just 1-2% of its plasma concentration of 5-10 μM.[185] This 50-100 nM CNS concentration might not be enough for complete clearance when just a single resistant TbAQP2 allele increased the IC_{50} 50 nM from 5 nM.[183] Given the complex multi-barrier structure of the CNS and the likely occurrence of reduced local concentrations, this increase in drug resistance might not allow for full clearance.

If concomitant expression were to develop in trypanosomes, melarsoprol, the only available treatment for *T.b. rhodesiense*, would become essentially redundant. Enhancing the risk is the existence of a multi-drug-resistant protein A (MRPA) present in some trypanosomes. *In vitro* studies have shown that over expression of this protein, which is responsible for exporting the active Mel-T agent from the cell, increased the drug resistance by ten-fold. [170]. The particular disadvantages of each treatment is summarised (**Table 1**):[186]

Table 1 - Summary of available HAT treatments[186]

	Discovery date	Disease stage; *Trypanosoma brucei* subspecies	Administration route	Adverse effect
Suramine	1922	Stage one; *T b rhodesiense*	Intravenous	Nephrotoxicity, allergic reactions
Pentamidine	1941	Stage one; *T b gambiense*	Intramuscular	Hypotension, glucose imbalances
Melarsoprol	1949	Both stages; *T b rhodesiense*	Intravenous	Painful injection, reactive encephalopathy, increasing number of treatment failures mostly because of toxicity
Nifurtimox	1967	Both stages; both subspecies	Oral	Gastrointestinal symptoms, neuropathies
Eflornithine	1981	Stage two; *T b gambiense*	Intravenous infusion	Reversible haematological abnormalities, diarrhoea, hair loss
Nifurtimox-eflornithine	2009	Stage two; *T b gambiense*	intravenous (eflornithine), oral (nifurtimox)	Gastrointestinal symptoms, headache, musculoskeletal, vertigo

Table: Available drugs for human African trypanosomiasis[4]

Poor oral adsorption – All chemotherapeutics, with the exception of nifurtimox, must be intravenously or intramuscularly administered by a trained professional, all requiring multiple doses over a course of days. Melarsoprol requires daily treatments for ten days, whilst eflornithine necessitates a very intensive regime of 56 IV doses over 14 days. NECT has shown some improvement[187] and is currently the best treatment strategy available. However, NECT still requires seven days of single IV eflornithine doses. IV administration is a substantial problem in HAT treatment particularly regarding logistics and affordability, as the disease is widespread across a poor, rural demographic. The affected individuals are unlikely to be able to afford to travel the necessary distances to

treatment centres for the days or weeks required to receive the available drug treatments.

Acute toxicities – While Phase 1 drugs are generally tolerated, traditionally treatments for Phase 2 have proven highly toxic. Melarsoprol is extremely painful to administer, is associated with severe reactive encephalopathies in 10% of cases and kills 5% of patients.[188,189] Eflornithine monotherapy has a 2.1% mortality[190] and toxicity problems result in gastrointestinal distress, bone marrow toxicity and seizures.[191] The high level and long duration (two months) of dosing in nifurtimox monotherapy was deemed unacceptably toxic.[192] Fortunately NECT has halved the toxicity compared to eflornithine but it remains unacceptably high.

Limited therapeutic spectrum – Eflornithine and pentamidine are only active against *T.b. gambiense* whilst suramin acts only on *T.b. rhodesiense*. The massively toxic melarsoprol, referred to as "arsenic antifreeze" by clinicians[193], is the only course for CNS-implicated illnesses involving *T.b. rhodesiense,* and the evolution of refractory parasite strains is affording it increasingly limited application. Indeed this development of melarsoprol resistance poses a serious risk, particularly if it becomes increasingly prevalent in acute *T. b. rhodesiense* HAT, as here treatment options would be completely limited to nifurtimox monotherapy.

Pharmacokinetics – Rapid metabolism and clearance of pentamidine, eflornithine, melarsoprol and nifurtimox necessitates increased dosings of these HAT trypanocidal agents to maintain the high serum concentrations necessary to minimize the high relapse rates observed in low dosing. [194] In contrast, the serum binding suramin, with a half-life of >50 days, is arguably at the other undesirable extreme, although toxicity from this appears limited.

Uncertain availability and price – In the past there have been zero-cost charity agreements between the World Health Organization (WHO) and the producers of anti-trypanosomal drugs, Sanofi and Bayer, as the patients are typically poor and unable to pay for treatment. However, long-term availability of such loss-making drugs is always precarious,[195] and in fact, for a period in the late 1990s, eflornithine became completely unavailable. Even with heavy international and government subsidies, if one member of

a household is infected with HAT the cost of treatment is calculated at roughly five months of the total family income. [196]

Parasite drug resistance - HAT chemotherapy began in the 1900s [197] and has been prevalent in animals and humans since. Partial treatment of animals or humans with anti-trypanosomal agents, due to incomplete application resulting in only semi-clearance of the parasite, unsuccessful treatments, or prophylactic use, have allowed the parasite to coexist in a host with non-lethal drug concentrations. These non-curative concentrations have provided a selective pressure in response to which anti-trypanocidal drug resistance has evolved for both melarsoprol and pentamidine. *In vitro* studies have shown that eflornithine and nifurtimox are similarly vulnerable to the development of resistance.[140,163]

African animal trypanosomiasis
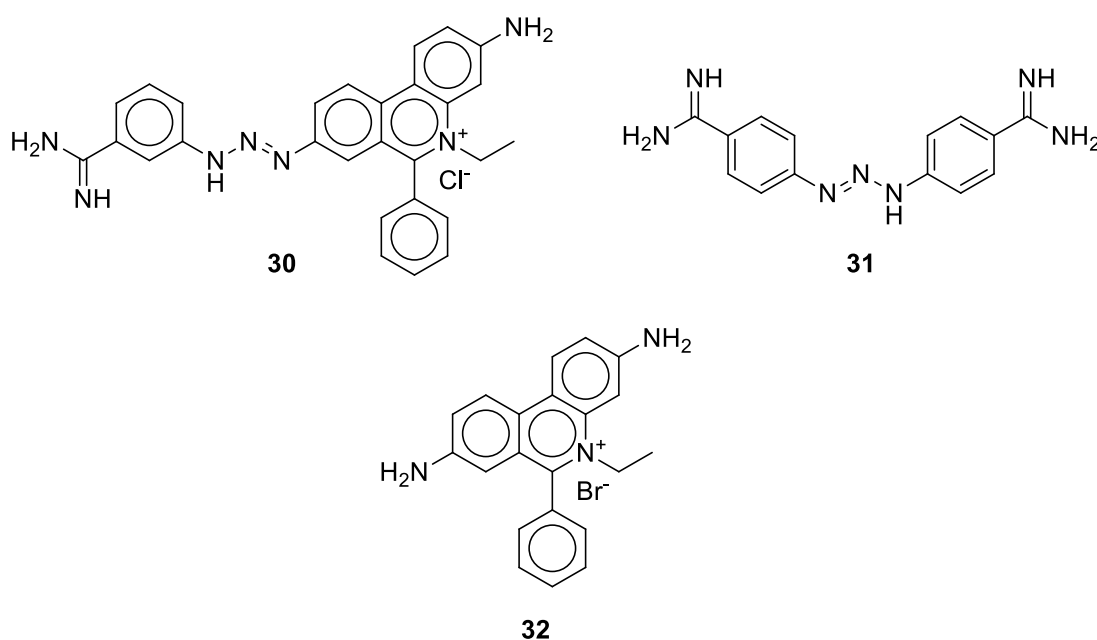
Figure 10 - Isometamidium chloride, ethidium bromide and diminazene aceturate

There are three main veterinary trypanocidal drugs administered, with isometamidium chloride (**30**) (ISM), diminazene aceturate (**31**) (DA) and ethidium bromide (**32**) (EB) (**Figure 10**) estimated to represent 40%, 33% and 26% respectively of the total trypanocidal drug market by value.[198] Despite being introduced in the 1950s the mechanism of action for both DA and ISM remain unclear.[199,200] DA is used primarily as

an active treatment[199] whilst ISM and EB are mainly prophylactic, but EB is a powerful mutagen and a poor trypanosomal prophylactic.[198] Inappropriately toxic treatments are thus common to AAT and HAT, as in fact is drug resistance. Drug resistance has been reported in 17 countries. Resistance to ISM is more widespread than to DA,[201] but increasingly often there are reports of multiple drug resistance. The challenge of multiple resistance is particularly well illustrated by a study of 800 cattle in south-east Mali.[202] Of the cattle tested across the area 125 (16%), were-trypanosome-positive. This subgroup was split in two, and half treated with ISM and half with DA. Any which remained infected after treatment were then retreated with a double dose of DA. 49% and 30% respectively of the ISM and DA treated cattle failed to clear the parasite and the doubled dose of DA failed to clear 26% of both the ISM and DA infections. Roughly a quarter of diseased animals were therefore deemed refractory to ISM and DA.

35 million doses of trypanocidals are given every year to animals.[54] This very high treatment rate is the result of ineffective treatments and high levels of resistance. The need for an effective, orally available, CNS-penetrant and non-toxic drug is evidently equally critical for AAT as HAT, with particularly incumbent issues of economics, livelihood, human nutrition and animal welfare.

Drug development

Advances towards new HAT treatments have received new attention in the past two decades with some compounds reaching clinical trial but none able to progress further. Therapies can be derived from alteration of known drugs, the re-ignition of old hits or from entirely new scaffolds and targets.

Development from the amidine agents has been common. These compounds have been known for a long period and have proven potent inhibitors, for example pentamidine with nM affinity. Most efforts have been in whole cell trypanosomal activities with no *in vivo*, pharmacokinetic or toxicology data with the exception of a study showing mammalian cell-line LD_{50},[203] thereby representing only preliminary drug discovery efforts.[203]

33
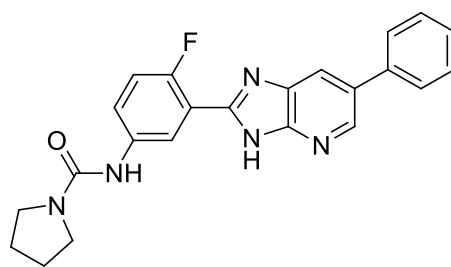
High throughput screens reported early in 2014[204] by Novartis identified 2-phenyl-imidazopyridines as a new scaffold (**Figure 11**) from their 700,000 compound library. Exploration around these gave compound **33**, which inhibits *T.b. brucei* with $IC_{50} < 5$ nM, has good CNS penetrance and dosing orally twice a day at 5 mg/kg for five days cured mice of Phase 1 infection. This compound requires further study but it seems promising and will hopefully become a candidate for clinical trial in the near future.

All of the issues discussed above clearly illustrate the urgent need for new African trypanosomiasis treatments. Ideally such a treatment should be targeted, non-toxic, orally bioavailable, and not require a complex dose regimen or administration by a professional clinician.[205,206] Despite the dire state of current treatment there has been some promising progress towards much-needed new drug treatments. NECT is an excellent breakthrough in comparison to the previous standards and the two potential treatments now in clinical trials represent genuine hope for some appropriate treatments.
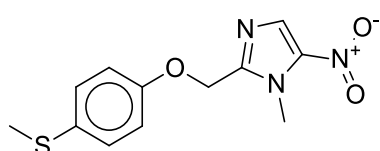
Feinidazole **34**
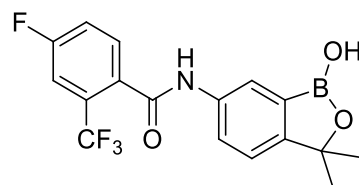
SCYX-7158 **35**

Fexinidazole and SCYX-7158

Fexinidazole (**34**) (**Figure 12**) was a preclinical antimicrobial developed in the 1970s and resurfaced in a profile of 700 nitroheterocyclic compounds.[113] It is oxidised from sulfide to sulfone in the body but an *in vitro* IC_{50} of ~2.3 μM has been observed for both of the two compounds against both variants of HAT. It successfully cleared mice infected with *T.b. brucei* in both Phase 1 and Phase 2 of the disease at 100 mg/kg/day. Extensive ADME (Absorption, Distribution, Metabolism, Excretion) studies, pharmacokinetic studies, repeated dose studies and toxicology studies (genetic, developmental and reproductive) were undertaken and the compound and its metabolized derivatives showed no markedly negative results. It is distributed well in the body and although, as mentioned, it is readily metabolised, it has a half-life of one to four hours. The drug is currently in Phase II/III studies, which are taking place in the Democratic Republic of the Congo and Central African Republic under the direction of the Drugs for Neglected Diseases Initiative in collaboration with the Swiss Tropical and Public Health Institute.

SCYX-7158 (**35**) (**Figure 12**) was identified in a screen of a library of boron-based compounds by Anacor Pharmaceuticals.[207] The lead was optimized to SCYX-7158 with IC_{50} 800 nM. It cures both forms of HAT infection in mice, is 55% orally bioavailable, CNS penetrant and metabolically stable. Preliminary toxicology is clean in Ames and hERG assays, and it is currently awaiting Phase II/III completion.[208]

Despite the promise of drugs currently in clinical trials, it would be imprudent, foolhardy and irresponsible for the scientific and medical community to ignore continued research into alternative treatments. Clinical trial failures are commonplace and even if both drugs are able to proceed to market, two drugs would represent a very limited pharmacological arsenal for the treatment of HAT and AAT, especially given their propensity to develop resistance.

In this regard we examined target proteins and lead compounds with potential for the rational design of new drugs against HAT and AAT. A trypanosomal protein, trypanosomal alternative oxidase (TAO), which emerged 30 years ago, shows promise for targeted treatment.

Trypanosomal alternative oxidase function

A number of desirable features make TAO a particularly promising target for drug development. Firstly, there is a published protein isolation procedure[209] that allows the production of the protein for established biological assays and drug potency measurements. There is also a published crystal structure of TAO,[210] which allows for increased understanding of the target's active site. TAO has been illustrated to be necessary for survival of the parasite.[211] Natural products have been identified that inhibit TAO, which can be used as lead compounds for further exploration,[212–214] and finally the trypanocidal activity of these natural products has been studied both *in vitro* and *in vivo* on the mammalian parasites.[215,216] Taken together, all of these factors make TAO an excellent focus for the development of a new chemotherapeutic to help address the dearth of acceptable and appropriate AT treatment options.

TAO function is the cytochrome-independent terminal oxidase of the mitochondrial electron-transport chain in the mammalian bloodstream trypanomastigote (**Figure 13**).[217] Unlike cytochrome-dependent oxidases (COXs), TAO is not sensitive to cyanide poisoning but is inhibited by salicylic hydroxamic acid (SHAM).[218] TAO transfers electrons from ubiquinol to oxygen, reducing the oxygen to water. It is not coupled to proton translocation but rather adenosine triphosphate (ATP) synthesis and heat production.[219] The bloodstream trypanosome must derive all its energy from the glucose of the host and as such has developed the glycosome organelle which undertakes glycolysis in addition to performing various other functions including purine salvage, beta oxidation of fatty acids, and ether lipid synthesis.[220] The mitochondrial TAO is ultimately coupled *via* the glycerol 3-phosphate/dihydroxyacetone cycle to the reoxidation of NADH to NAD$^+$ for use in aerobic respiration to afford the net gain of two ATP per glucose. Inhibition of the aerobic process leaves the parasite dependent on the less productive anaerobic process, where the net gain is only one ATP per glucose, but this does also produce glycerol 3 phosphate (G3P). This G3P can be processed into glycerol by glycerol kinasein an incredibly rare backward enzymatic activity. Glycerol kinase activity equilibrates however as glycerol levels rise, removing the net ATP gain. This inhibition by mass action can starve and kill the trypanosome.
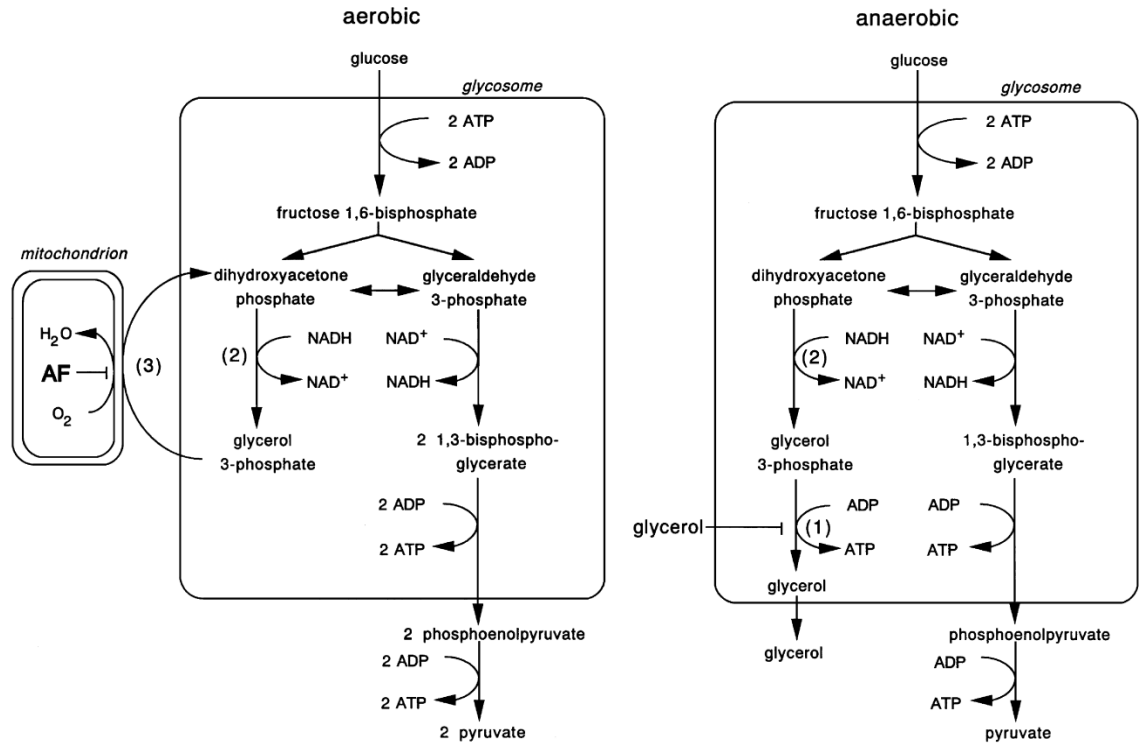
Figure 13 - Glucose metabolism in bloodstream form of *T. b. brucei* under aerobic and anaerobic conditions. (1) Glycerol kinase, (2) glycerol-3-phosphate[424]

TAO structure

TAO enzyme is a monomer[221] located in the mitochondrial organelle. It consists of α helices with a non-haem di-iron centre held by two conserved EXXH (Glutamic acid-X-X-Histidine) motifs at residues 162–165 and 266–269. It has two hydrophobic stretches, similar to other alternative oxidases.[222] The iron, which is crucial to function,[223] was detected initially by the EPR signal of the mixed valence reaction intermediate[224] and visualized recently *via* protein crystallisation.[210] TAO is an interfacial protein embedded only in the inner leaflet of the mitochondrial lipid bilayer[210,225] with its ubiquinol binding site opening into the mitochondrial cytoplasm.
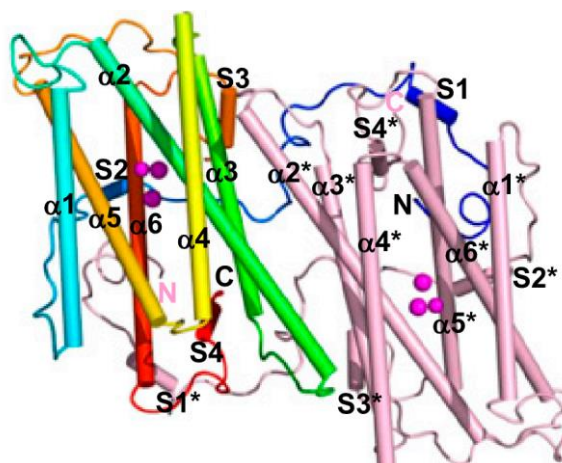
Figure 14 - Dimeric crystalised structure of TAO[226]

The recent publication of TAO's crystal structure at a resolution of 2.8 Å[210] is a great advance in understanding the nature of the protein however the crystal structure contains four monomers per asymmetric unit that associate to form homodimers (**Figure 14**) and so unfortunately data must be interpreted across these mildly divergent protein units not just a single monomer (**Figure 15**).
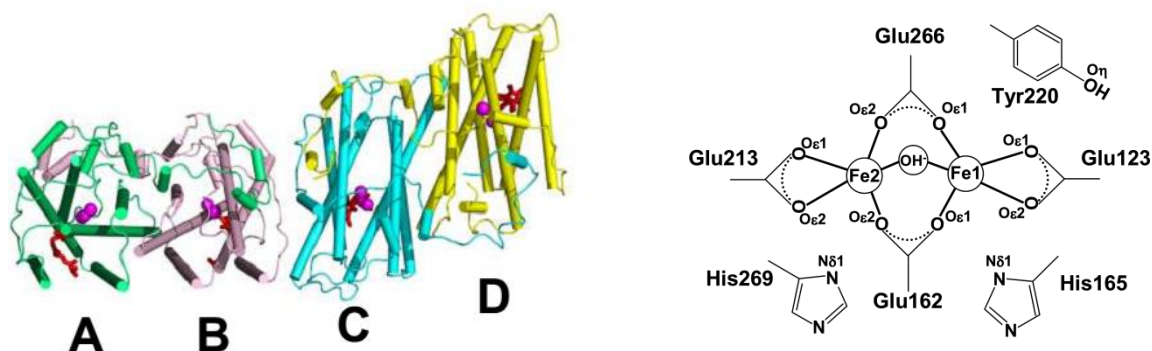
Figure 15 - Homodimeric crystalysed form of AOX monomer (left). Five co-ordinate diiron centres at TAO active site (right)[210]

All subunit's are convergent in their general structure. They each consist of a long N-terminal arm, six long α helices (α1–α6) and four short helices (S1–S4) (**Figure 14**). The long helices are arranged in an antiparallel fashion with α2, α3, α5, and α6 forming a four-helix bundle that accommodates the diiron centre. The diiron active site was confirmed as an oxidized Fe(III)-Fe(III) form with a single hydroxo-bridge (**Figure 15**), which agreed with predictions from existing spectroscopic evidence.[224]

The active site, which is located in a hydrophobic environment deep inside the TAO molecule (**Figure 17**), is composed of the diiron centre and four glutamate (E123, E162, E213, and E266) and two histidine residues (H165 and H269), all of which are completely conserved across alterative oxidases (AOXs).[223] These residues bind the diiron centre in a five co-ordinate manner possessing a distorted square pyramidal geometry, observed across all four crystallized units (**Figure 15** and **Figure 16**).
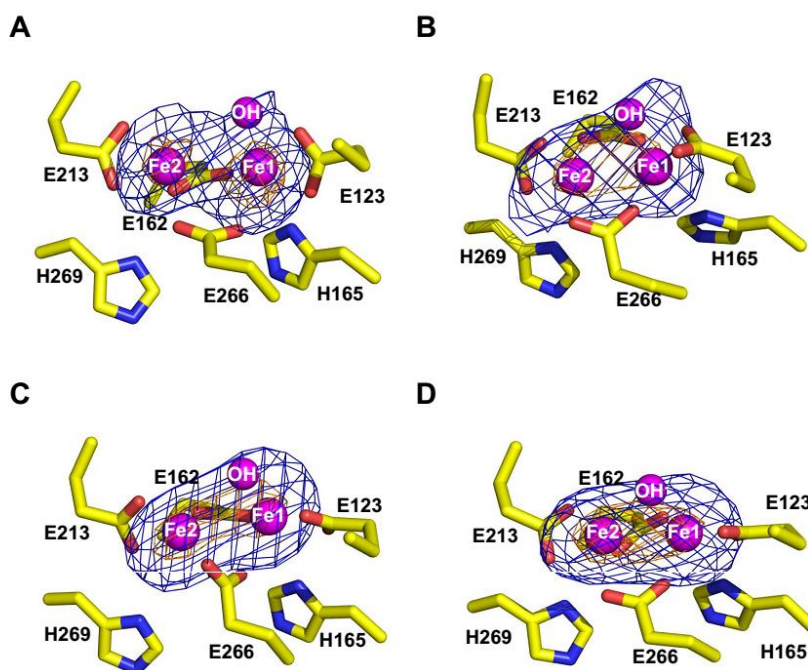
Figure 16 - The structure of diiron sites. Interaction between the diiron molecule and TAO with sigma-A weighted electron density map (Fo-Fc) calculated from the refined model of ligand-free TAO with the diiron molecule omitted from the phase calculation. The diiron molecules bound to (A) chain A, (B) chain B, (C) chain C and (D) chain D are shown as yellow sticks with nitrogen and oxygen atoms colored in blue and red. The diiron (Fe-OH--Fe) is drawn as magenta spheres. Contour levels are 1.0 σ (blue) and 3.0 σ (orange).[210]

CAVER protein-analysis software[210] predicted another possible hydrophobic cavity near the membrane surface and indeed this can observed in the crystal structure (**Figure 17**). This second cavity connects the di-iron active site with the membrane and interacts with the inhibitor-binding cavity on the opposite side of the di-iron core to the known ubiquinol binding site (green and orange respectively in **Figure 17**).

Although the exact four electron reduction mechanism is unknown, the mutation of the tyrosine 220 (Y220), which is entirely conserved across all known AOXs, abolishes enzymatic activity[223] (**Figure 15**). It is hypothesized that each hydrophobic cavity binds one ubiquinol close to the active site with the quinol rings located at the bottom of each

cavity, in a manner similar to that observed in known crystal structures for other proteins.[210]
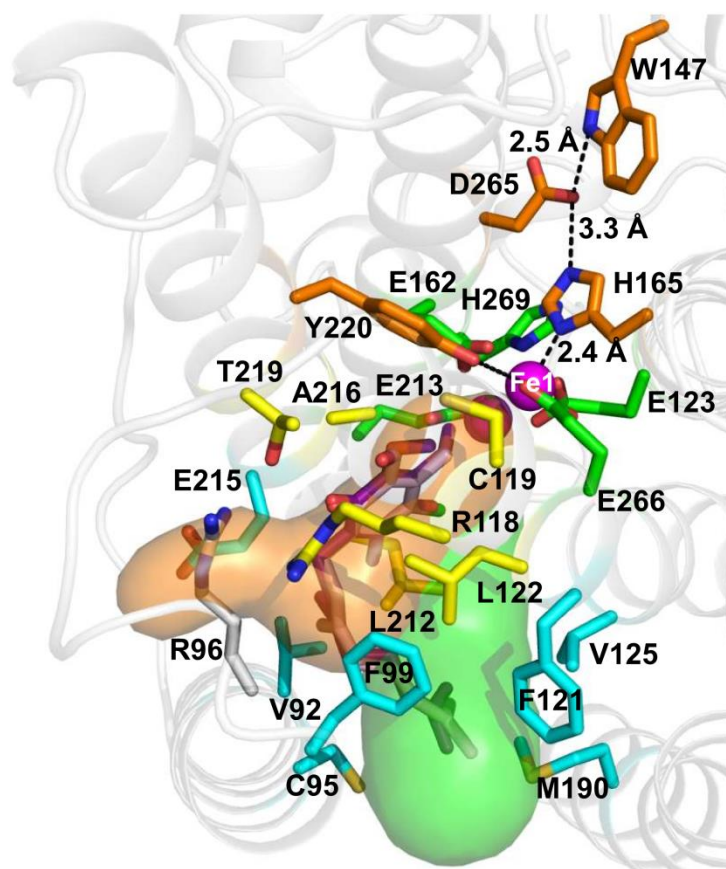

Figure 17 - Putative ubiquinol binding channels in CCB-TAO complex. Two hydrophobic cavities found by CAVER protein-analysis[227] software are shown in green and orange. Proposed residues involved in electron transfer are shown as orange sticks.
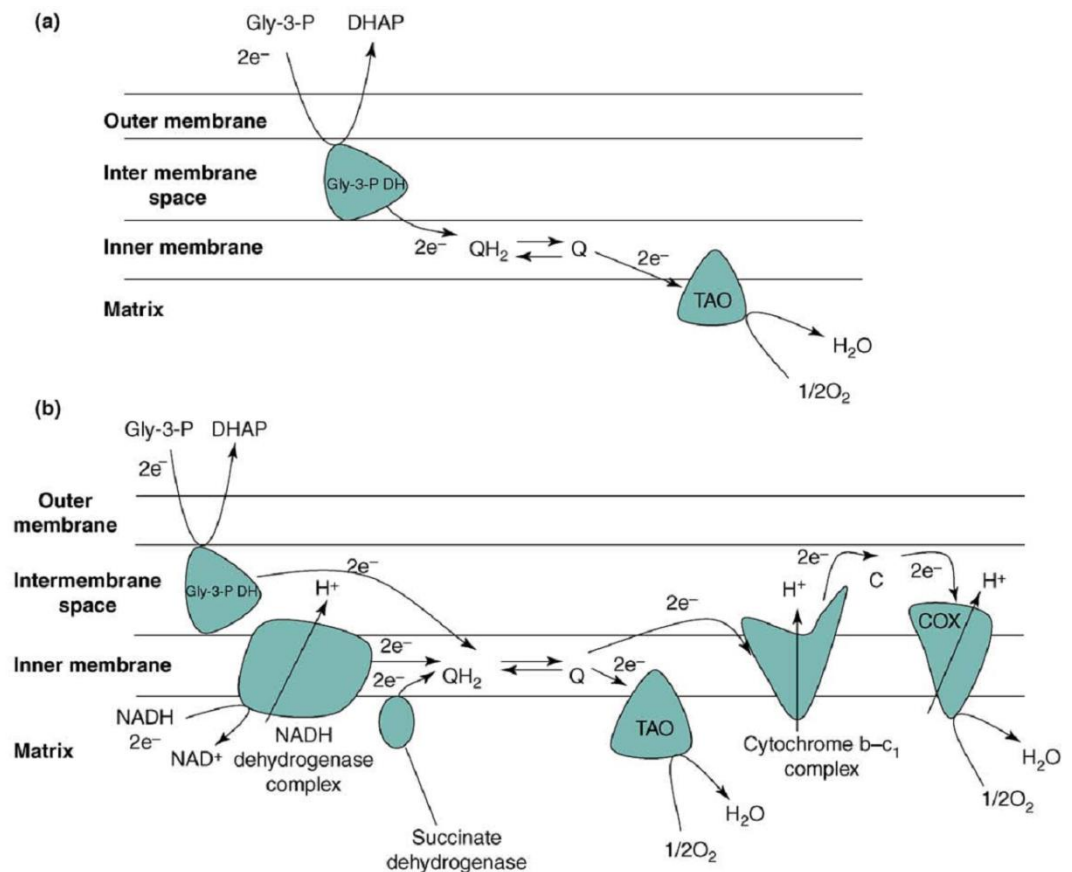
Figure 18 - The mitochondrial electron transport system in the bloodstream and procyclic forms of *T. brucei*. (a) The bloodstream form of *T. brucei* depends exclusively on TAO for respiration. (b) In the procyclic form TAO branches from the primary cytochrome-dependent pathway at the site of ubiquinol. Sub-mitochondrial localization of the enzymes and enzyme complexes are represented by their position in the outer mitochondrial membrane, inner mitochondrial membrane, intermembrane space, and mitochondrial matrix. Abbreviations: C, cytochrome c; COX, cytochrome oxidase; DHAP, dihydroxyacetone phosphate; Gly-3-P DH, glycerol-3-phosphate dehydrogenase; QH2, ubiquinol; Q, ubiquinone.[211]

Role of TAO across trypanosome lifecycle

TAO is expressed at nearly all stages in the life-cycle of the parasite and is developmentally regulated. In the Tsetse fly it is thought to allow for respiratory plasticity such that it can survive the harsh environment in the gut,[211] as it is expressed alongside COX and all citric acid cycle (CAC) proteins (**Figure 18**). The bloodstream form in mammals does not express COX or CAC proteins[228] but rather up-regulates TAO in a post-transcriptional manner so that the steady-state level of TAO transcript is about five-fold greater and the TAO protein level is 100-fold greater than in the Tsetse procyclic form.[229] TAO is the terminal oxidase in pyruvate producing glycolysis.[205] TAO inhibition induces anaerobic respiration,[230] whereby one glucose produces only one ATP, along with pyruvate and glycerol.[211] ATP is used in the cell, pyruvate exported into the

extracellular host medium, and glycerol, as described above, is itself an inhibitor of anaerobic ATP synthesis by mass action.[216] The combination of TAO inhibition and increasing cellular glycerol therefore derails bloodstream *T.brucei*'s only respiratory pathway.

Trypanosome alternative oxidase as a drug target

As discussed, TAO seems an excellent chemotherapeutic target. In addition to the plethora of advantages features already acknowledged, there is no mammalian homologue,[211] increasing the plausibility of designing a specific drug with minimal side effects. A genotypic assay has been used to screen for candidate molecules able to inhibit TAO and this assay has also been established in the Ward lab allowing rapid assessment of compound affinities. The published crystal structure allows also for computer-aided rational drug design and computational-chemical modelling of potential compound-protein interactions.

Potentially most encouraging is the existence of lead compounds from which medicinal chemical and synthetic exploration can begin. Trypanocidal inhibition of TAO by the natural products SHAM (**36**), colletochlorin B (**37**) and ascofuranone (**38**) (**Figure 19**) has been demonstrated.[215,231-233] All developmental stages of the bloodstream trypomastigotes in humans are crucially dependent on TAO for aerobic respiration making inhibition trypanocidal, rather than trypanostatic as with eflornithine.[234] Ascofuranone represents an exciting starting point on the journey towards a cure for African trypanosomiasis.
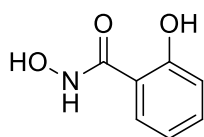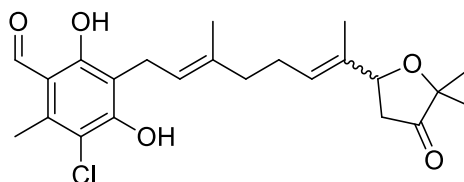
SHAM **36**
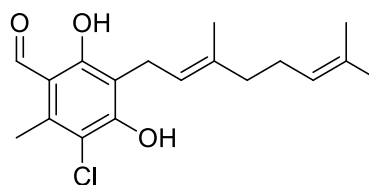
colletochlorin B **37**

(±)-ascofuranone **38**

Figure 19 - Established TAO inhibitors

Ascofuranone

Ascofuranone (**38**) (AF), a polyprenyl phenolic antibiotic, was first isolated from phytopathogenic fungus *Ascochyta visiae* in 1973.[235] Initially of interest was its hypolipidemic[236] effects and tumor-suppression[237] ability, thought to be mediated through activation of macrophages by respiratory inhibition.[238] However, in 1996 AF was shown to inhibit *T.b. brucei* with a K_i = 2 nM. It was later demonstrated that this affect was the result of incredibly potent inhibition of TAO. The compound exhibits mixed-type inhibition,[239] binding at the ubiquinol active site with picomolar activity (K_i = 0.13 ± 0.04 nM).[212] The trypanocidal activity of AF is orders of magnitude more potent than that of known concentrations for other trypanocidals like suramin (K_i= 4.1 µM),[240] n-propyl gallate (K_i = 6.3 µM)[241] and even melarsoprol (K_i = <10 nM).

Orientation of ascofuranone analogues in published crystal structure

AF analogues AF2779OH and colletochlorin B (**37**) (CCB) (**Figure 19**) were co-crystallized with TAO with resolution 2.6 Å and 2.3 Å respectively, which is not sufficiently high to draw very specific conclusions but is discussed below.

The structure indicates that AF2779OH is located close to the diiron active site and that the C2–OH forms hydrogen bonds with R118 and T219 (**Figure 20**). In addition, in the B and D subunits, the aldehyde oxygens at the C1 position interacts with E123 through a hydrogen bond network (**Figure 20**), whereas for the A and C subunits, the aldehyde oxygens form an intramolecular hydrogen bond with C2–OH *ortho*-phenol. While structural information is desirable, these crystal structures are not of sufficiently high resolution and the lack of consistency between the ABCD units makes determining the exact binding mode of the aldehyde head group futile. It is possible that the compound might bind to Fe, the bridging OH, outer-sphere water or H-bond amino acid (AA) residues near the iron.
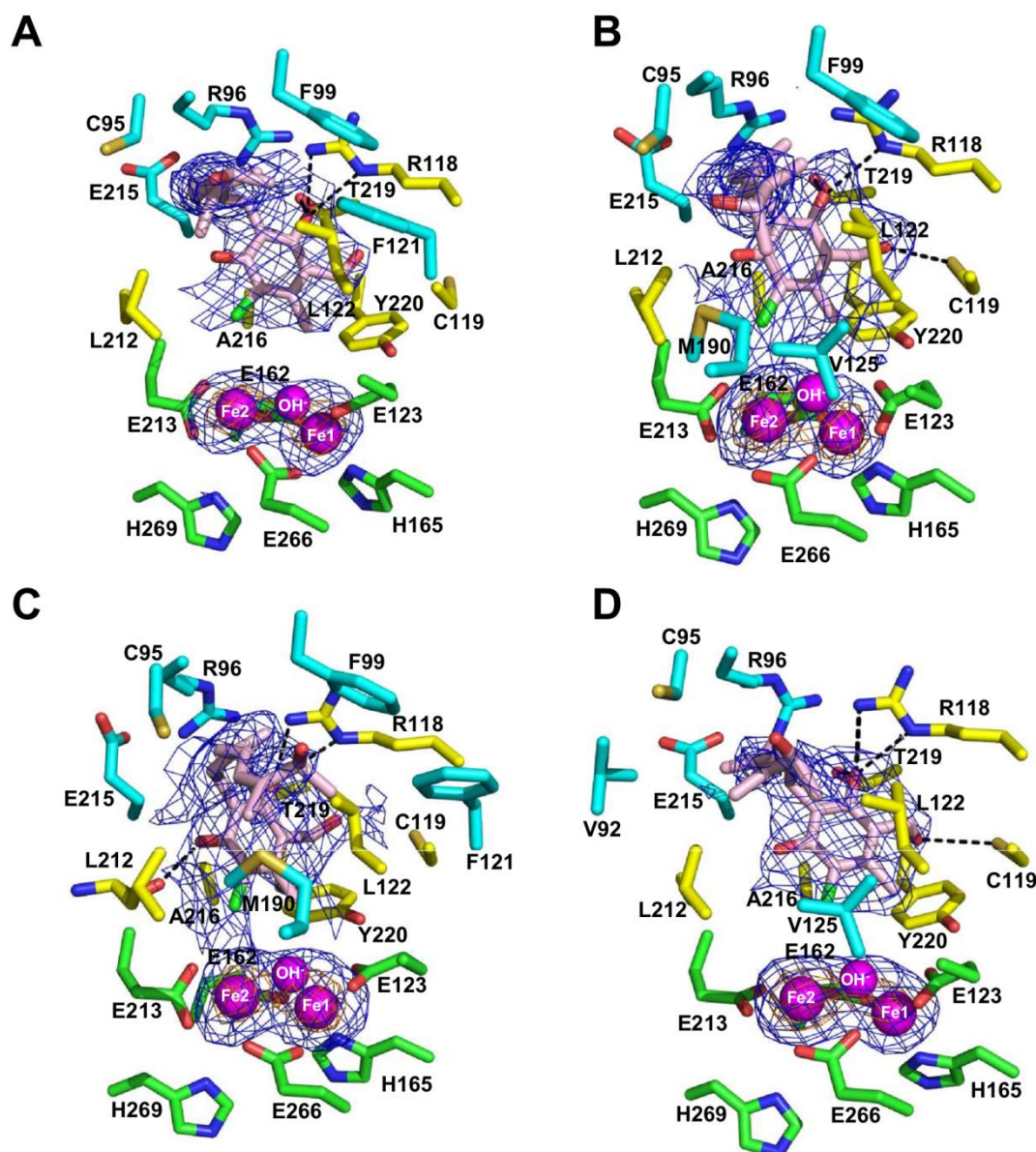
Figure 20 - Interaction between TAO and the bound AF2779OH molecules and their electron density maps. Interaction between the bound AF2779OH molecule and TAO with sigma-A weighted electron density map (Fo-Fc) calculated from the refined model of TAO-AF2779OH complex with theAF2779OH molecule omitted from the phase calculation. AF2779OH molecules bound to (A) chain A, (B) chain B, (C)chain C and (D) chain D are shown as pink sticks with nitrogen, oxygen and chlorine atoms coloured in blue, red and green, respectively. The diiron (Fe-OH--Fe) is drawn as magenta spheres. Contour levels are 1.0 σ (blue) and 3.0 σ (orange)[226] (Image and caption from reference)

Anti-trypanosomal evidence for AF

AF has been shown eradicate the parasite from bloodstream of mice with a high parasitic load, with curative dosings of 25 mg/kg AF and 3 g/kg glycerol for one day[216] or 100 mg/kg AF without glycerol for four days.[233] These results indicate that AF and AF-like

compounds show promise as non-toxic agents for mammalian trypanosomiasis. However, there are a number of drawbacks. For best effect the compounds must be administered intraperitoneally (IP), maintaining the need for a clinician. Curative oral doses were considerably higher with 100 mg/kg for one day AF and 3 g/kg glycerol, or 400 mg/kg for eight days with AF alone. Such doses are incredibly high considering that AF exhibits picomolar potency against TAO in genotypic and phenotypic assays, indicating that improving the pharmacokinetics (PK) could markedly improve prospects for TAO specific HAT inhibition.

Other known AF interactions

AF shows activity against a number of interesting targets including mitogen activated protein kinases,[242] G1 cell cycle arrest,[243] AMP activated protein kinases,[244] cytochrome bc1 complex,[213] and EGFR-mediated cell signaling.[245] It is also indicated as an antitumor agent by way of inhibiting MMP-9, which is implemented in tumour invasion and metastasis.[245]

The non-toxic clearance of trypanosomes in mice models indicates that AF is TAO-specific *in vivo*, however in its natural form there are a number of factors which make it unlikely that AF could be useful as a drug. Instead, TAO is adopted as a tantalizing lead compound for diversification.

Shortcomings of AF as a potential drug

AF has a number of structural features which should be addressed to make it more drug-like. The structure can be divided in 3 sections: 1) the aromatic head group; 2) prenyl linker; and 3) furanone tail group (**Figure 21**).

38
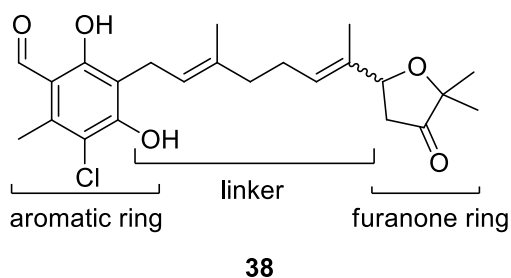
1) The crystal structure of TAO shows that the head group of AF analogues, with salicylaldehyde motif, interacts with the diiron active site. There are a number of potential problems in this region which must be addressed.[210]

The benzaldehyde is a prime target of metabolism *in vivo via* oxidation or attack by endogenous scavenging nucleophiles such as glutathione.[246]

The bisphenol moiety greatly increases the likelihood that AF-derived compounds would act as indiscriminate redox cycling agents. Redox cycling could potentially interfere with a plethora of electron transfer proteins, including, most critically, the human mitochondrial respiratory complex. Additionally, phenols have an innate toxicity for a wide variety of reasons.[247–250]

The hexa-substituted aryl motif is undesirable as these compounds tend to have poor solubility. They can also be synthetically idiosyncratic in both general reactivity and potential for side reactions because each addition, removal or substitution on any position will interact electronically and likely sterically with every other position on the ring.

2) The prenyl linker is a long hydrocarbon chain, and as such is likely to have poor metabolic stability. Cytochrome P450s (CYPs) are a superfamily of monooxygenases that account for ~75% of drug metabolism.[251] They add single hydroxyl/epoxy functionalities to a molecule which often deactivates it and increases its renal excretion from the body. The prenyl linker is particularly vulnerable to such oxidation and substitution for a shorter chain would be optimal, especially if that chain included a heteroatom. It would also be interesting to explore diverse linker and tail replacements by changing the linker-aryl bond from a carbon-carbon bond to a carbon-heteroatom bond.

3) The furanone tail group should have reasonable metabolic stability. However, analogues with simpler functionality and no chirality would be synthetically desirable. It is proposed that the furanone tail may help to afford selectivity because while AF is not toxic in mouse models, colletochlorin B is.[210]

Literature of the structure-activity relationship (SAR) around AF

It has been known since the 1990s[232] that AF is a TAO inhibitor, but it wasn't until 2013 that the structure-activity relationship (SAR) was explored.[212] As a result, most of the investigation detailed in this report was conducted prior to understanding of the SAR.

The synthetic alternatives explored in the study fall into several groups: 1) altered linker and tail group; 2) altered aldehyde functionality; 3) alteration and removal of remaining aryl substituents.

1)   Extensive changes were made to the linker and tail group. These include: removing the furanone or substituting it for various ethers, esters, and hydroxyl groups; saturating, partially saturating, branching, debranching, shortening or lengthening the linker.

39

Figure 22 - Most potent inhibitor to date: K_i= 0.06 nM

The changes illustrated that the furanone is not necessary for potency, in fact the most potent compound (**39**) (**Figure 22**), K_i= 0.06 nM, had no tail group, the optimum chain length is eight carbons, and a prenyl functionality beside the head group is mildly preferred. In summary, the chain appears to affect potency only non-specifically by lipophilic interactions.

2)   Aldehyde replacement was studied less extensively and unfortunately not conducted with matching tail groups, making direct comparison impossible, but seems

to indicate that substitution for the methyl ketone and nitro has little effect on potency (<10-fold), while introducing a nitrile, methyl ester or oxime moderately decreases potency (~10-fold) and chlorine and proton replacements had decidedly negative effects (100,000-fold and 40,000-fold respectively).

3)   Single changes on the ring at either the Me or Cl positions have negligible effect, both maintaining picomolar activity, but if both groups are removed potency decreases by 40-fold. These point changes do not confirm whether it is steric or electronic effects that are affecting potency but it is clear that these are non-essential functionalities. Methylation of the *para*-phenol decreases potency 100-fold and deletion results in almost complete loss of activity.

CHO replaced with Cl: 10 μM   CHO replaced with methylester: 45 nM

CHO replaced with NO$_2$: 10 μM   Methyl ketone: 0.15 nM

CHO replaced with CN: 6 nM   CHO replaced with aldoxime: 28 nM
(n-octyl pivilate ester tail)   (ascofuranone tail)

Various saturated and unsaturated tails showed similar levels of activity.

O-Methylation: 4 nM

Loss of 2-Methyl and 3-chloro individually shows only small effects but combined equates to >40 fold decrease.

colletochlorin B **37** : 0.20 nM

Figure 23 - SAR published by Kido *et al.*

To summarize (**Figure 23**), the nature of the tail is unimportant and the chlorine and methyl are not vital to function, but the para-phenol and potentially the *ortho*-phenol are necessary.

The exploration of chemical space in the study seems strangely directed. Only limited alterations were made to the headgroup, which would seem likely to have greater effect on potency given that ubiquinol is known to interact *via* its aromatic head group and SHAM only has this region. While hydrophilic interactions might be possible in the

channel leading to the active site, the linker is not an obvious starting point for diversification.

Positively, this exploration indicated that many desirable changes are viable, which should make AF more drug-like and tractable for analogue exploration. The linker and tail can be modified extensively, the aldehyde can be replaced with more suitable drug-like equivalents while retaining nM potency, and the Cl and Me can be removed, allowing space for possible SAR and growing off the ring. The necessity of the 4-hydroxy is clear but unfortunately the 2-hydroxy was not explored, although SHAM contains this 2-hydroxy and is efficacious, so it was assumed that the overall phenolic character of the lead compound is important. However, understanding can be improved by testing the effect of *para*-hydroxy methylation. Given that AF is mimicking electron-transferring ubiquinol it is understandable that the aldehyde and *ortho*, *para* phenolic character is necessary.

This work in combination with headgroup exploration undertaken in house prior to the commencement of this work unfortunately concluded that every position on the hexa-substituted aromatic group is required to give maximal potency. This greatly increased the synthetic challenge in producing novel analogues and severely limited the synthetic methods available. A thorough discussion of the synthetic difficulty involved in hexa-substituted aromatics and the literature around this topic is discussed in chapter 2.

Synthetic approaches to AF

There are several routes to AF and its analogues. There are numerous publications dedicated to synthesis of the furanone tail,[252–254] however, as it is irrelevant to AF's action, focus will be on preparation of the headgroup and how this is attached to the linker.
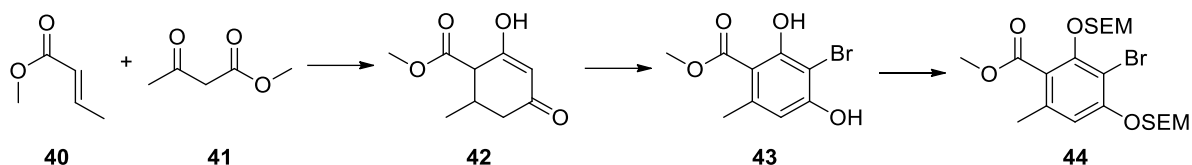
Scheme 6 - Penta-substituted headgroup synthesis from aliphatic staring materials

The headgroup, in almost all syntheses, is pre-formed as the 3-chloro-4,6-dihydroxy-2-methylbenzaldehyde (**47**) or the bromo methylbenzoate (**44**). This is obtained either by cyclisation (**Scheme 6**) or functionalization of orcinol (**45**) (**Scheme 7**). Unfortunately, in both of these routes the electrophilic carbonyl is installed early, limiting nucleophilic possibilities for later addition of the isoprenoid linker.
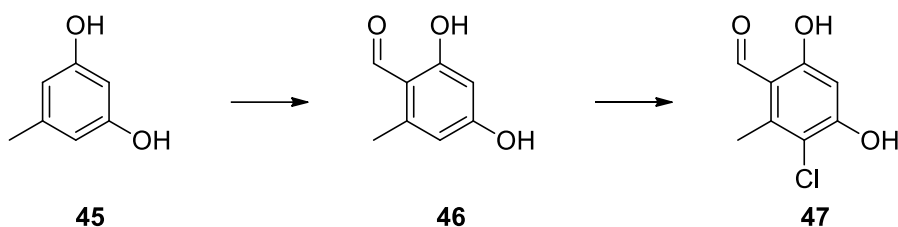
Scheme 7 - Penta-substituted headgroup synthesis from aromatic staring materials

There are two main routes for linker attachment from these two cores (**44**) and (**47**). For the free phenolic reagent (**47**), KOH and geranyl bromide enable electrophilic aromatic addition of the linker. The bromine of compound (**44**) is subjected to lithium-halogen exchange forming a nucleophile which attacks geranyl bromide *via* S_n2 displacement.

Prior to the commencement of this work, both of these methods had been tested in the Ward group but were found unsuccessful. The KOH method had been tried by several different labs and chemists at the University of Sussex and all had < 10% yields, much lower than the published 29%.[255] The second method involving lithium-halogen exchange, transmetallation to the cuprate and then S_n2 displacement with the geranyl bromide, reported a 70% yield,[256] but again this could not be repeated by post-doctoral fellows or students in the Ward lab.

This particular method does call for concern as it employs *n*-butyl lithium (*n*-BuLi) to exchange with the bromine, creating the aryl lithium intermediate in the presence of a methyl benzoate. Both of these could be expected to react with the methyl benzoate

and indeed this affect was observed in the Ward lab even when temperature, dilution and equivalents were carefully controlled. The choice of *n*-BuLi is also contrary to the recommendation in Victor Sneickus's comprehensive lithiation review,[257] where it is outlined that a *tert*-butyl benzoate, *sec* or *tert*-BuLi and low temperatures are needed to obtain yields comparable to those claimed for the AF synthesis.[258] This synthesis also requires SEM protecting groups which cannot be deprotected utilizing any of the various methods typically employed, including those quoted by the author. This deprotection problem was also identified by another group attempting to follow this synthesis of AF.[259]
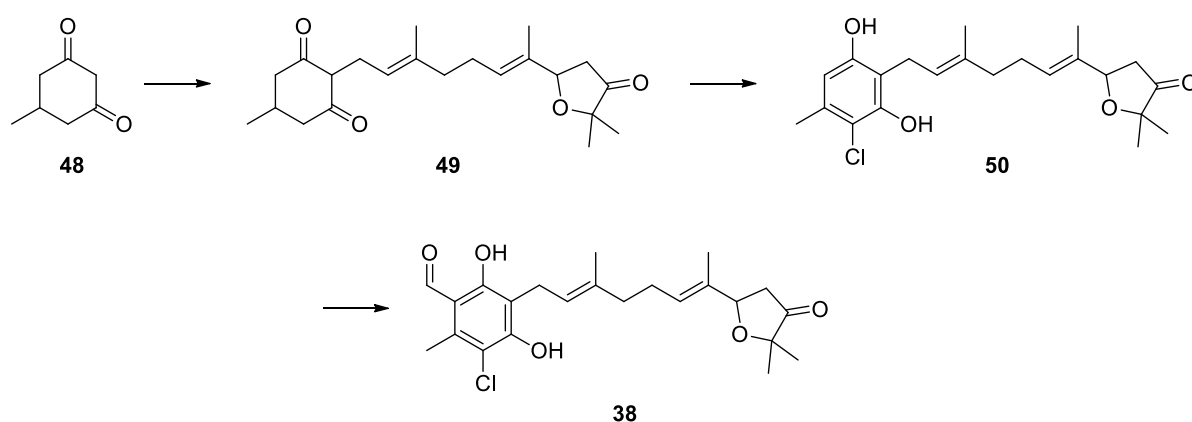
Scheme 8 - Synthesis employing late stage headgroup functionalisation[258]

In the only remaining published route[258] to AF the linker is attached early and the aryl headgroup functionalized afterwards by a chlorination, aromatization and formylation (**Scheme 8**). The yield for the complete 11-step synthesis was 0.8%, or omitting the formation of the tail group and linker, the 4 steps for simply attaching and functionalizing the headgroup, 2%. This is clearly not a viable route to AF for further derivatisation and SAR exploration.

Unfortunately none of the syntheses of AF have thus far proven to be high yielding, quick, reproducible or easily amenable to the diversity-orientated synthesis required for exploration of SAR. In spite of this AF represents an interesting and worthwhile subject for investigation because of its remarkable potency against an exciting protein candidate for the treatment of African trypanosomiasis. If a method could be developed for the diversification of this structure and/or the synthesis of the natural product improved,

this would be novel, constructive and important towards alleviating the suffering caused by the parasite *T.Brucei*.

Aims

The ultimate goal of this project was the development of the potent lead compound ascofuranone to produce a clinical candidate for the treatment of African trypanosomiasis. Towards this, three specific aims were determined which would become the focus of this work (**Figure 24**):

1) The existing chemistry around ascofuranone was limited in scope and not amenable to diversification of key functionalities. New synthetic routes were required which would enable improved exploration of chemical space and modification of metabolically labile features.

2) Once synthetic routes had been established, compounds could be developed which would afford enhanced drug-like properties, compared to AF, whilst retaining TAO activity. Pertinent to improving the drug-like properties of ascofuranone analogues was the removal of the headgroup aldehyde and bis phenols, which are particularly metabolically labile.

3) If a suitable alternate headgroup was discovered, which retained TAO activity, focus would shift to exploration at the tail. This would ideally involve substitution of the metabolically active geranyl motif with a variety of other tails with an aim to determine the optimum combination of pharmacodynamic and pharmacokinetic properties.

R_1= aldehyde replacement
R_2= phenol removed or altered
R_3= diversifiable tail group
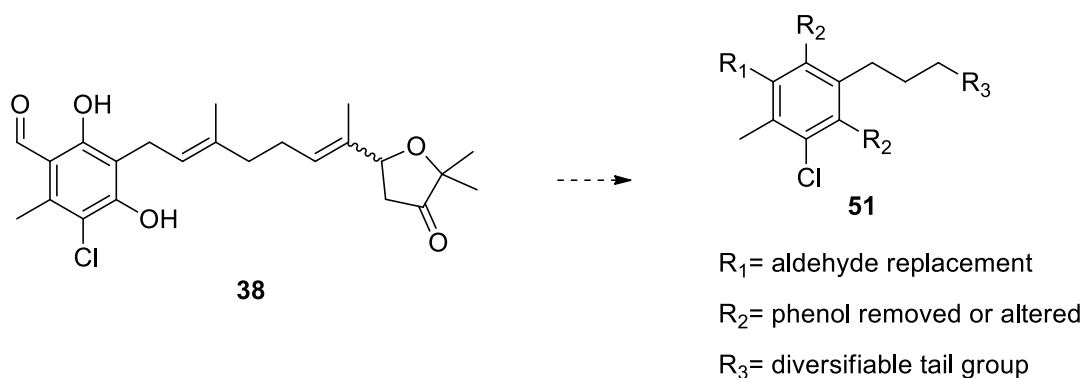
Figure 24 - Aims for developing ascofuranone towards a more drug-like analogue

Chapter 2 - Palladium cross-coupling and Fries-type rearrangement

The existing synthetic methods to synthesise ascofuranone (AF) and AF-analogues were limited. In addition, those methods reported had in large been tested by other chemists in the Ward group, prior to the commencement of this work, with little success. Several different methods were examined with the hope of developing an improved route to AF analogues. In particular, Suzuki coupling and Lewis acid catalysed Fries-type rearrangements were attempted as a means of installing the geranyl tail on to the aromatic headgroup. Also included in this chapter is a synthetic route to another AF analogue that had been designated as an interesting target.

Hexasubstituted arenes

When commencing this work there was no SAR around AF with which synthetic strategies could be directed and even when SAR was published,[212] it served only to reinforce the requirement of each of the six arene substituents. Polysubstituted aromatic compounds have long been a synthetic challenge[260] with the necessary presence of many functionalities decreasing the likelihood of obtaining the desired product. This is often due to steric or electronic incompatibility of these functionalities and the increased risk of side-reactions.

The functionalisation of aromatic rings is of critical importance in synthesis and nowhere more so than in medicinal chemistry where they are nearly ubiquitous across the field.[261] Naturally, by posing such a worthwhile challenge, the synthesis of polyfunctionalised arenes has been a massive field of chemical endeavor; these methods can be divided into classical approaches based on aromatic substitution of a given arene and benzannulation approaches that construct the aromatic backbone from acyclic precursors.

The main methods for decorating aromatic rings include: electrophilic aromatic substitution;[262] nucleophilic aromatic substitution;[263] benzyne reactivity;[264] coupling reactions catalyzed by transition metals;[265] and metalation-functionalisation reactions.[257]

Methods of polyfunctional benzannulation are innumerate, some examples of reactions classes include: [4 + 2] Diels-Alder cycloaddition,[266] particularly impressive when deployed to synthesise hexaarylbenzenes with six different aryl substituents;[267] the [3 + 2 + 1] Dotz reaction of Fisher carbene complexes;[268] alkyne-cyclobutenone [4 + 2] cyclisation;[269] [4 + 2] cycloaddition of metalacyclopentadienes and alkynes;[270] transition metal catalyzed [2 + 2 + 2] and [4 + 2] cycloadditions;[271,272] [4 + 2] benzannulation of o-alkynyl benzaldehyde and alkyne;[273–275] [3 + 3] cyclocondensation between bielectrophiles and binucleophiles;[276,277] 1,6-electrocyclization reaction;[278,279] [5 + 1] benzannulation strategy between alkenoyl keteneacetals and nitroalkane;[280,281] synthesis of acetophenones and methyl benzoates *via* the reaction of 1,3-dinitroalkanes with 2-ene-1,4- dione or 2-ene-4-oxo ester derivatives;[282] and [4 + 2] annulation strategy from the Baylis-Hillman reaction.[283]

Selection of the most appropriate synthetic method to synthesise AF analogues from the plethora of potential methods was a daunting prospect. Decisions were based primarily on literature precedent[284] as compound **51** (**Figure 25**) and similar compounds were available in good yield within three steps, and critically contained the correct substitution pattern.
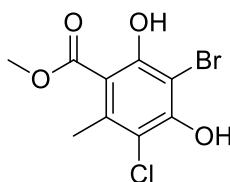
51

Figure 25 - Correctly hexasubtitued compound

In general, it was envisaged that the step-wise functionalisations of the ring would be more relevant as they potentially allow for greater generation of SAR data. Whereas, benzannulations, which would ideally install all functionalities at once, would not allow this.

In addition to this, the benzannulations referenced are often very limited in what functionalities can be used and prescriptive of their required position in the final ring. It is also common that these reactions have only be shown to work best with multiples of

the same functionality, which is unsuitable for AF-like synthesises. Additionally, the 1, 3 diphenol motif was poorly represented, with the 1, 4 and 1, 2 benzoquinones being much more widely available.[267] Of those examined the Diels-Alder cycloaddition did offer an interesting potential route to a hexasubstituted AF analogue or indeed for a total or formal synthesis of AF (**Scheme 9**). These sorts of annulations were unexplored in the course of this work and the methods employed: electrophilic aromatic substitution; palladium catalysed cross-coupling reactions; and metalation-functionalisation reactions are described at length where appropriate.
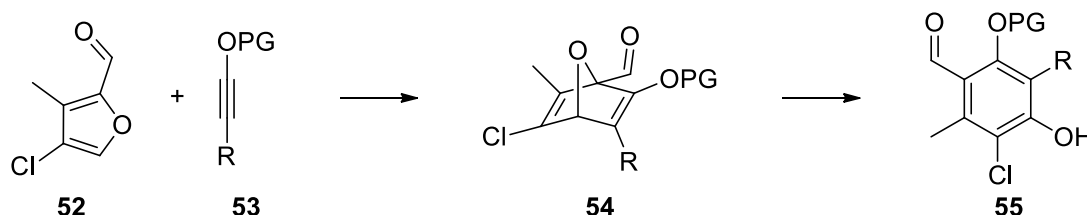
Scheme 9 - Potential formation of desired hexasubstituted arene *via* Diels-Alder chemistry

Suzuki coupling

When this work commenced, there was no published SAR around ascofuranone (AF) and as a result all molecules synthesised had to incorporate the geranyl chain so that headgroup changes could be compared directly to colletochlorin B (CCB). A useful general method to access CCB or AF analogues was not available, but compound **51** (**Figure 25**) was known from published work to be synthetically viable. With the aim to move away from the low yielding, unpredictable chemistry previously reported in the literature and toward more reliable reactions, the decision was taken to explore a palladium catalysed Suzuki coupling in an attempt to couple an easily synthesised aryl halide such as compound **51** with a boronate ester (**Scheme 10**).

The range of possible palladium couplings were considered: Negishi organozinc;[285] Kumada organomagnesium;[286] Hiyama organosilicon;[287] Stille organotin[288] or Suzuki organoboron[289] chemistry were all possible candidates for the sp^2-sp^3 C-C bond formation. However, as nucleophilic metalates were likely to attack the methyl ester, the Negishi and Kumada methods were inappropriate.

Of the remaining options, Stille and Suzuki have been most extensively explored and are the most versatile. Of these two, the Suzuki organoboron avoids the use of toxic tin which is undesirable in synthetic routes to compounds for biological assay.

A number of problems were foreseen including: that the possible η3-allylic palladium intermediate formed could isomerise the trans geranyl chain; the alkyl boronate would be unstable in the reaction; and the lone pair containing functionalities on the aryl headgroup could chelate and deactivate the palladium in solution. However, if these did develop into issues it was hoped they could be overcome by reaction optimisation.

$$\text{R--X} \quad \text{R'--B(R'')}_2 \quad \xrightarrow[\text{solvent}]{\text{Pd,}\ \text{base}} \quad \text{R--R'}$$

$$\textbf{56} \qquad\qquad \textbf{57} \qquad\qquad\qquad\qquad \textbf{58}$$

R/R' = alkyl, alkenyl, alkynyl, aryl
R'' = OH, alkyl, O-alkyl
X = OTf, I, Br, Cl
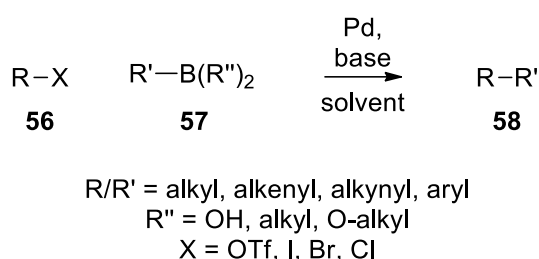
Scheme 10 – General Suzuki cross-coupling reaction

The Suzuki-Miyaura coupling reaction (**Scheme 10**) was first reported for aryl boronic acids with aryl halides and has since expanded to a vast range of C-C bond formations. The reaction now generally denotes palladium catalysed coupling of a C-BR$_n$ molecule with any molecule capable of oxidative addition to the palladium catalyst. The reaction can proceed with a large range of bases and solvents.[290] Typical bases include hydroxides, alkoxides, acetates, pivolates, carbonates, and flourides whilst some reaction is reported in nearly all organic solvents (polar/apolar, protic/aprotic) and additionally in water.

An assortment of organoboron compounds are used regularly (**Figure 26**): boronic acids[291] (**61**) are commonly used as they are cheap and a huge number of diverse compounds are available commercially, however these are the least stable and most prone to protodeborylation and oxidation; esters[292] (**60** and **64**) afford greater stability from enhanced oxygen lone-pair overlap with the vacant boron p-orbital than the boronic acid and enjoy wide commercial availability; 9-BBN borane[293] (**59**) was used initially because it was easily installed by hydroboration and remains a reagent of choice in alky couplings; trifluoroborates[294] (**62**), N-methyliminodiacetic (MIDA) boronates[295]

(**63**) and 1, 8 diaminonaphtyl boronamide[296] (**65**) all act as protecting groups allowing a boron moiety to proceed unaffected through various reaction conditions, this increases their synthetic utility and additionally allows for iterative Suzuki couplings;[297] the remaining charged boronates (**66** and **67**) benefit from requiring no addition of base, are crystalline solids to handle and can environmentally more benign, "greener".[298]

9-BBN
59

catechol boronic ester
60

boronic acid
61

organotrifluorborate
62

MIDA boranate
63

pinacol boronic ester
64

1, 8 diaminonaphtyl boronamide
65

triisopropyl borate
66

cyclictriol borate
67
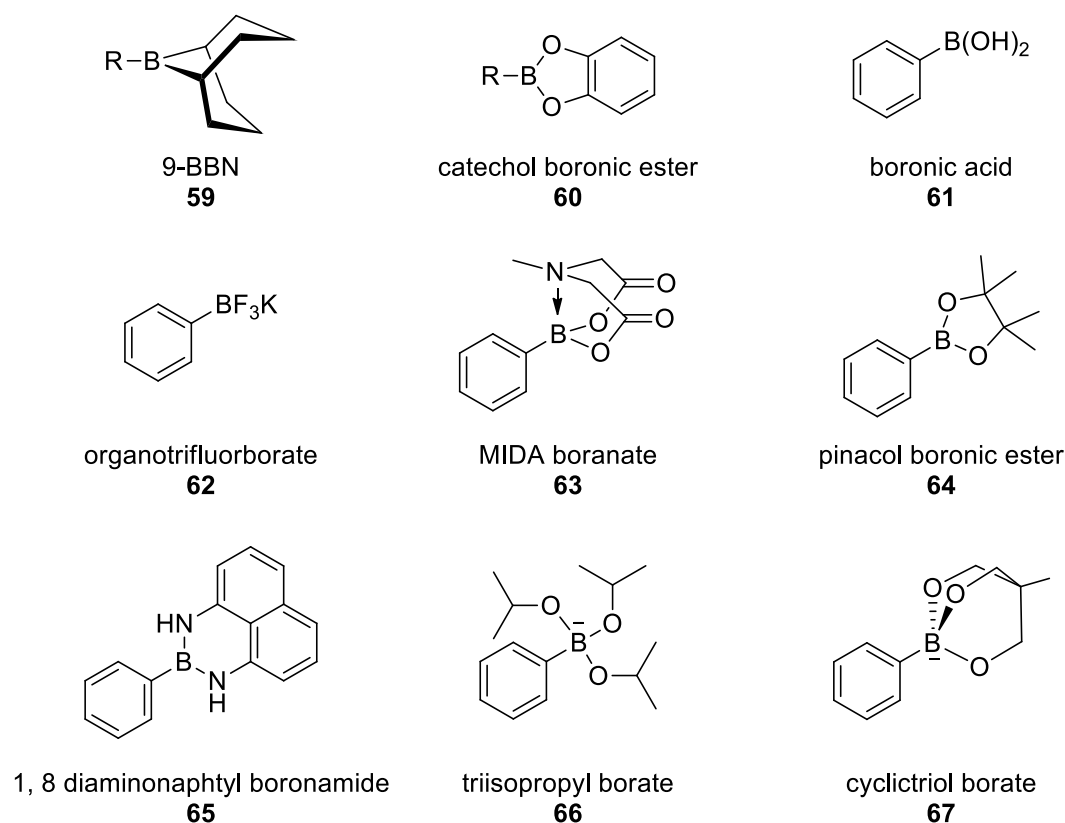
Figure 26 - Common organoboron reagents used in Suzuki reactions

When considering choice of palladium catalyst the list is enormous, from simple: Pd/C;[299] PdCl$_2$;[300] and Pd(OAc)$_2$[300] to elaborate preformed catalysts affording enhanced specific reactivities and/or low catalyst loadings: pincer ligands;[301] Buchwald ligands;[302] N-heterocyclic carbenes.[303] Palladium Suzuki catalysts is a large field in itself and will not be further reviewed here; the catalysts selected in this work were done so based on recommendations of reviews specific to the reactions undertaken and will be discussed, as appropriate, in line with the synthetic sequences undertaken.

The Suzuki-Miyaura coupling represents one of the most important synthetic transformations developed in the 20th century.[304] Palladium cross-coupling of alkenyboranes with alkenyl or aryl halides was performed by Suzuki, Miyaura and

Yamada and reported first in 1979.[289,290] Suzuki's work built upon the pioneering work of the previous 30 years in realising the catalytic potential of palladium: Hafner's development of the catalytic oxidation of ethylene in the Wacker process;[305,306] Heck's catalytic cross-coupling of alkenes with aryl halides;[307–313] Sonogashira's progression from stoichiometric copper to a catalytic Pd/Cu for coupling aryl halides and acetylenes;[314] Stille's coupling of organostannanes and aryl halides;[315,316] and Suzuki pursued the remaining element of the three previously identified by Negishi (zinc, boron, and tin).[304]

The Suzuki coupling has since outstripped all other palladium reactions in terms of articles published.[304] Several factors that have contributed to this success include: 1) easily handled and usually air- and moisture-stable organoboron starting materials; 2) mild and convenient reaction conditions; and 3) the facile removal of less-toxic inorganic byproducts. These aspects make the Suzuki–Miyaura coupling reaction especially useful for industrial applications and this compounding factor has acted to further accelerate research in this field.[304]

Despite its discovery in the late 1970s a definitive elucidation of the mechanism of the Suzuki-Miyaura coupling reaction was not reported until the 2010s and even this was only under a certain set of common conditions and reagents.[317] There were several mechanisms proposed (A-D, **Scheme 11**). All consisted of oxidative addition of the aryl halide onto the palladium, transmetalation from boron to palladium, endergonic rearrangement of the of *trans* diorganopalladium (**72**) to the *cis* isomer (**73**), and reductive elimination (**Scheme 11**).

$$[Pd(Ar)(L)_2X] + RO^- \rightleftharpoons [Pd(Ar)(L)_2(RO)] + X^-$$

68   **69**

transmetallation

Ar'B(OH)$_2$ or Ar'B(OH)$_2$(OR)$^-$ Ar'B(OH)$_2$ or Ar'B(OH)$_2$(OR)$^-$

A   B   C   D

70   **71**   **70**   **71**

$$\underset{L}{\overset{L}{Ar-Pd-Ar'}}$$

72

$$\underset{Ar}{\overset{L}{L-Pd-Ar'}}$$

reductive
elimination

$$\longrightarrow \quad Ar-Ar' \;+\; [Pd^0(L)_2]$$

74   **75**

73
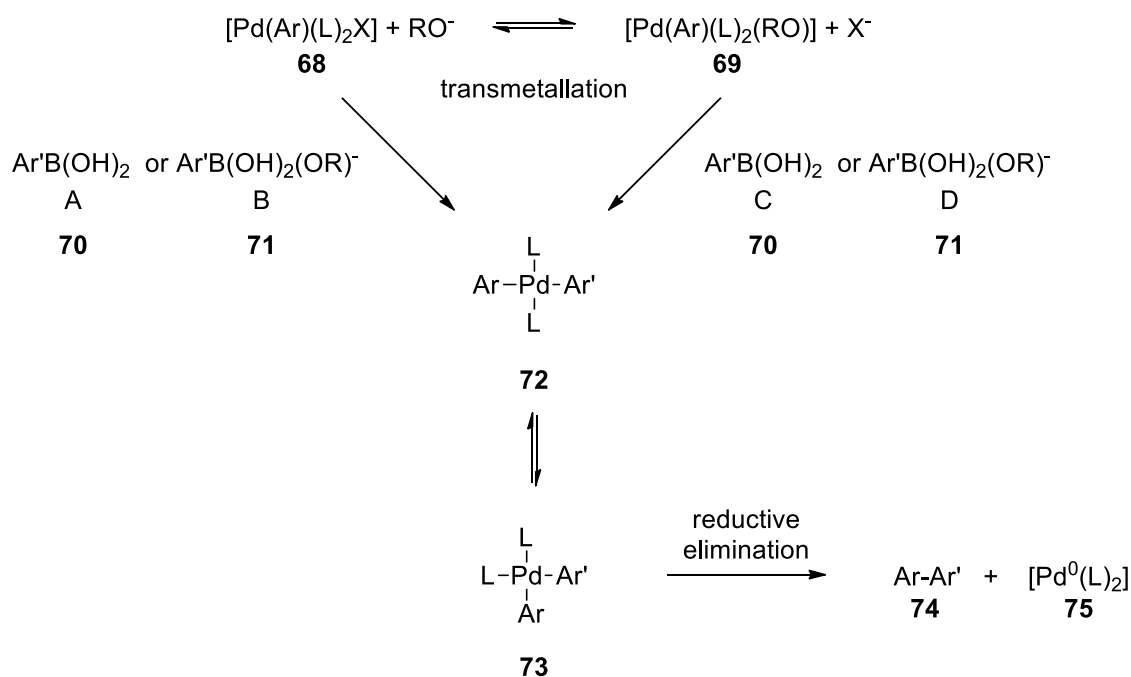
Scheme 11 – Proposed role of the base in Suzuki reaction[317] (R= H, alkyl)

The differences between the mechanisms arise from the role of the base in the catalytic cycle. Suzuki had observed in 1981 that even cross-couplings undergoing no deprotonation required a 'base', and in addition that not all bases were adequate with Lewis bases such as trialkylamines proving entirely unproductive[318] (although that has not remained the case).[319] Suzuki initially proposed the boronate pathway B[318] involving the reaction of alkoxides RO (R=Me, Et) with arylboronic acids to generate anionic arylborates Ar'B(OH)$_2$(OR)$^-$ (**71**) thought to be more active than Ar'B(OH)$_2$ (**70**) in the transmetalation with the complexes [Pd(Ar)(L)$_2$X] (**68**) generated in the oxidative addition of ArX to [Pd^0(L)$_n$] (**75**). Subsequently Suzuki proposed the oxopalladium of pathways D and C as a key intermediate based off the observation that reactions using only the preformed [Pd(Ar)(L)$_2$(OR)] (**69**) with a Ar'B(OH)$_2$ (**70**) reagent and in the absence of base proceeded in good yields.[320] Most published work, be it experimental[321,322] or computational,[323–325] demonstrated that pathway B, C or a combination was the most probable reaction mechanism. All mechanisms invariably arrived at the *trans*-[Pd(Ar)-(Ar')(L)$_2$] (**72**) species.

An excellent set of experiments by Amatore and Jutand[326–328] employed electrochemistry and NMR spectroscopy (^{11}B and ^{31}P) to measure in real-time the palladium and boron species present throughout the reaction and this allowed the

elucidation of the kinetics of simple Suzuki couplings. Through standard investigatory methods for probing reactions kinetics they increased and decreased amounts of different reagents and measured the rate change for different steps in the reaction, the results obtained were interesting. They found that both hydroxide and fluoride ions have three antagonistic functions (**Scheme 12**): 1) formation of the reactive *trans*-[Pd(Ar)(L)$_2$(OH)] (**69**) in the rds transmetallation with Ar'B(OH)$_2$ (**70**), the rate of which is controlled by the ratio: [OH]/[Ar'B(OH)$_2$]; 2) catalysis of the reductive elimination from trans-[Pd(Ar)(Ar')(L)$_2$]; and 3) formation of unreactive Ar'B(OH)$_3^-$ (**71**). This evidence clearly established pathway C (**Scheme 11**) as the productive mechanism even identifying the proposed active boronate (**71**) as an inactive reservoir of both boron compound and hydroxide. Unprecedented in the Suzuki reaction was the observation of a proposed pentacoordinate species (**80**) (**Scheme 12**) bypassing the slow classical reductive elimination requiring the endergonic *trans*/*cis* isomerisation. Finally, the cation associated with the base was found to retard the reaction based on its degree of conjugation to the oxopalladium complex (**79**), with larger cations affording greater retardation.

Pd^0L_3

76

L = PPh$_3$

$$\left[\begin{array}{c} Ar \\ Ar'-Pd^{\cdots L} \\ OH \quad L \end{array} \right]^{-}$$

80

ArAr'

74

+L $\updownarrow$ -L

Pd^0L_2

75

ArX

77

OH$^-$

L
|
Ar−Pd-Ar'
|
L

72

L
|
Ar−Pd-X
|
L

68

B(OH)$_3$

79

Ar'B(OH)$_2$

70

L
|
Ar−Pd-OH
|
L

69

m$^+$ OH$^-$

X$^-$ m = Na, Cs, K

OH$^-$ $\updownarrow$

m$^+$ $\updownarrow$

Ar'B(OH)$_3^-$

78

unreactive

L
|
Ar−Pd-OH
|
L m$^+$

76
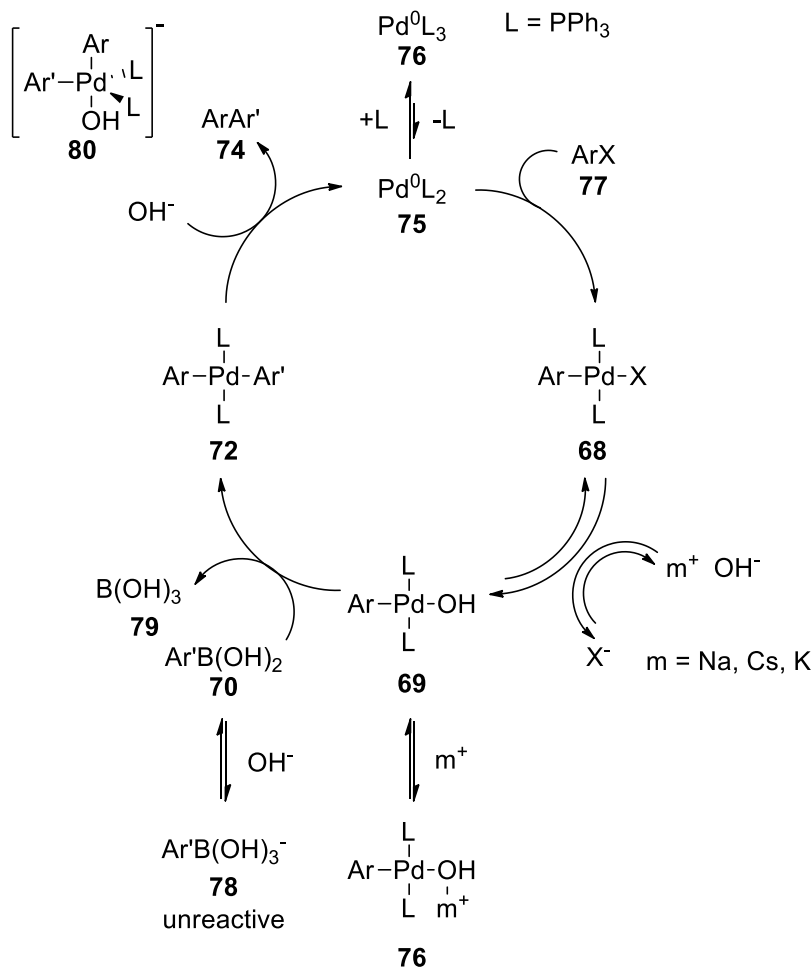
Scheme 12 – Mechanism accounting for role of the 'base' as proposed by Amatore[317]

The discussion thus far has been of an assumed homogeneous palladium catalyst and it has been suggested that catalysis occurred solely from leaching of low nuclearity palladium from metal particles suspended in solution.[329–334] However, strong evidence exists that Suzuki couplings occur at the five- and six-coordinate defect sites on the edge of palladium nanoparticles[335] and this was demonstrated adeptly by Fairlamb and Wilson using X-ray absorption spectroscopy (XAS). Polyvinylpyrrolidone stabilised palladium nanoparticles (PVP PdNP) of definite sizes below 5 nm in diameter were synthesised and their activity in Suzuki couplings investigated. The PdNP size and surface was monitored continuously by XAS and it was found that the catalytic rate associated with these < 5 nm particles was directly proportional to the number of low coordinate sites exposed. It was postulated that this could be a factor in the regular observation that highly dilute, 'homeopathic', quantities of palladium give higher reaction rates.[336] These highly dilute palladium suspensions could be more likely to exist in these active <

5 nm PdNPs and increased palladium loading would result only in an increased portion of the palladium being trapped in the inactive high coordinated bulk. Whilst this could have been assumed before, with this evidence its likelihood is increased. This work attempted to further preclude any activity arising from leached palladium atoms by adding a palladium binding silica network with pores small enough to exclude the PDNPs but not the solubilised palladium. They found only a small decrease in rate which was attributed to the adhering of the PdNPs to the exterior of the silica particles, indicating that the PdNPs are the drivers of catalysis. The authors stress that these are not generic results and alternate mechanisms are certainly taking place with varied solvents, temperatures, non PVP PdNPs etc. However, this work and others[337–341] indicate that both heterogeneous and homogeneous catalysis are possible in Suzuki reactions not involving preformed, homogeneous palladium catalysts such as N-heterocyclic carbene bound palladium; it suggests that a more complex reaction scheme is required to properly envisage the reaction (**Scheme 13**). Distinctly lacking from discourse of heterogeneous Suzuki reaction mechanisms was the requirement and role of the base and it appears this requires further elucidation.
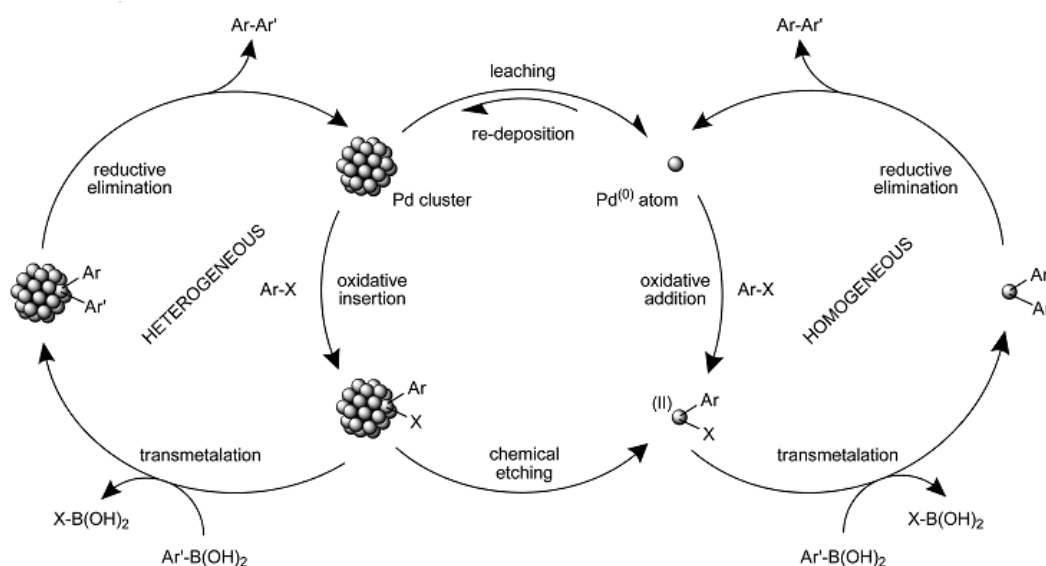
Scheme 13 - Proposed mechanism for the PdNP-catalyzed Suzuki cross-coupling involving both homogeneous and heterogeneous pathways.[342] Note: though only re-deposition is displayed in the scheme, re-clustering to form (new) smaller particles and/or formation of palladium black are also feasible but not displayed.

The scope of bond formations accessible by Suzuki reactions is truly staggering (only a hand-full of the multitudinous references possible will be given): any combination of alkyl, alkenyl, alkynyl, or aryl coupling;[343–347] synthesis of vinylic sulfides;[348] carbonylative coupling;[349] decarboxylative coupling reactions;[350] and regioselective and stereoselective bond formation[351] and these reactions can be utilised in: cascade reactions;[352] aqueous, aerobic, ligand free conditions;[353] C-H activation chemistry;[354] masked as stable N-methyliminodiacetic acid boronate and used in iterative reactions;[355] and amenable to industrially relevant processes like physycally[356] or magnetically[357] recoverable-nanoparticle-supported palladium catalysts. This barely touches on the massive field of Suzuki chemistry however fortunately included in this field is allylic-aryl cross-coupling which was the desired bond formation in the proposed synthesis of ascofuranone analogues.

Literature precedent existed for Suzuki mediated sp^2-sp^3 C-C bond formation at the allylic position of prenyl, crotyl and allyl boronates.[358] The optimum conditions were reported as Pd(dppf)Cl$_2$ in dioxane: water with K$_2$CO$_3$ as a base. This research had also concluded that potassium trifluoroborates, popularised by Molander,[359] gave particularly good yields, but simple pinacol boronate esters also performed well. The pinacol boronate ester was found to be more readily available and was therefore utilised.
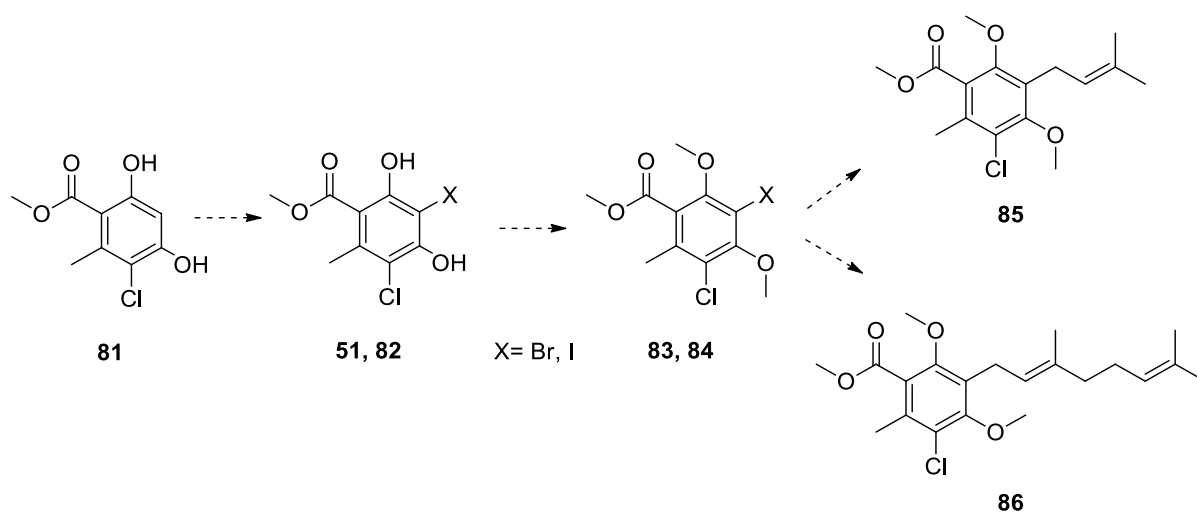
Target compounds

An interesting hydroxamic acid target, compound **87** (**Figure 27**), was generated from the combination of the CCB and SHAM motifs. This looked particularly interesting as the replacement of the aldehyde would test whether it was possible to remove this metabolically unattractive functionality. It would also serve as a target in the exploration of palladium chemistry towards AF-like compounds and could potentially have reasonable TAO activity given the high ligand efficiency of SHAM.

87
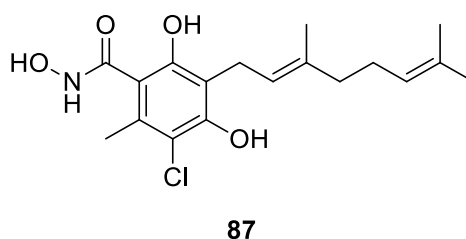
Figure 27- Hydroxamic acid target compound

This route also allows for the replacement of the geranyl chain in compound **86** with the synthetically simpler shorter prenyl chain compound **85** (**Scheme 14**). Isomerisation was a risk and was thought to have been observed using palladium for installing the geranyl in the Ward lab. It was hoped that a compound with this shorter chain would maintain sufficiently high potency to enable exploration of headgroup SAR in the event that olefin isomerisation could not be controlled for the geranyl chain.

Headgroup formation

88   **81**
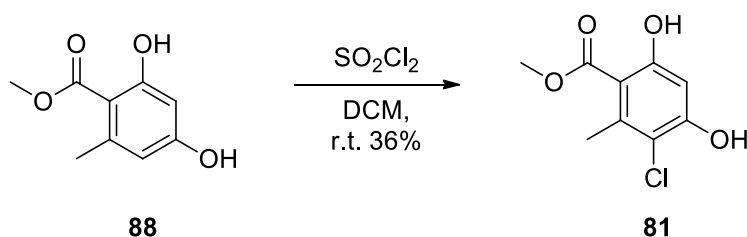
Scheme 15 - Chlorination reaction

The hexa-substituted headgroup compounds **51** and **82** were synthesised *via* two different routes.

Compound **82** was synthesized following an available procedure[255] (**Scheme 16**) from methyl 2,4-dihydroxy-6-methylbenzoate (**88**). Chlorination of compound **35** with sulfuryl chloride was reported with 75% yield. This yield was not obtained in any of the

various test scale and larger reactions attempted. A mixture of mono-chlorinated and di-chlorinated compounds **81**, **89** and **90** (**Figure 28**) was obtained.

These compounds were poorly soluble, poorly purified by recrystallisation and ultimately numerous silica column purifications were necessary to prepare the clean product. This difficult purification likely resulted in decreased isolated yields however even in ^{1}H NMR spectra of crude reaction mixture the observed proportion of methyl 3-chloro-4,6-dihydroxy-2-methylbenzoate (**81**) never reached that reported.

The product (**81**) was characterised in ^{1}H NMR spectroscopy by the disappearance of an aromatic CH and the elimination of 1, 3 proton coupling across the ring. ^{13}C NMR spectroscopy and two-dimensional HMBC spectroscopy allowed for accurate assignment of the chlorine to the C-5 position by the absence of coupling from the tolyl 6-CH$_3$.

88   **81**   **89**   **90**
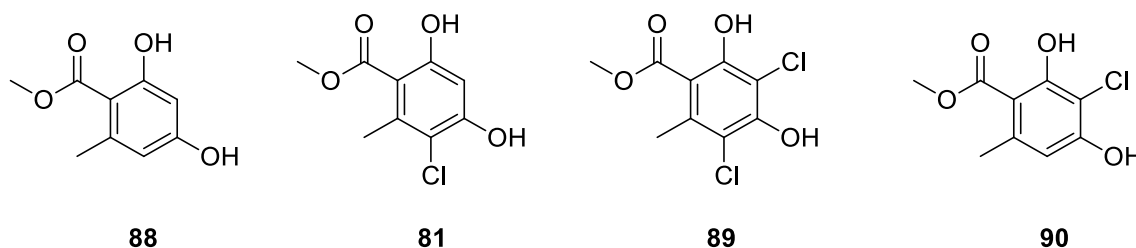
Figure 28 - Mixture of compounds obtained from chlorination

The chlorinated product (**81**) was then iodinated in a straightforward manner with benzyltrimethylammonium dichloroiodate (BTMA-ICl$_2$) (**Scheme 16**). This was evident by ^{1}H NMR spectroscopy with the disappearance of the only aromatic CH signal.

81   **82**   75
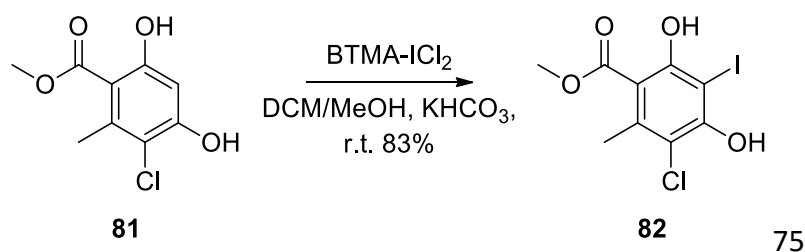
Scheme 16 - Iodination

The equivalent bromo headgroup was synthesised by known methods.[256] The cyclic ±-methyl 2-methyl-4,6-dioxocyclohexanecarboxylate (**42**) was prepared from acyclic

reagents (**40** and **41**) in a single step (**Scheme 17**). The product was identifiable in ^{1}H NMR spectroscopy by the 6-CH$_3$ doublet, the 1-OCH$_3$ methyl ester singlet and the vinylic 3-CH and by observation of the accurate mass of the molecular ion using HRMS. It also converted readily to the desired product compound **43** in the following bromination step (**Scheme 18**), which was fully characterised. The ^{1}H NMR spectrum exhibits only a *trans* proton-proton coupling for the two stereocentres 1-CH and 6-CH formed in the reaction and indicates the formation of a racemic mixture of compound **42**.
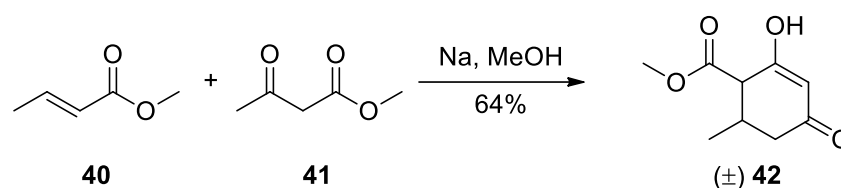
Scheme 17 - Formation of cyclic headgroup precursor

Compound **42** was brominated and oxidised in a single step using molecular bromine. A mixture of the mono and dibromo products was obtained but fortunately, in contrast to the chlorination attempted previously, formation of the desired 3-bromo product was favoured, affording a 69% yield. Chlorination of compound **43** with sulfuryl chloride occurred in excellent yield 98% (**Scheme 18**). Both products (**43** and **51**) were easily observable by ^{1}H NMR spectroscopy. Compound **43** was identified by the substantial simplification of the ^{1}H NMR spectrum in comparison to the staring material and by the appearance of distinct aryl and tolyl protons that couple to one another *via* two-dimensional HMBC spectroscopy. The chlorination was then observable by the disappearance of that aryl 5-CH singlet signal in the ^{1}H NMR spectrum of compound **28**.
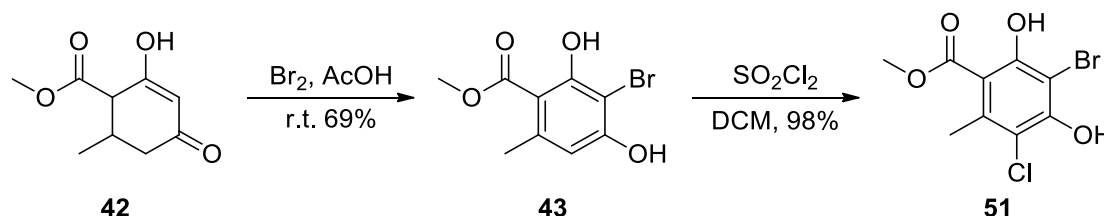
Scheme 18 - Aromatisation and decoration to the hexa-substituted headgroup

A similar halogenation and oxidation was attempted with molecular iodine (**Scheme 19**). However, this only partially reacted and the only observed product was the non-halogenated, oxidised ring (**88**). This was undesired but somewhat predictable as iodine

is a known oxidising agent. As there were already several known two-step methods for synthesising this ring and this was given no further attention.
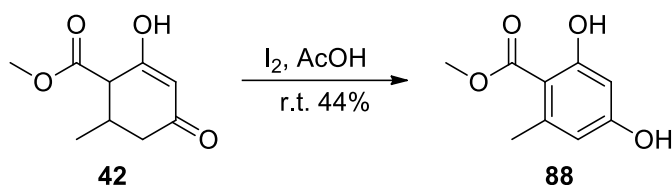
Scheme 19 - Attempted iodination reaction

It was expected that the phenols would interfere with the palladium coupling reactions, so the hexa-substituted headgroup compounds (**51** and **82**), were methylated with dimethyl sulfate (>90%) to give compounds **83** and **84** (**Scheme 20**) with two new distinct singlets for 3H observable in their ^{1}H NMR spectra. The reactivities of the free phenols were also assessed in subsequent palladium couplings to test the necessity of the protection step.
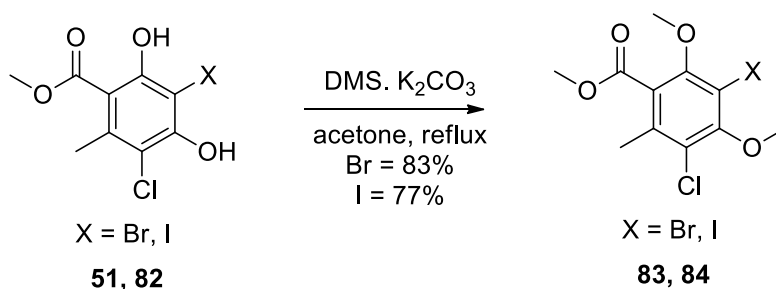
Scheme 20 - Dimethyl protection of phenols

Palladium catalysed Suzuki couplings

Coupling of compound **91** (**Figure 29**) utilising Pd(dppf)Cl$_2$ was reported in literature and had been previously employed in house. Encouragingly the protected iodo compound **84** coupled successfully to 3-methyl-2-butenylboronic acid pinacol ester (**92**) to give compound **85** in a 49% yield (**Scheme 21**). Although the yields were still not particularly high, they compared very favourably with those previously published for C-C bond formation between headgroup and linker (< 10%).
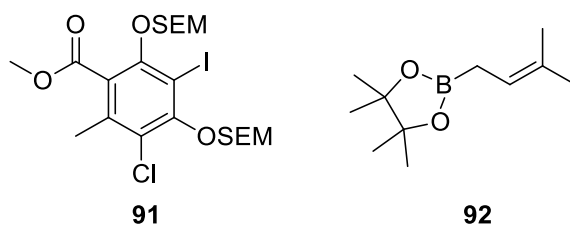
The reaction of compound **84** with 3-methyl-2-butenylboronic acid pinacol ester (**92**) using the established method formed two major products, the desired compound **85** and the deiodinated compound **98**. This dehalogenated side product is thought to result from beta-hydride elimination of the prenyl group as the allene **95** or diene **96** (**Scheme 22**), which would form the palladium hydride (**97**) that could reductively eliminate with the palladium bound aryl group to produce the deiodinated compound observed. Compound **85** was characterised only by ^{1}H NMR spectroscopy with the addition of the signals of the prenyl chain to those of the staring material (**84**). The small quantity of the product (**85**) produced was subsequently consumed in attempted deprotections of the methyl ethers. Any further resynthesis of compound **85** was deemed unproductive given the eventual failures in both deprotection and palladium coupling.
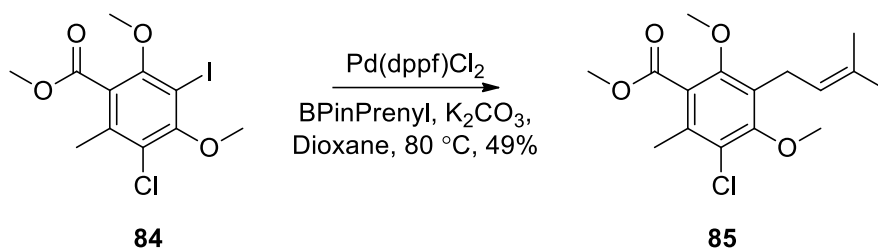
Scheme 21 - Palladium mediated prenyl installation
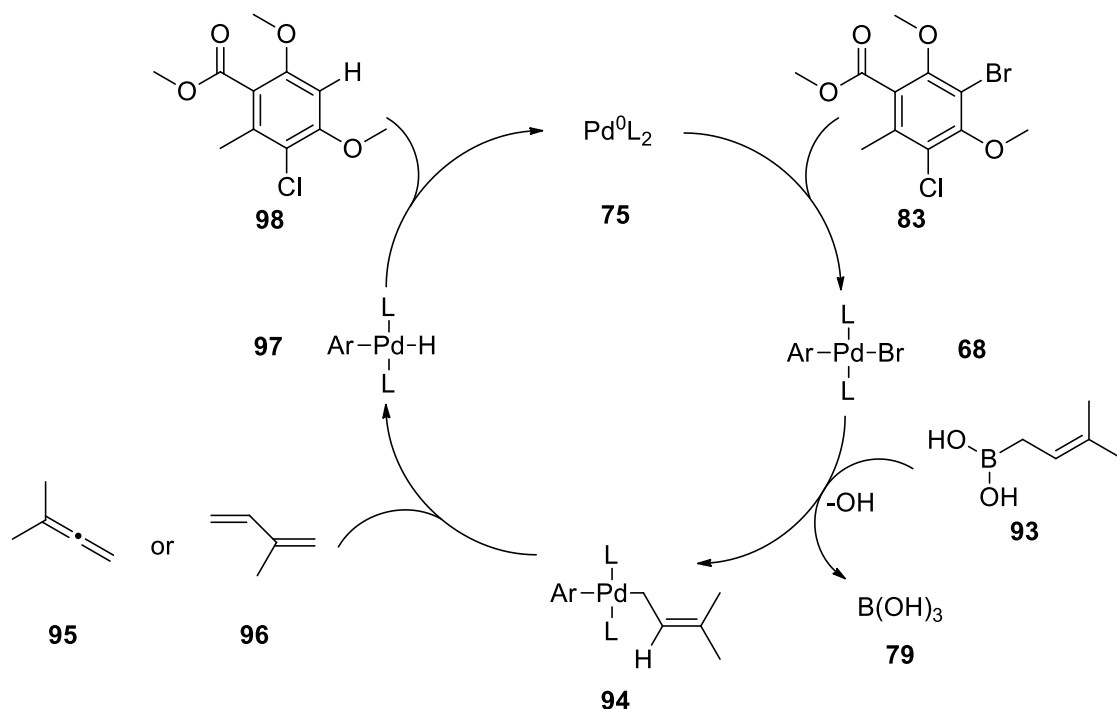
Scheme 22 - Proposed dehalogenation mechanism

Unfortunately, further Pd reactions proved entirely unsuccessful. Coupling of the bromo compounds **83** and **99** was unproductive using any of the applied conditions (**Table 3**) (all conditions were repeated several times and at increased temperatures), and the yield from the first attempted reaction with the iodo compound (**84**) could not be improved. Several catalysts were trialed in attempt to couple the free phenolic compounds **43**, **82** and **51** but this was also unsuccessful. Presumably the conditions for the successful Pd(dppf)Cl$_2$ reaction afford either an enhanced relative rate of reductive elimination over β-hydride elimination and/or sterically deter the agostic overlap required to form the side product. The free phenols seemingly interfered with the Pd couplings and even the Buchwald type ligand,[302] which donates substantial electron density to palladium and often allows previously unreactive substrates to undergo oxidative addition, was unable to activate these compounds sufficiently to enable successful reaction. Although this is by no means a thorough investigation of Pd catalysts and ligands, limited time was committed to further exploration due to the low chance of success.

R$_1$= H, Me
R$_2$= H, Cl
X= Br, I
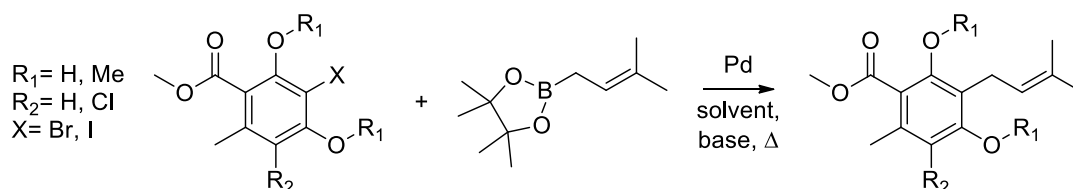
Scheme 23 – General reaction scheme for palladium couplings

Table 2 – Attempted palladium reactions with unprotected phenols
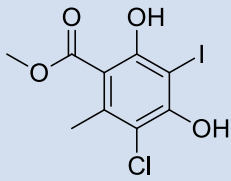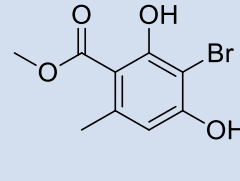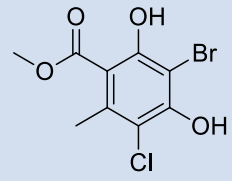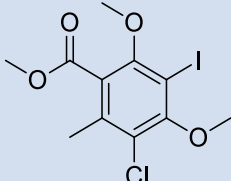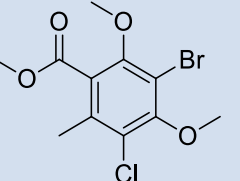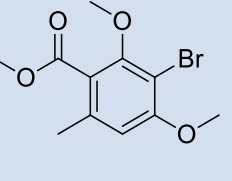
Conditions	82	43	51
Pd(dppf)Cl$_2$, dioxane, K$_2$CO$_3$, prenyl boronate, 100 °C	No reaction	No reaction	No reaction
Pd(acac)$_2$, dioxane, K$_2$CO$_3$, prenyl boronate, 100 °C	No reaction	No reaction	No reaction
Pd(OAc)$_2$, Ruphos toluene/water, K$_2$CO$_3$, prenyl boronate, 100 °C	No reaction	No reaction	No reaction

Table 3 - Attempted palladium reactions with methyl protected phenols

Conditions	84	83	99
PddppfCl$_2$, dioxane, K$_2$CO$_3$, prenyl boronate, 100 °C	49% coupled product	Little reaction Major product dehalogenated	No reaction
Pd(dba)$_3$, dioxane, K$_2$CO$_3$, prenyl boronate, 100 °C	< 5% coupled Major product dehalogenated arene	No reaction	No reaction
Pd(acac)$_2$, dioxane, K$_2$CO$_3$, prenyl boronate, 100 °C	< 5% coupled Major product dehalogenated arene	No reaction	No reaction

Pd(OAc)₂, XPhos Toluene/water, Cs₂CO₃, prenyl boronate, 100 °C	Major product dehalogenated arene	Little reaction Major product dehalogenated arene	No reaction
Pd(OAc)₂, RuPhos Toluene/water, K₃PO₄, prenyl boronate, 100 °C	Major product dehalogenated arene	No reaction	No reaction

Several deprotections of the bis methylated compound **85** were attempted (**Scheme 24**) with BBr$_3$ in DCM at 0 °C or NaSMe heated in both DMF and DMPU but no reaction attempted afforded the product. It was hypothesised that with the prenyl and *ortho*-phenol in close proximity, there was a likelihood of cyclisation, as in compound **101**, in the presence of acid, base or potentially high temperatures, resulting in an array of side products.
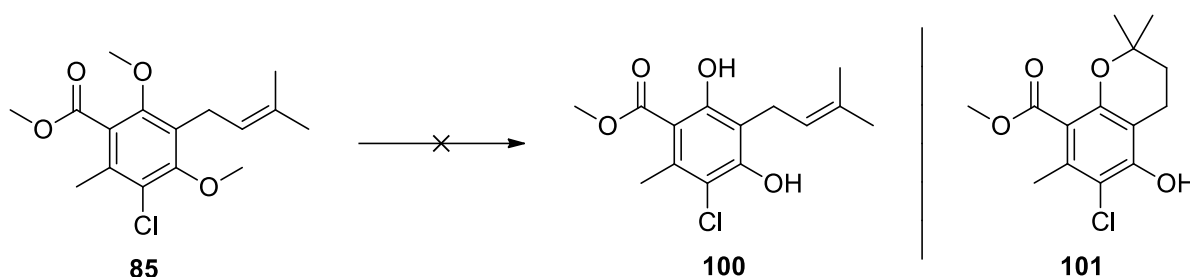
Scheme 24 - Deprotection of methyl ethers unsuccessful

This exploration of Suzuki couplings for installation of the geranyl linker had therefore regrettably come to several impasses:

1) The stereochemistry of the *trans* geranyl linker was an isomerisation risk and only one of the coupling conditions trialed gave any meaningful product formation, leaving no opportunity for improvement.

2) Most reactions proceeded only when the iodo headgroup was used and the major product was invariably the undesired dehalogenated material.

3) The coupled product that was formed could not be deprotected to compound **100**, with the various reactions attempted showing only decomposition.

At this point, further exploration of Suzuki couplings would have required the repeated synthesis of the iodo headgroup (**82**). In light of the number of serious hindering issues this was deemed a poor use of time and the route was abandoned.

Lewis-acid mediated rearrangement
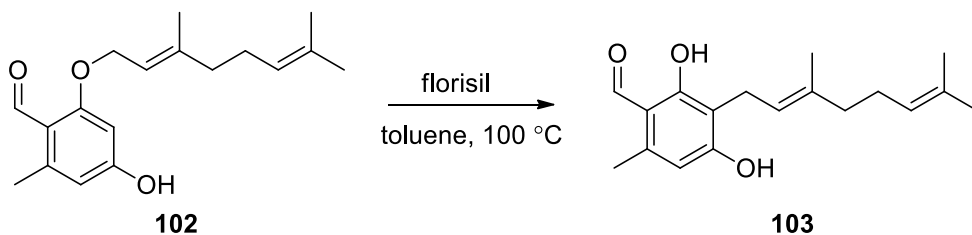
Scheme 25- Geranyl rearrangement

In addition to exploring the Suzuki coupling, there were ongoing investigations elsewhere in the Ward lab into the use of the Fries-type rearrangement[360] to form the C-C bond between linker and headgroup. Of all the conditions screened, it was found that only florisil (MgO:XSiO2•H2O) effected the transformation and only in 20-30% yield (**Scheme 25**).

The clay catalysed [1, 3] rearrangement of O-prenylated ethers was first discovered by Dauben in 1990.[361] The reaction was developed to overcome difficulties faced with the Claisen rearrangement,[362] which was also initially considered in this synthesis. The [3, 3] sigmatropic Claisen rearrangement demands the S_n2' addition of the prenyl equivalent, in this instance geranyl bromide (**104**), to arrive at the product with the desired connectivity following a Claisen rearrangement (**Scheme 26**). Selective formation of compound **105** was deemed unnecessarily challenging and therefore not explored. Interestingly, evolution has developed an enzyme that can selectively O-prenylate in the S_n2' manner displayed in compound **105** and this then undergoes a [3, 3] Claisen rearrangement to afford the appropriately *o*-prenylated phenol.[363]
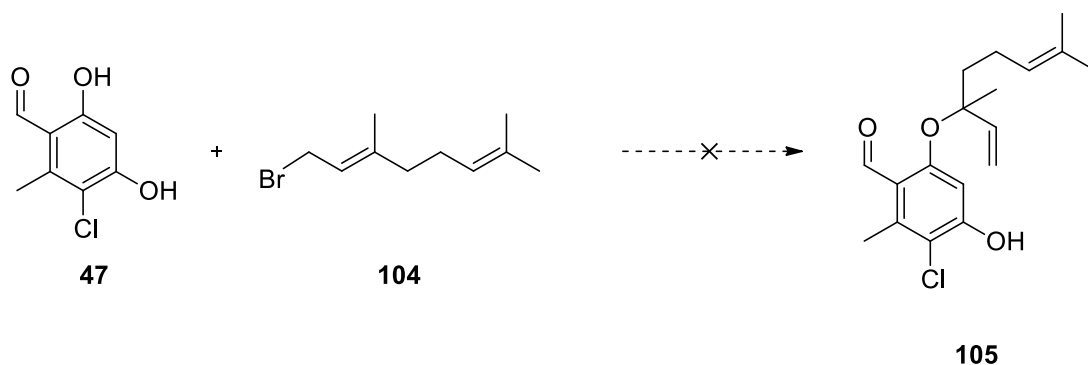
Scheme 26 - Improbable Sn₂' addition of geranyl bromide required to allow Claisen rearrangement

Subsequent publications around the clay catalysed [1, 3] shift have further explored the range of Lewis acids applicable and utilised the reaction for the synthesis of various natural products.[360,364,365] The mechanism is thought to involve the destabilisation of the C-O etheric bond (**107**) with the formation of an allylic carbocation and oxyanionic phenol (**108**). This carbocation then is irreversibly incorporated into the aryl ring *via* electrophilic aromatic substitution (**109**). Dauben rationalised that there must be an intermolecular mechanism available in addition to the likely intramolecular reaction (**Scheme 27**) because of the observation of multiply prenylated products. This was later explicitly established *via* crossover experiments.[364]
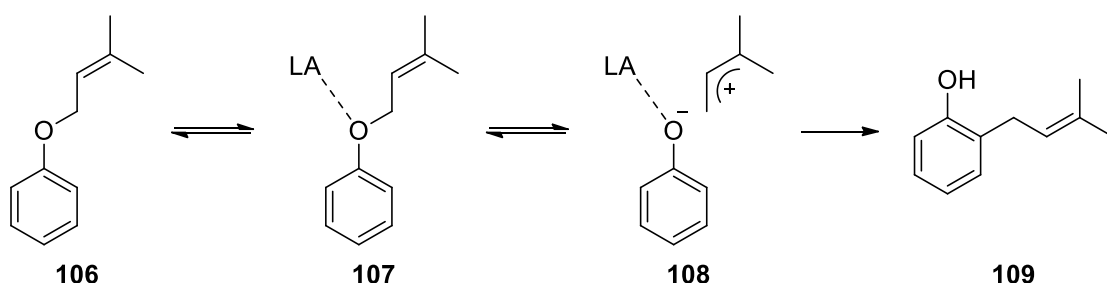
Scheme 27 – Proposed mechanism of [1, 3] shift

This Lewis catalysed rearrangement from a phenol in a [1, 3] manner is very similar to work first published by Fries early in the 20th century.[366,367] The Fries rearrangement entails the creation of *o*-phenol phenyl ketones from phenyl esters (**Scheme 28**) and was later reported by photochemical[368] and anionic[369] means. The Fries rearrangement itself was an extension of Friedel-Crafts[370] chemistry developed in the late 19th century which similarly used a Lewis acid to create an acylium cationic reactive intermediate that is electrophilically substituted onto an aryl ring.
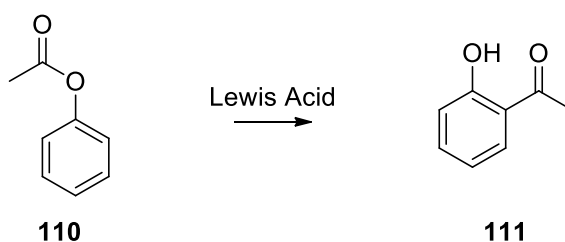
Scheme 28 – Freis rearrangement

Although the yield obtained for linker installation was again poor, 20-30%, it remained the most viable route to the hydroxamic acid, compound **87** (**Figure 30**). Fries-type rearrangement was explored in attempt to synthesise the chloro and deschloro compounds **87** and **112** (**Figure 30**). Although the most efficient route to produce **87** and **112** would require that chlorine was introduced at the final step, it was deemed necessary to install the chlorine first. This was in order to avoid complications arising from having the acid and electrophile sensitive geranyl chain present at this juncture.
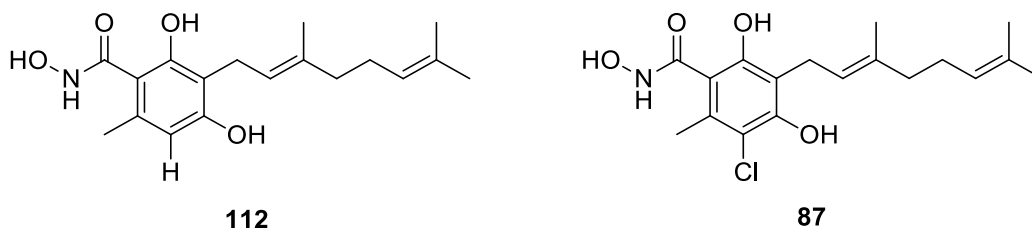
Figure 30 - Target compounds

Para-phenol reactivity and protection

It was hoped that the 4-geranyl ether (**113**) could rearrange to the desired product (**114**) as this is the more reactive of the phenols and alkylation preferentially occurs here (**Scheme 29**). This reactivity arises because the 2-OH is the less acidic alcohol due to the intramolecular hydrogen bond to the salicylaldehyde moiety. Interestingly, the H-bond holds the proton in plane with the aldehyde in a particularly de-shielded environment resulting in a characteristically high shift in proton NMR at ~12 ppm in comparison to unbound phenols at ~5.5 ppm (**Figure 31**).
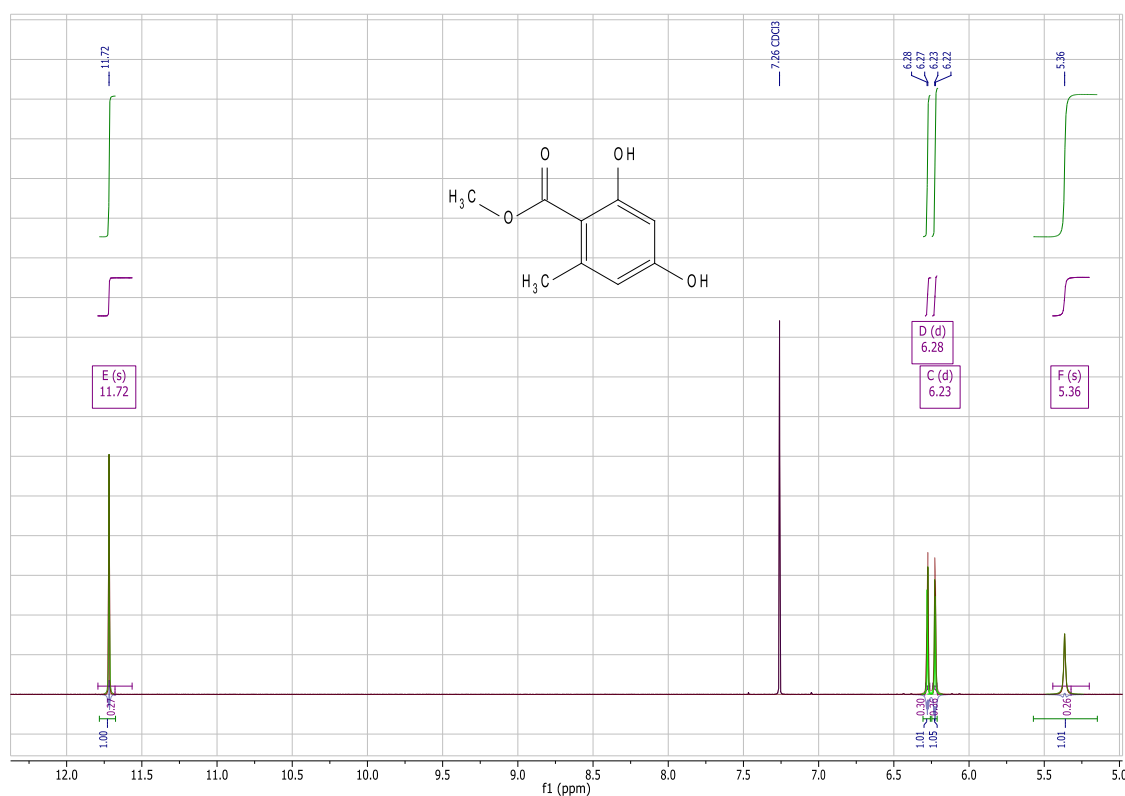
Figure 31 - Characteristic downfield *ortho*-phenol signal

The 4-O-geranyl compound **57** was available from other investigations within the group, and its reactivity was assessed. Unfortunately, even under forcing temperatures no rearrangement was observed (**Scheme 29**). This was not entirely unexpected as previous attempts to deprotect the bis-protected phenol would often readily deprotect the salicylic phenolic ether but leave the *para*-phenolic ether untouched.
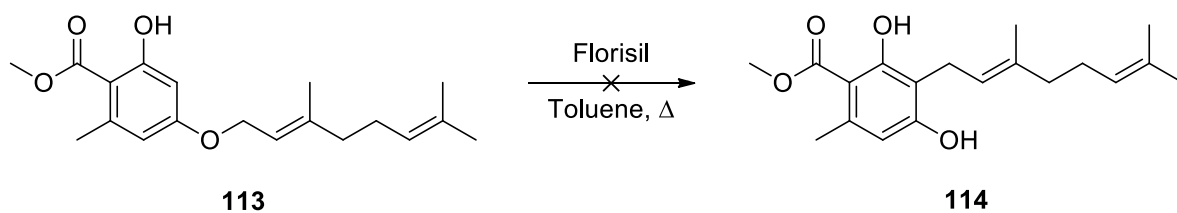
Scheme 29 - Unsuccessful *para*-phenol rearrangement

Rearrangement from the 2-OH had been previously shown in the Ward lab to afford the desired product. Presumably the lone-pair of the salicylaldehyde chelates the Lewis acidic Mg^{2+} ion of florisil (**Figure 32**) to destabilise the etheric O-C bond by polarising it. This is similar to the specific *ortho* directed deprotections of salicylaldehyde moiety with $AlCl_3$ reported in literature[371] and has been utilised previously in syntheses.[371,372]

115
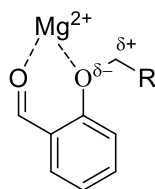
Only a small quantity of the bis phenol methyl ester, compound **88**, was available. With hindsight it should have been assumed that reaction at this crowded and complex head group would be non-trivial and time should have been dedicated to synthesising more starting material to enable more extensive exploration. However, although the subsequent chlorination of this bis phenol gave low yields of the desired regioisomer, a sufficient quantity was produced to attempt the following synthetic steps on small scale and the decision was taken to proceed.

The 4-OH was protected to force geranyl ether formation at the 2-OH position. It was decided that a simple acyl protecting group would be utilised (**Scheme 30**) as this could be installed easily and removal should be facile under a variety of conditions. Protection of the 4-OH of the des-chloro compound **88**, proceeded with good selectivity and very good yield, whilst that of the chloro compound **81**, was less selective and gave a lower yield. Both products were easily observed by ^{1}H NMR spectroscopy with the disappearance of a 4-OH phenolic proton and appearance of a singlet CH_3 signal.

AcCl, NEt$_3$
DCM, 0 °C → r.t.
H = 81%
Cl = 48%

X = H, Cl
88, 81

X = H, Cl
116, 117
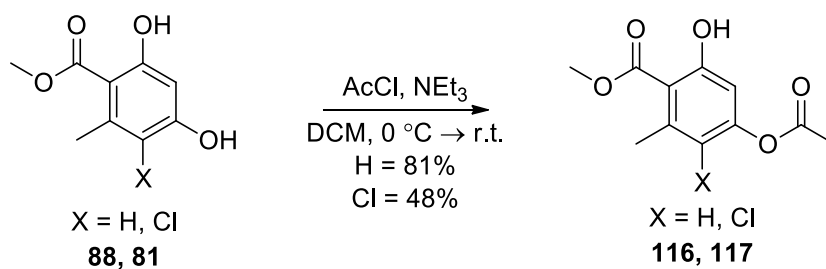
Scheme 30 - Acylation

Although the 2-OH geranyl ether formation (**Scheme 31**) gave a mixture of side products, most notably the bis geranyl ether (**122**) and deacylated geranyl ethers (**123** and **124**), the desired products (**118** and **119**) were obtained in moderate to good yield**.** The

disappearance of the characteristic phenol signal at ~12 ppm and the appearance of the geranyl chain were very clear by ^{1}H NMR spectroscopy.
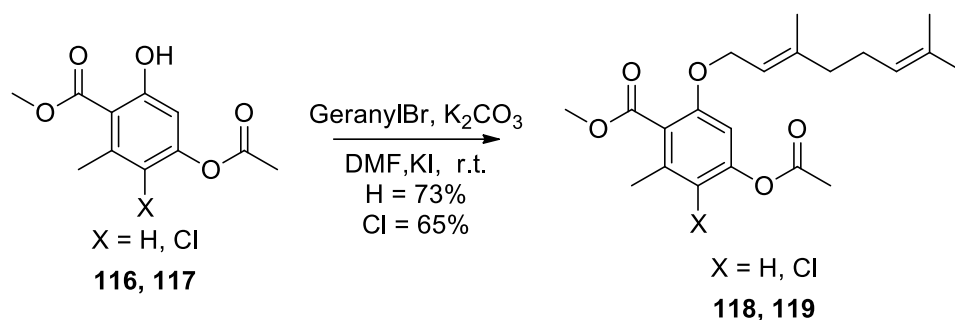
Scheme 31 - Geranyl ether formation

The Fries-type rearrangement of the des-chloro compound (**116**) gave a complex mixture of products, which were identified using two-dimensional HMBC and HSQC NMR spectroscopy, resulting in a low isolated yield of 21% for the desired compound **118** (**Table *4***).
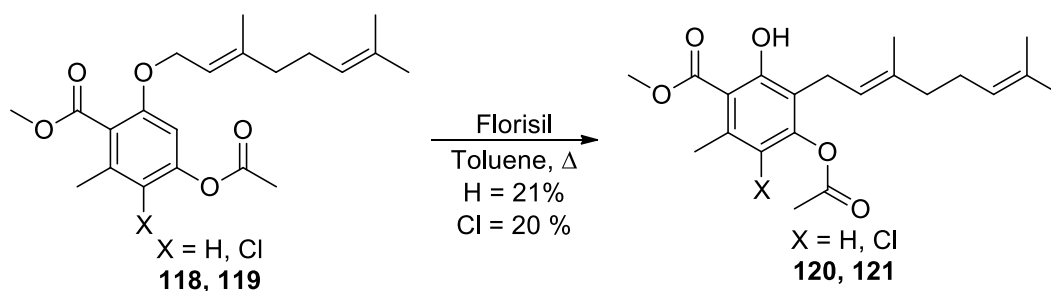
Table 4 - Compounds obtained following rearrangement of geranyl chain: R = geranyl chain

Compound			Yield
122	**123**	**124**	Trace
120			21%
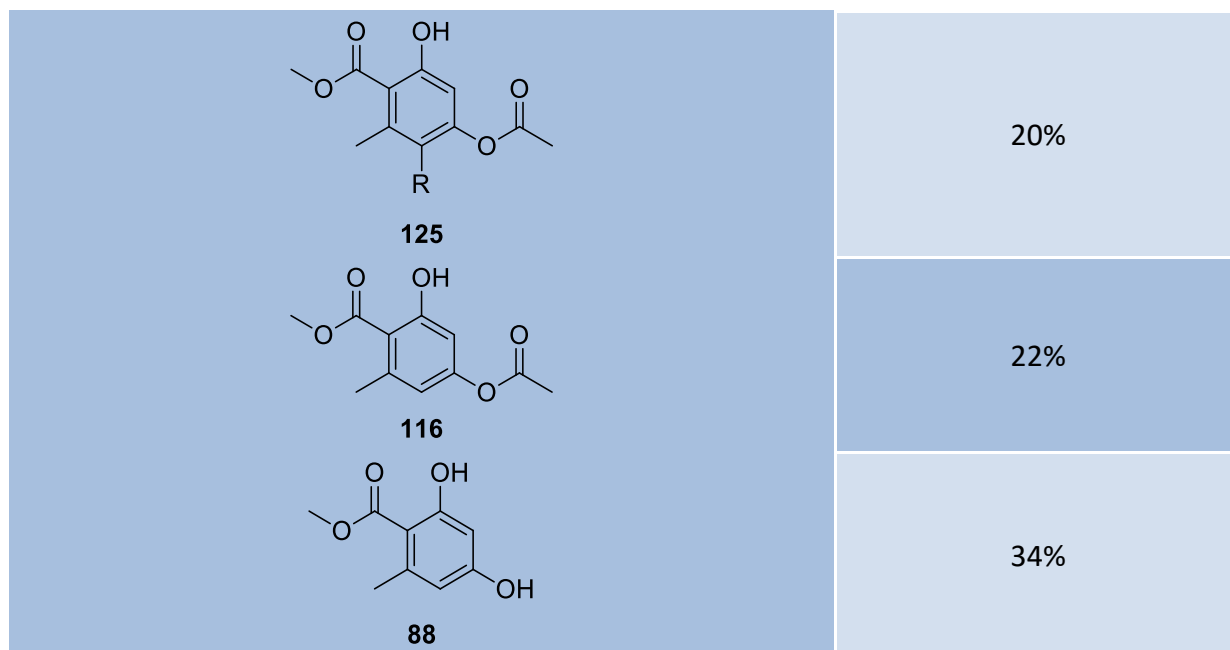
The desired product (**64**) was characterised in ^{1}H NMR spectroscopy by the reappearance of the salicylic phenol at 12 ppm, the continued presence of the geranyl signals and the indicative 1'-CH$_2$ triplet that shifts from 4 ppm to 2 ppm as a result of the change in connectivity, from etheric to phenylic. Two-dimensional HMBC NMR spectroscopy was utilised to confirm that the correct regioisomer was obtained.
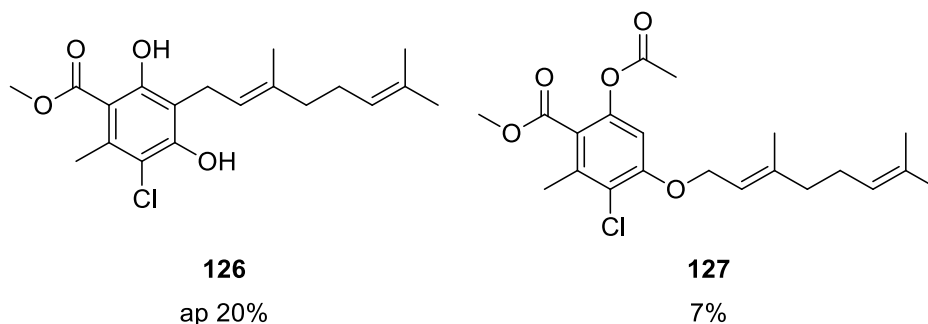
Figure 33 - Compounds obtained from rearrangement of CCB analogue

Predictably, the corresponding reaction with the penta-substituted chloro compound resulted in fewer side products. Three major products were obtained: compound **126**, having undergone the desired rearrangement and subsequent deacetylation; compound **127**, in which the protecting groups are swapped (**Figure 33**); and the bis phenolic compound **88**.

Ester alteration

Elsewhere in the group, test reactions of the simpler methyl benzoate (**88**), without any tail attached, had been successfully converted to the hydroxamic acid by heating in the presence of hydroxylamine. Unfortunately, this did not translate to the more complex methyl benzoate (**114**) which was completely unreactive to these conditions and in addition to this, deprotection attempts again proved non-trivial. ^{1}H NMR spectroscopy and TLC evidence showed that the NaOH, LiOH and NaSMe deacylated the 4-OH of the compounds but no saponification of the benzoate ester was observed.

If the reaction was heated, or even left at room temperature overnight (under inert atmosphere) the compound would degrade to result in a product with indecipherable collection of signals by ^{1}H NMR spectroscopy, from which no clean material could be purified; use of trimethylsilyl iodide and boron tribromide gave similarly poor results. Use of acidic conditions was inappropriate due to the known risk of annulation to give compounds such as **128** and **129** (**Scheme 32**). As a result of this inability to deprotect and expose the carboxylic acid motif required to employ any of the myriad of activated amide formations and with material low, the route was abandoned.
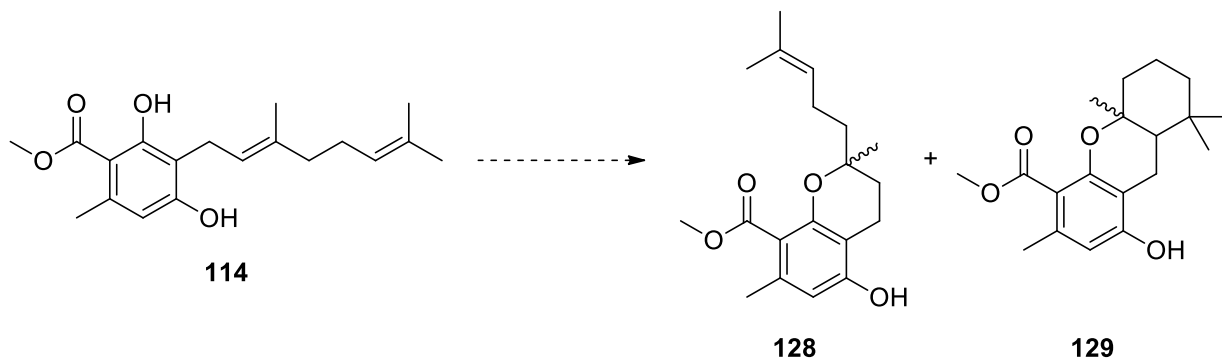
Scheme 32 - Potential undesired reactivity

Unfortunately, the routes attempted were low yielding and encountered many difficulties however the research did highlight the salicyl ester as unsuitable to late modification. This suggested a need for an alternate synthesis, in which, the problematic ester/aldehyde functionality is ideally installed at the latest possible stage.

Several alternate alpha phenol C-C bond formations were reported in literature. In particular, reaction of phenol with NaH and geranyl bromide in toluene had shown significant C-C formation over C-O (**Scheme 33**). This method was trialed several times but even at forcing temperatures did not show any formation of the desired product.


88   NaH, GeranylBr / Toluene   **114**
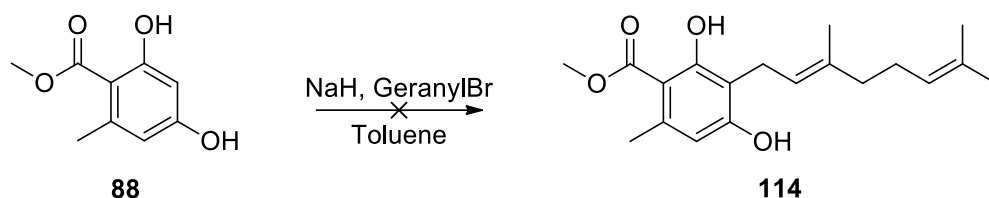
Scheme 33 - Failed alternative geranyl addition

With CCB synthesised and available in the lab there was the possibility of functionalising this to the hydroxamic acid, avoiding a lengthy full synthesis. Mild sodium chlorite, Pinnick oxidations, were attempted but no carboxylic acid could be obtained.

Trifluoromethylbenzisoxazole

While this work does not follow chronologically from the palladium and Fries-type chemistry, it represents a brief unsuccessful exploration and so has been included here.

The benzisoxazole motif of compound **130** was found to be active against TAO and will be discussed at length in subsequent chapters. The methyl compound **131** was under investigation elsewhere in the Ward group and the trifluoro methy compoundl **132** was a desired target (**Figure 34**). The iodo compound (**130**) had been shown to undergo Heck coupling to varying degrees and therefore we wished to synthesise the direct CF_3 analogue to enable accurate comparison of this point change.

R_1 = H, CH_3, CF_3
130, 131, 132
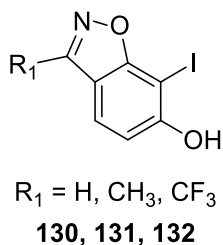
Figure 34 - Target benzisoxazole compounds

The halogenation of the 5,6-benzisoxazole was considered a liability and therefore the preferred synthetic path required iodination prior to isoxazole formation (**Scheme 34**). Acylation was known to occur selectively at the 4 and 6 positions of orcinol (**45**) and

there was precedent in the literature for iodination specifically in the required 2 position, giving compound **133**.[373] Unfortunately, despite several efforts, iodination gave a mix of the products that proved largely inseparable.
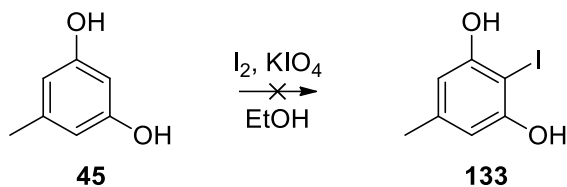
Scheme 34 - Selective iodination unsuccessful

By reversing the order of reactions the trifluoromethyl ketone could be installed easily in excellent yield (83%), however iodination of this ring (**135**) then proved challenging. As seen in previous chlorinations, no selectivity was obtained for the desired 3-C position between the two phenols and the ring was susceptible to dihalogenation. Purification of products was time consuming and challenging. It was hoped that formation of the oxime (**137**) would be trivial but instead it was quite particular. Typically, oxime formation will occur at room temperature, simply by mixing with hydroxylamine hydrochloride in methanol, but in this case this was unsuccessful. Higher conversion could be obtained by adding dry 3 Å molecular sieves and heating the reaction, but this resulted in deiodination. Several reaction conditions were trialed on small scale but with no improvement. At this point other avenues were available for exploration and this intractable route (**Scheme 35**) was discontinued in favour of more promising work.
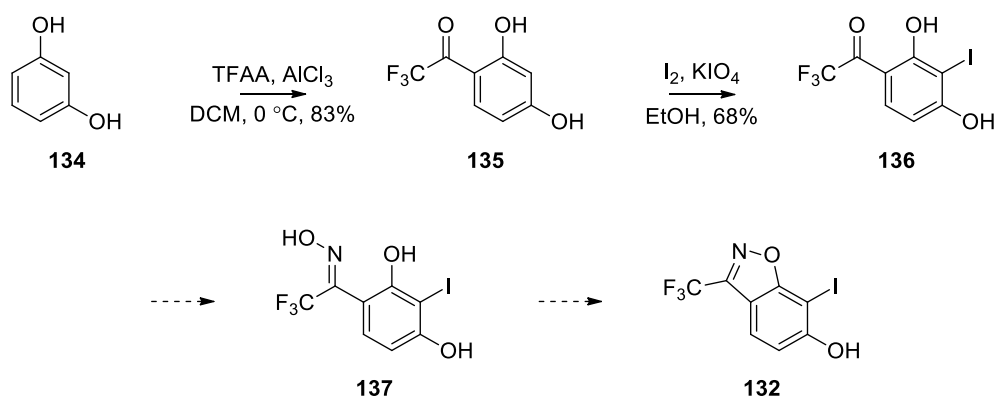
Scheme 35 - Partially completed synthetic route

Conclusion

Unfortunately, the synthetic routes discussed in this chapter were largely unsuccessful. The chemistry employed was found to be poorly suited for compound diversification and synthesis of novel AF analogues. The palladium chemistry had limited scope with only one reaction affording a reasonable yield. With additional problems arising from isomerisation of the geranyl chain and difficulties in deprotecting the phenols, the route was abandoned. The penta-substituted compound **81** was however still believed to represent a valuable starting material.

Further attempts were made to elaborate compound **81** by Fries-type rearrangement. In this approach the geranyl chain was successfully installed without isomerisation. However, multiple attempted reactions of the methyl ester (**114**), with an aim to introduce aldehyde alternatives, were unsuccessful and this route was also discontinued.

Whilst these two routes had proven unsuccessful they succeeded in highlighting the essential need for a completely new approach to AF-like compounds. In addition, having employed the phenolic motif in the rearrangement it was established that this pre-installed functionality could be exploited. This gave rise to the idea to use *ortho*-lithiation to elaborate the headgroup, which paved the way to future success.

Chapter 3 - Directed Litiation

As established, synthetic routes explored so far had not provided an adequate method for synthesis of ascofuranone (AF)-type compounds, and therefore others needed evaluating. The greatest success had been achieved by utilising the phenolic motif for Lewis acid catalysed rearrangement. It was hoped that this idea, in which the phenols are employed to direct subsequent reactions, could be exploited in a directed *ortho*-lithiation approach to the target compounds. This method was first employed in attempt to synthesise an AF analogue lacking the *ortho*-phenol, compound **138**, but was later developed to enable installation of the geranyl tail prior to installing functionality at the aldehyde position on compound **45** (**Figure 35**).
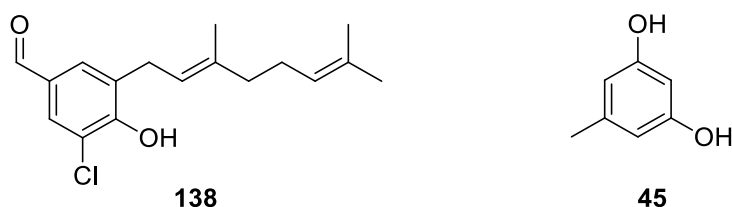
Figure 35 - Key compounds in development of lithiation methods

Acetal exploration and *ortho*-lithiations
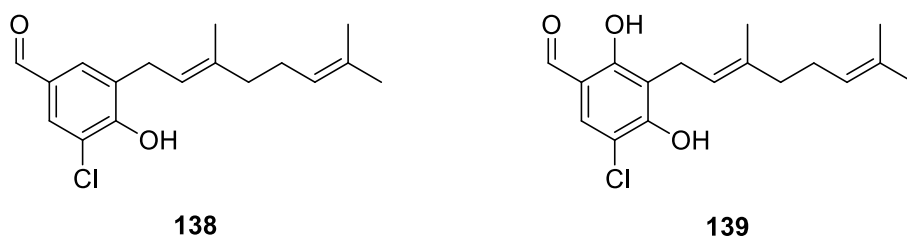
Figure 36 - Monophenolic target and previously synthesised analogue

Initially compound **138** (**Figure 36**) was selected as a primary target. The activity of compound **138** could be compared to that of compound **139**, previously synthesised in the Ward lab, to give some indication of the necessity of the 2-OH for TAO inhibition and it was also amenable to synthesis by this proposed synthetic route. The symmetry afforded by having the *para*-phenol benzaldehyde (**140**) would both benefit the lithiation and substitution reactions and selectively direct subsequent chlorination at

the desired 3-position by the combined effects of the *ortho-para* directing phenol and the *meta* directing aldehyde. The intended route (**Scheme 36**) would also indicate how accessible and stable the acetal might be in any future syntheses.
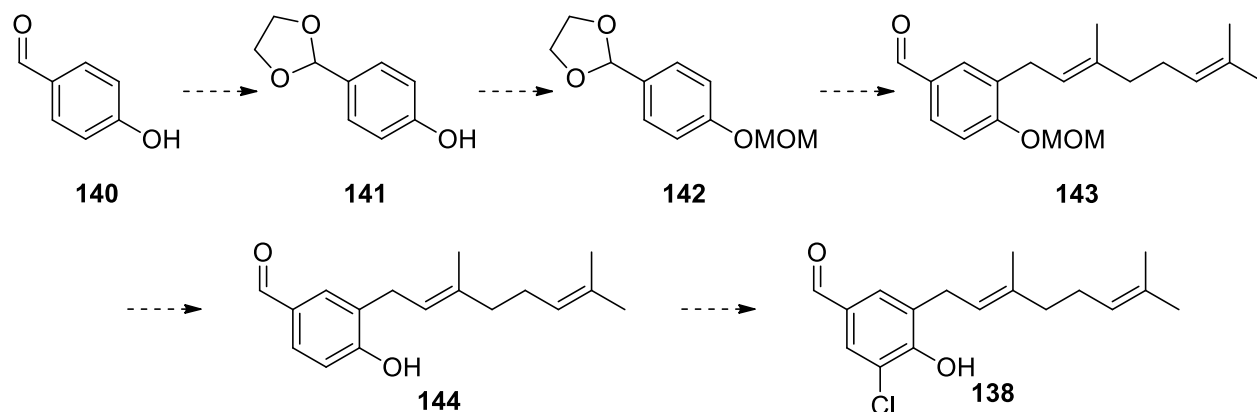
**Scheme 36 - Intended synthetic route employing acetal protection and *ortho*-lithiation**

Directing Metal Group chemistry
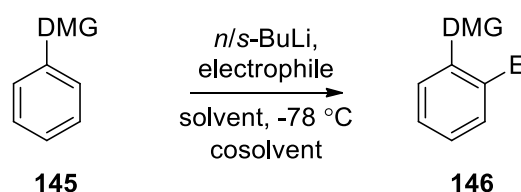
Scheme 37 – General directed *ortho* metalation

The key synthetic method in this and subsequent routes in this chapter is directed *ortho* metallation (DoM). This method consists primarily of the application of alkyllithium bases to aromatic rings containing a base-stable heteroatomic functionality (**147**) capable of chelating the powerful lithium base and regioselectively deprotonating the *ortho* position. The stabilised aryl lithiate formed can then be reacted with a wide range of electrophiles. This chemistry was independently discovered around 1940 by both Gilman and Bebb[374] and Wittig and Fuhrman[375] when anisole was selectively *ortho* deprotonated by *n*-BuLi. Thorough subsequent development Hauser[376,377] and others[378] advanced the scope of the field and this was further accelerated by the commercial availability of alkyllithiums arising from their necessity in industrial scale anionic polymerization.[379] DoM research has expanded vastly since this time thanks to the work

countless chemists, with Victor Snieckus preeminent among them, to be a key strategy in aromatic functionalisation alongside chemistry such as: cross-coupling; electrophilic aromatic substitution; benzyne utilisation; sigmatropic cyclisations; and radical reactions.
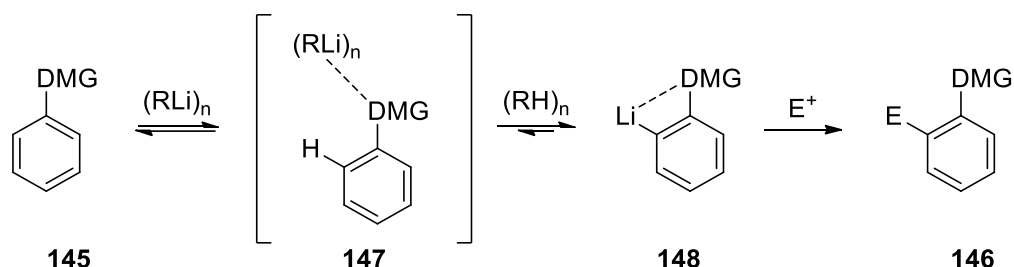
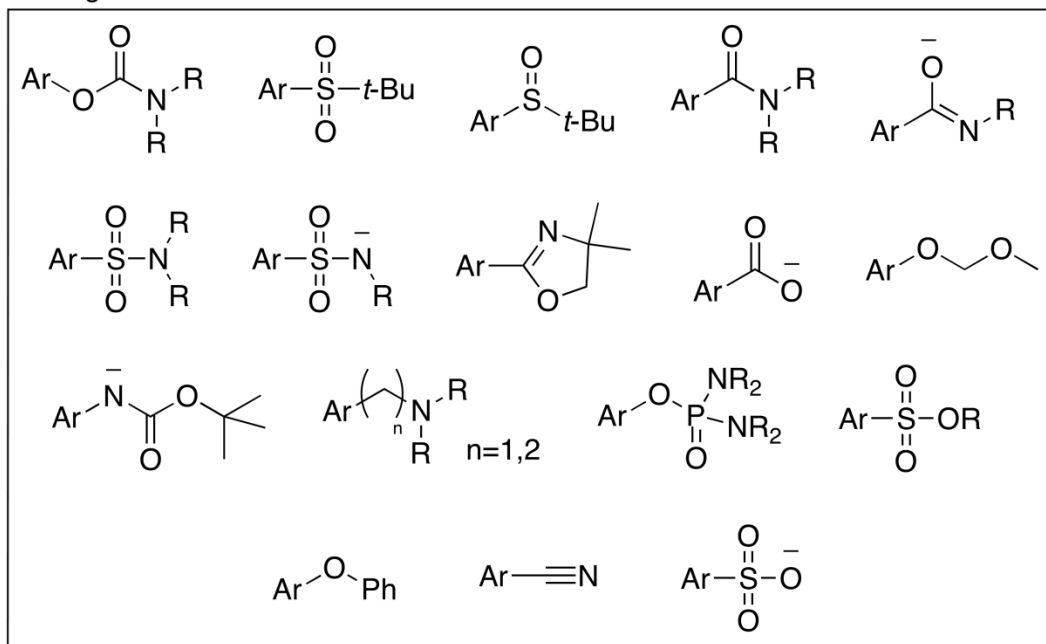**Scheme 38 – General directed *ortho* lithiation reaction mechanism**

Mechanistically the reaction is simple (**Scheme 38**): coordination of the alkyllithium aggregate to the heteroatom-containing DMG (**147**); deprotonation to give the coordinated ortho-lithiated species (**148**); and reaction with electrophile to yield product (**146**). This was established early: thermochemically with the observation that quenching (*p*-anisyl)lithium is 3.6 kcal/mol more exothermic than that of (*o*-anisyl)lithium;[380] rate enhancement of anisole deprotonation compared to benzene; pKa measurement;[381] steric effects;[382–384] and computational studies.[385,386]

The bases used most widely are *n*-BuLi and *s*-BuLi both of which exist as aggregates that vary greatly depending on the coordination of the chosen solvent. For instance, *n*-BuLi is mainly hexameric in hydrocarbon solvents,[387] tetrameric in diethyl ether,[388] and a tetramer–dimer mixture in THF.[389] This propensity to agglomerate reduces the bases reactivity through steric cumbrance and enhanced stability relative to disaggregate lithiates. This reduced activity has led to the inclusion of cosolvents with lone-pairs capable of coordinating the lithium atom. Such electron donation disassembles the aggregates to expose the solvated dimeric base and destabilises the C-Li bond, increasing its pKa. Examples of such bases are numerous however those routinely used include bidentate tetramethylethylenediamine (TMEDA), N,N'-dimethylpropyleneurea (DMPU) and the tridentate hexamethylphosphoric triamide (HMPA) and hexamethylphosphorous triamide (HMPT) which are significantly more coordinating Lewis bases although pose a much greater risk of toxicity and carcinogenicity.[390]
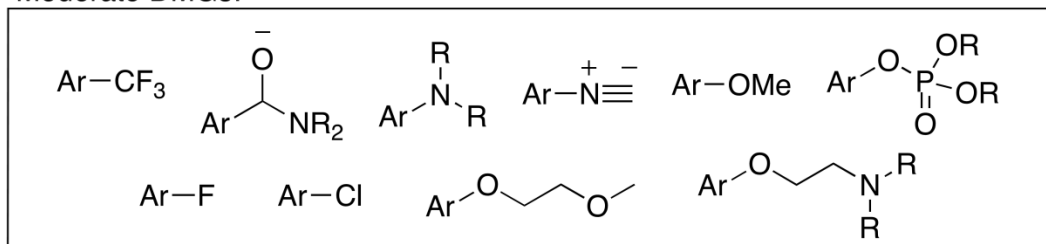
Temperature is also an important consideration in DoM reactions and they are usually cooled to −78 °C to minimise side reactions arising from the use of such powerful bases.
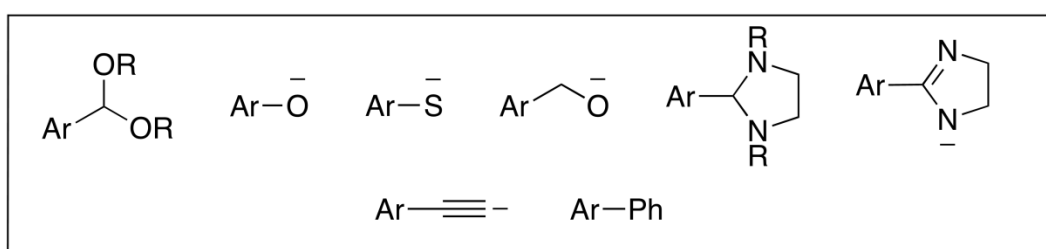

Figure 37 – Potential DMGs[257]

A wide array of DMGs are available to chemists and these have been ranked based on their relative ability to stabilise the *ortho* lithiate [OCONEt$_2$ > SO$_2$tBu > CONEt$_2$ > OMOM ~ NtBOC > OMe > Cl][391] (**Figure 37**). This stabilisation is a composite effect arising from factors such as: heteroatom lone-pair donation, sterics and inductive charge stabilisation.[257] These DMGs have allowed a myriad of synthetic transformations and methodologies: electrophile installation and subsequent functional-group

interconversion affording various moieties – alkyl,[392] allyl,[393] formyl,[394] silyl,[395] $B(OMe)_3$,[396] SnR_3,[397] OH,[398] NH_2,[399] NHR,[400] NR_2,[400] CO_2H,[401] CONHR,[401] $CONR_2$,[397] CN,[400] PR_2,[257] SH,[402] SR,[394] Se,[402] Br,[397] and I;[401] heterocycle functionalisation;[403,404] benzyne generation;[257] 2,6 dianion equivalents;[405] stabilised *o*-tolyl anions;[406] synthesis of heterocycles, including but not limited to, isocumarins,[407] 3-substituted 3,4-dihydro-1-(2H)-isoquinolones,[408] phthalides,[409] isobenzofurans,[410] isoquinolones,[411] quinolones,[412] and acridones.[400] These reactions represent the established chemistry of DoM however more current efforts have been to focus on novel DMGs such as O-sulfamates[413] and in particular DMGs that are amenable to a metal catalysed orthogonal coupling strategy. This means to varied arene polysubstitution is exemplified particularly by DMGs capable of undergoing subsequent Kumada–Corriu cross-couplings,[413] Suzuki cross-couplings,[414] feasible in one-pot,[415] and ruthenium catalysed C-O activation/coupling.[416]

Whilst the literature reviewed here was not exhaustive, interestingly absent were examples of direct transmetallation of an *ortho* lithiate to palladium in a catalytic cycle especially in the light of Feringa's 2013 high-impact reporting of Li-Pd transmetallation in catalytic biaryl cross-coupling in *Nature Chemistry*.[417]

The use of DMGs for DoM in this work was for the relatively facile addition of electrophiles, in particular the ascofuranone tail group, and the selection of DMG is discussed below as appropriate to the synthetic sequence.

Acetal formation

At first it was hoped that ethylene glycol could be used in the synthesis of the cyclic acetal, compound **141** (**Scheme 39**), given that the formation of the five-membered ring should be both kinetically favoured and stable. It was necessary that this reaction be conducted prior to MOM protection, as these protecting groups are potentially labile under the acidic conditions required for acetal formation. Reactions were found to be slow, and required multiple equivalents, molecular sieves and heat but the ^1H NMR spectrum of the reaction mixture showed > 95% conversion overnight, characterised by the disappearance of the aldehyde signal (~12 ppm) and appearance of benzyl acetal proton signal (~5 ppm). Inconveniently the product (**141**) had an almost identical R_f to the starting material (**140**) and therefore proved very difficult to purify by column

chromatography, and furthermore, ^{1}H NMR spectroscopy showed 20-30% of the acetal reverted to aldehyde after silica column chromatography.

140 → **141**

HO OH
PTSA, DCM,
MS 4 Å
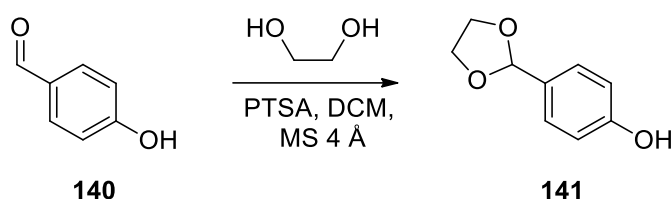
With an aim to alleviate some of the issues faced in using ethylene glycol, the decision was taken to instead use 2,2-dimethyl-1,3-propanediol. This diol reacts to form a stable six membered acetal[418] with restricted rotational freedom resulting from the Thorpe-Ingold effect. It was intended that this should afford faster reaction times, increased stability in silica column purification and most importantly a substantially different R_f, which would simplify purification.

The six-membered cyclic acetal was formed, as expected, using the same conditions as previously (**Scheme 40**). The increased divergence in R_f served to improve separation but did not fully alleviate the problem and as a result compound **149** was carried through to compound **150** with impurities present. As such compound **149** was not fully characterised.


140 → **149**

HO OH
PTSA, DCM,
MS 4 Å, ap 78%
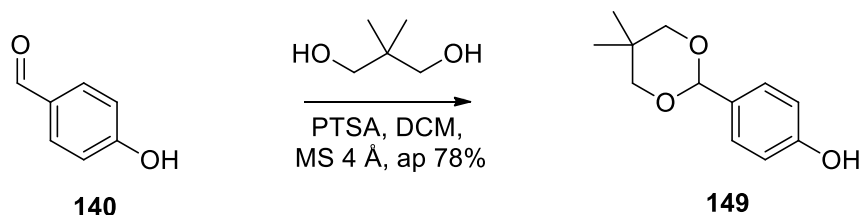
Scheme 40 - Improved acetal formation

Directing Metal Group selection

The proposed *ortho*-lithiation required prior installation of a suitable phenolic DMG. The previous literature precedents included -OMe, -OSEM, -OMOM and -OCON(Et)$_2$. The OMe and OSEM ethers were discounted, having previously proven difficult to deprotect on similar compounds. Of the remaining two options the OMOM ether was selected as

there were many reported examples of successful protection and, more notably in this work, deprotection with similar compounds with the *ortho* geranyl motif.[419] Of particular interest were examples of specific mild deprotections with P_2I_4[256] and $NaHSO_4 \cdot SiO_2$.[419] In this work it was found that the *para*-OMOM benzaldehyde, compound **150**, could be successfully deprotected with $NaHSO_4 \cdot SiO_2$. The MOM ether therefore appeared to be a reasonable selection for DMG.

Protection was expediently achieved using NaH and MOMCl (**Scheme 41**). ^{1}H NMR spectroscopy of the crude product showed addition of MOM with minimal reforming of the aldehyde (< 5%) however some acetal was again lost during column chromatography, lowering the isolated yield.
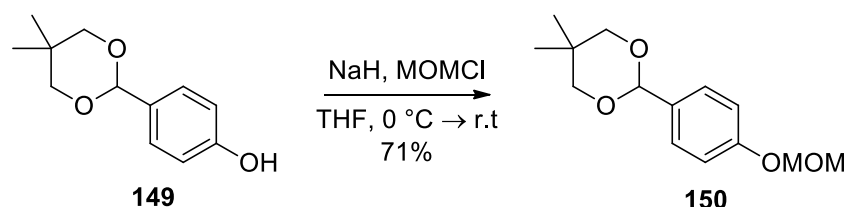
Scheme 41 - DMG installation

Initial lithiations

In a test reaction it was observed that compound **150** could be successfully lithiated (**Scheme 42**) and appeared by ^{1}H NMR spectroscopy to afford the desired compound **151** in good yield. The distinctive shift of the bromide methylene at 3.6 ppm to 3.1 ppm in the benzyl methylene became characteristic of successful linker installation in subsequent *ortho*-lithiation reactions. This compound was not fully characterised and the work set aside in favour of other research with the intention of it being completed at a later date, however, work was never resumed. If the route was continued, the MOM ether should first be deprotected using $NaHSO_4 \cdot SiO_2$ and then chlorinated with NCS to afford the desired compound **138.**
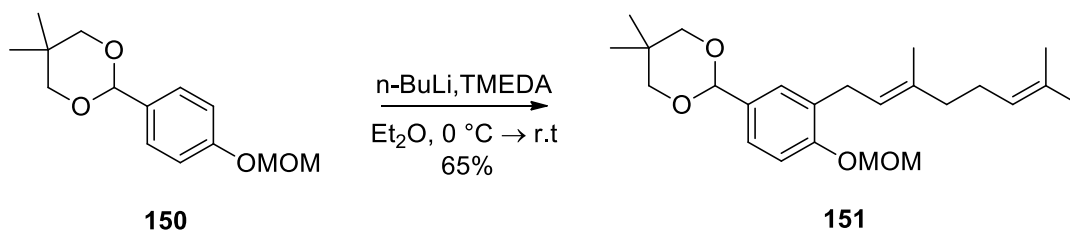
Although this route was discontinued, it successfully illustrated that the acetal compounds **150** and **151** could be obtained in decent yield and that *ortho*-lithiation is amenable to linker installation. Given the difficulties faced using the previous routes, this method for lithiation appeared far superior and represented a huge improvement in the search for a workable route to linker installation in AF-like compounds.

Ortho-lithiation for synthesis and diversification of CCB

Amid attempts to synthesise compound **151** using the *ortho*-lithiation route described another lithiation route to CCB and other AF analogues was proposed. In this route the linker would be installed first by *ortho*-lithiation, prior to the decoration of the aromatic ring (**Scheme 43**).
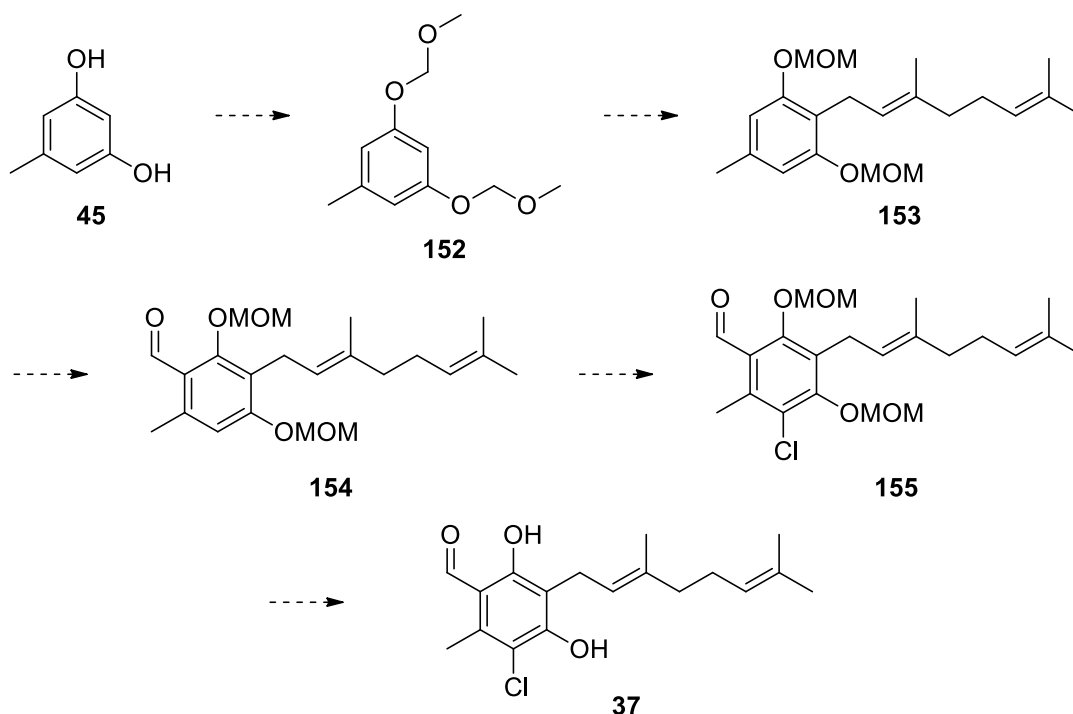

Scheme 43 - Proposed synthetic route to fully decorated AF analogue using *ortho*-lithiation

Most exciting about this route was the potential to "walk" around the CCB headgroup *via* multiple lithiation steps to fully substitute the ring in one-pot. The first lithiation should occur selectively α to both DMG groups at the 2-C position, allowing installation of the linker and affording a symmetrical molecule (**153**), which relieves any potential selectivity problems in the following two additions.

Although less efficient, an alternative step-wise construction of the head group could also be executed utilising lithiation to attach the linker and other reactions to install the aldehyde and chlorine.

Literature examples suggested that the protecting group best suited to this chemistry would again be the OMOM, which reportedly selectively lithiates at the aryl position over benzylic positions.[420]
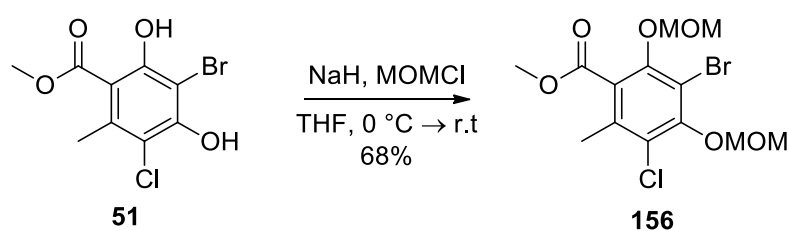
Scheme 44 - Bis MOM protection for deprotection condition screen

Deprotections have proven highly problematic throughout the TAO project. Therefore, even with many similar examples reported in which the bis OMOM geranyl motif was successfully removed, it was decided that deprotection should be tested. Compound **51**, a similar hexa-substituted compound available in-house, was bis protected with MOM ethers to compound **156** (**Scheme 44**) and screened against common reported deprotection conditions (**Table 5**).[418] The product was clearly characterised: in ^{1}H NMR spectroscopy by the appearance of four singlets corresponding to the MOM ethers and by the disappearance of the phenol signals; and by the observation of an accurate mass for the molecular ion using HRMS. Happily, two of the deprotection methods were successful, and particularly pleasingly, the mild $NaHSO_4 \cdot SiO_2$ worked cleanly in less than 10 minutes.
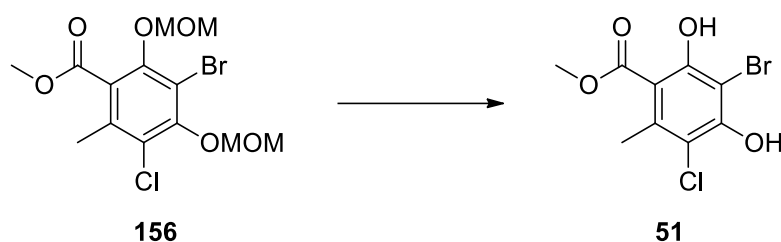
156 → **51**

Table 5 - Attempted deprotection conditions

Conditions	Deprotected
THF: 1N HCl 1:1 v/v	X
5 Eq TsOH·H$_2$O, MeOH	✓
Xs NaI, cat. HCl, acetone	X
NaHSO$_4$·SiO$_2$(2 Eq by weight), DCM	✓

These findings indicated that it should be possible to successfully remove the MOM ethers at the end of the synthesis and therefore the proposed route was initiated with protection of the orcinol (**45**) phenols in excellent yield (**Scheme 45**). The symmetrical product (**152**) clearly showed the addition of two singlets corresponding to the ethers by ^{1}H NMR spectroscopy and the correct molecular ion with accurate mass was observable by HRMS.


45 → **152**

NaH, MOMCl
THF, 0 °C → r.t
93%
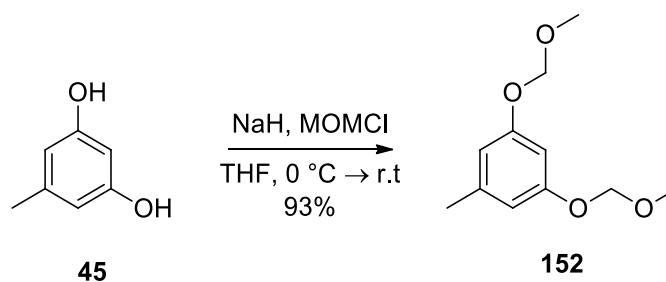
Scheme 45 - Orcinol DMG installation

Lithiation methodology

Initial lithiation attempts were unsuccessful and therefore less well-established, alternative methods had to be explored, firstly to confirm formation of the desired lithiate and secondly to give the desired product. The first two failed attempts followed a method outlined in the literature[421] (**Scheme 46**). This procedure called for the application of *n*-BuLi to compound **152** at 0 °C followed by 90 minutes stirring at room temperature before the addition of the electrophile. This method appeared to not account for the decomposition of THF in the presence of organolithium reagents. When no product was formed, the reactions were repeated at -78 °C and -40 °C, which afforded an improved yield of ~50-60%. The reaction mixture became bright yellow upon addition of *n*-BuLi, potentially indicative of formation of the aryl lithiate. Although this colour change was also observed in the reaction at 0 °C, it was noted that the colour was gradually lost during the hour-long stir.

It was determined, by eye, that the yellow colour was at its most intense at roughly 20 minutes and it was found that by quenching the reaction with the desired electrophile after 20 min the linker could reproducibly be inserted in excellent yield, and with no formation of the undesired S_n2' product. Compound **153** could be clearly identified: by a marked shift in R_f; by observation of an exact mass of the molecular ion using HRMS; and ^{1}H NMR spectroscopy clearly demonstrated the loss of the 2-CH singlet signal and the appearance of the geranyl chain signals. Retention of a single *trans* alkene 2'-CH triplet was also clear from this spectrum and when compared to that of the starting geranyl bromide.
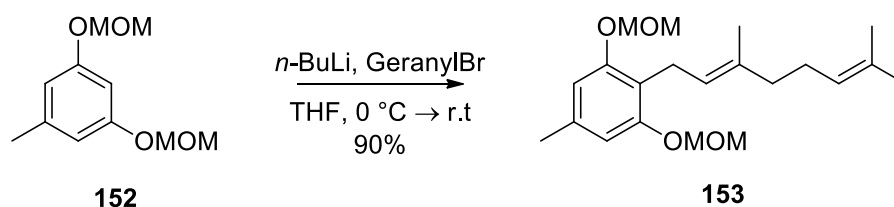

Scheme 46 - C-2 directed geranyl installation

Following this success, consecutive lithiations were attempted to further functionalise the ring. Initially the second lithiation was attempted immediately following the addition of the geranyl linker in the same pot and by ^{1}H NMR spectroscopy this appeared to have

gone to > 95% conversion (**Scheme 47**). Upon addition of *n*-BuLi, which was used in excess to quench any geranyl bromide still in solution, the reaction turned orange. When this was quenched with dry dimethyl formamide (DMF), the desired product (**154**) was obtained in 31% yield with the rest of the mixture comprising of the product of the first lithiation (**153**) and the starting material (**152**).

152

1) *n*-BuLi, GeranylBr
2) *n*-BuLi, DMF

THF, 0 °C → r.t
31%

154
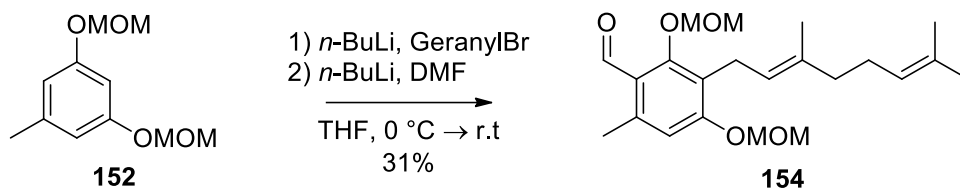
Scheme 47 - Consecutive one-pot electrophile additions

Several attempts were made to improve the yield of the second lithiation step (**Table 6**). ^{1}H NMR spectroscopy was used to monitor small-scale reactions to screen different solvents, temperatures and additives. Unfortunately, the yield could not be improved.


153   **154**
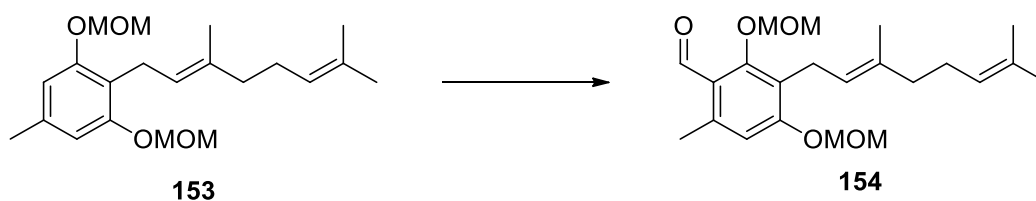
Table 6 - Conditions attempted to improve formylation yields

Number	Conditions
1	(i) THF, *n*-BuLi, -78 ˚C (ii) THF, *n*-BuLi, 0 ˚C
2	(i) Et$_2$O, *n*-BuLi, at -78 ˚C (ii) Et$_2$O, *n*-BuLi, 0 ˚C
3	(i) THF, TMEDA, *n*-BuLi -78 ˚C (ii) THF, TMEDA, *n*-BuLi, 0 ˚C
4	(i) Et$_2$O, TMEDA, *n*-BuLi, -78 ˚C (ii) Et$_2$O, TMEDA, *n*-BuLi, 0 ˚C
5	(i) THF, *s*-BuLi, -78 ˚C (ii) THF, *s*-BuLi, 0 ˚C
6	(i) THF, TMEDA, *s*-BuLi, -78 ˚C (ii)THF, TMEDA, *s*-BuLi, 0 ˚C

It is understood that poor solvation of lithiates can hinder reaction progress[390] and so TMEDA was added as a co-solvent in an attempt to relieve this, but unfortunately this had no observable impact. More donating solvents such as HMPA and HMPT were not explored. Unfortunately, no explanation was established as to why the second lithiation does not appear to proceed to completion.

It had been hoped that this second lithiation would allow sufficient scope to react with a range of electrophiles prior to deprotection. Disappointingly however, it did not seem that this was the case. A batch of the lithiate compound **153** was synthesised and this was then split into two and treated separately with CO_2 and $B(OMe)_3$ in an attempt to form the respective carboxylic and boronic acids. These reactions were unsuccessful over several repeats. The boronic acid would have been particularly valuable for use in palladium coupling reactions as the bromination of the ring elsewhere in the Ward lab had been challenging. In addition, the lithiate itself could potentially have been used to transmetallate to the palladium[417] in a catalytic cycle, but this was never attempted.

Although the yield was low, the second lithiation had progressed to some product and therefore the third consecutive lithiation was attempted. *N*-chlorosuccinamide (NCS) was utilised as an electrophilic source of chlorine. It was hoped that by using the DMF formyl equivalent, compound **157**, the aldehyde would be protected as the lithium stabilised hemi-aminal (**Scheme 48**) increasing the likelihood of successful reaction. Regrettably however, these attempts to fully functionalise the ring were not successful.
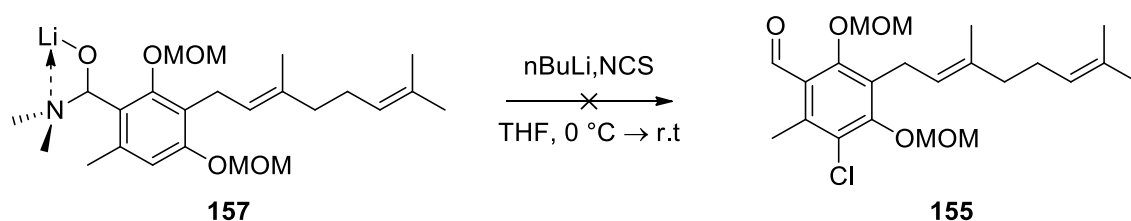
**Scheme 48 - Consecutive one-pot chlorination of the formylation intermediate was unsuccessful**

Functionalisation and Deprotection

Although conducting the three functionalisations in one pot had proven unsuccessful, compound **154** was available and an attempt was made to chlorinate this using NCS. Unfortunately, this showed no reaction even at forcing temperatures (140 °C in THF) in a microwave. This was not entirely surprising as the aldehyde acts to deactivate the ring and the electron donating ability of the phenols is attenuated upon addition of the MOM groups. As a result, the aromatic ring exhibits significantly decreased reactivity towards electrophiles.

154 → **103**
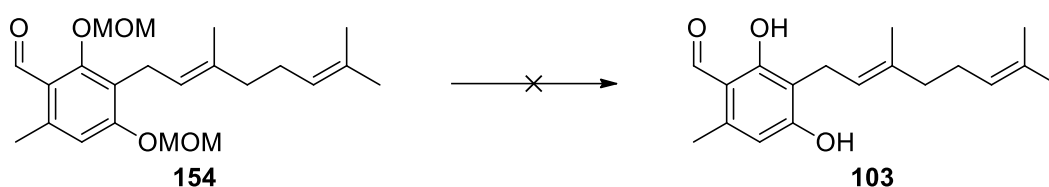
Scheme 49 -Removal of MOM DMGs proved challangeing

Chlorinations of compound **154** were not forthcoming but it was hoped that the deprotected compound **103** might yield better results so the deprotection conditions established previously were attempted. Using either reaction conditions the deprotection of the 2-OMOM was observed within five minutes at room temperature but the other 4-OMOM was unchanged after a day, and when heated or left for more time the mixture only turned red-black (**Scheme 49**). The deprotection of α-carbonyl OMOM ethers is documented[422] and has been observed previously in the Ward Lab with a related SEM protecting group. Potentially the test deprotections had worked only due to the presence of two flanking halogens on the 4-phenol of compound **156** and therefore deprotection of compound **154** was not possible with the same methods.


n-BuLi, Bromoctane

THF, 0 °C → r.t
83%

152 → **158**
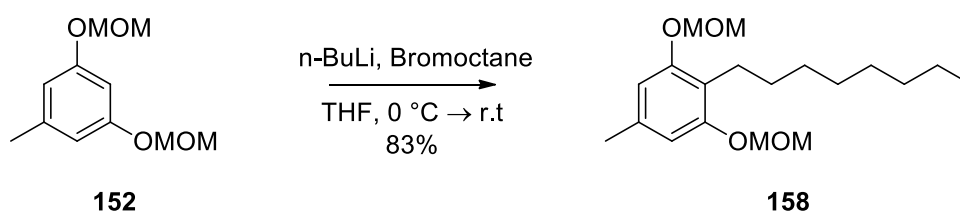
Scheme 50 - Inatallation of robust tail analogue

To circumvent the difficulties thought to be associated with the presence of the geranyl chain compound **158** was synthesised (**Scheme 50**). This could be used as a simpler example on which to test the bis MOM deprotection without the risk of the geranyl chain cyclising or interfering in the reaction. This decision to abandon the geranyl motif was also informed by the first publication of SAR[212] around AF-like compounds. As previously outlined in the introduction, the work in this paper showed that extensive changes to the lipophilic chain had surprisingly little impact. It appeared that, regarding the tail, the changes in activity corresponded only to general changes in the lipophilic hydrophobic interactions and it was found that optimal interaction required a tail length of eight carbons. It was understandable that having more lipophilic interactions should increase the retention of the compound in the lipophilic TAO pocket and active site and afford an increase in potency. In contrast, compounds with chains longer than eight carbons may be suffering from increased indiscriminate protein binding and decreased solubility or the chain may protrude from the protein, thereby exposing it to the polar intra-mitochondrial fluid.

Using many conditions reportedly used with similar compounds with a bis MOM geranyl motifs, deprotections were again screened (

Table 7). Excitingly the neutral deprotection utilising ethylene glycol and heat deprotected the C_8 chain compound, **158**, without degradation and in excellent yield.


158 → **159**
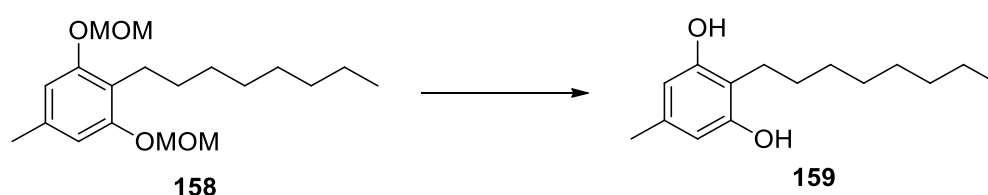
Table 7 - Attempted MOM ether deprotection conditions

Conditions	Result
THF: 1N HCl 1:1 v/v	No reaction
MeOH: 1N HCl 1:1 v/v	No reaction
5 Eq TsOH·H$_2$O, MeOH	No reaction
Xs NaI, cat. HCl, acetone	Removed the SM but no clear product
NaHSO$_4$·SiO$_2$(2 Eq by weight), DCM	No reaction
Conc HCl:THF, 1:2	Slow reaction and no clear product
Ethylene glycol, 160 °C	87% (conversion after two hours)

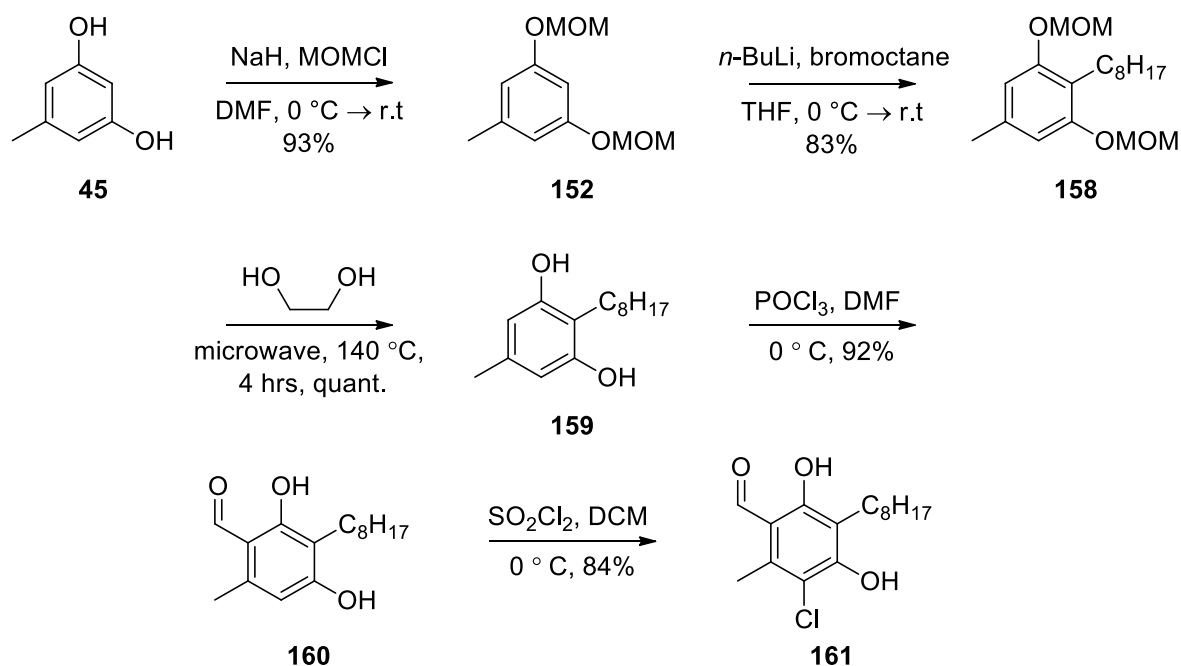| ZnBr$_2$, n-BuSH	Removed the SM but no clear product
EtSH, THF	No reaction
5mol% AcCl, MeOH	No reaction

Compound **158** was also used as a tool to test other potential reactivity of the ring in the absence of the geranyl chain. Several reactions were attempted to further elaborate the MOM protected ring but none were successful (**Scheme 51**).
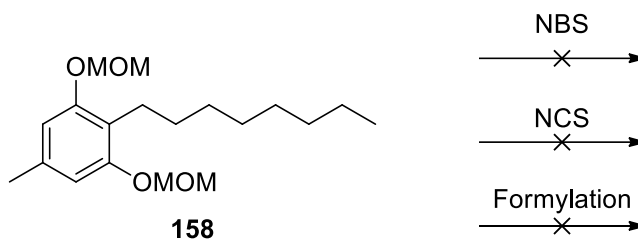
Scheme 51 - MOM protected compound unreactive to elctrophiles

The deprotection in ethylene glycol proved to be very fruitful initially but encountered reproducibility issues that proved insurmountable. Initially, the reaction yields were excellent to quantitative but unfortunately application of these methods to another batch of compound **158** synthesised only gave a maximum yield of 15%. Every effort was made to uncover the reason underpinning this issue and rectify it but no change made ever restored the initial success. The combined product obtained from the various reactions completed was taken forwards to investigate the subsequent reactions. The bisphenol compound (**159**) was formylated and chlorinated in excellent yields and gave a CCB analogue that proved very active against TAO K_i = 0.85 nM. Both compounds were fully characterised with the formylation observed by the appearance of salicylic signals in the ^{1}H NMR spectrum and the chlorination by disappearance of the aromatic CH.

Pleasingly, considering the best obtained yields of component reactions, the total yield of this CCB analogue from orcinol is 60% (**Scheme 52**). This constitutes a marked improvement over existing syntheses of other CCB and AF-like compounds.

OH → NaH, MOMCl / DMF, 0 °C → r.t / 93% → OMOM

45 → **152**

OMOM → *n*-BuLi, bromoctane / THF, 0 °C → r.t / 83% → OMOM, C$_8$H$_{17}$

158

HO—OH / microwave, 140 °C, 4 hrs, quant. → OH, C$_8$H$_{17}$, OH

159

POCl$_3$, DMF / 0 °C, 92%

O, OH, C$_8$H$_{17}$, OH

160 → SO$_2$Cl$_2$, DCM / 0 °C, 84% → O, OH, C$_8$H$_{17}$, OH, Cl

161

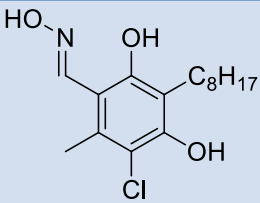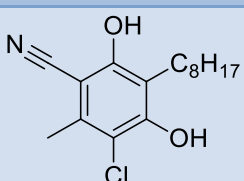Scheme 52 - Complete synthetic route to AF analogues

Benzisoxazole
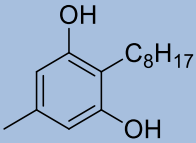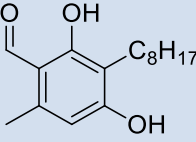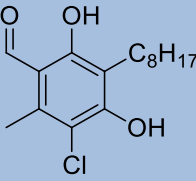
While the *ortho*-lithiation reactions were under investigation, it was discovered that the benzisoxazole functionality represents an active alternative for the salicylic motif in ascofuranone. The benzisoxazole was first synthesised *en route* to compound **164**, in which the nitrile replaces the aldehyde, and this chemistry was reconfirmed with the octyl chain analogue (**Scheme 53**). Oxime (**162**) formation was achieved straightforwardly in methanol, and once activated the nitrogen bound *trans*-hydroxyl is primed for intramolecular displacement by the *ortho*-phenol; this proceeds instantaneously at room temperature on treatment with triphenylphosphine (PPh$_3$) and 2,3-Dichloro-5,6-dicyano-1,4-benzoquinone (DDQ) to the heterocyclic benzisoxazole (**163**). Following this the base catalysed ring opening of the isoxazole affords the open nitrile phenol isomer (**164**).
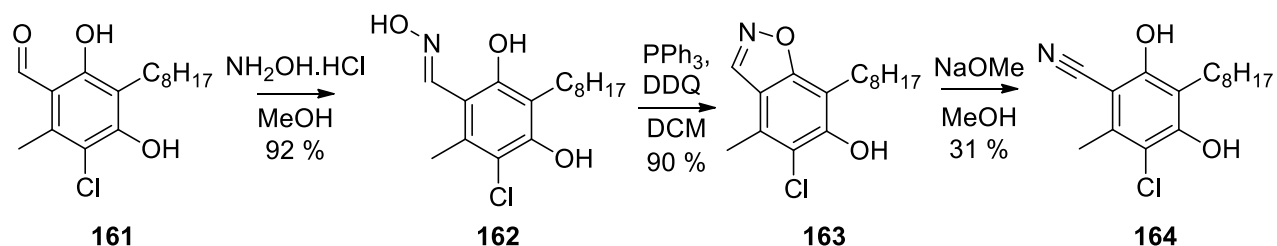
Scheme 53 - Synthesis of benzisoxazole and nitrile C$_8$ analogues

Benzisoxazoles like compound **163** represented a genuinely exciting development in the search for new TAO AF analogues. The 5,6-heterocycle is more drug-like, having removed many of the undesirable functionality of the head group. The benzaldehyde, which was a metabolism risk has been replaced, and the phenol which was a toxicity risk and might interfere with redox-cycling, has been masked. Importantly the compound retains high activity, with K_i = 25 nM, which is not significantly reduced compared to that of CCB and AF. Benzisoxazoles exist in drugs already on the market such as the antipsychotics Paliperidone and Risperidone. These compounds are generally metabolically stable with biological half-lives of approximately 20 hours, indicating that this heterocycle has good stability in the human body. It remained to be seen however whether such a highly substituted compound incorporating a *para*-phenol would behave in the same manner.

Table 8 - TAO inhibition of C$_8$ AF analogues

Structure	K_i (nM)
159	>1000
160	92
161	0.85
162	130
163	25
164	5

The above table (**Table 8**) summarises the measured activities of the compounds of interest from the *ortho*-lithiation mediated synthesis described above. The inhibition constants appear to be in agreement with the SAR findings which were published during the course of this work, in that it is essential that an electron withdrawing group is incorporated at the aldehyde position.

Benzisoxazole stability

Whilst the benzisoxazole illustrates an exciting breakthrough in this project, there were remaining concerns regarding its stability. As it is an intermediate in the synthesis of the nitrile and the two exhibit similar activity, it was suggested that the benzisoxazole could simply be isomerising to form the nitrile, and that in reality it was this that was the active compound. This hypothesis was substantiated when it was noted that the 3-methyl benzisoxazole, compound **166**, synthesised elsewhere in the Ward lab, had proven inactive, while the methyl ketone, compound **165**, retained activity (**Figure 38**). While this might represent genuine SAR around the benzisoxazole target, with the methyl disrupting a key orientation for the molecule, given that the active nitrile is an available isomer of compound **163** it was necessary that the stability was verified.
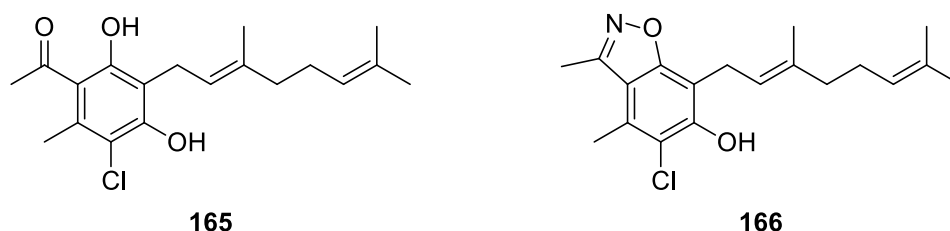

165   **166**

Figure 38 - Additional methyl containing AF analogues

An additional concern was the use of DDQ in the preceding synthetic sequence, which if present in residual quantities in the samples for biological testing, at levels below detection by NMR or LCMS, could potentially result in false positives through redox cycling. The C8 benzisoxazole was dissolved in D_6-DMSO and numerous ^{1}H NMR spectra were taken over the course of two weeks in attempt to monitor any degradation or isomerisation. No change was observed. Samples of the benzisoxazole were also dissolved in DMSO and separately in a solution of the buffers used in the biological assay, and these were followed over two weeks by LCMS. Again there was no detectable degradation to the nitrile, which gave us confidence that the benzisoxazole was stable under the conditions of the assay, particularly, since synthetically, the nitrile formation requires a few hours at room temperature in methanol and in the presence of excess NaOMe.

Alternative 5, 6-heterocycles

The benzisoxazole represented a very interesting new scaffold. In addition, the discovery that the geranyl could be swapped for the simpler octyl chain without loss of activity broadened the spectrum of applicable chemistry. With concerns over the stability of the 5,6 heterocycles still prevalent it was decided that analogues should be synthesised for testing. It was hoped that the indazole could be synthesised from the salicylic motif. This was of particular interest as it would afford the same arrangement of heteroatoms as the benzisoxazole, although a H-bond donor would replace a H-bond acceptor, but it would have no potential to ring open. There are reported examples of direct conversion of simple salicylaldehyde structures. The majority of these involve use of Lewis acids to activate the phenol, presumably such that it is displaced by the hydrazone formed at the benzaldehyde (**Scheme 54**).
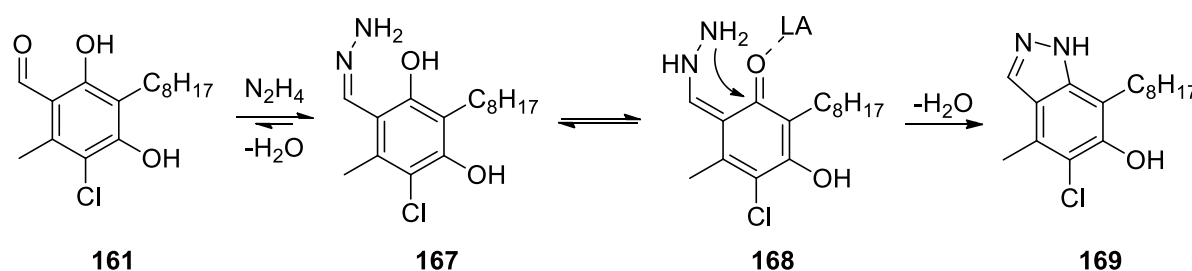
Scheme 54 - Proposed mechanism for indazole formation

The remaining reactions utilise forcing temperatures and polar solvents with excess hydrazine. Unfortunately, none of the desired product, compound **169**, was obtained using any of the reported conditions. It is plausible that the multitude of electron donating functionalities on the fully hexa-substituted ring may make it less amenable to attack by the hydrazone.
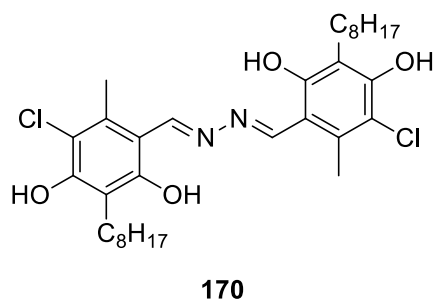
170

One potential explanation could be the formation of compound **170** (**Figure 39**). This might compete with formation of the indazole, but it was hoped that, because imine formation is reversible, excess hydrazine, heat, time and the presence of water would allow the thermodynamic formation of the indazole product. If it was present, its mass was not clear *via* LCMS and there was little shift in the NMR spectrum from the starting material but equally there were no observable NH signals. Methyl hydrazine was used in place of hydrazine in case this dimer was the cause of the problem as it would be unable to form such dimeric compounds. Regrettably, this didn't afford any methyl indazole either and it remains unclear why these indazole formations were unproductive. At this point there was little remaining material and as a result of the problems with both the MOM ether deprotections and indazole formations, another route to these compounds was required.

Conclusion

The *ortho*-lithiation approach facilitated the first successful synthesis of biologically active compounds achieved in this work, and represents a novel chemical route to AF-like compounds. In developing this chemistry novel headgroups were discovered, which should exhibit improved drug-like properties while hopefully retaining activity. It was found that the reactive geranyl chain could be replaced with the simplified octyl whilst retaining excellent biological activity. His greatly expanded the range of chemistry applicable. The benzisoxazole is a more drug-like headgroup than that of known AF analogues, having removed or masked both the benzaldehyde and phenol, which posed key metabolic and toxicity risks. To examine the available chemical space it was necessary that other bicycle heterocyclic headgroups were synthesised. It was hoped

that the indazole, which was of particular interest, could be accessed using this chemistry, but unfortunately efforts were unsuccessful.

At this stage the *ortho*-lithiation approach was of limited use in obtaining further desirable compounds, especially given the reproducibility problems faced with the ethylene glycol deprotection. In addition, only a limited number of 5, 6 heterocycles were accessible from the bisphenol aromatic motif. A new method was required which would enable access of a variety of bicyclic heterocycles and installation of a new functionalisable tail.

Chapter 4 - Benzisoxazole and Indazole synthesis

As a result of the irreproducibility problems faced with the *ortho*-lithiation chemistry and the lack of success in attempts to diversify any compounds that were obtained, it became imperative that an alternate synthetic route was developed. It was believed that use of an aliphatic starting material, compound **48**, as opposed to the aromatic compounds previously utilized, would enable synthesis of a greater number of novel heterocyclic headgroups.

New synthetic method

The benzisoxazole synthesised with the simple octane chain, compound **163**, showed excellent activity against TAO but frustratingly the *ortho*-lithiation approach utilised had become unreliable. In addition, attempts to further elaborate the compounds obtained were unsuccessful and the indazole could not be achieved *via* this route. A new synthetic method was required to enable access to the benzisoxazole and indazole and ideally a range of additional, correctly decorated heterocycles. Displacement of the salicyl *ortho*-phenol had proven unsuccessful but it was noted that the connectivity was identical to 1,3-diketones, which are prevalent in heterocycle formation. This suggested the potential to integrate a late stage aromatisation in any newly proposed synthetic route.
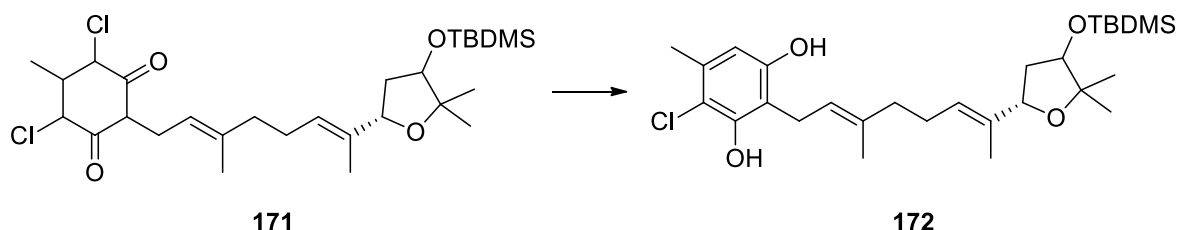

Scheme 55 - Late stage aromatisation reported in AF total synthesis

This is not an entirely novel concept. In one reported total synthesis of AF[254] a chlorination and aromatization had been combined in the final step (**Scheme 55**), although this had been very low yielding. In this work a formylation and aromatization of compound **48** would instead be employed.
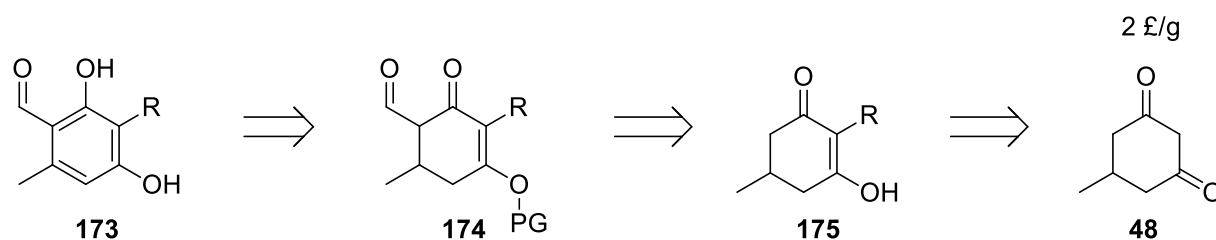
**Scheme 56 - Retrosynthetic analysis**

With this late stage aromatization in mind, retrosynthetic disconnections suggested synthesis *via* the 1,3-dicarbonyl (**48**) and early installation of the tail (**Scheme 56**). An appropriate synthetic route was devised from compound **48** as it benefits from being commercially available and is relatively cheap. Disappointingly, very little chemistry was reported around this compound, although the simpler 1,3-dicyclohexanone was better understood. It was sincerely hoped that this lack of published research was coincidental and not due to any inherent challenges with reactivity and stability. While in the above retrosynthesis the tail is added early in the synthetic route, ideally in order to achieve a range of different tails, diversification should be at late stage. The proposed route (**Scheme 57**) suggested protection of the diketone (**48**) as the enol (**176**) to confer regioselectivity and direct deprotonation at the C-6 position over the otherwise acidic C-2 methylene. This would be followed by lithiation, quench with a formyl equivalent, then cyclisation and deprotection to afford compounds **180** and **181**. The capacity of these compounds for both aromatisation and tail addition would then be examined.
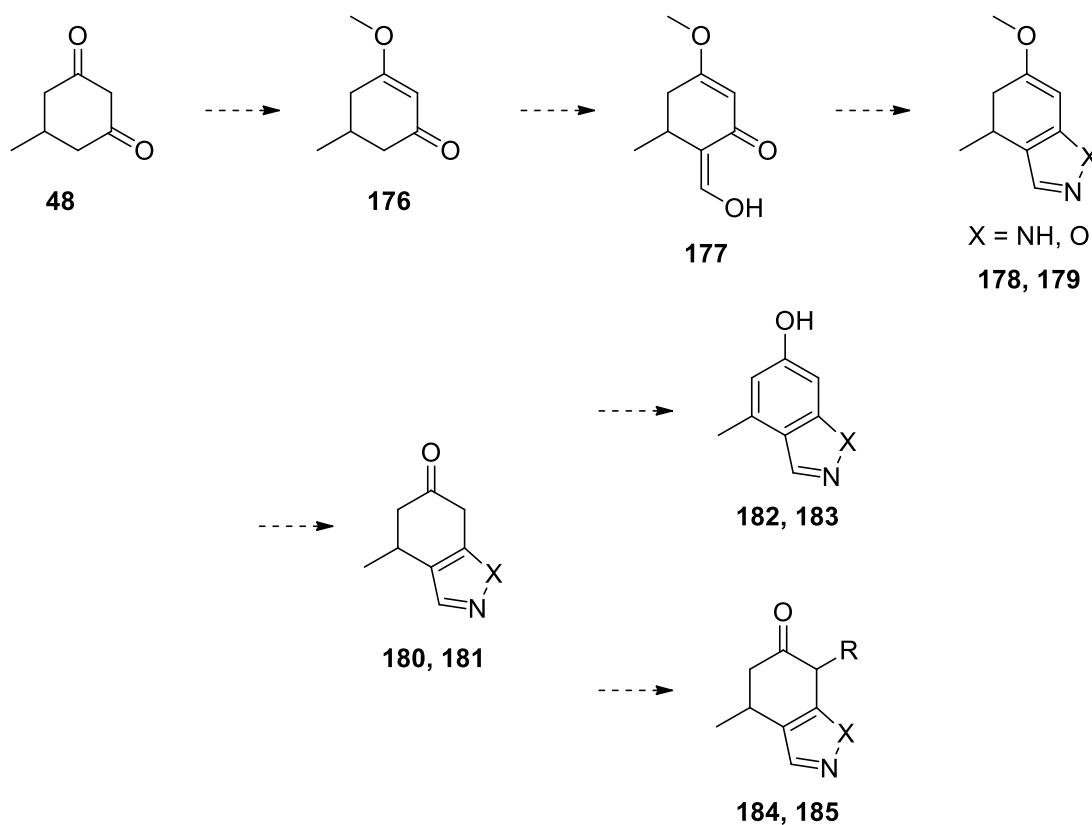
Scheme 57 - Proposed route to validate and explore headgroup formation from aliphatic precursors

Route Validation

Initially an attempt was made to doubly deprotonate the unprotected diketone (**48**) using lithium bases. It was anticipated that only the least stable position on the di-lithiate (**186**) would attack dimethyl formaldehyde (DMF) and thereby enable selective functionalisation without the requirement for protecting groups. These reactions (**Scheme 58**) were repeated several times with lithium diisopropylamide (LDA) in the presence of TMEDA but none of the desired product (**187**) was successfully obtained.
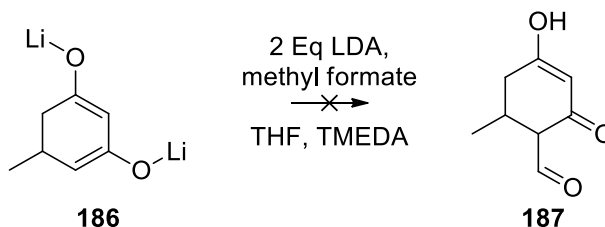
Scheme 58 - Dilithiation failed to yield the desired formylated product.

It appeared therefore that it would be necessary to protect compound **48**. It was decided that a methyl protecting group would be most appropriate as this would be resistant to lithiation conditions but also easy to remove prior to aromatisation using a simple aqueous acidic solution.

Initially there were concerns that use of electrophilic methylating reagents such as iodomethane might result in selectivity problems in which both the carbonyl and C-2 position were alkylated. Therefore, milder conditions using acid and dry methanol were trialed, but these reactions did not approach completion by TLC or ^{1}H NMR spectroscopic evidence. Striving to obtain a more complete conversion several bases and procedures were screened and it was found that addition of sodium hydride to a stirred solution of compound **48** and dimethylsulfate afforded the product in excellent yield (**Scheme 59**). The product (**176**) is clearly characterized: with the observation of the molecular ion with accurate mass by HRMS; the shift in R$_f$ which correlates with the decreased polarity of the product; and in ^{1}H NMR spectroscopy by the appearance of singlet with integration of three protons correlating to the methyl ether, the presence of the 2-CH vinyl signal and the disappearance of the 2-CH$_2$ signal for the bis-ketone tautomer.
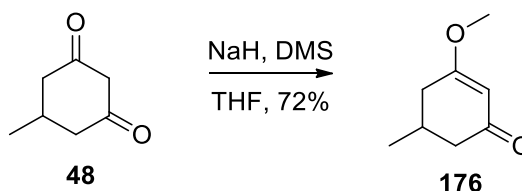

Scheme 59 - Methyl enol ether formation

Lithiation was undertaken with the non-nucleophilic base lithium diisopropylamide (LDA) and DMF was used in attempt to introduce the formyl functionality. Although this was repeated several times, with different sources of dry DMF, no product was successfully obtained. To ensure that the lithiate was being formed, an aliquot was taken from the lithiation reaction and quenched in deuterium oxide. A ^{1}H NMR spectrum of the product showed a ~50% reduction in the intensity of the C-2 methylene signal relative to that of other protons, indicating that the desired lithiate was being successfully formed in > 90% yield. It remains unclear why this reaction with DMF failed, but fortunately reaction with the methyl formate was found to afford the desired

product in > 50% yield. The observation of gentle bubbling upon addition of the formate was attributed to decomposition to carbon monoxide and methanol in the presence of the lithiate base, which may account for the moderate yields.

Eventually it was found that application of sodium methoxide to a solution of compound **176** in dry methyl formate gave the product more easily and in improved yields (**Scheme 60**). The product was clearly characterised: with the observation of the molecular ion with accurate mass by HRMS; the resulting shift from the R_f of the starting material; and in ^{1}H NMR spectroscopy by the appearance of a signal at ~7 ppm, assumed to correspond to the vinylic 6-CH proton. By ^{1}H NMR spectroscopy it appeared that the compound exists primarily (>90%) as the isomer **177** (**Scheme 60**). This can be justified by the improved stability afforded by the increased potential for H-bond interactions and extended conjugation compared to the isomer with the non-conjugated aldehyde. The ^{1}H NMR spectrum of this compound also exhibited a broad vinylic signal and a small signal at > 8 ppm, likely arising from the aldehyde tautomer, which suggests that the tautomers are able to interconvert.
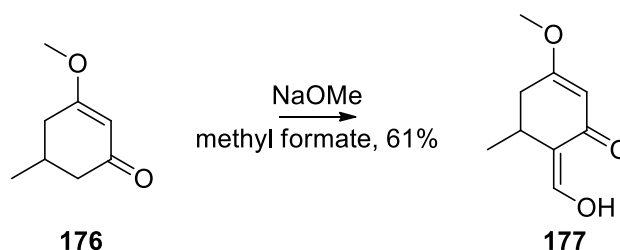
Scheme 60 - Simplified formylation conditions

It was hoped that this success would extend to enable addition of a range of different electrophiles and allow access to other heterocycles, but these reactions were unsuccessful. This was particularly regrettable as it was the potential for exploration that made this synthetic route so attractive initially. The addition of 2-bromo-1,1-diethoxyethane was of particular interest because the resulting methylene aldehyde compound (**188**) would have allowed access to rings with a single heteroatom, compounds **189-191**, which represent unexplored chemical space in TAO inhibitors (**Scheme 61**). It was hoped that in the event that addition of the 2-bromo-1,1-diethoxyethane was unsuccessful, addition of the alpha halo ester would provide an alternate route to the desired compounds after reduction and re-oxidation. In addition,

this route should have afforded other distinct heterocyclic derivatives, such as compound **194** (**Scheme 61**).

Unfortunately, although many reaction conditions were trialed for both electrophiles, none of the desired products were successfully obtained. With the prior success in addition of the formyl and with limited time available, further development from compound **123** was made a priority and the addition of novel electrophiles was discontinued.

Scheme 61 - Proposed route to diverse heterocyclic headgroups

Thankfully, the cyclisation to afford the pyrazole and isoxazole, which was crucial in the synthetic route, proved relatively facile. Stirring of compound **177** with hydrazine hydrochloride in methanol at room temperature afforded the pyrazole (**178**) in excellent yield within minutes. The isoxazole could not be obtained under the same conditions. Different bases and solvents were screened and it was found that stirring compound **177** in pyridine at 60 °C afforded the isoxazole in one hour (**Scheme 62**). The correct molecular ions of the products were observed by mass spectrometry and in the ^{1}H NMR spectrum of each heterocycle there was an indicative shift downfield for the signal corresponding to the vinyl/aldehyde.

It was plausible that the reactions had yielded the 1-*N* isoxazole isomer rather that the desired 1-*O* isomer, compound **179**, and none of the analytical methods employed were capable of distinguishing these. However, there is a strong rationale for selective formation of the 1-*O* isomer (**179**). Firstly, if a combination of both isomers were present this should result in two separate 3-CH signals in the ^{1}H NMR spectrum of the product, with this 3-CH proton being adjacent to two different heteroatoms. In this case however, only one signal was observed. It is expected that imine formation will occur selectively at the aldehyde/enol position, which has lower electron density and is better exposed, thereby affording the 1-*O* isomer. Production of the 1-*N* isomer would require imine formation at the α, β-unsaturated ketone, which has higher electron density due to conjugation with the methoxy ether and is more sterically hindered.
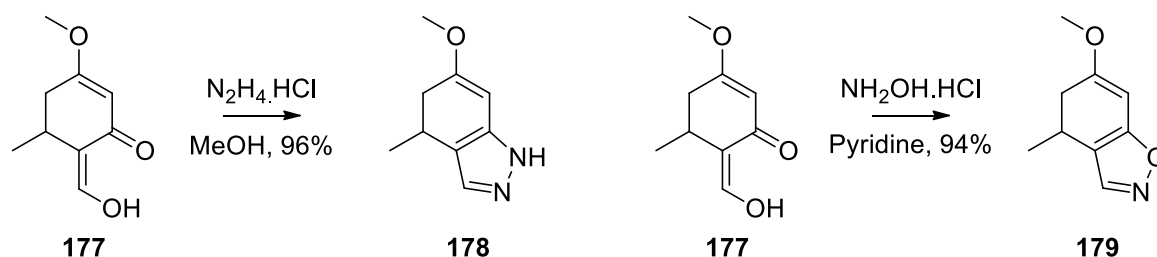
Scheme 62 - Straightforward heterocycle formation

Deprotection of the methyl ether enol proved to be trivial with the product obtained in good yield on first attempt. The starting material was stirred in THF: water with 1 M HCl added to afford the product (**Scheme 63**), and work up comprised a simple extraction, although frustratingly the products obtained were thick, sap-like gums, which were challenging to handle. For both compounds **180** and **181** correct molecular ions were observed by mass spectrometry and the ^{1}H NMR spectrum of each demonstrated the disappearance of both the methyl ether singlet and vinyl singlet signals as well as the appearance of the 7-CH$_2$ geminal signals.
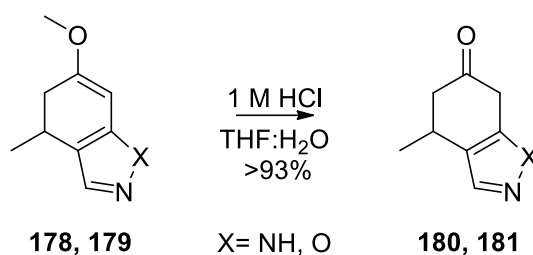
Gratifyingly, following the success of both the cyclisation and deprotection, test reactions suggested that the aromatisation would be equally forthcoming. LCMS results indicated successful product formation by overnight reaction either with palladium on carbon (Pd/C) in toluene at 90 °C, or with chloranil at room temperature. It was hoped that these conditions would prove equally successful in attempts to synthesise biologically relevant target compounds.

Overall this route had so far proven very successful in accessing the intended scaffolds with correct decoration and focus turned to the challenge of attaching the tail to compounds **180** and **181**. Unfortunately, repeated attempts to install a variety of different tails all proved unsuccessful. Reactions with bromooctane and allyl bromide and 1,4-addition of acrylate esters all failed under a variety of conditions. Fortunately, at this point another student tasked with developing the chemistry to attach the octyl chain had a breakthrough. It was found that a one pot l-proline catalyzed Knoevenagel condensation of octanal followed by sodium cyanoborohydride reduction afforded the desired product in nearly quantitative yields.

These reaction conditions were applied to both of the heterocyclic starting materials, **180** and **181**, and by examination of reaction mixtures using LCMS it appeared that the desired products, **195** and **196**, had been achieved. Unfortunately however, the compounds proved difficult to isolate and samples with the correct retention time and molecular ion by LCMS proved to be impure by ^{1}H NMR spectroscopy, even following further purification. At first, the Knoevenagel and reduction steps were attempted in one pot. With the mass of the indazole product was observed by LCMS but repeated attempts at isolation did not yield the desired product. The isoxazole behaved differently and by LCMS appeared to have been reduced twice, resulting in addition of 4 Da. A stepwise approach was also unsuccessful (**Scheme 64**).
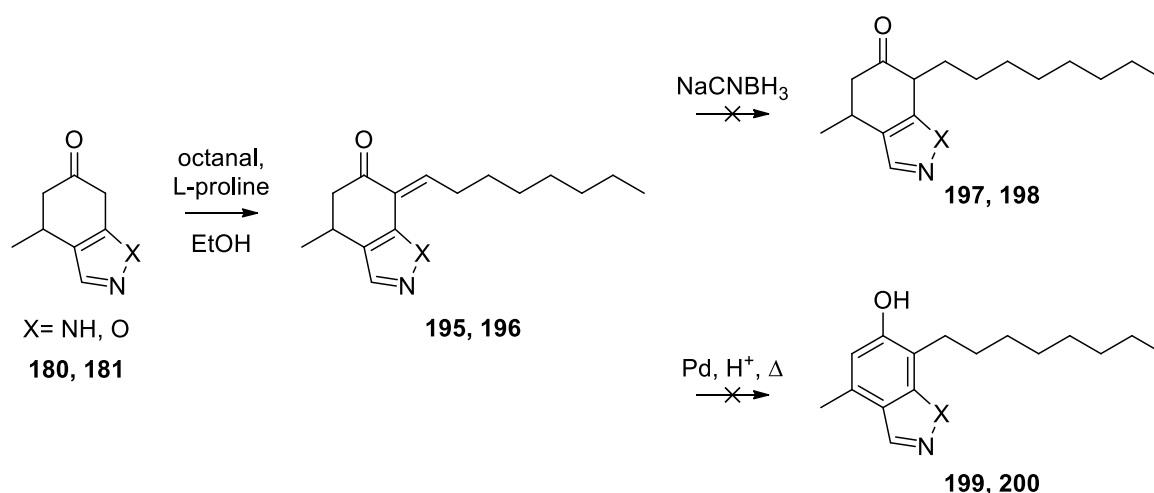
Scheme 64 - Late stage Knovenagel condensation failed to arrive at target compounds

It was clear that compounds **195** and **196** were identifiable by LCMS. Therefore, despite the futility of attempted reduction it was hoped that they could still be utilised in synthesis of the benzisoxazole and indazole, but, this was not achieved. Compounds **195** and **196** already represented a 10 π electron system, which was similar to the 5,6-heterocyclic targets, but containing an undesirable exocyclic olefin. It was hoped that this molecule would be amenable to rearrangement to the target compound. Direct intramolecular 1,4-hydride shift was impossible, with the planarity of the molecule prohibiting the required orbital overlap of the exocyclic olefin and the hydrogen on the 4-position. Instead it was hoped that either introduction of an acid or a metal might encourage aromatisation. The exocyclic compounds **195** and **196** were heated in the presence of acid and palladium on carbon, both separately and in combination.

Different solvents were screened, but all attempts returned the starting compound, which in fact proved highly stable in the presence of heat, acid and/or palladium. Unfortunately, at this point material was running low and with a lack of positive results in this endeavour the focus was diverted to the less preferred method of primary installation of the tail *via* the established Knoevenagel-reduction chemistry.

Synthesis of Octyl analogues
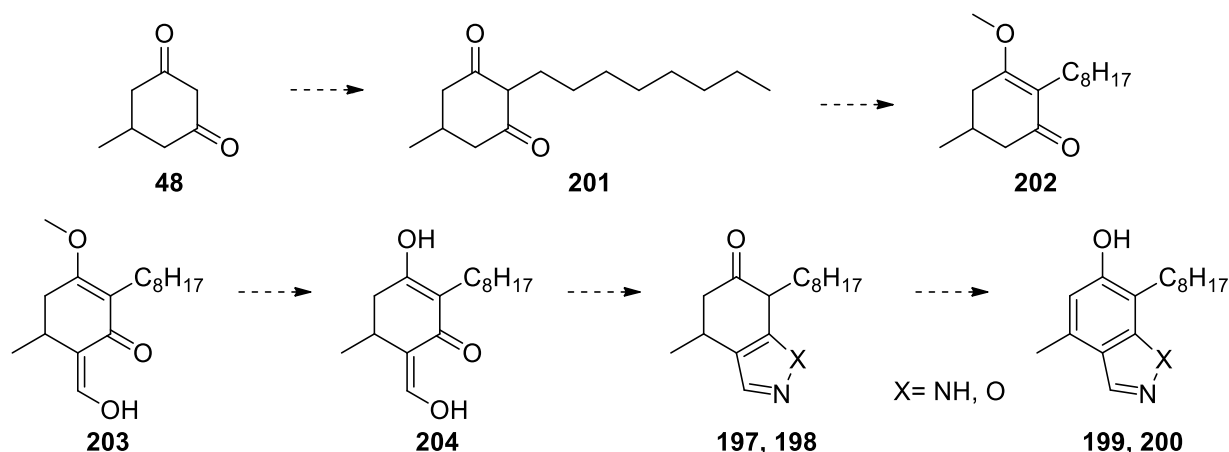
Scheme 65 - Proposed route to indazole and benzisoxazole targets requiring initial installation of the octyl chain

It was intended that following primary installation of the octyl chain the established chemistry would be repeated to resynthesise the benzisoxazole and afford the indazole for the first time (**Scheme 65**). The Knoevenagel condensation and reduction step proceeded repeatedly to excellent yields (> 90%) (**Scheme 66**). The product (**201**) was easily characterised: by the observation of the molecular ion with accurate mass using HRMS; the product provoked a distinct change in retention time *via* LCMS and R_f *via* TLC; and ^{1}H NMR spectrometry clearly exhibits the incorporation of the signals derived from the octyl chain alongside those of the starting material. Unfortunately, due to the complex mixture of isomers present, the ^{1}H and ^{13}C NMR spectra were not fully assigned, but successful onward reaction to the methyl enol ether (**202**), which was fully characterised, confirmed the identity of compound **201**.
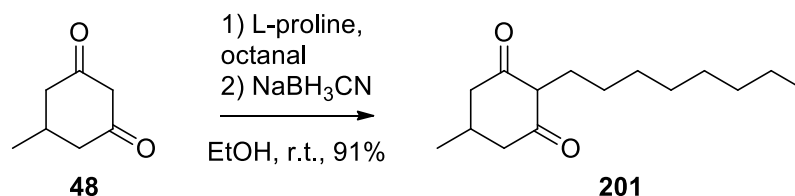
Scheme 66 - One-pot Knoevenagel condensation and reduction

Unfortunately, compound **201** proved unstable and quickly decomposed even when stored under nitrogen at -20 °C. As such, it was required that as material was generated it was immediately used and fortuitously the resulting methyl protected product (**202**) was very stable. The methylated compound **202** was achieved easily and in excellent

yield *via* the established reaction with dimethyl sulfate and the following lithium mediated formylation gave compound **203** in moderate yield (**Scheme 67**). This lithiation appeared more temperamental than those previously undertaken, on some occasions yielding very little product. This was disappointing but not entirely surprising, given that lithiations are often found to be sensitive and inconsistent, but extra care was taken in attempt to ensure the qualities of reagents and technique. Both compounds **202** and **203** were characterised fully: by the observation of the accurate mass of the molecular ion using HRMS; change in retention time *via* LCMS and R$_f$ *via* TLC; and by ^{1}H NMR spectroscopy where compound **202** was easily identified by the appearance of the methoxy singlet for 3H, and compound **203** by the appearance of a broad singlet signal at ~7 ppm corresponding to the vinylic proton and the loss of the C-6 methylene protons.
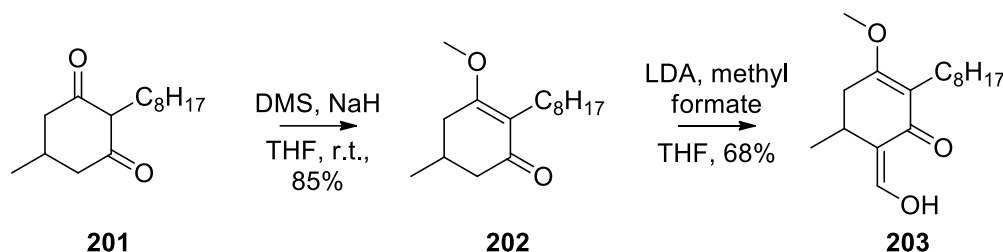
**Scheme 67 - Validated protection and formylation methods applied to C$_8$ compounds**

While previously deprotection of the methyl ether had proved trivial, in this case the same conditions yielded none of the desired product. By LCMS it appeared that the starting material was diminished but with no clear formation of any product and nothing was obtained when the mixture was purified by column chromatography. Various solvents and acids were screened in hope of improving the outcome but this was without success. Further to this, attempts to deprotect the heterocyclic products (**205** and **206**) formed in the subsequent cyclisation step were also unsuccessful. While this setback was disappointing there was a good chance that, even if the methyl could not ultimately be removed, these compounds would retain activity against TAO given that the *para* methoxy phenol of colletochlorin had been demonstrated to have high activity.

Thankfully, heterocycle formation proceeded in good yield (**Scheme 68**), although this was lower than obtained in the absence of the tail. The molecular ion was observable for both compounds **205** and **206**, there is a clear shift in retention time by LCMS, and ^{1}H NMR spectroscopy the vinylic signal is replaced by a distinct aromatic signal.

Treatment of **205** and **206** with Pd/C in toluene gave the aromatized compounds **207** and **208** in excellent yields and were characterised fully: by the observation of the accurate mass molecular ion using HRMS; change in retention time *via* LCMS; and by ^{1}H NMR spectroscopy which displayed obvious simplification with the disappearance of alkyl ring signals and the appearance of a clear aromatic CH singlet.
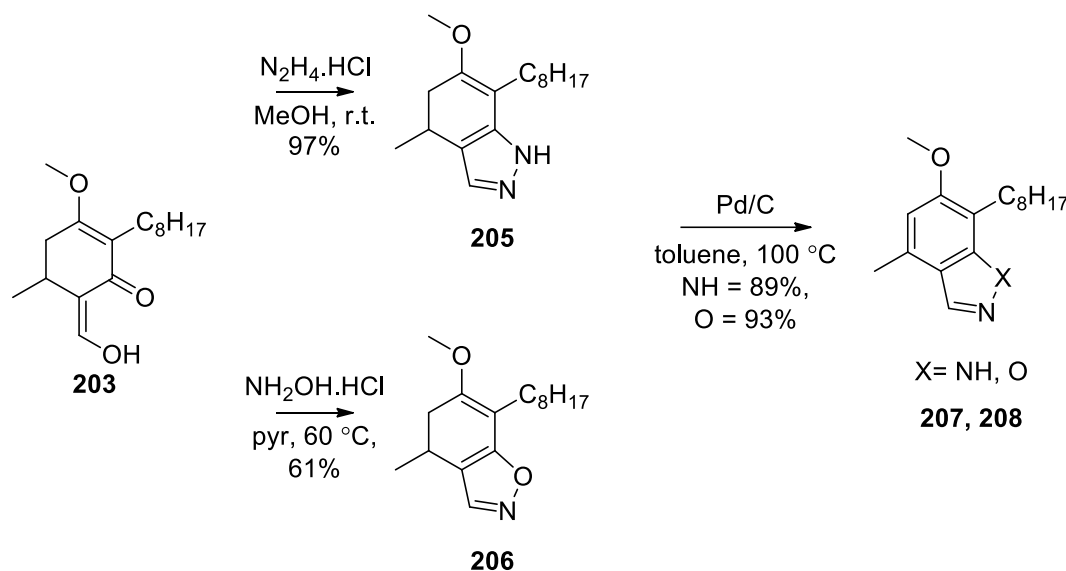
Scheme 68 - Validated chemistry successfully afforded target heterocycles

Although the methylated compounds **207** and **208** are excellent candidates to submit to the TAO assay, the free phenol would enable tighter exploration of SAR. Various methods were trialed for deprotection: organic and inorganic acids under forcing conditions; nucleophilic thiols; BBr$_3$ and TMSI, but all failed to deprotect either compounds **207** or **208**. At this point material was in low supply and the decision was made to focus on other more promising synthetic routes. The deprotection of the benzisoxazole was therefore not examined further.

Disappointingly, at the time of writing this thesis, the compounds synthesised by using this chemistry, that are expected to be biologically significant, have not yet been tested for TAO activity due to a lack of available TAO protein and collaborators. The isolated TAO enzyme assay was previously conducted in-house but unfortunately after the original stock of protein was exhausted, unexpected difficulties were encountered in expression and purification of a new batch of enzyme, which although now overcome, could not produce data in time for this report. Additionally, new collaborations were

being established during the final year of this work to access a wider spectrum of phenotypic, whole trypanosome assays, and unfortunately again, these data were not available in time to be included in this thesis.

Diversifiable synthesis

Having successfully synthesised the octyl compounds, there was a demand for compound diversification to enable exploration of the chemical space around the benzisoxazole tail. It was also intended that the indazole should be elaborated, although this was not yet confirmed active, on the assumption that it is biologically significant and because it can be synthesised *via* the same methodology.

During this work it became abundantly clear that a single change at any position of the multi-substituted aromatic head group could idiosyncratically alter the reactivity of the ring. In light of this, it was preferred that the electronics of the tail be disconnected from those of the head group and therefore conjugate styrene-like connections were discounted. Many different diversifiable tail groups were considered for installation (**Scheme 69**): (1) olefins would allow coupling *via* metathesis; (2) aldehydes could react with partners by reductive amination; (3) esters could be diversified by amide coupling; (4) a leaving group such as a halide or activated alcohol could be directly displaced by nucleophiles. This list of tail connections is in no way exhaustive but would enable very substantial scope for diversification. Unfortunately, at this point in the PhD time was very limited, and therefore only one of these options could be further investigated.
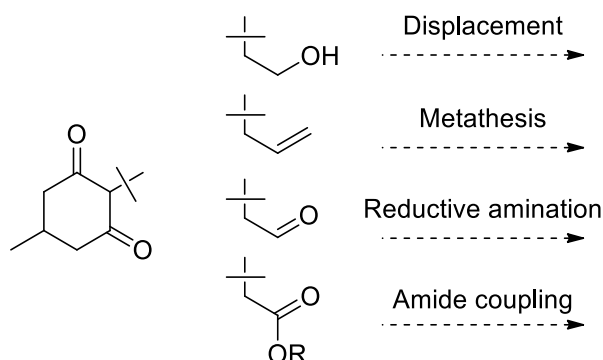
Scheme 69 - Selection of potential diversifiable tail groups

Of the various options available it was decided that the ester represented the best opportunity for diversification: the existing olefin in AF was known to be metabolically

labile and removing it with a selective hydrogenation was potentially challenging; both the alcohol and aldehyde would require specific protection to facilitate the established lithiation chemistry, increasing the number of steps required; the ester on the other hand would likely be stable under the basic and nucleophilic conditions required for lithiation chemistry, could be deprotected under mild conditions and could be diversified to a range of amides. If the synthesis proved facile and plenty of material could be produced, the ester also had the potential to be reduced to the aldehyde or the alcohol. In addition, synthetic methods to install the ester tail-linker had precedent in a successful test reaction between the diketone (**48**) and ethyl acrylate (**Scheme 70**), which was carried out earlier in this work. Although the compound had not been fully characterized, LCMS analysis of the reaction clearly showed product formation.
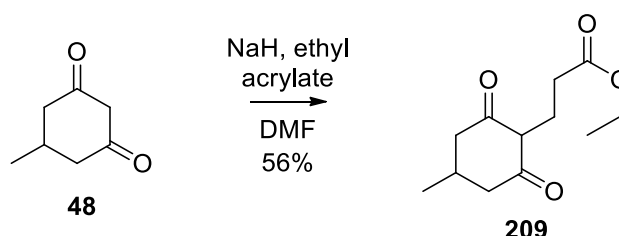

Scheme 70 - Test reaction for acrylate addition

The acrylate derived motif has several other desirable features in addition to enabling diversification: (1) it separates the head group and tail both electronically and sterically; (2) it introduces heteroatoms and increases the polarity, which is necessary in order to reduce the log P compared to that of colletochlorin B (CCB), > 6, and its octyl analogue compound **161** (**Table 8**); (3) with the tail already a minimum of four atoms long it is straightforward to extend it to achieve the empirically derived ideal length of eight atoms using a range of commercially available amines.
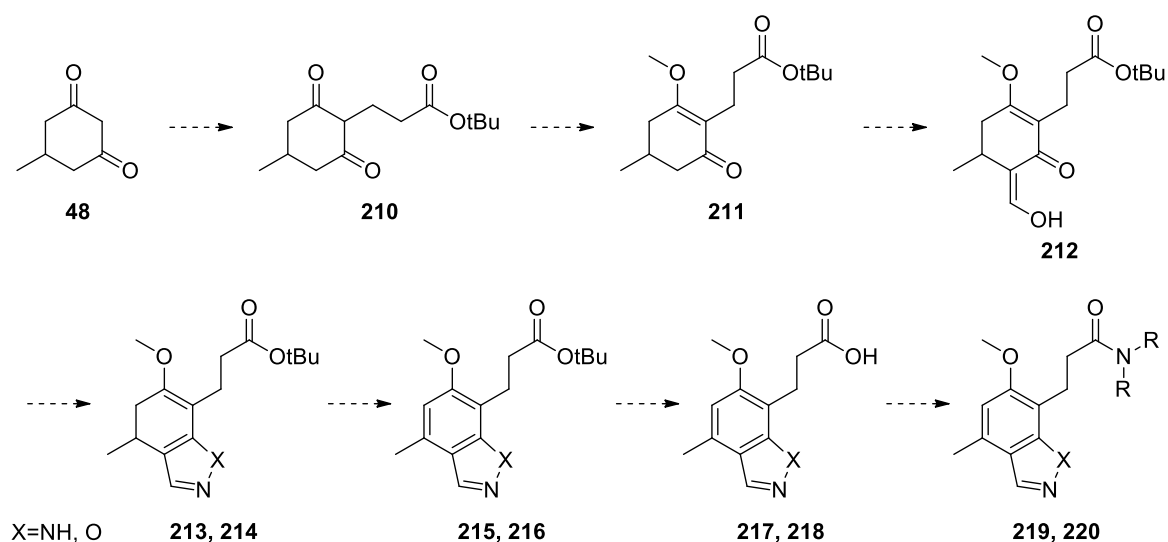
Scheme 71 - Proposed route to diversifiable compounds utilising established chemical methodology

It was proposed that a synthesis nearly identical to that of the octyl (**Scheme 65**) was used (**Scheme 71**). The ethyl acrylate was exchanged for a *tert* butyl ester in the hope that this would impede any reaction between the lithium enolate and the ester, and it could then be easily deprotected using acid.
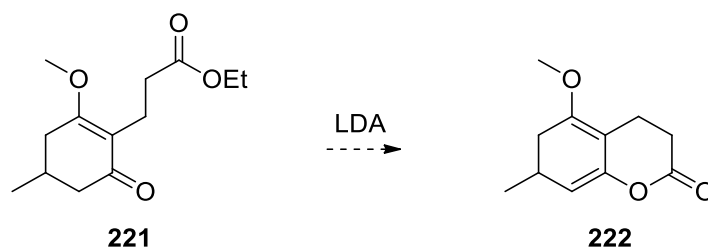
Scheme 72 - Lactone formation a potential risk

It was anticipated that this should alleviate complications resulting from formation of the intramolecular lactone (**222**) (**Scheme 72**). It was briefly considered that the lactone (**223**) (**Figure 40**) could be utilised as a more elegant means of protecting both the enol and ester throughout the synthesis. However, in the six-membered lactone (**Figure 40**) the lone-pairs of the oxygen are not correctly orientated to enable orbital overlap with the carbonyl π^* anti-bonding orbital, and it was feared that the resulting reduction of electron density at the carbonyl would lower the pK_a of the adjacent alpha hydrogens. It was thought that increasing the acidity of this alpha position could afford a competing site for deprotonation and lithiation as an alternative to the desired C-6 position. With

these concerns, and with limited time available, the use of the lactone was left unexplored.
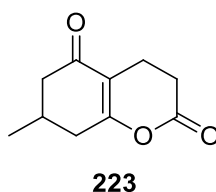

223

Figure 40 - Lactone functionality considered as a protection strategy

The proposed synthesis (**Scheme 71**) was not ideal. There was valid criticism of the continued use of the methyl ether protecting group which had repeatedly proved difficult or impossible to remove. The decision to retain this methyl protection was based principally on advancing the synthesis and avoiding problems associated with the development of unexplored chemistry. As previously stated, it was also anticipated that the methyl phenol derivatives would have similar potency to the free phenols and therefore, whilst the preference was to be able to biologically characterise both the methyl ether and free phenol derivatives, valuable information could be gained from the ethers alone in the event of an unsuccessful deprotection. Alternative protections of the initial diketone compound **48** utilising TBDMSCl and TIPSCl were attempted with no success. This was most likely reagent result of poor quality of reagents and choice of reaction conditions but this was not examined further.

Unfortunately, the synthesis outlined was plagued with repeated setbacks which would delay progress for weeks at a time. Small-scale test reactions to compounds **213** and **214**, prior to aromatization, were successful but not reproducible on larger scale.

Installation of the *t*-Bu acrylate ester was developed and for a period of time proved high yielding. While it appeared that the reaction with ethyl acrylate (**Scheme 70**) proceeded successfully in THF, a quick solvent screen demonstrated that the reaction with the *tert* butyl equivalent was only effective in DMF. This reaction was amenable to scale up and a reaction using 20 g of the diketone (**48**) formed the product in excellent yield >90%. The ability to simply use diethyl ether to extract the product from the reaction mixture followed by a recrystallization expedited this reaction on scale. The ^{1}H NMR spectrum of the product (**210**) has a very broad alkyl region but clearly shows the

t-Bu signal and the doublet ascribed to the methyl on the ring. Observation of an accurate molecular ion by HRMS also confirmed successful product formation. Unfortunately, due to the instability of compound **210**, the product was not further characterised, but, successful onward reaction to the methyl enol ether (**211**) which was fully characterised confirmed the identity of **210**.

Due to downstream problems in the synthesis it was necessary to repeat this reaction many times and infuriatingly, upon purchase of a new batch of starting material, compound **48**, the reaction became unreliable. Another batch was sourced but this too proved ineffectual. A solvent screen was conducted in attempt to circumvent the problem but with no success. The same diketone (**48**) was reordered from a variety of different suppliers and by screening these it was established that one example showed excellent conversion in dimethylacetamide (DMA). The whole process was time consuming and the solution unsatisfactory, especially considering that the cause remains unknown. LCMS and NMR spectroscopy could identify no fault in the starting materials.

The following protection step with dimethyl sulfate and NaH proceeded reliably (**Scheme 73**) in good yield. The product (**211**) was characterised fully: the ^{1}H NMR spectrum is simplified in comparison to that of the starting material, resulting from the lack of available tautomers and there is a distinct addition of a singlet at ~4 ppm corresponding to the methyl ether; there change in LCMS retention time and TLC R_f shift; and the accurate mass of the molecular ion is clearly observable using HRMS.
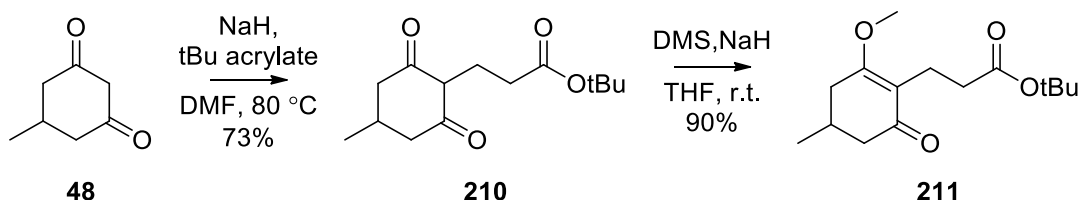

Scheme 73 - Acrylate addition and methylation

Lithiation by the established methyl formate method (**Scheme 74**) proved unreliable and difficult to reproduce. While the majority of reactions proceeded in good yield, around a third would fail to afford more than 10% of the desired product and the starting material could not be recovered even after careful column chromatography.

Accordingly, on a few occasions, large scale lithiations on over 15 g, gave very limited product necessitating synthesis of more starting material. The product obtained in successful reactions was characterised: in ^{1}H NMR spectroscopy by the appearance of the vinylic CH at 7 ppm and the disappearance of the two alkyl ring signals; by the change in retention time in LCMS and R_f in TLC; and by the accurate mass of the molecular ion is clearly observable using HRMS.
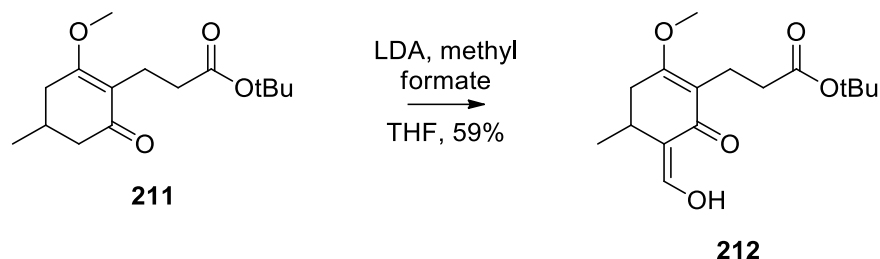

Scheme 74 - Unreliable formylation reaction

Approximately 10 g of the pre-divergent compound **212** was synthesised in several batches, which was then used to produce the pyrazole and isoxazole. The majority was used to in attempt to synthesise the benzisoxazole, which has confirmed activity against TAO and the remainder to be converted to the indazole in the hope that this would retain activity and to enable exploration of SAR. As observed previously, both heterocycle formations (**Scheme 75**) proceeded to product but the pyrazole formed in higher yield than the isoxazole. Both compounds **213** and **214** were characterised in their ^{1}H NMR spectra by a shift in the *exo*-vinylic proton signal to generate a new singlet further downfield and by observation of the correct molecular ion mass using LCMS.
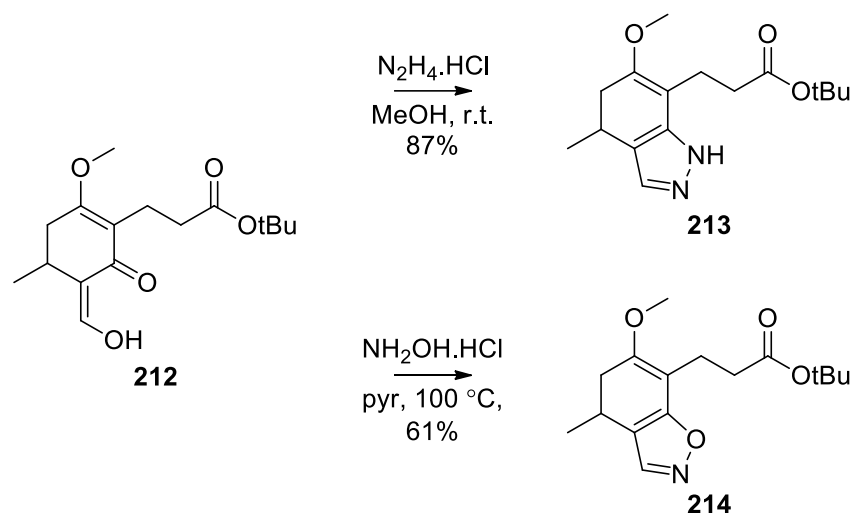
Scheme 75 - Heterocycle formation successful in presence of *tert* butyl ester

Around 5 g of the isoxazole (**214**) and 2 g of the pyrazole (**213**) were successfully synthesised but unfortunately, despite the apparent stability of the test samples, these larger samples decomposed when left for just two days to form unidentified products. Neither sample could be retrieved by column purification so disappointingly they had to be abandoned. As such the entire synthetic route had to be repeated.

The pyrazole had been obtained in sufficient quantities from smaller test reactions, which had not decomposed, to facilitate attempted diversification to some of the amide final products and the isoxazole was successfully resynthesised. The pyrazole and isoxazole were successfully aromatized using DDQ in toluene at room temperature to afford the indazole (**215**) and benzisoxazole (**216**) in excellent yield. The deprotection of the *tert* butyl ester proved similarly facile using trifluoroacetic acid in dichloromethane to produce the free acids **217** and **218** in excellent yield (**Scheme 76**). The products of both steps were clearly identified using ^{1}H NMR spectroscopy. The aromatised compounds **215** and **216** gave a clear 5-CH singlet and a singlet for the tolyl CH_3 with the distinct absence of the alkyl ring protons, whereas the carboxylic acids (**217** and **218**) lacked the characteristic *tert* butyl signal present throughout the synthesis. Both carboxylic acid compounds could also be identified by a change in LCMS retention time and R_f and by observation of the accurate molecular ion mass using HRMS.
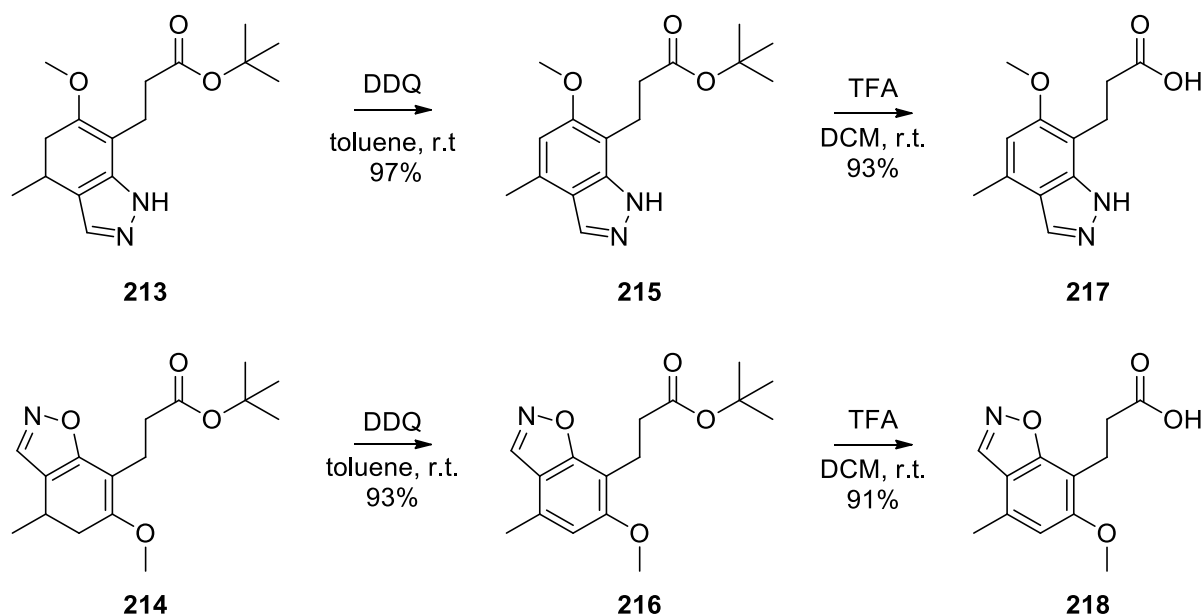
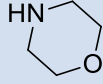**Scheme 76 - Aromatisation and deprotection proceeded in excellent yield**
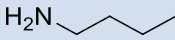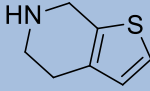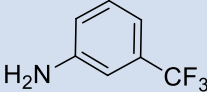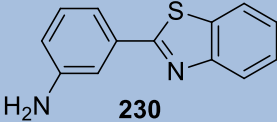
Amide synthesis

It was hoped that diversification of the tailgroup would enable tuning of the PSA and log P of the compound to improve the pharmacokinetic profile while retaining the activity afforded separately by the headgroup. This may be overly simplified considering the increase in potency which results simply from non-specific lipophilic tail-group interactions, as observed with the octyl compounds **160-164**, but nonetheless the compounds (**Table 9**) will enable exploration of SAR and optimisation against both the TAO protein and the whole organism.

**Table 9 - Log P and PSA values for the preliminary range of amide coupled compounds[423]**

Amine	Log P, PSA (Å²) of benzisoxazole amide	Log P, PSA (Å²) of indazole amide
	220	**219**
224	0.84, 71	0.77, 74

Amine		
HN—O (morpholine) **225**	0.96, 60	0.89, 64
HN (pyrrolidine) **226**	1.68, 51	1.60, 54
H_2N— (butylamine) **227**	2.37, 60	2.29, 63
HN—S **228**	2.88, 51	2.98, 54
H_2N—CF_3 **229**	3.71, 60	3.64, 63
H_2N— benzothiazole **230**	5.06, 72	4.98, 75

With a vast number of amines available for coupling to the carboxylic acid compounds **217** and **218**, criteria were applied to narrow the selection. Firstly, for expedience it was decided that the amines should be selected from the 111 available in-house, which we were confident represented an appropriate initial diversity set. Secondly, the most diverse of these amines should be selected whilst excluding undesirable and reactive functionalities. Finally, the coupled amide products should encompass a wide range of log P and PSA values to enable assessment of how these factors influence the inhibition of the TAO protein and whole parasite. With only a limited quantity of the free acids, **217** and **218**, available, only seven amines were selected for trial (**Table 9**).
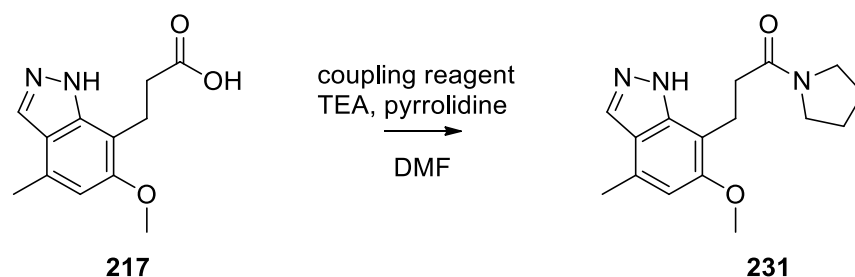
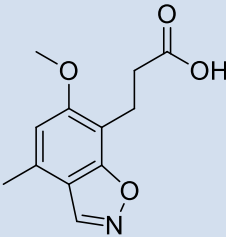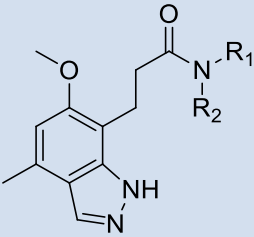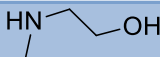Scheme 77 - Coupling reagents screened for amide formation

In order to determine suitable reaction conditions the simple amine pyrrolidine was utilised in a screen of amide coupling reagents (**Scheme 77**): HBTU; HATU; DCC; T_3P; EDAC; and oxalyl chloride. HBTU was found to give the best result and was therefore used in coupling all the amines selected. The amides formed in these initial reactions proved difficult to isolate *via* flash column chromatography so an alternate method of purification was necessary. The optimum process (**Scheme 78**) ultimately developed required that the reactions were executed in 1 mL of DMF and transferred directly to a mass directed auto-purification HPLC. In this way the coupled product was retrieved in much greater purity than other attempted methods.
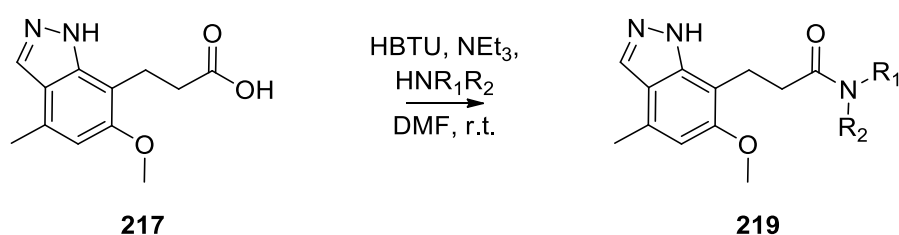
Scheme 78 - Coupling conditions employed in mini-library generation

Positively, for the majority of the reactions coupling preceded successfully, however, unfortunately there was a rather com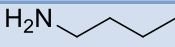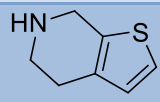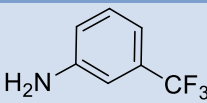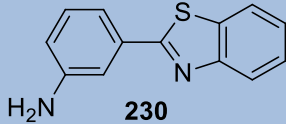plex array of different products obtained in many cases, summarised below (**Table 10**). Four of the couplings with the indazole and six with the isoxazole gave clean LCMS traces containing the accurate molecular ion masses. Of the compounds obtained, three indazoles and three isoxazoles, **231-236**, were characterised by ^{1}H NMR but the others could not be assigned. In addition to the major peaks, the indazoles exhibited a second smaller set of indazole signals that could not be removed by purifying. More disappointingly it was determined that in every example the isoxazole had reacted to form the ring opened *ortho*-phenol nitrile isomer.

Table 10 - Results of preliminary amide couplings

Amine coupled	Benzisoxazole reaction result	Indazole reaction result
	218	217
224	Product Obtained Clear LCMS, HRMS Ambiguous ^{1}H NMR	Product Obtained Clear LCMS, HRMS Ambiguous ^{1}H NMR
225	Nitrile Product Obtained Clear LCMS, HRMS, ^{1}H NMR	Product Obtained Clear LCMS, HRMS, Uninterruptable ^{1}H NMR
226	Nitrile Product Obtained Clear LCMS, HRMS, ^{1}H NMR	Product Obtained Clear LCMS, HRMS, ^{1}H NMR
227	Nitrile Product Obtained Clear LCMS, HRMS, ^{1}H NMR	Product Obtained Clear LCMS, HRMS, ^{1}H NMR
228	Product Obtained Clear LCMS, HRMS Ambiguous ^{1}H NMR	Failed
229	Failed	Failed
230	Product Obtained Clear LCMS, HRMS Ambiguous ^{1}H	Failed

Those compounds successfully obtained, **231-236**, were characterised by ^{1}H NMR spectroscopy and confirmed by a combination of the appropriate amide signals and well-established heterocycle signals, and by HRMS where the exact mass of each molecular ion was observable, which confirmed the atomic composition of the products; they were not characterised further due to time restraints. Evidently this coupling reaction requires further optimisation but this was beyond the scope of this work. The

six compounds (**Figure 41**) synthesised represent the first exploration of this 5,6-heterocycle for the inhibition of TAO and examination of their activity is eagerly anticipated.
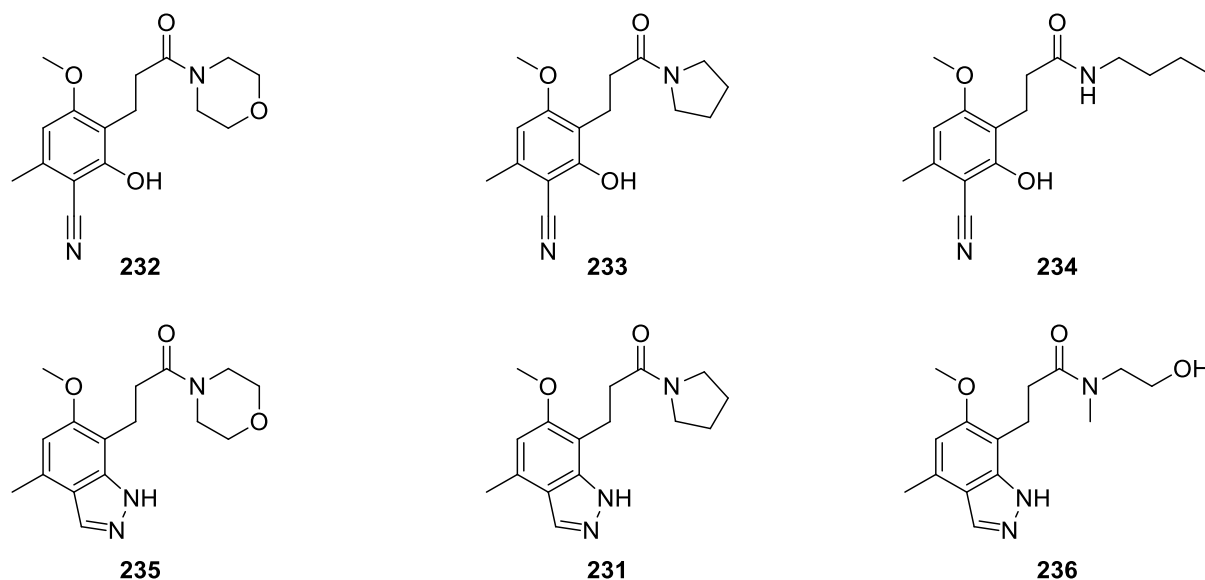
Figure 41 - Amides successfully observed and partially characterised

Conclusion

The limitations of the *ortho*-lithiation synthesis required the development of new synthetic methods to allow for both the synthesis of novel heterocyclic headgroups and the installation and diversification of a suitable tail. These goals were successfully achieved from the commercially available aliphatic diketone (**48**) as an alternative to the aromatic compounds (**45** and **51**) utilised previously. This choice greatly facilitated heterocycle formation, and by employing a late stage aromatisation an entirely novel range of drug-like AF analogues were synthesised.

Initial validation of this new synthesis was promising and confirmed that late stage aromatisation represented a viable method for constructing the 4-methyl-6-phenol indazole and benzisoxazole motifs, although regrettably other heterocyclic cores proved inaccessible. Attention then turned to synthesis of the octyl chain AF analogues for the indazole (**199**) and benzisoxazole (**200**). The successful synthesis of these compounds further validated the synthetic method and gave the first indazole ascofuranone

analogue, compound **207**. Finally, focus shifted to the synthesis of diversifiable analogues of the two heterocyclic cores, compounds **215** and **216**. Despite a plethora of synthetic challenges, the two carboxylic acid compounds **217** and **218** were synthesised in sufficient yield to enable development of an amide coupling reaction, which afforded a set of six novel amide compounds.

This work represents the preliminary exploration of this chemical space and although the products obtained were modest in number and potentially more complex than desired, they serve to validate this method for access to novel AF analogues. These methods permit synthesis of a variety of heterocycles, afford compounds with the required aromatic ornamentation and, in addition, facilitate installation of diverse tail groups. Another student has begun further investigation of this chemistry and elucidation of the SAR around these new analogues will add to this work and be published accordingly.

Chapter 5 - Experimental

All reactions were conducted under an atmosphere of nitrogen unless otherwise stated. Anhydrous solvents were used as purchased or were purified under nitrogen as follows using activated molecular sieves.

Thin layer chromatography was performed on glass plates pre-coated with Merck silica gel 60 F_{254}. Visualisation was achieved with U.V. fluorescence (254 nm) or by staining with a phosphomolybdic acid dip or a potassium permanganate dip. Flash column chromatography was carried out using pre-packed columns filled with Aldrich silica gel (40-63 µm) on an ISCO Combiflash Rf, or a Biotage Isolera Prime.

Proton nuclear magnetic resonance spectra were recorded at 500 MHz on a Varian 500 spectrometer (at 30 °C), using residual isotopic solvent (CHCl$_3$, δ_H = 7.27 ppm, DMSO δ_H = 2.50 ppm, 3.33 ppm (H$_2$O), MeOH δ_H = 3.31 ppm, 4.87 ppm (H$_2$O)) as an internal reference. Chemical shifts are quoted in parts per million (ppm). Coupling constants (J) are recorded in Hertz (Hz).

Carbon nuclear magnetic resonance spectra were recorded at 125 MHz on a Varian 500 spectrometer and are proton decoupled, using residual isotopic solvent (CHCl$_3$, δ_C = 77.00 ppm, DMSO δ_C = 39.52 ppm) as an internal reference. Carbon spectra assignments are supported by DEPT editing and chemical shifts (δ_C) are quoted in ppm.

Infrared spectra were recorded on a Perkin Elmer FT-IR Spectrum One spectrometer as a neat sample. Absorption maxima are reported in wave numbers (cm^{-1}). Only significant absorptions are presented in the data, with key stretches identified in brackets.

LCMS data was recorded on a Waters 2695 HPLC using a Waters 2487 UV detector and a Thermo LCQ ESI-MS. Samples were eluted through a Phenomenex Lunar 3µ C18 50 mm × 4.6 mm column, using acetonitrile and water (3 : 7 to 7 : 3) acidified by 0.01% formic acid

HPLC data and purification was performed on an Agilent 1100 series HPLC spectrometer, using a Phenominex Luna 10 µ C18 150 mm ×15 mm column, eluted using acetonitrile and water (3 : 7 to 7 : 3)

High resolution mass spectrometry data (ESI) were recorded on Bruker Daltonics Apex III ESI-MS, with an Apollo ESI using a methanol spray. Only molecular ions, fractions from molecular ions and other major peaks are reported as mass/charge (*m/z*) ratios.

Microwave reactions were performed using a Biotage Initiator 8+ microwave reactor in sealed reaction vials. Specific conditions for each reaction are reported separately.

Melting points were taken on a Griffin melting point apparatus.

Compounds were primarily bought from Sigma Aldrich however compound **24** was purchased from Acros Organic when the batch from Sigma Aldrich was found to not yield consistent results.

Methyl 3-chloro-4,6-dihydroxy-2-methylbenzoate[260] (**81**)
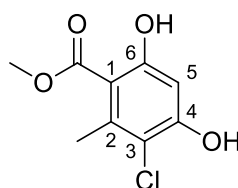
A dropping funnel was charged with sulfuryl chloride (0.82 mL, 10 mmol) in anhydrous diethyl ether (5 mL). This solution was added in a drop-wise manner to a solution of methyl 2,4-dihydroxy-6-methylbenzoate (1.87 g, 10.3 mmol) in diethyl ether (30 mL). The reaction was stirred for 1 hour at room temperature and then refluxed for 2 hours. Upon completion the reaction was allowed to cool to room temperature then water (15 mL) added and stirred for 5 minutes. The diethyl ether was separated and the aqueous layer extracted with diethyl ether (2 x 15 mL). The organic fractions were combined, dried over magnesium sulfate, filtered and concentrated under reduced pressure. Purification by flash column chromatography (25 g silica), eluting with a gradient of 40-60 °C petrol ether: ethyl acetate (100:0) to (90:10), gave the title compound as a cream coloured solid (0.79 g, 36%): MS (EI) m/z (%): 216 (72), 218 (62), 220 (22) $[M]^+$; R_f 0.35 (10% ethyl acetate / 90% 40-60 °C petrol ether); ^{1}H NMR (500 MHz, chloroform-d) δ 11.40 (1 H, s, 6-OH), 6.53 (1 H, s, 5-CH), 6.16 (1 H, s, 4-OH), 3.95 (3 H, s, 1-CH_3), 2.62 (3 H, s, 6-CH_3).

Methyl 3-chloro-4,6-dihydroxy-5-iodo-2-methylbenzoate (**82**)
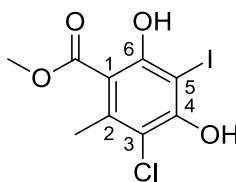
Benzyltrimethylammonium dichloroiodonate (2.66 g, 7.64 mmol) and potassium hydrogen carbonate (2.29 g, 20.8 mmol) were added to a stirred solution of methyl 3-chloro-4,6-dihydroxy-2-methylbenzoate (1.50 g, 6.94 mmol), methanol (40 mL) and dichloromethane (50 mL) then the reaction was left to stir for 16 hours. The reaction was diluted with water (50 mL) and the organic layer separated. The remaining aqueous layer was washed with dichloromethane (2 x 60 mL). The organic extracts were then combined, dried over magnesium sulfate, filtered and concentrated under reduced pressure. Purification by flash column chromatography (25 g silica), eluting with a gradient of 40-60 °C petrol ether: ethyl acetate (100:0) to (85:15), gave the title compound as a white solid (1.96 g, 83%): mp 98-103 °C; R_f 0.26 (10% ethyl acetate / 90% 40-60 °C petrol ether); HRMS-ESI m/z $[M+Na]^+$ calcd for $C_9H_9ClINaO_4$: 364.9048, found: 364.9050; ^1H NMR (500 MHz, chloroform-d) δ 12.40 (1 H, s, 6-OH), 6.53 (1 H, s, 4-OH), 3.98 (3 H, s, 1-CH$_3$), 2.60 (3 H, s, 6-CH$_3$); ^{13}C NMR (125 MHz, chloroform-d) δ 171.2 (C), 161.4 (C), 155.7 (C), 139.7 (C), 112.9 (C), 106.8 (C), 72.0 (C), 52.8 (CH$_3$), 20.0 (CH$_3$); IR (neat, v_{max}) cm^{-1} 3441, 1647, 1444, 1380, 1298, 1217, 1124, 1088, 799, 712.

± Methyl 2-hydroxy-6-methyl-4-oxocyclohex-2-enecarboxylate[261] (**42**)
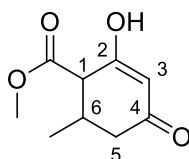
Sodium metal (5.75 g, 250 mmol) was fully dissolved in methanol (150 mL) at 0 ˚C. Methylacetoacetate (26.9 mL, 250 mmol) and methylcrotonate (26.4 mL, 250 mmol) were added and the reaction mixture was refluxed for 3 days. The reaction was allowed to cool to room temperature, the majority of the methanol was removed under reduced pressure and the remaining was diluted with water (70 mL) and acidified with 1 M aqueous hydrogen chloride solution (20 mL). The acidified mix was then extracted with ethyl acetate (3 x 100 mL). The combined organic extracts were dried over magnesium sulfate, filtered and concentrated under reduced pressure. Recrystallisation from diethyl ether afforded the title compound as a white powder (29.1 g, 64%): R_f 0.44 (100% ethyl acetate); HRMS-ESI m/z [M+H]$^+$ calcd for $C_9H_{13}O_4$: 185.0808, found: 185.0809; ^{1}H NMR (400 MHz, dmso-d_6) 5.19 (1 H, s, 3-CH), 3.61 (3 H, s, 1-CH_3), 3.07 (1 H, d, J = 11 Hz, 1-CH), 2.38-2.14 (3 H, m, 5-CH_2 and 6-CH), 0.93 (3 H, d, J = 6 Hz, 6-CH_3).

Methyl 3-bromo-2,4-dihydroxy-6-methylbenzoate[243] (**43**)
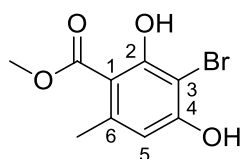
A solution of bromine (5.35 mL, 110 mmol) in acetic acid (40 mL) was added drop-wise to a stirred solution of methyl 2-hydroxy-6-methyl-4-oxocyclohex-2-enecarboxylate (10.1 g, 55.6 mmol) in acetic acid (40 mL) and the reaction was stirred at room temperature for 15 hours. The reaction was poured onto ice and the precipitated filtered off. Purification of this precipitate by flash column chromatography (100 g silica), eluting with a gradient of 40-60 °C petrol ether: ethyl acetate (100:0) to (85:15), gave the title compound as a white solid (10.0 g, 69%): R_f 0.16 (10% ethyl acetate / 90% 40-60 °C petrol ether); HRMS-ESI m/z [M+Na]$^+$ calcd for $C_9H_9BrNaO_4$: 282.9576, found: 282.9578; ^{1}H NMR (500 MHz, chloroform-d) δ 12.54 (1 H, s, 2-OH), 6.48 (1 H, s, 5-CH), 5.97 (1 H, s, 4-OH), 3.97 (3 H, s, 1-CH$_3$), 2.50 (3 H, s, 6-CH$_3$); ^{13}C NMR (125 MHz, chloroform-d) δ 171.9 (C), 161.0 (C), 156.8 (C), 142.6 (C), 110.6 (CH), 106.2 (C), 96.6 (C), 52.3 (CH$_3$), 24.1 (CH$_3$); IR (neat, ν$_{max}$) cm^{-1} 3397, 2953, 1626, 1577, 1440, 1439, 1308, 1260, 1208, 1074, 1022, 958, 794.

Methyl 3-bromo-5-chloro-2,4-dihydroxy-6-methylbenzoate[243] (**51**)
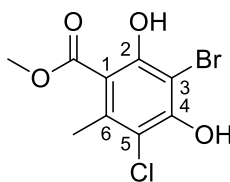
Methyl 3-bromo-2,4-dihydroxy-6-methylbenzoate (1.00 g, 3.71 mmol) was dissolved in dichloromethane (20 mL) and cooled to 0 °C. Sulfryl chloride (0.38 mL, 4.6 mmol) was added and the reaction allowed warm to room temperature over and was stirred for 3 hours. The reaction was quenched with saturated aqeous sodium hydrogen carbonate (20 mL) and the organic layer separated. The aqeous layer was extracted with dichloromethane (2 x 20 mL). The organics were dried over magnesium sulfate, filtered and concentrated under reduced pressure. This gave the title compound as a white solid (1.07 g, 98%): mp 68-72 °C; HRMS-ESI m/z [M+Na]$^+$ calcd for $C_9H_8BrClNaO_4$: 318.9167, found: 318.9160; ^{1}H NMR (500 MHz, chloroform-d) 12.18 (1 H, s, 2-OH), 6.46 (1 H, s, 4-OH), 3.99 (3 H, s, 1-CH$_3$), 2.63 (3 H, s, 6-CH$_3$).

Methyl 2,4-dihydroxy-6-methylbenzoate[262] (**88**)
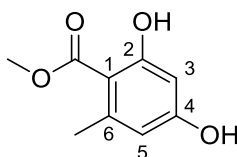
Iodine (1.95 g, 7.60 mmol) was added to a stirred solution of methyl 2-hydroxy-6-methyl-4-oxocyclohex-2-enecarboxylate (0.70 g, 3.8 mmol) in acetic acid (7.5 mL) and the reaction was stirred at room temperature for 15 hours. The reaction was diluted with water (30 mL) and extracted with ethyl acetate (3 x 30 mL). The combined extracts were washed with a saturated aqueous sodium bicarbonate solution (3 x 30 mL), brine (30 mL) and dried over magnesium sulfate. Purification by flash column chromatography (50 g silica), eluting with a gradient of 40-60 °C petrol ether: ethyl acetate (100:0) to (90:10), gave the title compound as a colourless solid (0.31 g, 44%): R_f 0.48 (10% ethyl acetate / 90% 40-60 °C petrol ether); MS (EI) m/z (%): 182 (72), 183 (10) [M]$^+$; ^{1}H NMR (500 MHz, chloroform-d) δ 11.70 (1 H, s, 2-OH), 6.28 (1 H, s, 3-CH), 6.23 (1 H, s, 5-CH), 5.08 (1 H, s, 4-OH), 3.94 (3 H, s, 9-CH$_3$), 2.53 (3 H, s, 7-CH$_3$).

Methyl 3-bromo-5-chloro-2,4-dimethoxy-6-methylbenzoate[263] (**83**)
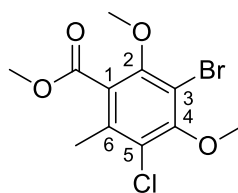
Dimethylsulfate (0.81 mL, 8.5 mmol) was added to a stirred suspension of methyl 5-bromo-3-chloro-4,6-dihydroxy-2-methylbenzoate (1.00 g, 3.40 mmol), potassium carbonate (1.07 g, 8.46 mmol) and acetone (10 mL). The reaction was refluxed for 3 hours then allowed to cool to room temperature and concentrated under reduced pressure. The concentrated mixture was transferred to a separating funnel with ethyl acetate (15 mL) and washed with a 1 M aqueous sodium hydroxide solution (3 x10 mL). The organics were dried over magnesium sulfate, filtered and concentrated under reduced pressure. Purification by flash column chromatography (10 g silica), eluting with a gradient of 40-60 °C petrol ether: ethyl acetate (100:0) to (90:10), gave the title compound as a colourless oil (0.90 g, 83%): R_f 0.16 (10% ethyl acetate / 90% 40-60 °C petrol ether); HRMS-ESI m/z [M+Na]+ calcd for $C_{11}H_{12}BrClNaO_4$: 344.9500, found: 344.9497; ^{1}H NMR (500 MHz, chloroform-d) δ 3.95 (3H, s, 1-CH$_3$), 3.90 (3H, s, 4-CH$_3$), 3.88 (3H, s, 2-CH$_3$), 2.30 (3H, s, 6-CH$_3$); ^{13}C NMR (125 MHz, chloroform-d) δ 166.9 (C), 155.1 (C), 153.5 (C), 134.4 (C), 127.2 (C), 125.7 (C). 111.2 (C), 62.3 (CH$_3$), 60.5 (CH$_3$), 52.6 (CH$_3$), 17.5 (CH$_3$).

Methyl 3-chloro-5-iodo-4,6-dimethoxy-2-methylbenzoate (**85**)
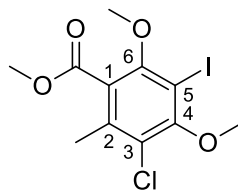
Dimethylsulfate (0.81 mL, 4.8 mmol) was added to a stirred suspension of methyl 3-chloro-4,6-dihydroxy-5-iodo-2-methylbenzoate (0.750 g, 2.19 mmol), potassium carbonate (0.67 g, 4.8 mmol) and acetone (10 mL). The reaction was refluxed for 5 hours then was allowed to cool to room temperature and concentrated under reduced pressure. The concentrated mixture was transferred to a separating funnel with ethyl acetate (15 mL) and washed with a 1 M aqueous sodium hydroxide solution (3 x 10 mL). The organics were dried over magnesium sulfate, filtered and concentrated under reduced pressure. Purification by flash column chromatography (10 g silica), eluting with a gradient of 40-60 °C petrol ether: ethyl acetate (100:0) to (90:10), gave the title compound as a clear oil with a yellow hue (0.62 g, 77%): R_f 0.50 (10% ethyl acetate / 90% 40-60 °C petrol ether); HRMS-EI m/z [M+Na]$^+$ calcd for $C_{11}H_{12}ClINaO_4$: 392.9361, found: 392.9358; ^{1}H NMR (500 MHz, chloroform-d) δ 3.95 (3 H, s, 1-CH_3), 3.88 (3 H, s, 4 or 6-CH_3), 3.85 (3 H, s, 4 or 6-CH_3), 2.31 (3 H, s, 2-CH_3); ^{13}C NMR (125 MHz, chloroform-d) δ 166.9 (C), 157.6 (C), 156.1 (C), 135.9 (C), 126.7 (C), 124.7 (C), 87.5 (C), 62.6 (CH_3), 60.5 (CH_3), 52.7 (CH_3), 17.5 (CH_3); IR (neat, v_{max}) cm^{-1} 2940, 1723, 1373, 1256, 1083, 961, 926, 708.

Methyl 3-chloro-4,6-dimethoxy-2-methyl-5-(3-methylbut-2-en-1-yl)benzoate (**86**)
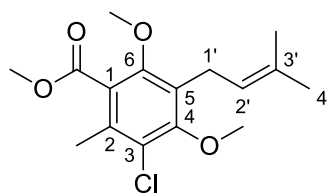
Methyl 3-chloro-5-iodo-4,6-dimethoxy-2-methylbenzoate (100 mg, 0.27 mmol), 3-methyl-2-butenylboronic acid pinacol ester (66 mg, 0.34 mmol) and an aqueous 1 M potassium carbonate solution (0.81 mL) was were combined in dioxane (0.8 mL). Nitrogen gas was bubbled through the reaction mixture for 10 minutes to degas the reaction. Pd(dppf)Cl$_2$ (22 mg, 0.03 mmol) was added and the reaction was heated to 100 °C for 2 hours. The reaction was allowed to cool to room temperature then transferred to a separating funnel with water (10 mL) and ethyl acetate (10 mL). The organic layer was separated and the aqueous layer was extracted further with ethyl acetate (2 x 10 mL). The combined organic extracts were washed with brine (20 mL), dried over magnesium sulfate, filtered and concentrated under reduced pressure. Purification by flash column chromatography (10 g silica), eluting with a gradient of 40-60 °C petrol ether: ethyl acetate (100:0) to (90:10), gave the title compound (42 mg, 49%) as a colourless oil: ^{1}H NMR (500 MHz, chloroform-d) δ 5.19-5.12 (1 H, m, 2'-CH), 3.93 (3 H, s, 1-CH$_3$), 3.82 (3 H, s, 4 or 6-CH$_3$), 3.76 (3 H, s, 4 or 6-CH$_3$), 3.36 (2 H, d, *J* = 7 Hz, 1'-CH$_2$), 2.29 (3 H, s, 2-CH$_3$), 1.77 (3 H, s, 3' or 4'-CH$_3$), 1.68 (3 H, s, 3' or 4'-CH$_3$).

Methyl 3-bromo-2,4-dimethoxy-6-methylbenzoate[264] (**99**)
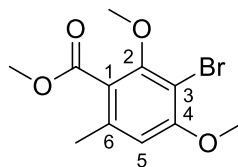
Dimethylsulfate (0.76 mL, 8.0 mmol) was added to a stirred suspension of methyl 3-bromo-4,6-dihydroxy-5-2-methylbenzoate (830 mg, 3.20 mmol), potassium carbonate (1.10g, 7.97 mmol) and acetone (10 mL). The reaction was refluxed for 3 hours then allowed to cool to room temperature and concentrated under reduced pressure. The concentrated mixture was transferred to a separating funnel with ethyl acetate (25 mL) and washed with a 1 M aqueous sodium hydroxide solution (3 x 15 mL). The organics were dried over magnesium sulfate, filtered and concentrated under reduced pressure. Purification by flash column chromatography (10 g silica), eluting with a gradient of 40-60 °C petrol ether: ethyl acetate (100:0) to (90:10), gave the title compound as a colourless oil (0.82 g, 89%): R_f 0.34 (10% ethyl acetate / 90% 40-60 °C petrol ether); MS (EI) m/z (%): 288 (70), 290 (65) [M]$^+$; ^{1}H NMR (500 MHz, chloroform-d) δ 6.52 (1 H, s, 5-CH), 3.91 (3 H, s, 2-CH$_3$), 3.89 (3 H, s, 4-CH$_3$), 3.88 (3 H, s, 1-CH$_3$), 2.30 (3 H, s, 6-CH$_3$).

Methyl 4-acetoxy-2-hydroxy-6-methylbenzoate (**116**)
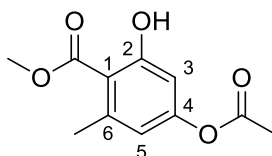
Methyl 2,4-dihydroxy-6-methylbenzoate (520 mg, 2.86 mmol) and triethylamine (400 µL, 2.86 mmol) were dissolved in dichloromethane (10 mL). The mixture was cooled to 0 ˚C and acetyl chloride (205 µL, 2.86 mmol) was added. The reaction was stirred at 0 ˚C for 30 minutes and then allowed to come to room temperature and stirred for 1 hour. The reaction was diluted with brine (20 mL) and the organic layer separated. The aqueous phase was washed with dichloromethane (2 x 15 mL) and the combined organic extracts were dried over magnesium sulfate, filtered and concentrated under reduced pressure onto silica gel (1 g). Purification by flash column chromatography (10 g silica), eluting with a gradient of 40-60 °C petrol ether: ethyl acetate (100:0) to (90:10), gave the title compound as a white powder (0.52 g, 81%): mp 56-60 °C; R_f 0.74 (20% ethyl acetate / 80% 40-60 °C petrol ether); HRMS-EI m/z $[M+H]^+$ calcd for $C_{11}H_{13}O_5$: 225.0757, found: 225.0757; ^{1}H NMR (500 MHz, chloroform-d) δ 11.50 (1 H, s, 2-OH), 6.62 (1 H, s, 3-CH), 6.50 (1 H, s, 5-CH), 3.96 (3 H, s, 1-CH$_3$) , 2.54 (3 H, s, 6-CH$_3$), 2.29 (3 H, s, 4-CH$_3$); ^{13}C NMR (126 MHz, chloroform-d) 171.7 (C), 168.5 (C), 164.2 (C), 154.7 (C), 143.1 (C), 116.4 (CH), 110.1 (C), 108.5 (CH), 52.1 (CH$_3$), 24.01 (CH$_3$), 21.01 (CH$_3$); IR (neat, ν_{max}) cm^{-1} 2957, 1761, 1656, 1316, 1264, 1190, 1136, 1066.

Methyl 4-acetoxy-3-chloro-6-hydroxy-2-methylbenzoate (**117**)
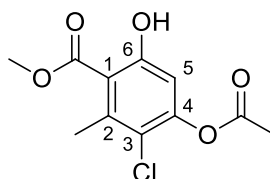
Methyl 3-chloro-4,6-dihydroxy-2-methylbenzoate (400 mg, 1.85 mmol) was dissolved in a solution of dichloromethane (4 mL) and triethylamine (270 μL, 1.94 mmol). The reaction mixture was cooled to 0 °C, acetyl chloride (139 μL, 1.94 mmol) was added drop-wise and the reaction was stirred for 1 hour. The solution was transferred to a separating funnel, diluted with ethyl acetate (20 mL) then washed with water (20 mL) and brine (20 mL). The organic layer was dried with magnesium sulfate, filtered, and concentrated under reduced pressure. Purification by flash column chromatography (10 g silica), eluting with a gradient of 40-60 °C petrol ether: ethyl acetate (100:0) to (90:10), gave the title compound as a white/yellow solid (230 mg, 48%): mp 60-61 °C; R$_f$ 0.32 (20% ethyl acetate / 80% 40-60 °C petrol ether); MS (EI) m/z (%): 258 (20), 260 (7) [M]$^+$ HRMS-ESI m/z [M+H]$^+$ calcd for $C_{11}H_{12}ClO_5$: 259.0368, found: 259.0370; ^{1}H NMR (500 MHz, chloroform-d) δ 11.02 (1 H, s, 6-OH), 6.55 (1 H, s, 5-CH), 3.92 (3 H, s, 1-CH$_3$), 2.58 (3 H, s, 6-CH$_3$), 2.30 (3 H, s, 4-CH$_3$); ^{13}C NMR (125 MHz, chloroform-d) δ 171.0 (C), 167.9 (C), 161.3 (C), 151.5 (C), 140.2 (C), 119.7 (C), 112.4 (C), 110.7 (C), 52.6 (CH$_3$), 20.7 (CH$_3$), 19.8 (CH$_3$); IR (neat, ν$_{max}$) cm^{-1} 2960, 1776, 1662, 1312, 1167, 1112, 1015, 885, 801.

(E)-Methyl 4-acetoxy-2-((3,7-dimethylocta-2,6-dien-1-yl)oxy)-6-methylbenzoate (**118**)
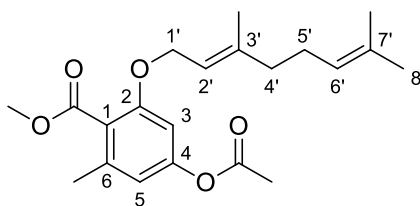
Geranyl bromide (500 mg, 2.31 mmol) was added to a suspension of methyl 4-acetoxy-2-hydroxy-6-methylbenzoate (260 mg, 1.16 mmol), potassium carbonate (481 mg, 3.48 mmol) and potassium iodide (18 mg, 0.12 mmol) in N,N-dimethylforamide (3 mL). The reaction was left stirring for 16 hours then diluted with water (10 mL) and it was extracted with diethyl ether (2 x 20 mL). The combined organic extracts were dried over magnesium sulfate, filtered and concentrated under reduced pressure onto silica gel (1 g). Purification by flash column chromatography (10 g silica), eluting with a gradient of 40-60 °C petrol ether: ethyl acetate (100:0) to (90:10), gave the tile compound as a colourless oil (280 mg, 73%): R$_f$ 0.82 (20% ethyl acetate / 80% 40-60 °C petrol ether); ^{1}H NMR (500 MHz, chloroform-d) δ 6.52 (1 H, s, 5-CH), 6.50 (1 H, s, 3-CH), 5.40-5.35 (1 H, m, 2'-CH), 5.08-5.03 (1 H, m, 6'-CH), 4.50 (2 H, d, *J* = 6 Hz, 1'-CH$_2$), 3.85 (3 H, s, 1-CH$_3$), 2.25 (3 H, s, 6-CH$_3$), 2.01 (3 H, s, 4-CH$_3$), 1.67 (3 H, s, 3'-CH$_3$), 1.65 (3 H, s, 8' or 10'-CH$_3$), 1.58 (3 H, s, 8' or 10'-CH$_3$); ^{13}C NMR (126 MHz, chloroform-d) δ 171.0 (C), 168.2 (C), 156.8 (C), 151.8 (C), 141.1 (C), 137.6 (C), 131.7 (C), 123.7 (CH), 121.9 (C), 119.1 (-CH), 115.3 (CH), 104.2 (CH), 66.0 (CH$_2$), 52.0 (CH$_3$), 39.4 (CH$_2$), 26.2 (CH$_2$), 25.5 (CH$_3$), 20.9 (CH$_3$), 19.3 (CH$_3$), 17.6 (CH$_3$), 16.6 (CH$_3$).

(E)-Methyl 4-acetoxy-3-chloro-6-((3,7-dimethylocta-2,6-dien-1-yl)oxy)-2-methylbenzoate (**119**)
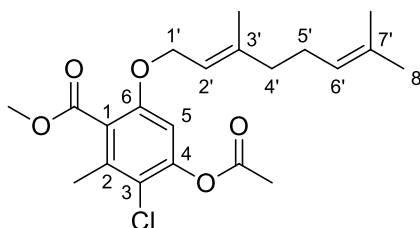

Geranyl bromide (500 mg, 2.31 mmol) was added to a suspension of methyl 4-acetoxy-3-chloro-6-hydroxy-2-methylbenzoate (260 mg, 1.16 mmol), potassium carbonate (481 mg, 3.48 mmol) and potassium iodide (18 mg, 0.12 mmol) in N,N-dimethylforamide (3 mL). The reaction was left stirring for 16 hours then diluted with water (10 mL) and extracted with diethyl ether (2 x 20 mL). The combined organic extracts were dried over magnesium sulfate, filtered and concentrated under reduced pressure onto silica gel (1 g). Purification by flash column chromatography (10 g silica), eluting with a gradient of 40-60 °C petrol ether: ethyl acetate (100:0) to (90:10), gave the title compound as a colourless oil (311 mg, 65%): R_f 0.57 (20% ethyl acetate / 80% 40-60 °C petrol ether); HRMS-ESI m/z [M+Na]$^+$ calcd for $C_{21}H_{27}ClNaO_5$: 417.1439, found: 417.1443; ^{1}H NMR (500 MHz, chloroform-d) δ 6.60 (1 H, s, 5-CH), 5.38 (1 H, t, J = 6 Hz, 2'-CH), 5.07 (1 H, t, J = 7 Hz, 6'-CH), 4.52 (2 H, d, J = 6 Hz, 1'-CH$_2$), 3.89 (3 H, s, 1-CH$_3$), 2.33 (3 H, s, 2-CH$_3$), 2.31 (3 H, s, 4-CH$_3$), 2.14-2.01 (4 H, m, 4' and 5'-CH$_2$), 1.68 (3 H, s, 3'-CH$_3$), 1.67 (3 H, s, 7' or 8'-CH$_3$), 1.60 (3 H, s, 7' or 8'-CH$_3$); ^{13}C NMR (125 MHz, chloroform-d) δ 168.0 (C), 167.4 (C), 154.5 (C), 148.2 (C), 141.6 (C), 135.5 (C), 131.7 (C), 123.7 (CH), 123.7 (C), 119.2 (CH), 118.8 (CH), 106.3 (CH$_2$), 66.3 (CH$_3$), 52.2 (CH$_2$), 26.3 (CH$_2$), 25.6 (CH$_3$), 20.6 (CH$_3$), 17.6 (CH$_3$), 17.4 (CH$_3$), 16.6 (CH$_3$); IR (neat, v_{max}) cm^{-1} 2924, 1779, 1733, 1590, 1256, 1185, 1105, 1033.

(E)-Methyl 4-acetoxy-3-(3,7-dimethylocta-2,6-dien-1-yl)-2-hydroxy-6-methylbenzoate

(120)
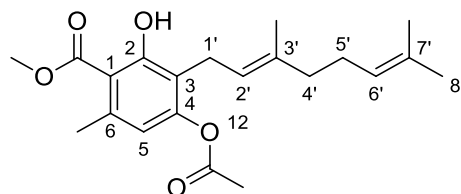
(E)-Methyl 4-acetoxy-2-((3,7-dimethylocta-2,6-dien-1-yl)oxy)-6-methylbenzoate (145 mg, 0.36 mmol) was dissolved in toluene (8 mL) and florisil 100-200 mesh (1.45 g) added. The reaction was heated to 100 ˚C for 4 hours, cooled to room temperature, filtered and the filtrate was concentrated under reduced pressure. Purification by flash column chromatography (10 g silica), eluting with a gradient of 40-60 °C petrol ether: ethyl acetate (100:0) to (90:10), gave title compound as a colourless oil (50 mg, 21%): R_f 0.30 (10% ethyl acetate / 90% 40-60 °C petrol ether); HRMS-ESI m/z [M+Na]$^+$ calcd for $C_{21}H_{28}NaO_5$: 383.1829, found: 383.1834; ^{1}H NMR (500 MHz, chloroform-d) δ 11.82 (1 H, s, 2-OH), 6.46 (1 H, s, 5-CH), 5.15 (1 H, t, *J* = 7 Hz, 2'-CH), 5.07 (1 H, t, *J* = 7 Hz, 6'-CH), 3.95 (3 H, s, 1-CH$_3$), 3.29 (2 H, d, *J* = 7 Hz, 1'-CH$_2$), 2.50 (3 H, s, 6-CH$_3$), 2.30 (3 H, s, 4-CH$_3$), 2.09-2.01 (2 H, m, 5'-CH$_2$), 2.01-1.94 (2 H, m, 4'-CH$_2$), 1.75 (3 H, s, 3'-CH$_3$), 1.66 (3 H, s, 8' or 10' CH$_3$), 1.58 (3 H, s, 8' or 10' CH$_3$); ^{13}C NMR (126 MHz, chloroform-d) δ 172.2 (C), 168.7 (C), 162.5 (C), 152.8 (C), 139.7 (C), 135.6 (C), 131.3 (C), 124.3 (CH), 121.3 (CH), 120.0 (C), 116.8 (CH), 110.0 (C), 52.1 (C), 39.7 (CH$_2$), 26.6 (CH$_2$), 25.6 (CH$_3$), 24.0 (CH$_3$), 22.9 (CH$_2$), 20.9 (CH$_3$), 17.6 (CH$_3$), 16.1 (CH); IR (neat, v$_{max}$) cm^{-1} 3328, 1653, 1439, 1368, 1317, 1245, 1191, 1139.

(E)-Methyl3-chloro-5-(3,7-dimethylocta-2,6-dien-1-yl)-4,6-dihydroxy-2-methylbenzoate[265] (**126**)
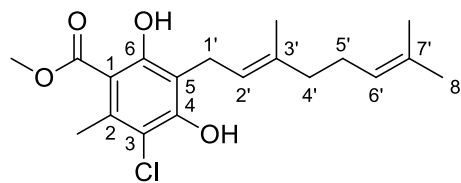
(E)-Methyl 4-acetoxy-3-chloro-6-((3,7-dimethylocta-2,6-dien-1-yl)oxy)-2-methylbenzoate (240 mg, 0.67 mmol) was dissolved in toluene (8 mL) and florisil 100-200 mesh (2.40 g) added. The reaction was heated to 100 ˚C for 4 hours, cooled to room temperature and filtered. The filtrate was concentrated under reduced pressure. Purification by flash column chromatography (10 g silica), eluting with a gradient of 40-60 °C petrol ether: ethyl acetate (100:0) to (90:10), gave title compound as a colourless oil (26 mg, ap 20%): HRMS-ESI m/z [M+H]$^+$ calcd for $C_{19}H_{26}ClO_4$: 353.1514, found: 253.1308; ^{1}H NMR (500 MHz, chloroform-d) δ 11.63 (1 H, s, 6-OH), 6.21 (1 H, s, 4-OH), 5.25 (1 H, t, J = 7 Hz, 2'-CH), 5.07 (1 H, t, J = 7 Hz, 6'-CH), 3.95 (3 H, s, 1-CH$_3$), 3.43 (2 H, d, J = 7 Hz, 1'-CH$_2$), 2.60 (3 H, s, 2-CH$_3$), 2.13-2.03 (2 H, m, 5'-CH$_2$), 2.03-1.92 (2 H, m, 4'-CH$_2$), 1.80 (3 H, s, 3'-CH$_3$), 1.66 (3 H, s, 7' or 8'-CH$_3$), 1.58 (3 H, s, 7' or 8'-CH$_3$).

1-(2,4-Dihydroxyphenyl)-2,2,2-trifluoroethanone[266] (**135**)
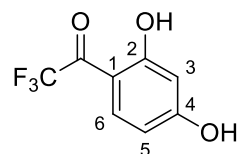
Trifluoroacetic acid anhydride (16.3 mL, 115 mmol) was added drop-wise to a stirred suspension of resorcinol (10.0 g, 91 mmol) and aluminum chloride (39.5 g, 296 mmol) in dichloromethane (750 mL) at 0 ˚C. The reaction was allowed to come to room temperature and was stirred for 15 hours. The mixture was poured onto ice (300 g), transferred to separating funnel and the organic layer separated. The aqueous layer was then washed with dichloromethane (3 x 300 mL). The combined organics were neutralised with a saturated aqueous sodium bicarbonate solution (200 mL), washed with a saturated brine solution (200 mL), dried over magnesium sulfate and concentrated under reduced pressure. Purification by flash column chromatography (70 g silica), eluting with a gradient of 40-60 °C petrol ether: ethyl acetate (100:0) to (75:25), gave the title compound as a pale yellow powder (15.4 g, 83%): MS (EI) m/z (%): 207 (15) [M+H]$^{+}$; ^{1}H NMR (500 MHz, chloroform-d) δ 11.49 (1 H, s, 2-OH), 7.75 (1 H, d, J = 9 Hz, 6-CH), 6.49 (1 H, d, J = 9 Hz, 5-CH), 6.47 (1 H, s, 3-CH), 5.63 (1 H, s, 4-OH).

1-(2,4-Dihydroxy-3-iodophenyl)-2,2,2-trifluoroethanone (**136**)
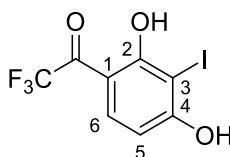
Iodine (4.61 g, 18.2 mmol) and potassium iodate (1.54 g, 7.2 mmol) were added to a stirred solution of 1-(2,4-dihydroxyphenyl)-2,2,2-trifluoroethanone (4.35 g, 21.1 mmol) in ethanol (50 mL) and the mixture was stirred for 16 hours. The reaction was diluted with water (50 mL) and a 1M hydrochloric acid solution added until pH 4 achieved. The solution was then extracted with diethyl ether (3 x 50 mL) and the combined organic layers were washed with a saturated aqueous sodium thiosulfate solution (50 mL) and a saturated brine solution (50 mL). The organics were dried over magnesium sulfate, filtered and concentrated under reduced pressure. Purification by flash column chromatography (50 g silica, eluting with a gradient of 40-60 °C petrol: ethyl acetate (100:0) to (80:20), gave the title compound as an white/brown powder (4.60 g, 68%): mp 56-59 °C; R_f 0.58 (20% ethyl acetate / 80% 40-60 °C petrol ether); MS (EI) m/z (%): 332 (56) [M]$^+$; ^{1}H NMR (500 MHz, chloroform-d) δ 12.43 (1 H, s, 2-OH), 7.77 (1 H, d, J = 9 Hz, 6-CH), 6.72 (1 H, d, J = 9 Hz, 5-CH), 6.50 (1 H, br s, 4-OH); ^{13}C NMR (125 MHz, chloroform-d) 182.09 (q, $^2J_{FC}$ = 36 Hz, C), 165.71 (C), 163.92 (C), 132.85 (q, $^3J_{FC}$ = 4 Hz, CH), 116.32 (q, $^1J_{FC}$ = 289 Hz, C), 108.45 (CH), 108.31 (C), 77.49 (C); IR (neat, ν$_{max}$) cm^{-1} 3399, 1607, 1481, 1363, 1287, 1130, 1016, 957, 783.

4-(5',5'-Dimethyl-1',3'-dioxan-2'-yl)phenol[267] (**149**)
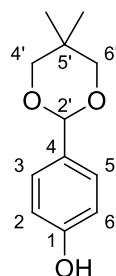
2, 2 Dimetyl 1, 3 propanediol (4.26 g, 40.9 mmol) was added to a stirred solution of *para*-hydroxybenzaldehyde (2.00 g, 16.4 mmol) in dry dichloromethane (15 mL) containing 4 Å activated molecular sieves. *Para*-toluylsulfonic acid (150 mg, 0.82 mmol) was added and the reaction was refluxed for 14 hours. The reaction was cooled to room temperature, transferred to a separating funnel and washed with saturated aqueous sodium bicarbonate (20 mL). The layers were separated and the aqueous layer washed with ethyl acetate (2 x 20 mL). The combined extracts were dried over magnesium sulfate, filtered, concentrated under reduced pressure. Purification by flash column chromatography (20 g silica), eluting with a gradient of 40-60 °C petrol ether: ethyl acetate (100:0) to (70:30), gave the title compound as an impure product that was used directly in the next reaction to 2-(4-(methoxymethoxy)phenyl)-5,5-dimethyl-1,3-dioxane (2.66 g, ap 78%): HRMS-ESI m/z [M+H]$^+$ calcd for $C_{12}H_{17}O_3$: 209.1172, found: 209.1173; ^{1}H NMR (500 MHz, chloroform-d) δ 7.38 (2 H, d, *J* = 9 Hz), 6.78 (2 H, d, *J* = 9 Hz), 5.36 (1 H, s), 3.77 (2 H, d, *J* = 11 Hz), 3.65 (2 H, d, *J* = 11 Hz), 1.31 (3 H, s), 0.80 (3 H, s).

2-(4-(Methoxymethoxy)phenyl)-5,5-dimethyl-1,3-dioxane (**150**)
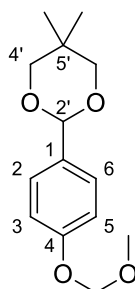
4-(5',5'-Dimethyl-1',3'-dioxan-2'-yl)phenol (1.95 g, 9.46 mmol) was dissolved in dry tetrahydrofuran (15 mL) and cooled to 0 ˚C. 60% sodium hydride on mineral oil (454 mg, 11.4 mmol) was added to the reaction in three portions and stirred for 30 minutes. Chloromethyl methyl ether (790 µL, 10.4 mmol) was added drop-wise *via* syringe and the reaction was allowed come up to room temperature over 30 minutes. Saturated aqueous sodium bicarbonate (20 mL) was added and the solution was extracted with ethyl acetate (3 x 30 mL). The combined organic extracts were, dried over sodium sulfate, filtered and concentrated under reduced pressure. Purification by flash column chromatography (20 g silica), eluting with a gradient of 40-60 °C petrol ether: ethyl acetate (100:0) to (85:15), gave the title compound as a clear oil (1.67 g, 71%): R_f 0.30 (20% ethyl acetate / 80% 40-60 °C petrol ether); HRMS-ESI m/z [M+H]$^+$ calcd for $C_{14}H_{21}O_4$: 253.1434, found: 253.1432; ^{1}H NMR (500 MHz, chloroform-d) δ 7.46 (2 H, d, *J* = 8 Hz, 2 and 6-CH), 7.06 (2 H, d, *J* = 8 Hz, 3 and 5-CH), 5.37 (1 H, s, 2'-CH), 5.17 (2 H, s, 4-CH$_2$), 3.77 (2 H, d, *J* = 11 Hz, 4'-CH$_2$), 3.64 (2 H, d, *J* = 11 Hz, 4'-CH$_2$), 3.46 (3 H, s, 4-CH$_3$), 1.31 (3 H, s, 5'-CH$_3$), 0.80 (3 H, s, 5'-CH$_3$); ^{13}C NMR (126 MHz, chloroform-d) δ 157.6 (C), 132.4 (C), 127.4 (CH), 116.0 (CH), 101.5 (CH), 94.4 (CH$_2$), 77.6 (CH$_2$), 55.8 (CH$_3$), 30.1 (C), 23.1 (CH$_3$), 21.9 (CH$_3$).

(E)-2-(3-(3,7-Dimethylocta-2,6-dien-1-yl)-4-(methoxymethoxy)phenyl)-5,5-dimethyl-1,3-dioxane (**151**)
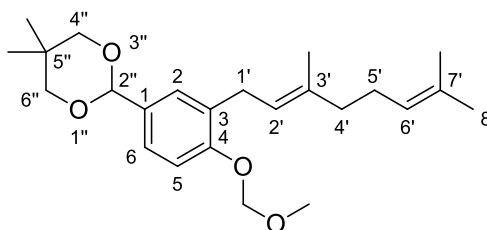
2.0 M n-butyl lithium (297 μL, 0.60 mmol) was added drop-wise to a 0 ˚C stirred solution of 2-(4-(methoxymethoxy)phenyl)-5,5-dimethyl-1,3-dioxane (100 mg, 0.4 mmol) and N1,N1,N2,N2-tetramethylethane-1,2-diamine (90 μL, 0.60 mmol) in dry tetrahydrofuran (3 mL). This was allowed come to room temperature over 30 minutes and was cooled again to 0 ˚C before the addition of geranyl bromide (174 mg, 0.80 mmol) drop-wise. The reaction was allowed to come to room temperature, brine added (10 mL) and this was extracted with diethyl ether (3 x 10 mL). The combined organics were washed with brine (2 x 10 mL), dried over sodium sulfate and concentrated under reduced pressure. Purification by flash column chromatography (10 g silica), eluting with a gradient of 40-60 °C petrol ether: ethyl acetate (100:0) to (95:5), gave the title compound as a clear oil (79 mg, 65%): ^{1}H NMR (500 MHz, chloroform-d) δ 7.33-7.28 (2 H, m, 2 and 6-CH), 7.09-7.01 (1 H, d, *J* = 9 Hz, 5-CH), 5.36-5.29 (2 H, m, 2'' and 2'-CH), 5.19 (2 H, s, CH$_2$), 5.12 (1 H, t, *J* = 7 Hz, 6'-CH), 3.76 (2 H, d, *J* = 11 Hz, 6'' and 4''-CH$_2$), 3.63 (2 H, d, *J* = 11 Hz, 6'' and 4''-CH$_2$), 3.46 (3 H, s, 5-CH$_3$), 3.37 (2 H, d, *J* = 7 Hz, 1'-CH$_2$), 2.17-2.06 (2 H, m, 5'-CH$_2$), 2.06-1.98 (2 H, m, 4'-CH$_2$), 1.73 (3 H, s, 3'-CH$_3$), 1.69 (3 H, s, 7' or 8'-CH$_3$), 1.61 (3 H, s, 7' or 8'-CH$_3$), 1.30 (3 H, s, 5''-CH$_3$), 0.80 (3 H, s, 5''-CH$_3$); ^{13}C NMR (126 MHz, chloroform-d) δ 155.3 (C), 135.83 (C), 131.93 (C), 131.33 (C), 130.7 (C), 127.5 (CH), 124.7 (CH), 124.4 (CH), 122.5 (CH), 113.7 (CH), 101.8 (CH), 94.4 (CH$_2$), 77.7 (CH$_2$), 55.8 (CH$_3$), 39.8 (CH$_2$), 30.2 (C), 28.7 (CH$_2$), 26.7 (CH$_2$), 25.7 (CH$_3$), 23.0 (CH$_3$), 21.9 (CH$_3$), 17.6 (CH$_3$), 16.1 (CH$_3$).

Methyl 3-bromo-5-chloro-2,4-bis(methoxymethoxy)-6-methylbenzoate (**156**)
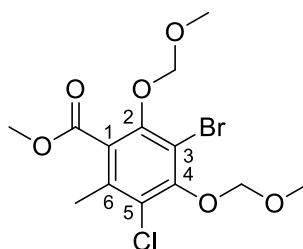
60% sodium hydride on mineral oil (267 mg, 6.76 mmol) was added in three portions to a stirred solution of methyl 3-bromo-5-chloro-2,4-dihydroxy-6-methylbenzoate (1.00 g, 3.41 mmol) in dry tetrahydrofuran (15 mL) at 0 ˚C. This was stirred for 40 minutes and methyl chloromethoxy ether (506 µL, 76.8 mmol) added drop-wise. The reaction was stirred for 16 hours and then diluted with water (100 mL) and extracted with diethyl ether (3 x 100 mL). The combined ether fractions were dried over sodium sulfate, filtered and concentrated, under reduced pressure. Purification by flash column chromatography (20 g silica), eluting with a gradient of 40-60 °C petrol ether: ethyl acetate (100:0) to (95:5), gave the title compound as a clear colourless oil (878 mg, 68%): R_f 0.34 (20% ethyl acetate / 80% 40-60 °C petrol ether); HRMS-ESI m/z [M+Na]$^+$ calcd for $C_{13}H_{16}BrClNaO_6$: 404.9711, found: 404.9700 ; ^{1}H NMR (500 MHz, chloroform-d) δ 5.19 (2 H, s, 2-CH$_2$), 5.10 (2 H, s, 4-CH$_2$), 3.94 (3 H, s, 1-CH$_3$), 3.71 (3 H, s, 4-CH$_3$), 3.58 (3 H, s, 2-CH$_3$), 2.32 (3 H, s, 6-CH$_3$) ; ^{13}C NMR (126 MHz, chloroform-d) δ 166.6 (C), 152.6 (C), 150.6 (C), 134.6 (C), 127.8 (C), 126.2 (C), 112.1 (C), 100.4 (CH$_2$), 99.6 (CH$_2$), 58.4 (CH$_3$), 57.9 (CH$_3$), 52.6 (CH$_3$), 17.9 (CH$_3$); IR (neat, v_{max}) cm^{-1} 1733, 1588, 1487, 1184, 1159, 1024, 879, 753, 689, 588.

Methyl 3-bromo-5-chloro-2,4-dihydroxy-6-methylbenzoate[243] (**51**)
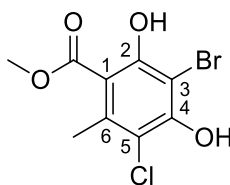
Various conditions were attempted to deprotect the methyl 3-bromo-5-chloro-2,4 bis(methoxymethoxy)-6-methylbenzoate esters on a 50 mg scale. Reactions were monitored over 24 hours and deprotection determined *via* ^{1}H NMR: mp 68-72 °C; HRMS-ESI m/z [M+Na]$^+$ calcd for $C_9H_8BrClNaO_4$: 318.9167, found: 318.9160; ^{1}H NMR (500 MHz, chloroform-d) 12.18 (1 H, s, 2-OH), 6.46 (1 H, s, 4-OH), 3.99 (3 H, s, 1-CH$_3$), 2.63 (3 H, s, 6-CH$_3$).

Conditions	Result
Tetrahydrofuran (2 mL) and 1M HCl (2 mL)	✗
*Para*toluylsulfonic acid (121 mg) and methanol (5 mL)	✓
Catalytic HCl, NaI (100 mg) and acetone (5 mL)	✗
1:1 NaHSO$_4$:SiO$_2$ (50 mg)	✓
Acetic acid (1 mL) and methanol (4 mL)	✗

1,3-Bis(methoxymethoxy)-5-methylbenzene[255] (152)
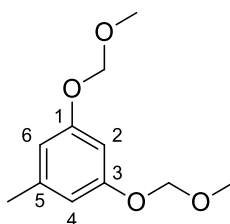
60% sodium hydride on mineral oil (742 mg, 18.5 mmol) was added in three portions to a stirred solution of orcinol (1.00 g, 8.06 mmol) in dimethylformamide (20 mL) at 0 ˚C. This was stirred for 40 minutes and methyl chloromethoxy ether (1.35 mL, 17.7 mmol) added drop-wise. The reaction was stirred for 16 hours and then diluted with water (100 mL) and extracted with diethyl ether (3 x 100 mL). The combined organics were washed with 1 M sodium hydroxide solution (2 x 50 mL), saturated brine solution (50 mL), dried over sodium sulfate, filtered and concentrated under reduced pressure. Purification by flash column chromatography (20 g silica), eluting with a gradient of 40-60 °C petrol ether: ethyl acetate (100:0) to (95:5), gave the title compound as a clear oil (1.59 g, 93%): HRMS-ESI m/z [M+H]$^+$ calcd for $C_{11}H_{17}O_4$: 213.1121, found: 213.1120; ^{1}H NMR (500 MHz, chloroform-d) δ 6.56 (1 H, s, 2-CH), 6.54 (2 H, s, 4 and 6-CH), 5.15 (4 H, s, 1 and 3-CH$_2$), 3.49 (6 H, s, 1 and 3-CH$_3$), 2.31 (3 H, s, 5-CH$_3$).

(E)-2-(3,7-Dimethylocta-2,6-dienyl)-1,3-bis(methoxymethoxy)-5-methylbenzene (**153**)

3-Bis(methoxymethoxy)-5-methylbenzene (2.50 g, 11.8 mmol) was dissolved in dry tetrahydrofuran (90 mL) and cooled to 0 ˚C. 2.1 M *n*-butyl lithium (8.41 mL, 17.7 mmol) was added drop-wise and the reaction was left to stir for 1 hour at 0 ˚C. Geranyl bromide (4.48 g, 20.6 mmol) was added to the reaction mixture in a drop-wise manner, this was stirred for 1 hour and allowed to come to room temperature. The reaction was diluted with water (300 mL) and extracted with diethyl ether (3 x 200 mL). The combined organics were dried over sodium sulfate, filtered and concentrated under reduced pressure. Purification by flash column chromatography (50 g silica), eluting with a gradient of 40-60 °C petrol ether: ethyl acetate (100:0) to (95:5), gave the title compound as a colourless clear oil (3.70 g, 90%): R_f 0.60 (20% ethyl acetate / 80% 40-60 °C petrol ether); HRMS-ESI m/z [M+H]$^+$ calcd for $C_{21}H_{33}O_4$: 349.2373, found: 349. 2376; ^{1}H NMR (500 MHz, chloroform-d) δ 6.60 (2 H, s, 4 and 6-CH), 5.22 (1 H, t, *J* = 7 Hz, 2'-CH), 5.18 (4 H, s, 1 and 3-CH$_2$), 5.08 (1 H, t, *J* = 7 Hz, 6'-CH), 3.48 (6 H, s, 1 and 3-CH$_3$), 3.38 (2 H, d, *J* = 7 Hz, 1'-CH$_2$), 2.31 (3 H, s, 5-CH$_3$), 2.09-2.02 (2 H, m, 4' or 5'-CH$_2$), 1.99-1.92 (2 H, m, 4' or 5'-CH$_2$), 1.79 (3 H, s, 3'-CH$_3$), 1.66 (3 H, s, 7' or 8'-CH$_3$), 1.58 (3 H, s, 7' or 8'-CH$_3$); ^{13}C NMR (125 MHz, chloroform-d) δ 155.6 (C), 136.8 (C), 134.3 (C), 131.1 (C), 124.4 (CH), 123.1 (C), 117.4 (CH), 108.9 (CH), 94.5 (CH$_2$), 55.9 (CH$_3$), 39.8 (CH$_2$), 26.8 (CH$_2$), 25.6 (CH$_3$), 22.4 (CH$_2$), 21.7 (CH$_3$), 17.6 (CH$_3$), 16.0 (CH$_3$); IR (neat, v_{max}) cm^{-1} 2952, 2900, 1464, 1356, 1297, 1215, 1162, 1094, 1000, 904, 876, 704, 685, 674.

(E)-3-(3,7-Dimethylocta-2,6-dienyl)-2,4-bis(methoxymethoxy)-6-methylbenzaldehyde

(154)
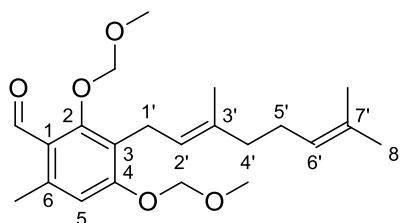
3-Bis(methoxymethoxy)-5-methylbenzene (2.50 g, 11.8 mmol) was dissolved in dry tetrahydrofuran (90 mL) and cooled to 0 ˚C. 2.1 M *n*-butyl lithium (8.41 mL, 1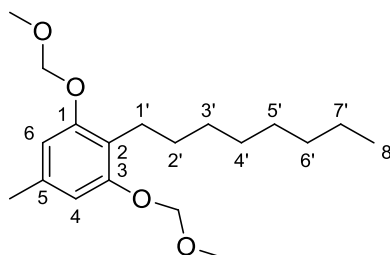7.7 mmol) was added drop-wise and the reaction was left to stir for 1 hour at 0 ˚C. Geranyl bromide (4.48 g, 20.6 mmol) was added to the reaction mixture in a drop-wise manner. This was stirred for 1 hour and allowed to come to room temperature. The reaction was cooled to 0 ˚C again and 2.1 M *n*-butyl lithium (8.41 mL, 17.67 mmol) added followed by another 1 hour stirring at 0 ˚C. Excess dry N, N-dimethylformamide was added and the reaction was allowed to come to room temperature over 1 hour. The reaction was diluted with water (300 mL) and extracted with diethyl ether (3 x 200 mL). The combined organics were dried over sodium sulfate, filtered and concentrated under reduced pressure. Purification by flash column chromatography (50 g silica), eluting with a gradient of 40-60 °C petrol ether: ethyl acetate (100:0) to (95:5), gave the title compound as a yellow tinted clear oil (1.28 g, 31%): HRMS-ESI m/z [M+Na]$^+$ calcd for $C_{23}H_{32}NaO_5$: 399.2142, found: 399.2147; ^{1}H NMR (500 MHz, chloroform-d) δ 10.38 (1 H, s, 1-CH), 6.74 (1 H, s, 5-CH), 5.24 (2 H, s, 2 or 4-CH$_2$), 5.17 (1 H, t, *J* = 7 Hz, 2'-CH), 5.04 (2 H, s, 2 or 4-CH$_2$), 5.01 (1 H, t, *J* = 6 Hz, 6'-CH), 3.57 (3 H, s, 2 or 4-CH$_3$), 3.46 (3 H, s, 2-CH$_3$ or 4-CH$_3$), 3.36 (2 H, d, *J* = 7 Hz, 1'-CH$_2$), 2.57 (3 H, s, 5-CH$_3$), 2.07-2.01 (2 H, m, 4' or 5'-CH$_2$), 1.99-1.93 (2 H, m, 4' or 5'-CH$_2$), 1.76 (3 H, s, 3'-CH$_3$), 1.63 (3 H, s, 7' or 8'-CH$_3$), 1.56 (3 H, s, 7' or 8'-CH$_3$); IR (neat, v$_{max}$) cm^{-1} 2932, 1682, 1595, 1560, 1440, 1375, 1315, 1284, 1220, 1152, 1039, 1007, 924.

1,3-Bis(methoxymethoxy)-5-methyl-2-octylbenzene (**158**)

3-Bis(methoxymethoxy)-5-methylbenzene (2.00 g, 9.42 mmol) was dissolved in dry tetrahydrofuran (60 mL) and cooled to 0 ˚C. 2.5 M *n*-butyl lithium (4.90 mL, 12.3 mmol) was added drop-wise and the reaction was left to stir for 1 hour at 0 ˚C. Bromooctane (2.44 mL, 14.1 mmol) was added to the reaction mixture and this was stirred for 1 hour at 0 ˚C before being allowed to come to room temperature. The reaction was diluted with water (100 mL) and extracted with diethyl ether (3 x 100 mL). The organic fractions were dried over sodium sulfate, filtered and concentrated under reduced pressure. Purification by flash column chromatography (25 g silica), eluting 40-60 °C petrol ether: ethyl acetate (100:0) to (95:5), gave the title compound as a colourless oil (2.75 g, 83%): R_f 0.79 (10% ethyl acetate / 90% 40-60 °C petrol ether); HRMS-ESI m/z [M+H]$^+$ calcd for $C_{19}H_{32}NaO_4$: 347.2193, found: 347.2187; ^{1}H NMR (500 MHz, chloroform-d) 6.59 (2 H, s, 4 and 6-CH), 5.17 (4 H, s, 1 and 3-CH$_2$), 3.49 (6 H, s, 1 and 3-OMe), 2.64 (2 H, t, *J* = 8 Hz, 1'-CH$_2$), 2.30 (3 H, s, 5-CH$_3$), 1.55-1.46 (2 H, m, 2'-CH$_2$), 1.39-1.23 (10 H, m, 3' to 7'CH$_2$), 0.89 (3 H, t, *J* = 7 Hz, 8'-CH$_3$); ^{13}C NMR (126 MHz, chloroform-d) δ 155.7 (C), 136.6 (C), 118.4 (C), 108.7 (CH), 94.5 (CH$_2$), 56.0 (CH$_3$), 31.9 (CH$_2$), 29.8 (CH$_2$), 29.7 (CH$_2$), 29.5 (CH$_2$), 29.3 (CH$_2$), 23.2 (CH$_2$), 22.7 (CH$_2$), 21.8 (CH$_3$), 14.1 (CH$_3$); IR (neat, v$_{max}$) cm^{-1} 2924, 2854, 1612, 1586, 1463, 1394, 1154, 1122, 1036, 923, 823;

5-Methyl-2-octylbenzene-1,3-diol (**159**)
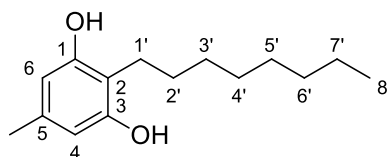
1,3-bis(methoxymethoxy)-5-methyl-2-octylbenzene (350 mg, 1.08 mmol) was suspended in ethylene glycol (10 mL) and heated to 160 °C by microwave irradiation for 5 hours in a sealed vial. The reaction mixture was diluted with water (40 mL) and extracted with diethyl ether (3 x 30 ml). The combined extracts were washed with water (30 mL), dried over magnesium sulfate, filtered and concentrated under reduced pressure. Purification by flash column chromatography (10 g silica), eluting 40-60 °C petrol ether: ethyl acetate (100:0) to (70:30), gave the title compound as an orange/white powder (255 mg, quant.): mp 63-65 °C; R_f 0.32 (10% ethyl acetate / 90% 40-60 °C petrol ether); HRMS-ESI m/z [M+H]$^+$ calcd for $C_{15}H_{25}O_2$: 237.1849, found: 237.1853; ^{1}H NMR (500 MHz, chloroform-d) δ 6.23 (2 H, s, 4 and 6-CH), 4.69 (2 H, s, 1 and 3-OH), 2.59 (2 H, t, *J* = 8 Hz, 1'-CH$_2$), 2.22 (3 H, s, 5-CH$_3$), 1.60-51 (2 H, m, 2'-CH$_2$), 1.43-1.23 (10 H, m, 3' to 7'-CH$_2$), 0.89 (3 H, t, *J* = 7 Hz, 8'-CH$_3$); ^{13}C NMR (126 MHz, chloroform-d) δ 154.4 (C), 137.0 (C), 112.4 (C), 108.7 (CH), 75.4 (CH$_2$), 31.9 (CH$_2$), 29.8 (CH$_2$), 29.5 (CH$_2$), 29.3 (CH$_2$), 23.0 (CH$_2$), 22.7 (CH$_2$), 21.0 (CH$_3$), 14.1 (CH$_3$); IR (neat, v_{max}) cm^{-1} 3427, 3280, 2956, 2918, 2850, 1635, 1584, 1522, 1467, 1328, 1268, 1160, 1112, 829, 534.

2,4-Dihydroxy-6-methyl-3-octylbenzaldehyde (**160**)
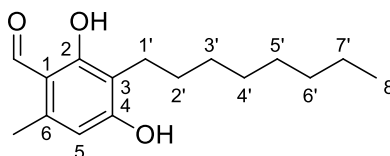
5-methyl-2-octyl-benzene-1,3-diol (500 mg, 2.12 mmol) was dissolved in dry N, N-dimethylformamide (4.1 mL, 53 mmol) and cooled to 0 °C. Phosphorus oxychloride (0.39 mL, 4.2 mmol) was added slowly by syringe and the reaction was then allowed to come to room temperature. After 2 hours the reaction was cooled to 0 °C and diluted with 1M aqueous sodium hydroxide solution (10 mL). This was stirred for 10 minutes then acidified with 1M aqueous hydrogen chloride solution (30 mL) and transferred to a separating funnel. The mixture was extracted with diethyl ether (3 x 40 mL). The combined organic layers were washed with water (50 mL) and brine (50 mL), dried over magnesium sulfate and concentrated under reduced pressure. Purification by flash column chromatography (10g silica), eluting 40-60 °C petrol ether: ethyl acetate (100:0) to (80: 20), gave the title compound as an orange/white powder (0.54 g, 92%): mp 101-103 °C; R_f 0.18 (10% ethyl acetate / 90% 40-60 °C petrol ether); HRMS-ESI m/z [M+H]$^+$ calcd for $C_{16}H_{25}O_3$: 265.1798, found: 265.1805; ^{1}H NMR (500 MHz, chloroform-d) δ 12.63 (1 H, s, 2-OH), 10.09 (1 H, s, 1-CH), 6.20 (1 H, s, 5-CH), 5.52 (1 H, s, 4-OH), 2.60 (2 H, d, J = 7 Hz, 1'-CH$_2$), 2.50 (3 H, s, 6-CH$_3$), 1.59-1.47 (2 H, m, 2'-CH$_2$), 1.42-1.21 (10 H, m, 3' to 7'-CH$_2$), 0.89 (3 H, d, J = 7 Hz, 8'-CH$_3$); ^{13}C NMR (126 MHz, chloroform-d) δ 193.0 (CH), 164.2 (C), 161.0 (C), 141.5 (C), 114.0 (C), 113.4 (C), 110.2 (CH), 31.9 (CH$_2$), 29.7 (CH$_2$), 29.5 (CH$_2$), 29.3 (CH$_2$), 28.7 (CH$_2$), 22.6 (CH$_2$), 22.0 (CH$_2$), 17.9 (CH$_3$), 14.1 (CH$_3$); IR (neat, v$_{max}$) cm^{-1} 3111, 2916, 2849, 1605, 1509, 1466, 1284, 1250, 1216, 1135, 829, 773, 644, 567.

3-Chloro-4,6-dihydroxy-2-methyl-5-octylbenzaldehyde (**161**)
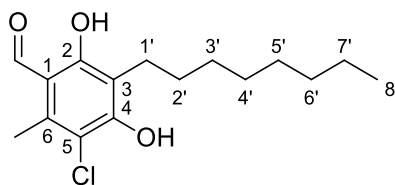
2,4-dihydroxy-6-methyl-3-octylbenzaldehyde (70 mg, 0.27 mmol) was dissolved in dry diethyl ether (5 mL) and sulfuryl chloride (32 µL, 0.40 mmol) added. The reaction was stirred for 1 hour at room temperature before being quenched with saturated aqueous sodium hydrogen bicarbonate solution (25 mL). The mixture was then extracted with diethyl ether (2 x 15 mL). The combined organic phases were dried over magnesium sulfate, filtered and concentrated onto celite (1 g). Purification by flash column chromatography over silica (10 g) eluting 40-60 °C petrol ether: ethyl acetate (100:0) to (80:20) gave the title compound as a colourless powder (67 mg, 84%): mp 64-66 °C; R_f 0.58 (10% ethyl acetate / 90% 40-60 °C petrol ether); HRMS-ESI m/z [M+H]$^+$ calcd for $C_{16}H_{24}ClO_3$: 299.1408, found: 299.1421; ^{1}H NMR (500 MHz, chloroform-d) δ 12.65 (1 H, s, 2-OH), 10.14 (1 H, s, 1-CH), 6.34 (1 H, s, 4-OH), 2.69 (2 H, d, J = 7 Hz, 1'-CH$_2$), 2.60 (3 H, s, 6-CH$_3$), 1.54--1.47 (2 H, m, 2'-CH$_2$), 1.30-1.23 (10 H, m, 3' to 7'-CH$_2$), 0.88 (3 H, d, J = 7 Hz, 8'-CH$_3$); ^{13}C NMR (126 MHz, chloroform-d) δ 193.1 (CH), 162.5 (C), 156.2 (C), 137.2 (C), 115.8 (C), 113.5 (C), 113.0 (C), 31.9 (CH$_2$), 29.6 (CH$_2$), 29.5 (CH$_2$), 29.3 (CH$_2$), 28.4 (CH$_2$), 22.9 (CH$_2$), 22.6 (CH$_2$), 14.4 (CH$_3$), 14.1 (CH$_3$); IR (neat, ν$_{max}$) cm^{-1} 3327, 2924, 2856, 1606, 1452, 1416, 1374, 1233, 1132, 791, 767, 710, 555.

3-Chloro-4,6-dihydroxy-2-methyl-5-octylbenzaldehyde oxime (**162**)
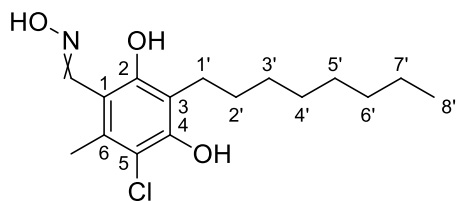
3-chloro-4,6-dihydroxy-2-methyl-5-octylbenzaldehyde (250 mg, 0.84 mmol), hydroxylamine monohydrochloride (178 mg, 2.51 mmol) and sodium acetate (275 mg, 3.35 mmol) were dissolved in a mixture of tetrahydrofuran: ethanol: water (2:3:2) (2 mL) and stirred for 16 hours at room temperature. The reaction mixture was diluted with diethyl ether (10 mL), this mixture was dried over magnesium sulfate, filtered and concentrated on celite (1 g). Purification by flash column chromatography over silica (10 g) eluting 40-60 °C petrol ether: ethyl acetate (100:0) to (90: 10) gave the title compound as a white powder (243 mg, 92%): mp 68-70 °C; R_f 0.40 (10% ethyl acetate / 90% 40-60 °C petrol ether); HRMS-ESI m/z [M+H]$^+$ calcd for $C_{16}H_{25}ClNO_3$: 314.1517, found: 314.1527; ^{1}H NMR (500 MHz, chloroform-d) δ 10.60 (1 H, s, 2-OH), 8.54 (1 H, s, 1-CH), 7.14 (1 H, s, 1-OH), 5.88 (1 H, s, 4-OH), 2.69 (2 H, t, *J* = 7 Hz, 1'-CH$_2$), 2.43 (3 H, s, 6-CH$_3$), 1.58-1.52 (2 H, m, 2'-CH$_2$), 1.30-1.21 (10 H, m, 3' to 7'-CH$_2$), 0.91-0.87 (3 H, m, 8'-CH$_3$); ^{13}C NMR (126 MHz, chloroform-d) δ 156.2 (C), 151.5 (C), 151.0 (CH), 132.5 (C), 115.6 (C), 112.6 (C), 108.5 (C), 31.9 (CH$_2$), 29.7 (CH$_2$), 29.5 (CH$_2$), 29.3 (CH$_2$), 28.7 (CH$_2$), 23.7 (CH$_2$), 22.7 (CH$_2$), 15.9 (CH$_3$), 14.1 (CH$_3$); IR (neat, v_{max}) cm^{-1} 3290, 2912, 2850, 1604, 1466, 1360, 1314, 1287, 1211, 1183, 1119, 853, 764, 722, 593.

5-Chloro-6-hydroxy-4-methyl-7-octylbenzo[d]isoxazole (**163**)
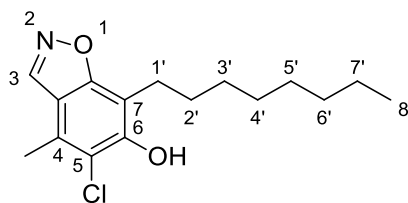
Triphenylphosphine (220 mg, 0.84 mmol) was dissolved in dry dichloromethane (3 mL) and 2,3-dichloro-5,6-dicyanobenzoquinone (190 mg, 0.84 mmol) added. A 3-chloro-4,6-dihydroxy-2-methyl-5-octylbenzaldehyde oxime (175 mg, 0.56 mmol) solution in dichloromethane (3 mL) was prepared and added in one portion. The reaction was stirred for 5 minutes at room temperature then concentrated under reduced pressure onto celite (1 g). Purification by flash column chromatography over silica (10 g) eluting 40-60 °C petrol ether: ethyl acetate (100:0) to (90:10) gave the title compound as a white powder (150 mg, 90%): mp 102-103 °C; R_f 0.55 (10% ethyl acetate / 90% 40-60 °C petrol ether); HRMS-ESI m/z $[M+H]^+$ calcd for $C_{16}H_{23}ClNO_2$: 296.1412, found: 296.1424; ^{1}H NMR (500 MHz, chloroform-d) δ 8.60 (1 H, s, 1-CH), 6.00 (1 H, s, 4-OH), 2.94 (2 H, t, J = 7 Hz, 1'-CH$_2$), 2.43 (3 H, s, 6-CH$_3$), 1.70-1.59 (2 H, m, 2'-CH$_2$), 1.37-1.25 (10 H, m, 3' to 7'-CH$_2$), 0.92-0.88 (3 H, m, 8'-CH$_3$); ^{13}C NMR (126 MHz, chloroform-d) δ 160.7 (C), 150.4 (C), 145.0 (CH), 126.9 (C), 118.1 (C), 115.2 (C), 109.2 (C), 31.8 (CH$_2$), 29.5 (CH$_2$), 29.3 (CH$_2$), 29.2 (CH$_2$), 28.7 (CH$_2$), 24.5 (CH$_2$), 22.6 (CH$_2$), 16.7 (CH$_3$), 14.0 (CH$_3$); IR (neat, ν$_{max}$) cm^{-1} 3386, 2926, 2857, 1604, 1508, 1419, 1328, 1238, 1122, 973, 950, 723, 639.

3-Chloro-4,6-dihydroxy-2-methyl-5-octylbenzonitrile (**164**)
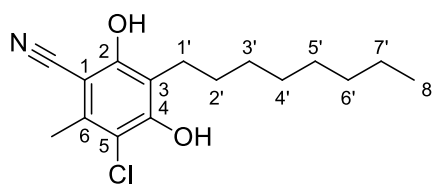
5-Chloro-4-methyl-7-octylbenzo[d]isoxazol-6-ol (50 mg, 0.17 mmol) was dissolved in a mixture of ethanol (10 mL) and 1 M aqueous sodium hydroxide (1.7 mL) and stirred for 2 hours at room temperature. The reaction was acidified with 1 M aqueous hydrogen chloride (3 mL) and extracted with diethyl ether (3 x 20 mL). The combined organic phases were dried over magnesium sulfate, filtered and concentrated under reduced pressure onto celite (1 g). Purification by flash column chromatography over silica (10 g), eluting 40-60 °C petrol ether: ethyl acetate (100:0) to (85:15), gave the title compound as a white powder (16 mg, 31%): mp 68 °C; R$_f$ 0.42 (10% ethyl acetate / 90% 40-60 °C petrol ether); HRMS-ESI m/z [M+H]$^+$ calcd for C$_{16}$H$_{23}$ClNO$_2$: 296.1412, found: 296.1422; ^{1}H NMR (500 MHz, chloroform-d) δ 6.13 (2 H, s, 2 and 4-OH), 2.70-2.63 (2 H, m, 1'-CH$_2$), 2.51 (3 H, s, 6-CH$_3$), 1.57-1.49 (2 H, m, 2'-CH$_2$), 1.37-1.23 (10 H, m, 3' to 7'-CH$_2$), 0.89 (3 H, s, 8'-CH$_2$); ^{13}C NMR (126 MHz, chloroform-d) δ 156.3 (C), 154.0 (C), 137.0 (C), 115.7 (C), 115.4 (C), 113.4 (C), 93.8 (C), 31.8 (CH$_2$), 29.5 (CH$_2$), 29.4 (CH$_2$), 29.2 (CH$_2$), 28.4 (CH$_2$), 23.8 (CH$_2$), 22.6 (CH$_2$), 18.8 (CH$_3$), 14.0 (CH$_3$); IR (neat, v$_{max}$) cm^{-1} 2924, 2855, 2234, 1592, 1487, 1185, 1026, 864, 750, 688, 591.

3-Methoxy-5-methylcyclohex-2-enone[268] (**176**)
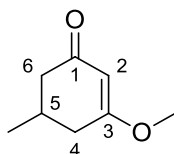
5-Methylcyclohexane-1,3-dione (10.0 g, 79.3 mmol) and dimethylsulfate (7.5 mL, 79 mmol) were dissolved in anhydrous tetrahydrofuran (30 mL) and 60% sodium hydride on mineral oil (3.5 g, 87 mmol) was added in portions. The reaction was stirred for 18 hours at room temperature concentrated under reduced pressure, diluted with ethyl acetate (20 mL), quenched with water (20 mL) and transferred to a separating funnel. The organics were washed with water (30 mL) and brine (30 mL), dried over magnesium sulfate, filtered and concentrated under reduced pressure onto celite (2 g). Purification by column chromatography over silica (50 g), eluting with a gradient of 40-60 °C petrol ether: ethyl acetate (100:0) to (50:50) and concentration under reduced pressure, gave the title compound as a white solid (10.8 g, 72%): HRMS-ESI m/z [M+Na]$^+$ calcd for $C_9H_{12}NaO_3$: 163.0730, found: 163.0727; ^{1}H (500 MHz, chloroform-d) δ 5.37 (1 H, s, 2-CH), 3.70 (3 H, s 3-CH$_3$), 2.44 (1 H, t, J = 5 Hz, 6-CH), 2.41 (1 H, t, J = 5 Hz, 4-CH), 2.28-2.20 (1 H, m, 5-CH), 2.15 (1 H, dd, J = 17, 10 Hz, 4-CH), 2.05 (1 H, dd, J = 16, 11 Hz, 6-CH), 1.09 (3 H, d, J = 6 Hz, 5-CH$_3$).

(Z)-6-(Hydroxymethylene)-3-methoxy-5-methylcyclohex-2-enone (**177**)
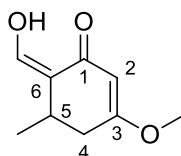
3-Methoxy-5-methyl-cyclohex-2-en-1-one (2.50 g, 17.8 mmol) was dissolved in methyl formate (20 mL, 0.32 mol). Sodium methoxide (4.8 g, 89 mmol) was added and the reaction was stirred for 20 hours. The reaction was concentrated under reduced pressure, diluted with water (20 mL) and neutralised by careful addition of 1M aqueous hydrochloric acid. The neutral solution was extracted with ethyl acetate (3 x 20 mL). The combined organics were dried over magnesium sulfate, filtered and concentrated under reduced pressure onto celite (2 g). Purification by flash column chromatography over silica (25 g) 40-60 °C petrol ether: ethyl acetate (100:0) to (70:30) gave the title compound as a clear yellow oil (1.83 g, 61%): R_f 0.30 (20% ethyl acetate / 80% 40-60 °C petrol ether); HRMS-ESI m/z [M+H]$^+$ calcd for $C_9H_{13}O_3$: 169.0859, found: 169.0858; ^{1}H (500 MHz, chloroform-d) δ 7.24 (1 H, s, 6-CH), 5.35 (1 H, s, 2-CH), 3.74 (3 H, s, 3-CH$_3$), 2.76 (1 H, h, *J* = 7 Hz, 5-CH), 2.54 (1 H, dd, *J* = 17, 6 Hz, 4-CH$_2$), 2.19 (1 H, dd, *J* = 17, 7 Hz, 4-CH$_2$), 1.16 (3 H, d, *J* = 7 Hz, 3-CH$_3$); ^{13}C NMR (126 MHz, cdcl$_3$) δ 192.7 (C), 175.8 (C), 161.6 (CH), 111.7 (C), 100.0 (CH), 55.8 (CH$_3$), 36.6 (CH$_2$), 28.6 (CH), 20.3 (CH$_3$); IR (neat, ν$_{max}$) cm^{-1} 2962, 1635, 1598, 1406, 1383, 1167, 1000, 831.

6-Methoxy-4-methyl-4,5-dihydro-1H-indazole (**178**)
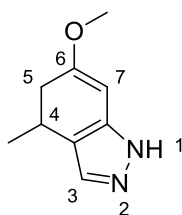
4-Methoxy-6-methyl-2-oxo-cyclohex-3-ene-1-carbaldehyde (1.75 g, 10.4 mmol) was dissolved in dry methyl alcohol (6 mL) and hydrazine monohydrochloride (855 mg, 12.5 mmol) added to this solution and stirred at room temperature for 1 hour. The reaction was concentrated under reduced pressure to near dryness, diluted with ethyl acetate (15 mL), transferred to a separating funnel and was washed with water (3 x 10 mL). The organics were dried over magnesium sulfate, filtered and concentrated under reduced pressure onto celite (2 g). Purification by flash column chromatography over silica (10 g) eluting 40-60 °C petrol ether: ethyl acetate (100:0) to (50:50) gave the title compound as a dark red gum (1.66 g, 96%): HRMS-ESI m/z [M+H]$^+$ calcd for $C_9H_{13}N_2O$: 165.1022, found: 165.1023; ^{1}H (500 MHz, chloroform-d) δ 9.33 (1 H, s, 1-NH), 7.21 (1 H, s, 3-CH), 5.64 (1 H, s, 7-CH), 3.67 (3 H, s, 6-CH$_3$), 3.11-2.98 (1 H, m, 4-CH), 2.44 (1 H, dd, *J* = 16, 7 Hz, 5-CH$_2$), 2.22 (1 H, dd, *J* = 16, 11 Hz, 5-CH$_2$), 1.26 (3 H, d, *J* = 7 Hz, 4-CH$_3$).

6-Methoxy-4-methyl-4,5-dihydrobenzo[d]isoxazole (**179**)
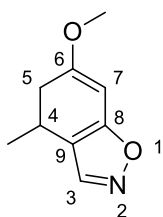
4-Methoxy-6-methyl-2-oxo-cyclohex-3-ene-1-carbaldehyde (2.00 g, 11.9 mmol) and hydroxylamine hydrochloride (825 mg, 11.9 mmol) were dissolved in pyridine (7 mL) and heated to 70 °C for 2 hours. The reaction was concentrated under reduced pressure then diluted with ethyl acetate (30 mL) and washed with 1M aqueous hydrogen chloride solution (30 mL). The combined organics were dried over magnesium sulfate, filtered and concentrated under reduced pressure onto celite (2 g). Purification by flash column chromatography over silica (25 g) eluting 40-60 °C petrol ether: ethyl acetate (100:0) to (50:50) gave the title compound as a viscous red oil (1.85 g, 94%): MS (ESI) m/z (%): 166 (100) [M+H]$^+$; ^{1}H (500 MHz, chloroform-d) δ 7.98 (1 H, s, 3-CH), 5.62 (1 H, s 7-CH), 3.71 (3 H, s, 6-CH$_3$), 3.08-2.99 (1 H, m. 4-CH), 2.60 (1 H, dd, J = 17, 8 Hz, 5-CH$_2$), 2.31 (1 H, dd, J = 17, 10 Hz, 5-CH$_2$), 1.24 (3 H, d, J = 7 Hz, 4-CH$_3$).

4-Methyl-4,5-dihydro-1H-indazol-6(7H)-one (**180**)
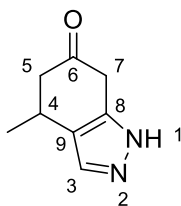
6-Methoxy-4-methyl-4,5-dihydro-1H-indazole (750 mg, 4.57 mmol) was suspended in water (4 mL), 12 M aqueous hydrogen chloride (0.5 mL, 5 mmol) added and the reaction stirred for 16 hours at room temperature. The reaction was neutralised with excess saturated aqueous sodium hydrogen carbonate solution (20 mL) and extracted with ethyl acetate (3 x 20 mL). The combined organics were dried over magnesium sulfate, filtered and concentrated under reduced pressure giving the product as a dark red gum (643 mg, 94%): HRMS-ESI m/z [M+H]$^+$ calcd for $C_8H_{11}N_2O$: 151.0866, found: 151.0871; ^{1}H (500 MHz, chloroform-d) δ 7.47 (1 H, s, 3-CH), 7.04 (1 H, s, 1-NH), 3.68-3.50 (2 H, m, 7-CH$_2$), 3.23-3.12 (1 H, m, 4-CH), 2.72 (1 H, dd, *J* = 14, 5 Hz, 5-CH$_2$), 2.36 (1 H, dd, *J* = 14, 9 Hz, 5-CH$_2$), 1.33 (3 H, d, *J* = 7 Hz, 4-CH$_3$); ^{13}C NMR (126 MHz, chloroform-d) δ 207.6 (C) 143.0 (C), 127.5 (CH), 121.1 (C), 48.1 (CH$_2$), 37.8 (CH$_2$), 26.1 (CH), 21.5 (CH$_3$).

4-Methyl-4,5-dihydrobenzo[d]isoxazol-6(7H)-one (**181**)
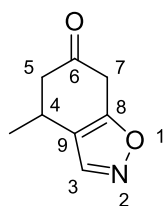
6-Methoxy-4-methyl-4,5-dihydro-1,2-benzoxazole (900 mg, 5.45 mmol) was suspended as an oil in water (3 mL) and concentrated hydrochloric acid (0.45 mL, 5.5 mmol) was added. The reaction was stirred for 16 hours and was then extracted with ethyl acetate (2 x 20 mL). The organics were dried over magnesium sulfate, filtered and concentrated under reduced pressure onto celite (2 g). Purification by flash column chromatography over silica (20 g) eluting 40-60 °C petrol ether: ethyl acetate (100:0) to (50:50) gave the title compound as a yellow gum (764 mg, 93%): MS (EI) m/z (%): 151 (51), 152 (8) [M]$^+$; ^{1}H (500 MHz, chloroform-d) δ 8.21 (1 H, s, 3-CH), 3.69-3.50 (2 H, m, 7-CH$_2$), 3.17-3.04 (1 H, m, 4-CH), 2.77 (1 H, dd, *J* = 14, 6 Hz, 5-CH$_2$), 2.38 (1 H, dd, J 14, 8 Hz, 5-CH$_2$), 1.31 (3 H, d, *J* = 7 Hz, 4-CH$_3$); ^{13}C NMR (126 MHz, chloroform-d) δ 204.2 (C), 163.1 (C), 148.1 (CH), 117.5 (C), 47.2 (CH$_2$), 37.7 (CH$_2$), 24.6(CH), 21.2 (CH$_3$).

5-Methyl-2-octylcyclohexane-1,3-diol (**201**)
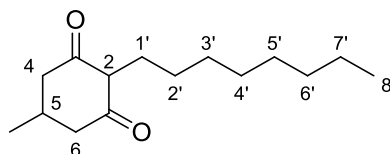
5-Methylcyclohexane-1,3-dione (10.3 g, 81.9 mmol), octanal (8.54 mL, 54.6 mmol) and L-proline (1.26 g, 10.9 mmol) were dissolved in ethanol (150 mL) and stirred for 1 hour. Sodium cyanoborahydride (3.43 g, 54.6 mmol) and molecular sieves (350 mg per mmol of aldehyde) were added and the reaction heated to 80 °C for 2 hours. The reaction was poured onto ice (100 g) and the white solid suspension that formed was vacuum filtered. The solids were dissolved in ethyl acetate (40 mL) and washed with water (2 x 40 mL). The organics were dried over magnesium sulfate, filtered and concentrated under reduced pressure to give the title compound as a white powder (11.9 g, apparent yield 91%) Product was a complex mixture of isomers and full characterisation was confirmed after successful subsequent reaction to 3-methoxy-5-methyl-2-octylcyclohex-2-enone: R_f 0.12 (20% ethyl acetate / 80% 40-60 °C petrol ether); HRMS-ESI m/z [M+H]$^+$ calcd for $C_{15}H_{27}O_2$: 239.2006, found: 239.2005

3-Methoxy-5-methyl-2-octylcyclohex-2-enone (**202**)
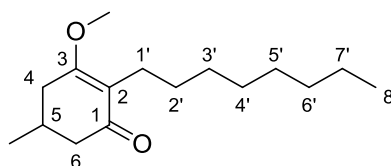
5-Methyl-2-octyl-cyclohexane-1,3-dione (567 mg, 2.38 mmol) and dimethylsulfate (0.23 mL 2.4 mmol) were dissolved in anhydrous tetrahydrofuran (30 mL) and 60% sodium hydride on mineral oil (3.49 g, 87.1 mmol) was added in portions. The reaction was stirred for 18 hours at room temperature concentrated under reduced pressure, diluted with ethyl acetate (20 mL), quenched with water (20 mL) and transferred to a separating funnel. The organics were washed with water (30 mL) and brine (30 mL), dried over magnesium sulfate, filtered and concentrated under reduced pressure onto celite (2 g). Purification by column chromatography over silica (50 g), eluting with a gradient of 40-60 °C petrol ether: ethyl acetate (100:0) to (50:50) and concentration under reduced pressure, gave the title compound as a yellow oil (508 mg, 85%): R_f 0.26 (20% ethyl acetate / 80% 40-60 °C petrol ether); HRMS-ESI m/z [M+H]$^+$ calcd for $C_{16}H_{29}O_2$: 253.2162, found: 253.2163; ^{1}H (500 MHz, chloroform-d) δ 3.80 (3 H, s, 3-CH$_3$), 2.71-2.61 (1 H, m, 4 or 6-CH), 2.44 (1 H, dd, J = 16, 3 Hz, 4 or 6-CH), 2.28-2.11 (4 H, m, 4 or 6-CH, 5-CH and 1'-CH$_2$), 2.07-1.98 (1 H, m, 4 or 6-CH), 1.26 (12 H, s, 2' to 7'-CH$_2$), 1.10 (3 H, d, J = 6 Hz, 5-CH$_2$), 0.88 (3 H, t, J = 7 Hz, 8'-CH$_3$); ^{13}C NMR (126 MHz, chloroform-d) δ 198.0 (C), 170.8 (C), 119.6 (C), 54.9 (CH$_3$), 44.8 (CH$_2$), 33.0 (CH$_2$), 31.8 (CH$_2$), 29.6 (CH$_2$), 29.4 (CH$_2$), 29.2 (CH$_2$), 28.6 (CH$_2$), 28.4(CH), 22.6(CH$_2$), 21.9 (CH$_2$), 21.1 (CH$_3$), 13.9 (CH$_3$); IR (neat, v_{max}) cm^{-1} 2924, 1709, 1377, 1230, 1128, 1061, 1033, 722.

4-Methoxy-6-methyl-3-octyl-2-oxocyclohex-3-enecarbaldehyde (**203**)
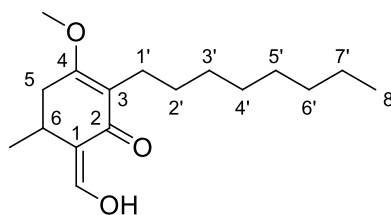
N-Isopropylpropan-2-amine (2.67 mL, 19.0 mmol) was dissolved in dry tetrahydrofuran (150 mL), cooled to -78 °C and *n*-butyllithium (6.18 mL, 15.5 mmol) added. The mixture was allowed to come to room temperature. This was cooled to -78 °C again and a solution of 3-methoxy-5-methyl-2-octyl-cyclohex-2-en-1-one (3.00 g, 11.9 mmol) in dry tetrahydrofuran (5 mL) was added *via* syringe. This was stirred for 1 hour and then dry methyl formate (1.47 mL, 23.8 mmol) was added and the reaction was allowed to come to room temperature overnight slowly. The reaction mixture was concentrated under reduced pressure and diluted with ethyl acetate (30 mL). This was neutralised with 1 M aqueous hydrogen chloride, the organics separated and washed with water (30 mL). The organics were dried over magnesium sulfate, filtered and concentrated under reduced pressure onto celite (2 g). Purification by flash column chromatography over silica (25 g) eluting 40-60 °C petrol ether: ethyl acetate (100:0) to (90:10) gave the title compound as a clear yellow oil (2.25 g, 68%): R_f 0.46 (20% ethyl acetate / 80% 40-60 °C petrol ether); HRMS-ESI m/z [M+H]$^+$ calcd for $C_{17}H_{29}O_3$: 281.2111, found: 281.2113; ^{1}H (500 MHz, chloroform-d) δ 7.19 (1 H, d, J = 1 Hz, 1-CH), 3.79 (3 H, s, 4-CH$_3$), 2.75 (1 H, q, *J* = 7 Hz, 5-CH), 2.65 (1 H, dd, *J* = 17, 6 Hz, 5-CH), 2.37-2.27 (3 H, m, 1'-CH$_2$ and 6-CH), 1.39-1.32 (2 H, m, 2'-CH$_2$), 1.32-1.23 (10 H, m, 3' to 7'-CH$_2$), 1.18 (3 H, d, *J* = 7 Hz, 6-CH$_3$), 0.88 (3 H, t, *J* = 7 Hz, 8'-CH$_3$); ^{13}C NMR (126 MHz, chloroform-d) δ 191.9 (C), 169.3 (C), 160.5 (CH), 111.3 (CH$_3$), 55.0 (CH$_2$), 31.9 (CH$_2$), 31.8 (CH$_2$), 29.6 (CH$_2$), 29.4 (CH$_2$), 29.2 (CH$_2$), 28.6 (CH$_2$), 28.3 (CH), 22.6 (CH$_2$), 21.6 (CH$_2$), 20.4 (CH$_3$), 14.0 (CH$_3$); IR (neat, v_{max}) cm^{-1} 2923, 1608, 1378, 1238, 1159, 1130, 1006, 953.

6-Methoxy-4-methyl-7-octyl-4,5-dihydro-1H-indazole (**205**)
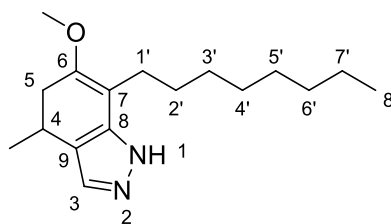
4-Methoxy-6-methyl-3-octyl-2-oxo-cyclohex-3-ene-1-carbaldehyde (500 mg, 1.78 mmol) was dissolved in methanol (5 mL), hydrazine monohydrochloride (134 mg, 1.96 mmol) was added and the reaction was stirred at room temperature for 2 hours. The reaction was concentrated to near dryness under reduced pressure, diluted with water (30 mL) and extracted with ethyl acetate (2 x 30 mL). The combined organics were dried over magnesium sulfate, filtered and concentrated under reduced pressure onto celite (2 g). Purification by flash column chromatography over silica (10 g) eluting 40-60 °C petrol ether: ethyl acetate (100:0) to (75:25) gave the title compound as a red gum (481 mg, 97%). Product unstable, full characterisation after subsequent reaction to 6-methoxy-4-methyl-7-octyl-1H-indazole: MS (ESI) m/z (%): 171 (100) [M+H]$^+$; ^{1}H NMR (500 MHz, chloroform-d) δ 7.25 (1 H, s, 3-CH), 3.64 (3 H, s, 6-CH$_3$), 3.09-2.96 (1 H, m, 4-CH), 2.57 (1 H, dd, *J* = 16, 7 Hz, 5-CH), 2.49 (2 H, t, *J* = 8 Hz, 1'-CH$_2$), 2.22 (1 H, dd, *J* = 16, 10 Hz, 5-CH), 1.58-1.47 (2 H, m, 2'-CH$_2$), 1.40-1.14 (13 H, m, 4-CH$_3$ and 3' to 7'-CH$_2$), 0.87 (3 H, t, *J* = 7 Hz, 8'-CH$_3$).

6-Methoxy-4-methyl-7-octyl-4,5-dihydrobenzo[d]isoxazole (**206**)
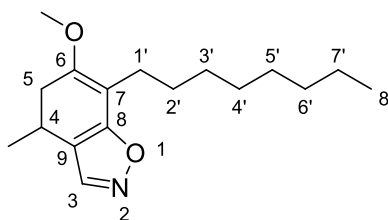
4-Methoxy-6-methyl-3-octyl-2-oxo-cyclohex-3-ene-1-carbaldehyde (375 mg, 1.34 mmol) was dissolved in pyridine (6 mL) and hydroxylamine hydrochloride (102 mg, 1.47 mmol) added. The reaction was heated to 100 °C in a microwave for 1 hour then concentrated under reduced pressure to near dryness. The residue was diluted with ethyl acetate (30 mL) and this was washed with 1 M aqueous hydrochloric acid (2 x 20 mL) then water (2 x 30 mL). The organics were dried over magnesium sulfate, filtered and concentrated under reduced pressure onto celite (2 g). Purification by flash column chromatography over silica (10 g) eluting 40-60 °C petrol ether: ethyl acetate (100:0) to (90:10) gave the title compound as a clear viscous oil (224 mg, 61%). Product unstable, full characterisation after subsequent reaction to 6-methoxy-4-methyl-7-octylbenzo[d]isoxazole: MS (ESI) m/z (%): 178 (100) [M+H]$^+$; ^{1}H (500 MHz, chloroform-d) δ 7.99 (1 H, s, 3-CH), 3.69 (3 H, s, 6-CH$_3$), 3.14-2.99 (1 H, m, 4-CH), 2.71 (1 H, dd, *J* = 17, 8 Hz, 5-CH), 2.44 (2 H, t, *J* = 8 Hz, 1'-CH$_2$), 2.32 (1 H, dd, *J* = 17, 10 Hz, 5-CH), 1.55-1.46 (2 H, m, 2'-CH$_2$), 1.36-1.20 (13 H, m, 3' to 7'-CH$_2$ and 4-CH$_3$), 0.88 (3 H, t, *J* = 7 Hz, 8'-CH$_3$).

6-Methoxy-4-methyl-7-octyl-1H-indazole (**207**)
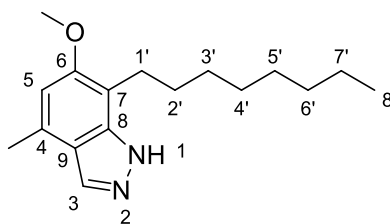
6-Methoxy-4-methyl-7-octyl-4,5-dihydro-1H-indazole (50 mg, 0.18 mmol) and palladium on carbon 60% (3.2 mg, 0.02 mmol) were added to toluene (5 mL) and the reaction was heated to 100 °C for 15 hours. The reaction was cooled, filtered and concentrated under reduced pressure to give the title compound as a pale yellow solid (44 mg, 89%): mp 55-58 °C; R_f 0.28 (20% ethyl acetate / 80% 40-60 °C petrol ether); HRMS-ESI m/z [M+H]$^+$ calcd for $C_{17}H_{27}N_2O$: 275.2118, found: 275.2112; δ H (500 MHz, chloroform-d) 8.06 (1 H, s, 3-CH), 7.28-7.25 (1 H, m, 1-NH), 6.75 (1 H, s, 5-CH), 3.92 (3 H, s, 6-CH$_3$), 2.86 (2 H, t, J = 8 Hz, 1'-CH$_2$), 2.59 (3 H, s, 4-CH$_3$), 1.68-1.60 (2 H, m, 2'-CH$_2$), 1.47-1.14 (10 H, m, 3'-7'-CH$_2$), 0.88 (3 H, t, J =7 Hz, 8'-CH$_3$); ^{13}C NMR (126 MHz, chloroform-d) δ 156.1 (C), 141.0 (C), 133.7 (CH), 129.2 (C), 118.8 (C), 109.0 (CH), 108.4 (C), 56.9 (CH$_3$), 31.9 (CH$_2$), 29.8 (CH$_2$), 29.5 (CH$_2$), 29.3 (CH$_2$), 29.2 (CH$_2$), 25.0 (CH$_2$), 22.6 (CH$_2$), 18.7 (CH$_3$), 14.0 (CH$_3$); IR (neat, v_{max}) cm^{-1} 2921, 2852, 1619, 1460, 1219, 949, 839.

6-Methoxy-4-methyl-7-octylbenzo[d]isoxazole (**208**)
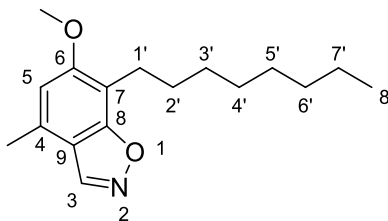
6-Methoxy-4-methyl-7-octyl-4,5-dihydrobenzo[d]isoxazole (50 mg, 0.18 mmol) and palladium on carbon 60% (3.2 mg, 0.02 mmol) were added to toluene (5 mL) and the reaction was heated to 100 °C for 15 hours. The reaction was cooled, filtered and concentrated under reduced pressure to give the title compound as a clear pale yellow oil (46 mg, 93%): mp 48-50 °C; R_f 0.47 (10% ethyl acetate / 90% 40-60 °C petrol ether); HRMS-ESI m/z [M+H]$^+$ calcd for $C_{17}H_{26}NO_2$: 276.1958, found: 276.1950; ^{1}H (500 MHz, chloroform-d) δ 8.59 (1 H, s, 3-CH), 6.74 (1 H, s, 5-CH), 3.91 (3 H, s, 6-CH$_3$), 2.92-2.82 (2 H, m, 1'-CH$_2$), 2.54 (3 H, s, 4-CH$_3$), 1.71-1.59 (2 H, m, 2'-CH$_2$), 1.46-1.18 (10 H, m, 3' to 7'-CH$_2$), 0.88 (3 H, t, J = 7 Hz, 8'-CH$_3$); ^{13}C NMR (126 MHz, chloroform-d) δ 162.4 (C), 158.8 (C), 145.1 (CH), 129.9 (C), 115.4 (C), 110.0 (C), 109.6 (CH), 56.5 (CH$_3$), 31.9 (CH$_2$), 29.6 (CH$_2$), 29.4 (CH$_2$), 29.2 (CH$_2$), 29.1 (CH$_2$), 23.6 (CH$_2$), 22.6 (CH$_2$), 18.7 (CH$_3$), 14.1 (CH$_3$); IR (neat, v_{max}) cm^{-1} 2953, 2851, 2919, 1623, 1600, 1461, 1314, 1219.

Ethyl 3-(2-hydroxy-4-methyl-6-oxocyclohex-1-en-1-yl)propanoate (**209**)
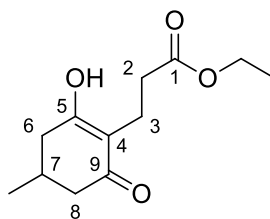
60% Sodium hydride on mineral oil (698 mg, 17.4 mmol) was dissolved in dry N, N-dimethylformamide (30 mL). A dropping funnel was charged with 5-methylcyclohexane-1,3-dione (2.00 g, 15.8 mmol) in N, N-dimethylformamide (10 mL) and was added drop-wise over 5 minutes. The reaction was left to stir for 1 hour before the addition of ethyl acrylate (1.90 mL, 17.4 mmol). The reaction was stirred for a further 2 hours then neutralised with 1 M aqueous hydrogen chloride and diluted with water (50 mL). The quenched solution was transferred to a separating funnel and extracted with diethyl ether (3 x 100 mL). The combined organics were washed with water (2 x 50 mL) followed by saturated brine solution (50 mL). The organics were dried over magnesium sulfate, filtered and concentrated under reduced pressure onto celite (3 g). Purification by flash column chromatography over silica (25 g), eluting petrol ether: ethyl acetate (100: 0) to (50: 50), gave the title compound as a white powder (2.01 g, 56%): HRMS-ESI m/z [M+Na]$^+$ calcd for $C_{12}H_{18}NaO_4$: 249.1097, found: 249.1102; ^{1}H (500 MHz, chloroform-d) δ 9.47 (1 H, s, 5-OH), 4.22-4.16 (1 H, m, 1-CH$_2$), 2.63-2.39 (6 H, m, 2, 6 and 8-CH$_2$), 2.23-2.10 (2 H, m, 3-CH$_2$), 2.08-1.96 (1 H, m, 7-CH), 1.27 (3 H, t, *J* = 7 Hz, 1-CH$_3$), 1.06 (3 H, d, *J* = 6 Hz, 7-CH$_3$).

Tert-butyl 3-(4-methyl-2,6-dioxocyclohexyl)propanoate (**210**)
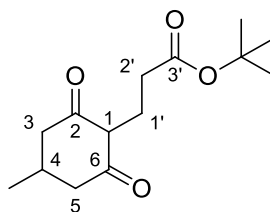
5-Methylcyclohexane-1,3-dione (2.00 g, 15.9 mmol) and *tert* butyl acrylate (2.55 mL, 17.4 mmol) were dissolved in N,N-dimethylformamide (10 mL) and sodium hydride (635 mg, 15.8 mmol) added slowly. The reaction was stirred for 1 hour at room temperature then heated to 80 °C for 16 hours. The reaction was allowed cool to room temperature, acidified to pH 4 with acetic acid then neutralised and diluted with saturated aqueous sodium hydrogen carbonate solution (30 mL). This was extracted with ethyl acetate (3 x 30 mL). The combined organics were washed with saturated aqueous sodium hydrogen carbonate (30 mL), dried over magnesium sulfate, filtered and concentrated under reduced pressure onto celite (4 g). Purification by flash column chromatography over silica (25 g) eluting 40-60 °C petrol ether: ethyl acetate (100:0) to (60:40) gave the title compound as a pale yellow powder (2.94 g, 73%). Product unstable, full characterisation after subsequent reaction to tert-butyl 3-(2-methoxy-4-methyl-6-oxocyclohex-1-en-1-yl)propanoate: HRMS-ESI m/z [M+Na]$^+$ calcd for $C_{14}H_{22}NaO_4$: 277.1410, found: 277.1415; ^{1}H (500 MHz, chloroform-d) δ 2.49-2.36 (6 H, m), 2.18-2.02 (3 H, m), 1.42 (9 H, s, 1'-tBu), 1.02 (3 H, d, *J* = 6 Hz, 4-CH$_3$)

Tert-butyl 3-(2-methoxy-4-methyl-6-oxocyclohex-1-en-1-yl)propanoate (**211**)
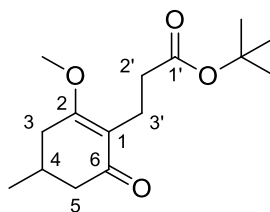
Tert-butyl 3-(2-hydroxy-4-methyl-6-oxo-cyclohexen-1-yl)propanoate (16.0 g, 62.9 mmol) and dimethyl sulfate (7.1 mL, 76 mmol) were dissolved in tetrahydrofuran (200 mL) and 60% sodium hydride on mineral oil (3.0 g, 76 mmol) added slowly. The reaction was stirred at room temperature for 3 hours then the reaction was concentrated under reduced pressure and rediluted with ethyl acetate (25 mL) and water (25 mL). This mixture was neutralised using excess sodium phosphate monobasic. The ethyl acetate was separated and the aqueous layer extracted with ethyl acetate (2 x 30 mL). The combined organics were dried over magnesium sulfate, filtered and concentrated under reduced pressure onto celite (2 g). Purification by flash column chromatography over silica (100 g) eluting 40-60 °C petrol ether: ethyl acetate (100:0) to (80:20) gave the title compound as a clear colourless oil (15.2 g, 90%): R_f 0.17 (20% ethyl acetate / 80% 40-60 °C petrol ether); HRMS-ESI m/z [M+Na]$^+$ calcd for $C_{15}H_{24}NaO_4$: 291.1567, found: 291.1572; ^{1}H (600 MHz, chloroform-d) 3.78 (3 H, s, 2-CH$_3$), 2.69-2.58 (1 H, m, 3 or 5-CH$_3$), 2.55-2.43 (2 H, m, 3'-CH$_2$), 2.43-2.34 (1 H, m, 3 or 5-CH$_3$), 2.24-2.17 (2 H, m, 2'-CH$_3$), 2.17-2.09 (2 H, m, 3 or 5-CH$_2$ and 4-CH), 2.05-1.93 (1 H, m, 3 or 5-CH$_2$), 1.40 (9 H, s, 1'-tBu), 1.07 (3 H, d, *J* = 6 Hz, 4-CH$_2$); ^{13}C NMR (126 MHz, chloroform-d) δ 197.6 (C), 172.9 (C), 171.5 (C), 117.7 (C), 79.6 (C), 55.1 (C), 44.7 (CH$_2$), 34.3 (CH$_2$), 33.0 (CH$_2$), 28.4 (CH), 28.1 (CH$_3$), 21.1 (CH$_3$), 17.8 (CH$_2$); IR (neat, v_{max}) cm^{-1} 2973, 1723, 1611, 1367, 1233, 1148, 1084, 846.

(Z)-Tert-butyl 3-(5-(hydroxymethylene)-2-methoxy-4-methyl-6-oxocyclohex-1-en-1-yl)propanoate (**212**)
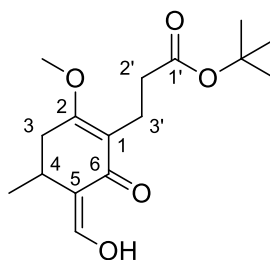
Diisopropylamine (4.6 mL, 32 mmol) was dissolved in dry tetrahydrofuran (550 mL), cooled to -78 °C and 2.5 M *n*-butyllithium (12.2 mL, 30.4 mmol) added. The reaction was warmed to room temperature then cooled to -78 °C and *tert*-butyl 3-(2-methoxy-4-methyl-6-oxo-cyclohexen-1-yl)propanoate (6.80 g, 23.4 mmol) added. The reaction was stirred for 1 hour at -78 °C then methyl formate (2.34 mL, 38.0 mmol) was added and the reaction was allowed to warm to room temperature overnight. The reaction was concentrated under reduced pressure, diluted water (50 mL) and neutralised by careful addition of 1M aqueous hydrogen chloride solution. The organics were dried over magnesium sulfate, filtered and concentrated under reduced pressure onto celite (5 g). Purification by flash column chromatography over silica (100 g) eluting 40-60 °C petrol ether: ethyl acetate (100:0) to (70:30) gave the title compound as a yellow oil (4.41 g, 59%): R_f 0.26 (20% ethyl acetate / 80% 40-60 °C petrol ether); HRMS-ESI m/z [M+H]$^+$ calcd for $C_{16}H_{24}NaO_5$: 319.1510, found: 319.1521; ^{1}H NMR (500 MHz, chloroform-d) 7.21-7.07 (1 H, m, 5-CH), 3.79 (3 H, s, 2-CH$_3$), 2.76-2.69 (1 H, m, 4-CH), 2.67-2.60 (1 H, m, 3-CH$_2$), 2.60-2.56 (2 H, m, 3'-CH$_2$), 2.35-2.25 (3 H, m, 2'-CH and 3-CH$_2$), 1.41 (9 H, s, 1'-tBu), 1.16 (3 H, d, J = 7 Hz, 4-CH$_3$); ^{13}C NMR (126 MHz, chloroform-d) δ 191.7 (C), 172.7 (C), 170.0 (C), 160.3 (CH), 116.5 (C), 111.2 (C), 79.7 (C), 55.2 (CH$_3$), 34.3 (CH$_2$), 32.0 (CH$_2$), 28.3 (CH), 28.1 (CH$_3$), 20.3 (CH$_3$), 17.5 (CH$_2$); IR (neat, v_{max}) cm^1 2973, 1723, 1611, 1367, 1233, 1148, 1084, 846.

Tert-butyl 3-(6-methoxy-4-methyl-4,5-dihydro-1H-indazol-7-yl)propanoate (**213**)
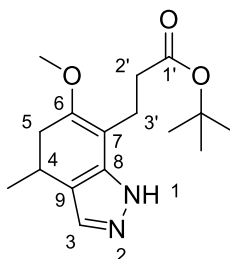
(Z)-*Tert*-butyl 3-(5-(hydroxymethylene)-2-methoxy-4-methyl-6-oxocyclohex-1-en-1-yl) propanoate (3.25 g, 11.0 mmol) was dissolved in methanol (15 mL), hydrazine monohydrochloride (0.939 g, 13.7 mmol) was added and the reaction was stirred at room temperature for 2 hours. The reaction was concentrated to near dryness under reduced pressure, diluted with water (30 mL) and extracted with ethyl acetate (2 x 30 mL). The combined organics were dried over magnesium sulfate, filtered and concentrated under reduced pressure onto celite (2 g). Purification by flash column chromatography over silica (10 g) eluting 40-60 °C petrol ether: ethyl acetate (100:0) to (80:20) gave the title compound as a yellow gum (2.80 g, 87%). Product unstable, full characterisation after subsequent reaction to *tert*-butyl 3-(6-methoxy-4-methyl-1H-indazol-7-yl)propanoate: MS (ESI) m/z (%): 237 (47) 293 (100) [M+H]$^+$; ^{1}H NMR (500 MHz, chloroform-d) δ 7.25 (1 H, s, 3-CH), 3.65 (3 H, s, 6-CH$_3$), 3.10-2.95 (1 H, m, 4-CH), 2.76 (2 H, t, *J* = 8 Hz, 3'-CH$_3$), 2.57 (1 H, dd, *J* = 16, 7 Hz, 5-CH$_2$), 2.49 (2 H, t, *J* = 8 Hz, 2'CH$_3$), 2.21 (1 H, dd, *J* = 16, 11 Hz, 5-CH$_2$), 1.43 (9 H, s, 1'-tBu), 1.28 (3 H, d, *J*= 7 Hz, 4'-CH$_3$).

Tert-butyl 3-(6-methoxy-4-methyl-4,5-dihydrobenzo[d]isoxazol-7-yl)propanoate (**214**)
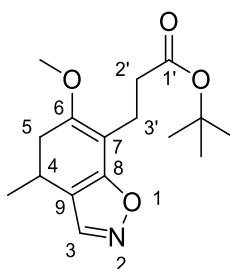
4-Methoxy-6-methyl-3-octyl-2-oxo-cyclohex-3-ene-1-carbaldehyde (3.00 g, 10.3 mmol) was dissolved in pyridine (10 mL) and hydroxylamine hydrochloride (880 mg, 12.6 mmol) added. The reaction was heated to 100 °C in a microwave for 1 hour then concentrated under reduced pressure to near dryness. The residue was diluted with ethyl acetate (30 mL) and this was washed with 1 M aqueous hydrochloric acid (20 mL) and water (2 x 30 mL). The organics were dried over magnesium sulfate, filtered and concentrated under reduced pressure onto celite (2 g). Purification by flash column chromatography over silica (10 g) eluting 40-60 °C petrol ether: ethyl acetate (100:0) to (90:10) gave the title compound as a yellow oil (1.86 g, 61%). Product unstable, full characterisation after subsequent reaction to *tert*-butyl 3-(6-methoxy-4-methylbenzo[d]isoxazol-7-yl)propanoate: MS (ESI) m/z (%): 238 (47), 294 (52) [M+H]$^+$; ^{1}H NMR (500 MHz, chloroform-d) δ 7.99 (1 H, s, 3-CH), 3.71 (3 H, s, 6-CH$_3$), 3.11-2.97 (1 H, m, 4-CH), 2.77-2.67 (3 H, m, 5-CH$_2$ and 3'-CH$_2$), 2.49-2.41 (2 H, m, 2'-CH$_2$), 2.32 (1 H, dd, *J* = 17, 10 Hz, 5-CH$_2$), 1.42 (9 H, s, 1'-tBu), 1.25 (3 H, d, *J* = 7 Hz, 4-CH$_3$).

Tert-butyl 3-(6-methoxy-4-methyl-1H-indazol-7-yl)propanoate (**215**)
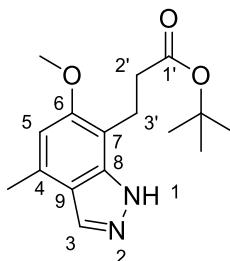
Tert-butyl 3-(6-methoxy-4-methyl-4,5-dihydro-1H-indazol-7-yl)propanoate (600 mg, 2.05 mmol) was dissolved in toluene (20 mL) and 2,3-dichloro-5,6-dicyano-p-benzoquinone (583 mg, 2.57 mmol) added. The reaction was stirred for 16 hours at room temperature then diluted with ethyl acetate (50 mL) and washed with water (5 x 50 mL). The organics were dried over magnesium sulfate, filtered and concentrated under reduced pressure on to celite (2 g). Purification by flash column chromatography over silica (100 g) eluting 40-60 °C petrol ether: ethyl acetate (100:0) to (80:20) gave the title compound as a white/yellow gum (576 mg, 97%): R_f 0.28 (20% ethyl acetate / 80% 40-60 °C petrol ether); MS (ESI) m/z (%): 175 (54), 217 (18), 235 (32), 291 (100) [M+H]$^+$; ^{1}H (500 MHz, chloroform-d) 8.03 (1 H, s, 3-H), 6.69 (1 H, s, 5-CH), 3.91 (3 H, s, 6-CH$_3$), 3.13 (2 H, t, J = 7 Hz, 3'-CH$_2$), 2.61-2.56 (5 H, m, 2'CH$_2$ and 4-CH$_3$), 1.37 (9 H, s, 1'-tBu); ^{13}C NMR (126 MHz, chloroform-d) 174.0 (C), 156.20 (CH), 141.10 (C), 133.40 (C), 130.10 (C), 118.80 (C), 108.40 (CH), 106.60 (C), 80.8, 56.60 (CH$_3$), 35.00 (CH$_2$), 28.0 (CH$_3$), 20.1 (CH$_2$), 18.7(CH$_3$); IR (neat, ν_{max}) cm^1 2971, 2936, 1705, 1624, 1603, 1276, 1232, 1118, 862, 767.

3-(6-Methoxy-4-methyl-1H-indazol-7-yl)propanoic acid (**217**)
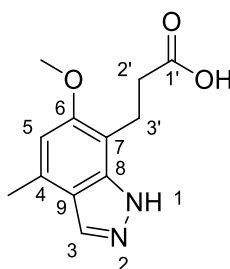
Tert-butyl 3-(6-methoxy-4-methyl-1H-indazol-7-yl)propanoate (250 mg, 0.86 mmol) was dissolved in dichloromethane and trifluoroacetic acid (0.25 mL, 3.3 mmol) added. The reaction was stirred at room temperature for 16 hours and then concentrated under reduced pressure onto celite (1 g). Purification by flash column chromatography over silica (100 g) eluting 40-60 °C petrol ether: ethyl acetate (100:0) to (80:20) gave the title compound as a white/brown solid (189 mg, 93%): mp 153-159 °C; R_f 0.10 (50% ethyl acetate / 50% 40-60 °C petrol ether); HRMS-ESI m/z $[M+H]^+$ calcd for $C_{12}H_{15}N_2O_3$: 235.1077, found: 235.1068; ^1H (500 MHz, dmso-d_6) δ 7.97 (1 H, s, 3-CH), 6.73 (1 H, s, 5-CH), 3.83 (3 H, s, 6-CH$_3$), 3.08-2.85 (2 H, m, 3'-CH$_2$), 2.46-2.40 (2 H, m, 2'-CH$_2$); ^{13}C NMR (126 MHz, dmso-d_6) 174.4 (C), 155.5 (C), 140.9 (C), 133.1 (CH), 129.3 (C), 119.2 (C), 108.6 (CH), 106.2 (C), 57.1 (CH$_3$), 33.7 (CH$_2$), 20.7 (CH$_2$), 18.9 (CH$_3$); IR (neat, v_{max}) cm^1 2921, 1716, 1623, 1297, 1215, 1033, 827.

Tert-butyl 3-(6-methoxy-4-methylbenzo[d]isoxazol-7-yl)propanoate (**216**)
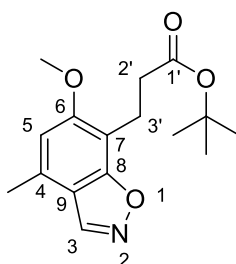
Tert-butyl 3-(6-methoxy-4-methyl-4,5-dihydro-1H-indazol-7-yl)propanoate (1.75 g, 5.97 mmol) was dissolved in toluene (20 mL) and 2,3-dichloro-5,6-dicyano-p-benzoquinone (1.69 g, 7.46 mmol) added. The reaction was stirred for 3 hours at room temperature then diluted with ethyl acetate (50 mL) and washed with water (5 x 50 mL). The organics were dried over magnesium sulfate, filtered and concentrated under reduced pressure on to celite (2 g). Purification by flash column chromatography over silica (100 g) eluting 40-60 °C petrol ether: ethyl acetate (100:0) to (80:20) gave the title compound as a white solid (1.61 g, 93%): mp 63-66 °C; R_f 0.15 (20% ethyl acetate / 80% 40-60 °C petrol ether MS (ESI) m/z (%): 176 (25), 218 (12), 236 (100), 292 (9) [M+H]$^+$; ^{1}H (500 MHz, chloroform-d) 8.60 (1 H, s, 3-CH), 6.74 (1 H, s, 5-CH), 3.92 (3 H, s, 6-CH$_3$), 3.19-3.13 (2 H, m, 3'-CH$_2$), 2.63-2.57 (2 H, m, 2'-CH), 2.55 (3 H, s, 4-CH$_3$), 1.42 (9 H, s, 1'-tBu); ^{13}C NMR (126 MHz, chloroform-d) 172.3 (C), 162.2 (C), 159.0 (C), 145.1 (C), 130.8 (CH), 115.5 (C), 109.5 (CH), 107.7 (C), 80.1 (C), 56.5 (CH$_3$), 34.5 (CH$_2$), 28.0 (CH$_3$), 19.5 (CH$_2$), 18.7 (CH$_3$).

3-(6-Methoxy-4-methylbenzo[d]isoxazol-7-yl)propanoic acid (**218**)
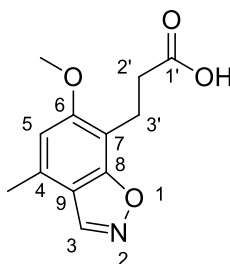
Tert-butyl 3-(6-methoxy-4-methylbenzo[d]isoxazol-7-yl)propanoate (320 mg, 1.10 mmol) was dissolved in dichloromethane and trifluoroacetic acid (0.32 mL, 4.2 mmol) added. The reaction was stirred at room temperature for 16 hours and then concentrated under reduced pressure onto celite (1 g). Purification by flash column chromatography over silica (100 g) eluting 40-60 °C petrol ether: ethyl acetate (100:0) to (80:20) gave the title compound as a white solid (235 mg, 91%): mp 143-147 °C; R_f 0.25 (50% ethyl acetate / 50% 40-60 petrol ether); HRMS-ESI m/z [M+H]$^+$ calcd for $C_{12}H_{14}NO_4$: 236.0917, found: 236.0915; ^{1}H (500 MHz, chloroform-d) δ 8.61 (1 H, s, 3-CH), 6.75 (1 H, s, 5-CH), 3.92 (3 H, s, 6-CH$_3$), 3.26-3.19 (2 H, m, 3'-CH$_2$), 2.76-2.71 (2 H, m, 2'-CH$_2$), 2.56 (3 H, s, 4-CH$_3$); ^{13}C NMR (126 MHz, chloroform) δ 178.2 (C), 162.1 (C), 159.0 (C), 145.1 (CH), 131.1 (C), 115.5 (C), 109.5 (CH), 107.1 (C), 56.5 (CH$_3$), 32.9 (CH$_2$), 19.1 (CH$_2$), 18.8 (CH$_3$); IR (neat, v_{max}) cm^{-1} 2924, 1695, 1304, 1221, 1173, 1125, 835, 826, 658, 645.

General amide coupling procedure:

The desired carboxylic acid (20 mg) was dissolved in N, N-dimethyl formamide (1 mL), triethylamine (3 Eq) was added and this was stirred for 20 minutes. N,N,N′,N′-Tetramethyl-O-(1H-benzotriazol-1-yl)uronium hexafluorophosphate (2.2 Eq) and the selected amine (2.5 Eq) were added and the reaction stirred for 20 hours. Direct purification of reaction mixture by a mass directed auto purification HPLC machine gave the coupled products below:

2-Hydroxy-4-methoxy-6-methyl-3-(3-morpholino-3-oxopropyl)benzonitrile (**232**)
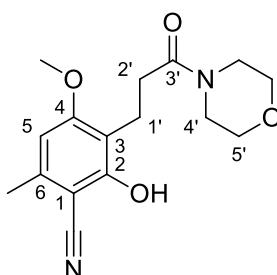
White/brown solid (11 mg, 42%): HRMS-ESI m/z [M+H]$^+$ calcd for $C_{16}H_{20}N_2O_4$: 305.1496, found: 305.1495; ^{1}H (500 MHz, chloroform-d) δ 6.33 (1 H, s, 5-CH), 3.85 (3 H, s, 4-CH$_3$), 3.78-3.52 (6 H, m, 4′ and 5′-CH$_2$), 3.47-3.40 (2 H, m, 4′-CH$_2$), 2.95-2.85 (2 H, m, 1′ or 2′-CH$_2$), 2.67-2.59 (2 H, m, 1′ or 2′-CH$_2$), 2.46 (3 H, s, 6-CH$_3$).

2-Hydroxy-4-methoxy-6-methyl-3-(3-oxo-3-(pyrrolidin-1-yl)propyl)benzonitrile (**233**)
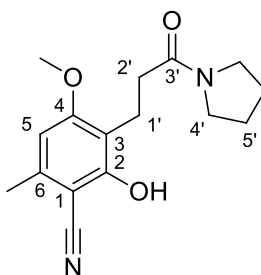
White solid (9 mg, 37%): HRMS-ESI m/z [M+H]$^+$ calcd for $C_{12}H_{14}NO_4$: 236.0917, found: 236.0915; ^{1}H (500 MHz, chloroform-d) δ 6.31 (1 H, s, 5-CH), 3.84 (3 H, s), 3.47 (2 H, t, *J* = 7 Hz), 3.34 (2 H, t, *J* = 7 Hz), 2.98-2.84 (2 H, m), 2.64-2.55 (2 H, m), 2.46 (3 H, s, 6-CH$_3$), 1.95 (2 H, ap p, *J* = 7 Hz, 5′-CH$_2$), 1.85 (2 H, ap p, *J* = 7 Hz, 5′-CH$_2$).

N-Butyl-3-(3-cyano-2-hydroxy-6-methoxy-4-methylphenyl)propanamide (**234**)
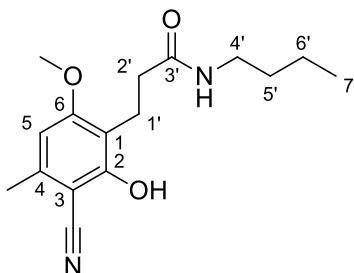
White/brown solid (8 mg, 32%): HRMS-ESI m/z [M+H]$^+$ calcd for $C_{16}H_{23}N_2O_3$: 291.1703, found: 291.1703; ^{1}H (500 MHz, chloroform-d) δ (500 MHz, cdcl$_3$) 10.41 (1 H, br s, 3'-NH), 6.32 (1 H, s, 5-CH), 5.52 (1 H, br s, 2-OH), 3.83 (3 H, s, 6-CH$_3$), 3.33-3.18 (2 H, m, 4'-CH$_2$), 2.93-2.81 (2 H, m, 1' or 2'-CH$_2$), 2.60-2.51 (2 H, m, 1' or 2'-CH$_2$), 2.46 (3 H, s, 4-CH$_3$), 1.51-1.40 (2 H, m, 5'-CH$_2$), 1.34-1.24 (2 H, m, 6'-CH$_2$), 0.91 (3 H, t, J = 7 Hz, 7'-CH$_3$).

3-(6-Methoxy-4-methyl-1H-indazol-7-yl)-1-morpholinopropan-1-one (**235**)
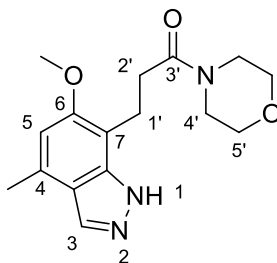
White solid (15 mg, 59%): HRMS-ESI m/z [M+H]$^+$ calcd for $C_{16}H_{21}N_3O_3$: 304.1656, found: 304.1655; ^{1}H (500 MHz, chloroform-d) δ 8.05 (1 H, s, 3-H), 6.70 (1 H, s, 5-CH), 3.92 (3 H, s, 6-CH$_3$), 3.59-3.53 (2 H, m, 4'-CH$_2$), 3.49-3.45 (2 H, m, 4'-CH$_2$), 3.40-3.31 (4 H, m, 5-CH$_2$), 3.26 (2 H, t, J = 6 Hz, 1' or 2'-CH$_2$), 2.67 (2 H, t, J = 6 Hz, 1' or 2'-CH$_2$), 2.59 (3 H, s, 4-CH$_3$).

3-(6-Methoxy-4-methyl-1H-indazol-7-yl)-1-(pyrrolidin-1-yl)propan-1-one (**231**)
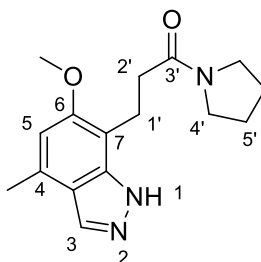
Brown solid (6 mg, 25%): HRMS-ESI m/z [M+H]$^+$ calcd for $C_{16}H_{22}N_3O_2$: 288.1707, found: 288.1705; ^{1}H (500 MHz, chloroform-d) δ 8.04 (1 H, s, 3-CH), 6.70 (1 H, s, 5-CH), 3.93 (3 H, s, 6-CH$_3$), 3.43 (2 H, t, J = 7 Hz, 1'-CH$_2$), 3.28 (4 H, ap q, J = 7 Hz, 4'-CH$_2$), 2.64-2.60 (2 H, m, 2'-CH$_2$), 2.59 (3 H, s, 4-CH$_2$), 1.85 (2 H, ap p, J = 7, 6 Hz, 5'-CH$_2$), 1.78 (2 H, ap p, J = 8, 7 Hz, 5'-CH$_2$).

N-(2-Hydroxyethyl)-3-(6-methoxy-4-methyl-1H-indazol-7-yl)-N-methylpropanamide

(**236**)
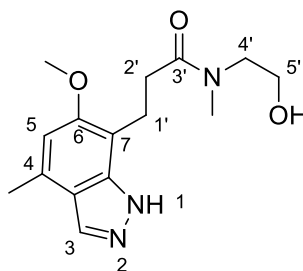
White /brown solid (11 mg, 45%): HRMS-ESI m/z [M+H]$^+$ calcd for $C_{15}H_{23}N_3O_3$: 292.1656, found: 292.1653; ^{1}H (500 MHz, chloroform-d) δ 8.05 (1 H, s), 6.70 (1 H, s), 3.93 (3 H, s), 3.73 (2 H, t, J = 5 Hz), 3.54 (2 H, t, J = 5 Hz), 3.29-3.21 (2 H, m), 2.99 (3 H, s), 2.71 (2 H, t, J = 7 Hz), 2.59 (3 H, s).

Overview and Future work

When this work was initiated it was expected that the development of synthetic methods would occupy no more than two years, leaving time to develop SAR around ascofuranone. The synthesis proved a great deal more challenging than anticipated, expanding to fill the entire PhD and therefore much remains to be investigated around these compounds. Whilst the aromatic head group structure looks deceptively simple, the presence of substituents on most, if not all, constituent atoms often frustrated attempts to transfer developed routes between different headgroup analogues. This was not aided by the difficulty encountered in deprotections across various routes employed. Particularly the *para* phenol, which was discovered to be vital for activity, was challenging to deprotect. In spite of these problems the aims outlined initially were largely achieved.

There was a lack of synthetic means available when commencing and many potential routes were explored. Early forays into palladium chemistry and Fries-like rearrangement afforded only limited results although attachment of the tail to the headgroup was higher yielding than previously reported syntheses. A combination of *ortho* lithiation chemistry and late stage aromatisaiton of aliphatic heterocycles were more successful and allowed the synthesis of a range of novel inhibitors.

The entire ascofuranone molecule required modification to remove the undesirable metabolically labile functionalities. The discovery in the Ward lab of the active benzisoxazole headgroup seemingly addresses the aldehyde and bisphenol which were at the greatest risk of metabolic alteration. The indazoles synthesised have yet to be confirmed as active compounds, however if inhibition of TAO is confirmed then these compounds will be another exciting novel class of TAO inhibitors.

These 5, 6-hetercyclic compounds were developed further and synthetic methods were established to allow diversification of these headgroups. Ultimately little time remained for exploration of the SAR however the synthetic methods validated will allow future exploration of the chemical space around these compounds.

Clearly further exploration is required of the chemical space around the heterocycles with the amide tail. A range of amides should be synthesised with a diverse array of

chemical functionalities in attempt to optimise the medicinal chemistry parameters such as log P and PSA. It is hoped that compounds could be identified which lack the undesirable lipophilicity and metabolic instability associated with the ascofuranone lead compound but which retain activity.

Given that the benzisoxazole appears to isomerise under amide coupling conditions it has become imperative that the activity of the indazoles against TAO be ascertained. If this compound retains activity it would be prudent to shift focus to the indazole core, given that it has proven more easily achievable. If x-ray crystal structures of sufficient quality could be achieved, a computationally guided exploration of point changes on the indazole and benzisoxazole headgroup would be compelling and novel.

Further work to access a range of other heterocycles from the diketone starting material would be of great interest and was underexplored in this work due to time constraints. Of particular interest are the mono heteroatomic indole and thiophene due to their improved stability and common use in pharmaceutical drugs at present. Elsewhere in the Ward lab Beckmann rearrangement of the salicylic motif has successfully generated the benzoxazole and synthesis of a colletochlorin B octyl analogue is underway.

If the heterocyclic compounds synthesised prove to be active inhibitors of TAO it would be necessary to conduct a counter screen against other electron transport chain enzymes to assess selectivity.

References

1   J. Haag, C. O'Huigin and P. Overath, *Mol. Biochem. Parasitol.*, 1998, **91**, 37.

2   A. L. Hughes and H. Piontkivska, *Mol. Biol. Evol.*, 2003, **20**, 644.

3   L. Simpson, O. H. Thiemann, N. J. Savill, J. D. Alfonzo and D. A. Maslov, *Proc. Natl. Acad. Sci. U.S.A*, 2000, **97**, 6986.

4   T. A. Shapiro, *Proc. Natl. Acad. Sci. USA*, 1993, **90**, 7809.

5   V. W. Pollard, S. P. Rohrer, E. F. Michelotti, K. Hancock and S. L. Hajduk, *Cell*, 1990, **63**, 783.

6   S. Vaughan and K. Gull, *J. Cell Sci.*, 2003, **116**, 757.

7   C. Vedrenne, C. Giroud, D. R. Robinson, S. Besteiro, C. Bosc, F. Bringaud and T. Baltz, *Mol. Biol. Cell*, 2002, **13**, 1058–1070.

8   C. A. Hoare, *Adv. Parasitol.*, 1967, **5**, 47.

9   A. K. Davis and W. A. Hopkins, *Parasitol. Res.*, 2013, **112**, 453.

10   J. Votypka and M. Svobodova, *Parasitol. Res.*, 2004, **92**, 147.

11   F. Agüero, V. Campo, L. Cremona, J. M. Di Noia, P. Overath, D. O. Sánchez and A. C. Frasch, *Infect. Immun.*, 2002, **70**, 7140.

12   S. Podlipaev, *Int. J. Parasitol.*, 2001, **31**, 648.

13   E. P. Camargo, *Advances in Parasitology Volume 42*, Academic Press, London, 1999, vol. 42.

14   P. Borst and A. H. Fairlamb, *Annu. Rev. Microbiol.*, 1998, **52**, 745.

15   R. Morty, P. Bulau, R. Pelle, S. Wilk and K. Abe, *Biochem. J.*, 2006, **394**, 635.

16   F. N. Motta, I. M. D. Bastos, E. Faudry, C. Ebel, M. M. Lima, D. Neves, M. Ragno, J. A. R. G. Barbosa, S. M. de Freitas and J. M. Santana, *PLoS One*, 2012, **7**, e30431, doi: 10.1371/journal.pone.0030431.

17   L. Piacenza, G. Peluffo, M. N. Alvarez, A. Martínez and R. Radi, *Antioxid. Redox Signal.*, 2013, **19**, 723.

18   J. Donelson, K. Hill and N. El-Sayed, *Mol. Biochem. Parasitol.*, 1998, **91**, 51.

19   P. T. Manna, C. Boehm, K. F. Leung, S. K. Natesan and M. C. Field, *Trends Parasitol.*, 2014, **30**, 251.

20   B. Namangala, *Parasite Immunol.*, 2011, **33**, 430.

21   D. Jackson, M. Owen and H. Vooreis, *Biochem. Journalm*, 1985, **230**, 195.

22   C. G. Grunfelder, M. Engstler, F. Weise, H. Schwarz, Y.-D. Stierhof, M. Boshart and P. Overath, *Traffic*, 2002, **3**, 547.

23   G. Warren, *Histochem. Cell Biol.*, 2013, **140**, 235.

24   C. M. R. Turner and J. D. Barry, *Parasitology*, 1989, **99**, 67.

25   S. Cencig, N. Coltel, C. Truyens and Y. Carlier, *PLoS Negl. Trop. Dis.*, 2011, **5**, e1216, doi: 10.1371/journal.pntd.0001216.

26   L. Marcello and J. D. Barry, *Genome Res.*, 2007, **17**, 1344.

27   N. M. El-Sayed, P. J. Myler, G. Blandin, M. Berriman, J. Crabtree, G. Aggarwal, E. Caler, H. Renauld, E. A. Worthey, C. Hertz-Fowler, E. Ghedin, C. Peacock, D. C. Bartholomeu, B. J. Haas, A. Tran, J. R. Wortman, U. C. M. Alsmark, S. Angiuoli, A. Anupama, J. Badger, F. Bringaud, E. Cadag, J. M. Carlton, G. C. Cerqueira, T. Creasy, A. L. Delcher, A. Djikeng, T. M. Embley, C. Hauser, A. C. Ivens, S. K. Kummerfeld, J. B. Pereira-Leal, D. Nilsson, J. Peterson, S. L. Salzberg, J. Shallom, J. C. Silva, J. Sundaram, S. Westenberger, O. White, S. E. Melville, J. E. Donelson, B. Andersson, K. D. Stuart and N. Hall, *Science*, 2005, **309**, 404.

28   C. Hertz-Fowler, L. M. Figueiredo, M. A. Quail, M. Becker, A. Jackson, N. Bason, K. Brooks, C. Churcher, S. Fahkro, I. Goodhead, P. Heath, M. Kartvelishvili, K. Mungall, D. Harris, H. Hauser, M. Sanders, D. Saunders, K. Seeger, S. Sharp, J. E. Taylor, D. Walker, B. White, R. Young, G. A. M. Cross, G. Rudenko, J. D. Barry, E. J. Louis and M. Berriman, *PLoS One*, 2008, **3**, e3527, doi: 10.1371/journal.pone.0003527.

29   B. Wickstead, K. Ersfeld and K. Gull, *Genome Res.*, 2004, **14**, 1014.

30   A. Y. C. Liu, L. H. T. Van der Ploeg, F. A. M. Rijsewijk, P. Borst and P. Chambon, *J. Mol. Biol.*, 1983, **167**, 57.

31   C. E. Boothroyd, O. Dreesen, T. Leonova, K. I. Ly, L. M. Figueiredo, G. A. M. Cross and F. N. Papavasiliou, *Nature*, 2009, **459**, 278.

32   E. Pays, M. Guyaux, D. Aerts, N. Van Meirvenne and M. Steinert, *Nature*, 1985, **316**, 562.

33   M. McConville and M. Ferguson, *Biochem. J.*, 1993, **294**, 305.

34   J. D. Bangs, T. L. Doering, P. T. Englund and G. W. Hart, *J. Biol. Chem.*, 1988, **263**, 17697.

35   C. Bern, *N. Engl. J. Med.*, 2011, **30**, 2527.

36   R. Brun, J. Blum, F. Chappuis and C. Burri, *Lancet*, 2010, **375**, 148.

37   R. Forde, *J Trop Med*, 1902, **5**, 261.

38   F. Cox, *Infect Dis Clin N Am*, 2004, **18**, 231.

39   J. Dutton, *Thompson Yates Lab Rep*, 1902, **4**, 455.

40   A. Castellani, *Proc R Soc L.*, 1903, **71**, 501.

41   *The history of sleeping sickness, P. de Raadt, http://www.who.int/trypanosomiasis_african/country/history/en/print.html (accessed February 2015)*.

42   *WHO Trypanosomiasis, Human African (factsheet), http://www.who.int/mediacentre/factsheets/fs259/en/ (accessed February 2015)*.

43   N. Baker, H. P. De Koning, P. Ma and D. Horn, *Trends. Parasitol.*, 2013, **29**, 110.

44   R. Lozano, M. Naghavi, K. Foreman, S. Lim, K. Shibuya, V. Aboyans, J. Abraham, T. Adair, R. Aggarwal, S. Y. Ahn, M. Alvarado, H. R. Anderson, L. M. Anderson, K. G. Andrews, C. Atkinson, L. M. Baddour, S. Barker-Collo, D. H. Bartels, M. L. Bell, E. J. Benjamin, D. Bennett, K. Bhalla, B. Bikbov, A. Bin Abdulhak, G. Birbeck, F. Blyth, I.

Bolliger, S. Boufous, C. Bucello, M. Burch, P. Burney, J. Carapetis, H. Chen, D. Chou, S. S. Chugh, L. E. Coffeng, S. D. Colan, S. Colquhoun, K. E. Colson, J. Condon, M. D. Connor, L. T. Cooper, M. Corriere, M. Cortinovis, K. C. de Vaccaro, W. Couser, B. C. Cowie, M. H. Criqui, M. Cross, K. C. Dabhadkar, N. Dahodwala, D. De Leo, L. Degenhardt, A. Delossantos, J. Denenberg, D. C. Des Jarlais, S. D. Dharmaratne, E. R. Dorsey, T. Driscoll, H. Duber, B. Ebel, P. J. Erwin, P. Espindola, M. Ezzati, V. Feigin, A. D. Flaxman, M. H. Forouzanfar, F. G. R. Fowkes, R. Franklin, M. Fransen, M. K. Freeman, S. E. Gabriel, E. Gakidou, F. Gaspari, R. F. Gillum, D. Gonzalez-Medina, Y. A. Halasa, D. Haring, J. E. Harrison, R. Havmoeller, R. J. Hay, B. Hoen, P. J. Hotez, D. Hoy, K. H. Jacobsen, S. L. James, R. Jasrasaria, S. Jayaraman, N. Johns, G. Karthikeyan, N. Kassebaum, A. Keren, J.-P. Khoo, L. M. Knowlton, O. Kobusingye, A. Koranteng, R. Krishnamurthi, M. Lipnick, S. E. Lipshultz, S. L. Ohno, J. Mabweijano, M. F. MacIntyre, L. Mallinger, L. March, G. B. Marks, R. Marks, A. Matsumori, R. Matzopoulos, B. M. Mayosi, J. H. McAnulty, M. M. McDermott, J. McGrath, G. A. Mensah, T. R. Merriman, C. Michaud, M. Miller, T. R. Miller, C. Mock, A. O. Mocumbi, A. A. Mokdad, A. Moran, K. Mulholland, M. N. Nair, L. Naldi, K. M. V. Narayan, K. Nasseri, P. Norman, M. O'Donnell, S. B. Omer, K. Ortblad, R. Osborne, D. Ozgediz, B. Pahari, J. D. Pandian, A. P. Rivero, R. P. Padilla, F. Perez-Ruiz, N. Perico, D. Phillips, K. Pierce, C. A. Pope, E. Porrini, F. Pourmalek, M. Raju, D. Ranganathan, J. T. Rehm, D. B. Rein, G. Remuzzi, F. P. Rivara, T. Roberts, F. R. De León, L. C. Rosenfeld, L. Rushton, R. L. Sacco, J. A. Salomon, U. Sampson, E. Sanman, D. C. Schwebel, M. Segui-Gomez, D. S. Shepard, D. Singh, J. Singleton, K. Sliwa, E. Smith, A. Steer, J. A. Taylor, B. Thomas, I. M. Tleyjeh, J. A. Towbin, T. Truelsen, E. A. Undurraga, N. Venketasubramanian, L. Vijayakumar, T. Vos, G. R. Wagner, M. Wang, W. Wang, K. Watt, M. A. Weinstock, R. Weintraub, J. D. Wilkinson, A. D. Woolf, S. Wulf, P.-H. Yeh, P. Yip, A. Zabetian, Z.-J. Zheng, A. D. Lopez, C. J. L. Murray, M. A. AlMazroa and Z. A. Memish, *Lancet*, 2012, **380**, 2095.

45   B. Devleesschauwer, A. H. Havelaar, C. Maertens de Noordhout, J. A. Haagsma, N. Praet, P. Dorny, L. Duchateau, P. R. Torgerson, H. Van Oyen and N. Speybroeck, *Int. J. Public Health*, 2014, **59**, 571.

46   P. Desjeux, *Comp Immunol Microbiol Infect Dis.*, 2004, **27**, 305.

47   E. M. Fèvre, B. V Wissmann, S. C. Welburn and P. Lutumba, *PLoS Negl. Trop. Dis.*, 2008, **2**, e333, doi: 10.1371/journal.pntd.0000333.

48   B. S. Salgado, C. T. Battaglia, R. S. Stuchi, F. A. Cadioli, D. B. Rozza and G. F. Machado, *Vet. Clin. Pathol.*, 2011, **40**, 103.

49   A. F. Mulla and L. R. Rickman, *Parasitol. Today*, 1988, **4**, 352.

50   C. O. Orenge, L. Munga, C. N. Kimwele, S. Kemp, A. Korol, J. P. Gibson, O. Hanotte and M. Soller, *BMC Genet.*, 2012, **13**, 87.

51   H. Noyes, A. Brass, I. Obara, S. Anderson, A. L. Archibald, D. G. Bradley, P. Fisher, A. Freeman, J. Gibson, M. Gicheru, L. Hall, O. Hanotte, H. Hulme, D. McKeever, C. Murray, S. J. Oh, C. Tate, K. Smith, M. Tapio, J. Wambugu, D. J. Williams, M. Agaba and S. J. Kemp, *Proc. Natl. Acad. Sci. U. S. A.*, 2011, **108**, 9304.

52   O. Hanotte, Y. Ronin, M. Agaba, P. Nilsson, A. Gelhaus, R. Horstmann, Y. Sugimoto, S. Kemp, J. Gibson, A. Korol, M. Soller and A. Teale, *Proc. Natl. Acad. Sci. U. S. A.*, 2003, **100**, 7443.

53 J. Naessens, *Int. J. Parasitol.*, 2006, **36**, 521.

54 *Trypanosomiasis (African), http://www.discontools.eu/Diseases/Detail/61 (accessed February 2015).*

55 E. Wilsion, S Morris, K Krog, *Bull. Wld. Hlth. Org.*, 1963, **28**, 595.

56 R. Thomson, G. Genovese, C. Canon, D. Kovacsics, M. K. Higgins, M. Carrington, C. A. Winkler, J. Kopp, C. Rotimi, A. Adeyemo, A. Doumatey, G. Ayodo, S. L. Alper, M. R. Pollak, D. J. Friedman and J. Raper, *Proc. Natl. Acad. Sci. U. S. A.*, 2014, **111**, E2130–9, doi: 10.1073/pnas.1400699111.

57 L. Vanhamme, F. Paturiaux-Hanocq, P. Poelvoorde, D. P. Nolan, L. Lins, J. Van Den Abbeele, A. Pays, P. Tebabi, H. Van Xong, A. Jacquet, N. Moguilevsky, M. Dieu, J. P. Kane, P. De Baetselier, R. Brasseur and E. Pays, *Nature*, 2003, **422**, 83.

58 S. L. Hajduk, D. R. Moore, J. Vasudevacharya, H. Siqueira, A. F. Torri, E. M. Tytler and J. D. Esko, *J. Biol. Chem.*, 1989, **264**, 5210.

59 J. Raper, R. Fung, J. Ghiso, V. Nussenzweig and S. Tomlinson, *Infect. Immun.*, 1999, **67**, 1910.

60 J. Widener, M. J. Nielsen, A. Shiflett, S. K. Moestrup and S. Hajduk, *PLoS Pathog.*, 2007, **3**, 1250.

61 B. Vanhollebeke, G. De Muylder, M. J. Nielsen, A. Pays, P. Tebabi, M. Dieu, M. Raes, S. K. Moestrup and E. Pays, *Science*, 2008, **320**, 677.

62 K. M. Hager, *J. Cell Biol.*, 1994, **126**, 155.

63 D. P. Nolan, M. Geuskens and E. Pays, *Curr. Biol.*, 1999, **9**, 1169.

64 W. Bullard, R. Kieft, P. Capewell, N. J. Veitch, A. Macleod and S. L. Hajduk, *Virulence*, 2012, **3**, 72.

65 D. Pérez-Morga, B. Vanhollebeke, F. Paturiaux-Hanocq, D. P. Nolan, L. Lins, F. Homblé, L. Vanhamme, P. Tebabi, A. Pays, P. Poelvoorde, A. Jacquet, R. Brasseur and E. Pays, *Science*, 2005, **309**, 469.

66 B. Vanhollebeke and E. Pays, *Mol. Microbiol.*, 2010, **76**, 806.

67 G. Genovese, D. J. Friedman, M. D. Ross, L. Lecordier, P. Uzureau, B. I. Freedman, D. W. Bowden, C. D. Langefeld, T. K. Oleksyk, A. L. Uscinski Knob, A. J. Bernhardy, P. J. Hicks, G. W. Nelson, B. Vanhollebeke, C. A. Winkler, J. B. Kopp, E. Pays and M. R. Pollak, *Science*, 2010, **329**, 841.

68 A. Parsa, W. H. L. Kao, D. Xie, B. C. Astor, M. Li, C. Hsu, H. I. Feldman, R. S. Parekh, J. W. Kusek, T. H. Greene, J. C. Fink, A. H. Anderson, M. J. Choi, J. T. Wright, J. P. Lash, B. I. Freedman, A. Ojo, C. a Winkler, D. S. Raj, J. B. Kopp, J. He, N. G. Jensvold, K. Tao, M. S. Lipkowitz and L. J. Appel, *N. Engl. J. Med.*, 2013, **369**, 2183.

69 E. Pays, B. Vanhollebeke, P. Uzureau, L. Lecordier and D. Pérez-Morga, *Nat. Rev. Microbiol.*, 2014, **12**, 575.

70 R. Brun and O. Balmer, *Curr. Opin. Infect. Dis.*, 2006, **19**, 415.

71 P. P. Simarro, G. Cecchi, M. Paone, J. R. Franco, A. Diarra, J. A. Ruiz, E. M. Fèvre, F. Courtin, R. C. Mattioli and J. G. Jannin, *Int. J. Health Geogr.*, 2010, **9**, 57.

72 M. Odiit, F. Kansiime and J. Enyaru, *East Afr Med J*, 1997, **74**, 792.

73   N. A. Stephens, R. Kieft, A. Macleod and S. L. Hajduk, *Trends Parasitol.*, 2012, **28**, 539.

74   J. C. K. Enyaru, E. Matovu, B. Nerima, M. Akol and C. Sebikali, *Ann. N. Y. Acad. Sci.*, 2006, **1081**, 311.

75   S. Welburn, K. Picozzi, E. Fèvre, P. Coleman, M. Odiit, M. Carrington and I. Maudlin, *Lancet*, 2001, **358**, 2017.

76   L. M. MacLean, M. Odiit, J. E. Chisi, P. G. E. Kennedy and J. M. Sternberg, *PLoS Negl. Trop. Dis.*, 2010, **4**, e906, doi: 10.1371/journal.pntd.0000906.

77   G. Hide, *Clin. Microbiol. Rev.*, 1999, **12**, 112.

78   T. Koerner, P. de Raadt and I. Maudlin, *Parasitol. Today*, 1995, **11**, 303.

79   H. Van Xong, L. Vanhamme, M. Chamekh, C. E. Chimfwembe, J. Van Den Abbeele, A. Pays, N. Van Meirvenne, R. Hamers, P. De Baetselier and E. Pays, *Cell*, 1998, **95**, 839.

80   N. Campillo and M. Carrington, *Mol. Biochem. Parasitol.*, 2003, **127**, 79.

81   L. Vanhamme, H. Renauld, L. Lecordier, P. Poelvoorde, J. Van Den Abbeele and E. Pays, *Mol. Biochem. Parasitol.*, 2004, **135**, 39.

82   N. A. Stephens and S. L. Hajduk, *Eukaryot. Cell*, 2011, **10**, 1023.

83   M. W. Oli, L. F. Cotlin, A. M. Shiflett and S. L. Hajduk, *Eukaryot. Cell*, 2006, **5**, 132.

84   J. Wang, U. Böhme and G. A. M. Cross, *Mol. Biochem. Parasitol.*, 2003, **128**, 135.

85   L. Lecordier, B. Vanhollebeke, P. Poelvoorde, P. Tebabi, F. Paturiaux-Hanocq, F. Andris, L. Lins and E. Pays, *PLoS Pathog.*, 2009, **5**, e1000685, doi: 10.1371/journal.ppat.1000685.

86   R. Thomson, P. Molina-Portela, H. Mott, M. Carrington and J. Raper, *Proc. Natl. Acad. Sci. U. S. A.*, 2009, **106**, 19509.

87   F. B. Piel, A. P. Patil, R. E. Howes, O. A. Nyangiri, P. W. Gething, T. N. Williams, D. J. Weatherall and S. I. Hay, *Nat. Commun.*, 2010, **1**, 104.

88   F. Checchi, J. a N. Filipe, D. T. Haydon, D. Chandramohan and F. Chappuis, *BMC Infect. Dis.*, 2008, **8**, 16.

89   D. Sudarshi, S. Lawrence, W. O. Pickrell, V. Eligar, R. Walters, S. Quaderi, A. Walker, P. Capewell, C. Clucas, A. Vincent, F. Checchi, A. MacLeod and M. Brown, *PLoS Negl. Trop. Dis.*, 2014, **8**, e3349, doi: 10.1371/journal.pntd.0003349.

90   D. Malvy and F. Chappuis, *Clin. Microbiol. Infect.*, 2011, **17**, 986.

91   F. Njiokou, C. Laveissière, G. Simo, S. Nkinin, P. Grébaut, G. Cuny and S. Herder, *Infect. Genet. Evol.*, 2006, **6**, 147.

92   M. Berberof, D. Pérez-Morga and E. Pays, *Mol. Biochem. Parasitol.*, 2001, **113**, 127.

93   P. Capewell, C. Clucas, E. DeJesus, R. Kieft, S. Hajduk, N. Veitch, P. C. Steketee, A. Cooper, W. Weir and A. MacLeod, *PLoS Pathog.*, 2013, **9**, e1003686, doi: 10.1371/journal.ppat.1003686.

94   P. Uzureau, S. Uzureau, L. Lecordier, F. Fontaine, P. Tebabi, F. Homblé, A. Grélard,

V. Zhendre, D. P. Nolan, L. Lins, J.-M. Crowet, A. Pays, C. Felu, P. Poelvoorde, B. Vanhollebeke, S. K. Moestrup, J. Lyngsø, J. S. Pedersen, J. C. Mottram, E. J. Dufourc, D. Pérez-Morga and E. Pays, *Nature*, 2013, **501**, 430.

95   R. E. Symula, J. S. Beadell, M. Sistrom, K. Agbebakun, O. Balmer, W. Gibson, S. Aksoy and A. Caccone, *PLoS Negl. Trop. Dis.*, 2012, **6**, e1728, doi: 10.1371/journal.pntd.0001728.

96   E. DeJesus, R. Kieft, B. Albright, N. A. Stephens and S. L. Hajduk, *PLoS Pathog.*, 2013, **9**, e1003317, doi: 10.1371/journal.ppat.1003317.

97   R. Kieft, P. Capewell, C. M. R. Turner, N. J. Veitch, A. MacLeod and S. Hajduk, *Proc. Natl. Acad. Sci. U. S. A.*, 2010, **107**, 16137.

98   *Parasites   -   African   Trypanosomiasis, http://www.cdc.gov/parasites/sleepingsickness/biology.html (accessed February 2015).*

99   P. G. Kennedy, *Lancet. Neurol.*, 2013, **12**, 186.

100   J. Atouguia and P. Kennedy, *Neurological aspects of human African trypanosomiasis*, Oxford, 2000.

101   P. Kennedy, *The fatal sleep*, Luath Press, Edinburgh, 2010.

102   A. Duggan and M. Hutchington, *J .Trop. Med. Hyg.*, 1966, **69**, 124.

103   P. G. E. Kennedy, *J. Clin. Invest.*, 2004, **113**, 496.

104   J. H. Adams, L. Haller, F. Y. Boa, F. Doua, A. Dago and K. Konian, *Neuropathol. Appl. Neurobiol.*, 1986, **12**, 81.

105   J. Blum, C. Schmid and C. Burri, *Acta Trop.*, 2006, **97**, 55.

106   P. G. E. Kennedy, *Ann. Neurol.*, 2008, **64**, 116.

107   A. Buguet, S. Bisser, T. Josenando, F. Chapotot and R. Cespuglio, *Acta Trop.*, 2005, **93**, 107.

108   P. J. Hotez, A. Fenwick, L. Savioli and D. H. Molyneux, *Lancet*, 2009, **373**, 1570.

109   R. T. Jacobs, B. Nare and M. a Phillips, *Curr. Top. Med. Chem.*, 2011, **11**, 1255.

110   R. Shechter, A. London and M. Schwartz, *Nat. Rev. Immunol.*, 2013, **13**, 206.

111   R. Daneman and A. Prat, *Cold Spring Harb. Perspect. Biol.*, 2015, **7**, a020412, doi: 10.1101/cshperspect.a020412.

112   B. Obermeier, R. Daneman and R. M. Ransohoff, *Nat. Med.*, 2013, **19**, 1584.

113   W. F. Ganong, *Clin. Exp. Pharmacol. Physiol.*, 2000, **27**, 422.

114   T. Llewellyn, H. Zheng, X. Liu, B. Xu and K. P. Patel, *Am. J. Physiol. Regul. Integr. Comp. Physiol.*, 2012, **302**, R424.

115   P. M. Smith and A. V Ferguson, *J. Neuroendocrinol.*, 2012, **24**, 504.

116   G. Burnstock, *Purinergic Signal.*, 2014, **10**, 189.

117   S. Zini, M. C. Fournie-Zaluski, E. Chauvel, B. P. Roques, P. Corvol and C. Llorens-Cortes, *Proc. Natl. Acad. Sci. U. S. A.*, 1996, **93**, 11968.

118   J. Borjigin, L. S. Zhang and A.-A. Calinescu, *Mol. Cell. Endocrinol.*, 2012, **349**, 13.

119   J. Rodgers, *Parasitology*, 2010, **137**, 1995.

120   J. Halper and M. Kjaer, *Adv. Exp. Med. Biol.*, 2014, **802**, 31.

121   W. Masocha, M. E. Rottenberg and K. Kristensson, *Physiol. Behav.*, 2007, **92**, 110.

122   W. Masocha, B. Robertson, M. E. Rottenberg, J. Mhlanga, L. Sorokin and K. Kristensson, *J. Clin. Invest.*, 2004, **114**, 689.

123   U. Boehm, T. Klamp, M. Groot and J. C. Howard, *Annu. Rev. Immunol.*, 1997, **15**, 749.

124   C. T. Prendergast and S. M. Anderton, *Endocrine, Metab. Immune Disord. Targets*, 2009, **9**, 315.

125   M. H. Abdulla, T. O'Brien, Z. B. Mackey, M. Sajid, D. J. Grab and J. H. McKerrow, *PLoS Negl. Trop. Dis.*, 2008, **2**, e298, 10.1371/journal.pntd.0000298.

126   O. V Nikolskaia, A. P. C. de A Lima, Y. V Kim, J. D. Lonsdale-Eccles, T. Fukuma, J. Scharfstein and D. J. Grab, *J. Clin. Invest.*, 2006, **116**, 2739.

127   M. P. Barrett, D. W. Boykin, R. Brun and R. R. Tidwell, *Br. J. Pharmacol.*, 2007, **152**, 1155.

128   C. A. Lanteri, R. R. Tidwell and S. R. Meshnick, *Antimicrob. Agents Chemother.*, 2008, **52**, 875.

129   R. Brun, R. Don, R. T. Jacobs, M. Z. Wang and M. P. Barrett, *Future Microbiol.*, 2011, **6**, 677.

130   R. R. Tidwell, S. K. Jones, J. D. Geratz, K. A. Ohemeng, M. Cory and J. E. Hall, *J. Med. Chem.*, 1990, **33**, 1252.

131   S. M. Bakunova, S. A. Bakunov, D. A. Patrick, E. V. K. S. Kumar, K. A. Ohemeng, A. S. Bridges, T. Wenzler, T. Barszcz, S. K. Jones, K. A. Werbovetz, R. Brun and R. R. Tidwell, *J. Med. Chem.*, 2009, **52**, 2016.

132   C. J. Bacchi, *Interdiscip. Perspect. Infect. Dis.*, 2009, **2009**, 195040, doi: 10.1155/2009/195040.

133   B. Bouteille, O. Oukem, S. Bisser and M. Dumas, *Fundam. Clin. Pharmacol.*, 2003, **17**, 171.

134   F. R. Opperdoes, *J. Cell Biol.*, 1984, **98**, 1178.

135   S. Alsford, S. Eckert, N. Baker, L. Glover, A. Sanchez-Flores, K. F. Leung, D. J. Turner, M. C. Field, M. Berriman and D. Horn, *Nature*, 2012, **482**, 232.

136   H. Ullmann, S. Meis, D. Hongwiset, C. Marzian, M. Wiese, P. Nickel, D. Communi, J.-M. Boeynaems, C. Wolf, R. Hausmann, G. Schmalzing and M. U. Kassack, *J. Med. Chem.*, 2005, **48**, 7040.

137   D. Legros, G. Ollivier, M. Gastellu-Etchegorry, C. Paquet, C. Burri, J. Jannin and P. Büscher, *Lancet*, 2002, **2**, 437.

138   S. Bisser, F. X. N'Siesi, V. Lejon, P. M. Preux, S. Van Nieuwenhove, C. Miaka Mia Bilenge and P. Büscher, *J. Infect. Dis.*, 2007, **195**, 322.

139   G. Gonzalez-Martin, S. Thambo, C. Paulos, I. Vasquez and J. Paredes, *Eur. J. Clin. Pharmacol.*, 1992, **42**, 671.

140   S. R. Wilkinson, M. C. Taylor, D. Horn, J. M. Kelly and I. Cheeseman, *Proc. Natl. Acad. Sci. U. S. A.*, 2008, **105**, 5022.

141   B. S. Hall, C. Bot and S. R. Wilkinson, *J. Biol. Chem.*, 2011, **286**, 13088.

142   S. Patterson and S. Wyllie, *Trends Parasitol.*, 2014, **30**, 289.

143   A. Baliani, G. J. Bueno, M. L. Stewart, V. Yardley, R. Brun, M. P. Barrett and I. H. Gilbert, *J. Med. Chem.*, 2005, **48**, 5570.

144   N. Maina, K. J. Maina, P. Mäser and R. Brun, *Acta Trop.*, 2007, **104**, 84.

145   S. Jeganathan, L. Sanderson, M. Dogruel, J. Rodgers, S. Croft and S. A. Thomas, *J. Pharmacol. Exp. Ther.*, 2011, **336**, 506.

146   L. S. Filardi and Z. Brener, *Trans. R. Soc. Trop. Med. Hyg.*, 1987, **81**, 755.

147   S. R. Wilkinson, M. C. Taylor, D. Horn, J. M. Kelly and I. Cheeseman, *Proc. Natl. Acad. Sci. U. S. A.*, 2008, **105**, 5022.

148   J. A. Castro, M. M. de Mecca and L. C. Bartel, *Hum. Exp. Toxicol.*, 2006, **25**, 471.

149   J. Pépin, F. Milord, F. Meurice, L. Ethier, L. Loko and B. Mpia, *Trans. R. Soc. Trop. Med. Hyg.*, 1992, **86**, 254.

150   M. Romdhani-Younes and M. M. Chaabouni, *J. Sulfur Chem.*, 2012, **33**, 223.

151   WO2008091946, 2008.

152   US4052419 A1, 1977.

153   US3541090, 1970.

154   DE1170957, 1964.

155   L. Kurian, R. Palanimurugan, D. Gödderz and R. J. Dohmen, *Nature*, 2011, **477**, 490.

156   S. M. Oredsson, *Biochem. Soc. Trans.*, 2003, **31**, 366.

157   M. Malumbres, E. Harlow, T. Hunt, T. Hunter, J. M. Lahti, G. Manning, D. O. Morgan, L. H. Tsai and D. J. Wolgemuth, *Nat. Cell Biol.*, 2009, **11**, 1275.

158   D. L. T. Koomoa, D. Geerts, I. Lange, J. Koster, A. E. Pegg, D. J. Feith and A. S. Bachmann, *Int. J. Oncol.*, 2013, **42**, 1219.

159   M. Iten, H. Mett, A. Evans, J. Enyaru, R. Brun and R. Kaminsky, *Antimicrob. Agents Chemother.*, 1997, **41**, 1922.

160   A. L. W. de Gee, P. H. B. Carstens, P. P. McCann and J. M. Mansfield, *Tissue Cell*, 1984, **16**, 731.

161   A. J. Bitonti, P. P. Mccann and A. Sjoerdsma, *Biochem. Pharmacol.*, 1986, **35**, 331.

162   M. A. Phillips and C. C. Wang, *Mol. Biochem. Parasitol.*, 1987, **22**, 9.

163   I. M. Vincent, D. Creek, D. G. Watson, M. A. Kamleh, D. J. Woods, P. E. Wong, R. J. S. Burchmore and M. P. Barrett, *PLoS Pathog.*, 2010, **6**, e1001204, doi: 10.1371/journal.ppat.1001204.

164   S. Alsford, J. M. Kelly, N. Baker and D. Horn, *Parasitology*, 2013, **140**, 1478.

165   E. Zweygarth and R. Kaminsky, *Acta Trop.*, 1991, **48**, 223.

166   J. Franco, S. Pere, A. Diarra, J. A. Ruiz-Postigo, M. Samo and J. Jannin, *Res. Rep. Trop. Med.*, 2012, **31**, 93.

167   G. Priotto, S. Kasparian, W. Mutombo, D. Ngouama, S. Ghorashian, U. Arnold, S. Ghabri, E. Baudin, V. Buard, S. Kazadi-Kyanza, M. Ilunga, W. Mutangala, G. Pohlig, C. Schmid, U. Karunakara, E. Torreele and V. Kande, *Lancet*, 2009, **374**, 56.

168   US4330559 A, 1995.

169   M. Balasegaram, S. Harris, F. Checchi, S. Ghorashian, C. Hamel and U. Karunakara, *Bull. World Health Organ.*, 2006, **84**, 783.

170   S. K. Shahi, R. L. Krauth-Siegel and C. E. Clayton, *Mol. Microbiol.*, 2002, **43**, 1129.

171   A. H. Fairlamb, G. B. Henderson and A. Cerami, *Proc. Natl. Acad. Sci.*, 1989, **86**, 2607.

172   A. H. Fairlamb, G. B. Henderson and A. Cerami, *Proc. Natl. Acad. Sci. U.S.A*, 1989, **86**, 2607.

173   C. K. Banks, O. M. Gruhzit, E. W. Tillitson and J. Controulis, *J. Am. Chem. Soc.*, 1944, **66**, 1771.

174   S. Gibaud, R. Alfonsi, P. Mutzenhardt, I. Fries and A. Astier, *J. Organomet. Chem.*, 2006, **691**, 1081.

175   I. M. Rollo and J. Williamson, *Nature*, 1951, **167**, 147.

176   N. Baker, H. P. de Koning, P. Mäser and D. Horn, *Trends Parasitol.*, 2013, **29**, 110.

177   P. Mäser, C. Sutterlin, A. Kralli and R. Kaminsky, *Science (80-.).*, 1999, **285**, 242.

178   M. L. Stewart, R. J. S. Burchmore, C. Clucas, C. Hertz-Fowler, K. Brooks, A. Tait, A. Macleod, C. M. R. Turner, H. P. De Koning, P. E. Wong and M. P. Barrett, *Eukaryot. Cell*, 2010, **9**, 336.

179   B. Nerima, E. Matovu, G. W. Lubega and J. C. K. Enyaru, *Trop. Med. Int. Health*, 2007, **12**, 1361.

180   E. Matovu, F. Geiser, V. Schneider, P. Mäser, J. C. K. Enyaru, R. Kaminsky, S. Gallati and T. Seebeck, *Mol. Biochem. Parasitol.*, 2001, **117**, 73.

181   A. J. N. Kazibwe, B. Nerima, H. P. de Koning, P. Mäser, M. P. Barrett and E. Matovu, *PLoS Negl. Trop. Dis.*, 2009, **3**, e523, doi: 10.1371/journal.pntd.0000523.

182   N. Baker, L. Glover, J. C. Munday, D. Aguinaga Andrés, M. P. Barrett, H. P. de Koning, D. Horn, D. Aguinaga, M. P. Barrett, H. P. De Koning and D. Horn, *Proc. Natl. Acad. Sci. U. S. A.*, 2012, **109**, 10996.

183   F. E. Graf, P. Ludin, T. Wenzler, M. Kaiser, R. Brun, P. P. Pyana, P. Büscher, H. P. de Koning, D. Horn and P. Mäser, *PLoS Negl. Trop. Dis.*, 2013, **7**, e2475, doi:10.1371/journal.pntd.0002475.

184   J. C. Munday, A. A. Eze, N. Baker, L. Glover, C. Clucas, D. Aguinaga Andrés, M. J. Natto, I. A. Teka, J. McDonald, R. S. Lee, F. E. Graf, P. Ludin, R. J. S. Burchmore, C. M. R. Turner, A. Tait, A. MacLeod, P. Mäser, M. P. Barrett, D. Horn and H. P. De Koning, *J. Antimicrob. Chemother.*, 2014, **69**, 651.

185   C. Burri, T. Baltz, C. Giroud, F. Doua, H. A. Welker and K. Brun, *Chemotherapy*, 1993, **39**, 225.

186   A. Stich, A. Ponte-Sucre and U. Holzgrabe, *Lancet. Infect. Dis.*, 2013, **13**, 733.

187   E. Alirol, D. Schrumpf, J. Amici Heradi, A. Riedel, C. de Patoul, M. Quere and F. Chappuis, *Clin. Infect. Dis.*, 2013, **56**, 195.

188   D. W. P. Pépin J, Milord F, Khonde AN, Niyonsenga T, Loko L, Mpia B, *Trans. R. Soc. Trop. Med. Hyg.*, 1995, **89**, 92.

189   J. Blum, S. Nkunku and C. Burri, *Trop. Med. Int. Heal.*, 2001, **6**, 390.

190   G. Priotto, S. Kasparian, W. Mutombo, D. Ngouama, S. Ghorashian, U. Arnold, S. Ghabri, E. Baudin, V. Buard, S. Kazadi-Kyanza, M. Ilunga, W. Mutangala, G. Pohlig, C. Schmid, U. Karunakara, E. Torreele and V. Kande, *Lancet*, 2009, **374**, 56.

191   P. Seeback, T Maser, *Parasitol. Res.*, 2003, **90**, 24.

192   B. M. J. Pépin, F. Milord, F. Meurice, L. Ethier, L. Loko, *Trans. R. Soc.Trop. Med. Hyg.*, 1992, **86**, 254.

193   *http://www.newscientist.com/article/mg18524821.800-curing-diseases-modern-medicine-has-left-behind.html (accessed February 2015)*.

194   N. S. Pepin J, Khonde N, Maiso F, Doua F, Jaffar S, *Bull. World. Heal. Organ.*, 2000, **78**, 1284.

195   M. P. Barrett, R. J. S. Burchmore, A. Stich, J. O. Lazzari, A. C. Frasch, J. J. Cazzulo and S. Krishna, *Lancet*, 2003, **362**, 1469.

196   P. Lutumba, E. Makieya, A. Shaw, F. Meheus and M. Boelaert, *Emerg. Infect. Dis.*, 2007, **13**, 248.

197   M. Wrry, *Int. J. Antimicro. Ag*, 1994, **4**, 227.

198   V. Delespaux, D. Geysen, P. Van den Bossche and S. Geerts, *Trends Parasitol.*, 2008, **24**, 236.

199   a. S. Peregrine and M. Mamman, *Acta Trop.*, 1993, **54**, 185.

200   A. Sahin, C. Asencio, J. Izotte, D. Pillay, V. Coustou, H. Karembe and T. Baltz, *Vet. Parasitol.*, 2014, **203**, 270.

201   S. Geerts, P. H. Holmes, M. C. Eisler and O. Diall, *Trends Parasitol.*, 2001, **17**, 25.

202   E. O. Mungube, H. S. Vitouley, E. Allegye-Cudjoe, O. Diall, Z. Boucoum, B. Diarra, Y. Sanogo, T. Randolph, B. Bauer, K. H. Zessin and P. H. Clausen, *Parasit. Vectors*, 2012, **5**, 155.

203   A. S. Nagle, S. Khare, A. B. Kumar, F. Supek, A. Buchynskyy, C. J. N. Mathison, N. K. Chennamaneni, N. Pendem, F. S. Buckner, M. H. Gelb and V. Molteni, *Chem. Rev.*, 2014, **114**, 11305.

204   H. B. Tatipaka, J. R. Gillespie, A. K. Chatterjee, N. R. Norcross, M. A. Hulverson, R. M. Ranade, P. Nagendar, S. A. Creason, J. McQueen, N. A. Duster, A. Nagle, F. Supek, V. Molteni, T. Wenzler, R. Brun, R. Glynne, F. S. Buckner and M. H. Gelb, *J. Med. Chem.*, 2014, **57**, 828.

205   J. Keiser, a Stich and C. Burri, *Trends Parasitol.*, 2001, **17**, 42.

206   S. Geerts, P. H. Holmes, M. C. Eisler and O. Diall, *Trends Parasitol.*, 2001, **17**, 25.

207   D. Ding, Y. Zhao, Q. Meng, D. Xie, B. Nare, D. Chen, C. J. Bacchi, N. Yarlett, Y.-K.

Zhang, V. Hernandez, Y. Xia, Y. Freund, M. Abdulla, K.-H. Ang, J. Ratnam, J. H. McKerrow, R. T. Jacobs, H. Zhou and J. J. Plattner, *ACS Med. Chem. Lett.*, 2010, **1**, 165.

208   R. T. Jacobs, B. Nare, S. A. Wring, M. D. Orr, D. Chen, J. M. Sligar, M. X. Jenks, R. A. Noe, T. S. Bowling, L. T. Mercer, C. Rewerts, E. Gaukel, J. Owens, R. Parham, R. Randolph, B. Beaudet, C. J. Bacchi, N. Yarlett, J. J. Plattner, Y. Freund, C. Ding, T. Akama, Y.-K. Zhang, R. Brun, M. Kaiser, I. Scandale and R. Don, *PLoS Negl. Trop. Dis.*, 2011, **5**, e1151.

209   C. Nihei, Y. Fukai, K. Kawai, A. Osanai, Y. Yabu, T. Suzuki, N. Ohta, N. Minagawa, K. Nagai and K. Kita, *FEBS Lett.*, 2003, **538**, 35.

210   T. Shiba, Y. Kido, K. Sakamoto, D. Ken, C. Tsuge and R. Tatsumi, *Proc. Natl. Acad. Sci. U.S.A*, 2013, **110**, 4580.

211   M. Chaudhuri, R. D. Ott and G. C. Hill, *Trends Parasitol.*, 2006, **22**, 484.

212   H. Saimoto, Y. Kido, Y. Haga, K. Sakamoto and K. Kita, *J. Biochem*, 2013, **153**, 267.

213   E. A. Berry, L. S. Huang, D.-W. Lee, F. Daldal, K. Nagai and N. Minagawa, *Biochim. Biophys. Acta*, 2010, **1797**, 360.

214   R. Ott, K. Chibale, S. Anderson, A. Chipeleme, M. Chaudhuri, A. Guerrah, N. Colowick and G. C. Hill, *Acta Trop.*, 2006, **100**, 172.

215   Y. Yabu, T. Suzuki, C. Nihei, N. Minagawa, T. Hosokawa, K. Nagai, K. Kita and N. Ohta, *Parasitol. Int.*, 2006, **55**, 39.

216   Y. Yabu, N. Minagawab, K. Kitac, K. Nagaid, M. Honmab, S. Sakajob, T. Koide and N. Ohta, *Parasitol. Int.*, 1998, **47**, 131.

217   A. B. Clarkson, E. J. Bienen, G. Pollakis and R. W. Grady, *J. Biol. Chem.*, 1989, **264**, 17770.

218   A. Moore and J. Siedow, *Biochim. Biophys. Acta*, 1991, **1059**, 703.

219   G. C. Vanlerberghe and L. McIntosh, *Annu. Rev. Plant Physiol. Plant Mol. Biol.*, 1997, **48**, 703.

220   M. Parsons, T. Furuya, S. Pal and P. Kessler, *Mol. Biochem. Parasitol.*, 2001, **115**, 19.

221   M. Chaudhuri, R. D. Ott, L. Saha, S. Williams and G. C. Hill, *Parasitol. Res.*, 2005, **96**, 178.

222   M. Chaudhuri, W. Ajayi and G. C. Hill, *Mol. Biochem. Parasitol.*, 1998, **95**, 53.

223   W. U. Ajayi, M. Chaudhuri and G. C. Hill, *J. Biol. Chem.*, 2002, **277**, 8187.

224   D. a Berthold, N. Voevodskaya, P. Stenmark, A. Gräslund and P. Nordlund, *J. Biol. Chem.*, 2002, **277**, 43608.

225   M. E. Andersson and P. Nordlund, *FEBS Lett.*, 1999, **449**, 17.

226   T. Shiba, Y. Kido, K. Sakamoto, D. K. Inaoka, C. Tsuge, R. Tatsumi, G. Takahashi, E. O. Balogun, T. Nara, T. Aoki, T. Honma, A. Tanaka, M. Inoue, S. Matsuoka, H. Saimoto, a. L. Moore, S. Harada and K. Kita, *Proc. Natl. Acad. Sci. U.S.A*, 2013, **110**, 4580.

227 M. Zemek, I. Kolingerová, P. Medek, J. Sochor, M. Zemek, I. Kolingerová, P. Medek and J. Sochor, *Regular Triangulation and Tunnels in Proteins*, 2007.

228 G. Hill, *Biochim. Biophys. Acta*, 1976, **456**, 149.

229 M. Chaudhuri, R. Sharan and G. Hill, *J. Eukaryot. Microbiol.*, 2002, **49**, 263.

230 B. Bakker, P. Michels, C. Clayton, S. Helfert and A. M. Este, *Biochem. J.*, 2001, **125**, 117.

231 F. H. Brohn and A. B. J. Clarkson, *Acta Trop.*, 1978, **35**, 23.

232 N. Minagawa, Y. Yabu, K. Kita, K. Nagai, N. Ohta, K. Meguro, S. Sakajo and A. Yoshimoto, *Mol. Biochem. Parasitol.*, 1997, **84**, 271.

233 Y. Yabu, A. Yoshida, T. Suzuki, C. Nihei and K. Kawai, *Parasitol. Int.*, 2003, **52**, 155.

234 E. J. Bienen, M. Saric, G. Pollakis, R. W. Grady and a B. Clarkson, *Mol. Biochem. Parasitol.*, 1991, **45**, 185.

235 T. Hosokawa, M. Sawada and K. Ando, *J. Antibiot. (Tokyo).*, 1973, **5**, 676.

236 M. Sawada, T. Hosokawa, T. Okutomi and K. Ando, *J. Antibiot*, 1973, **26**, 681.

237 J. Magae, T. Hosokawa, K. Ando, K. Nagai and G. Tamura, *J. Antibiot*, 1983, **35**, 1547.

238 G. Tamura and K. Ando, *J. Antibiot*, 1980, **12**, 361.

239 Y. Kido, K. Sakamoto, K. Nakamura, M. Harada, T. Suzuki, Y. Yabu, H. Saimoto, F. Yamakura, D. Ohmori, A. Moore, S. Harada and K. Kita, *Biochim. Biophys. Acta*, 2010, **1797**, 443.

240 A. H. Fairlamb and I. B. Bowman, *Exp. Parasitol.*, 1977, **43**, 353.

241 R. W. Grady, E. J. Bienen and A. B. Clarkson, *Mol. Biochem. Parasitol.*, 1986, **21**, 55.

242 Y. Chang and H. Cho, *Biochem. Biophys. Res. Commun.*, 2012, **422**, 423.

243 J. H. Jeong, S. S. Kang, K. K. Park, H. W. Chang, J. Magae and Y. C. Chang, *Mol. Cancer Ther.*, 2010, **9**, 2102.

244 S. L. Hwang, H. W. Chang, I. K. Lee, B. K. Yang, J. Magae and Y. C. Chang, *Biochem. Biophys. Res. Commun.*, 2010, **396**, 967.

245 H. J. Cho, J. H. Kang, T. Kim, K. K. Park, C. H. Kim, I.-S. Lee, K. S. Min, J. Magae, H. Nakajima, Y. S. Bae and Y. C. Chang, *J. Cell. Biochem.*, 2009, **107**, 335.

246 M. Deponte, *Biochim. Biophys. Acta*, 2013, **1830**, 3217.

247 A. O. Aptula, T. I. Netzeva, I. V. Valkova, M. T. D. Cronin, T. W. Schultz, R. Kühne and G. Schüürmann, *Quant. Struct. Relationships*, 2002, **21**, 12.

248 E. Argese, C. Bettiol, D. Marchetto, S. De Vettori, A. Zambon, P. Miana and P. F. Ghetti, *Toxicol. In Vitro*, 2005, **19**, 1035.

249 M. Y. Moridani, A. Siraki and P. J. O'Brien, *Chem. Biol. Interact.*, 2003, **145**, 213.

250 C. D. Selassie, A. J. Shusterman, S. Kapur, R. P. Verma, L. Zhang and C. Hansch, *J. Chem. Soc. Perkin Trans. 2*, 1999, 2729.

251 F. P. Guengerich, *Chem. Res. Toxicol.*, 2008, **21**, 70.

252   M. A. Tabrizi, P. G. Baraldi, M. Guameri, S. Manfredini, G. P. Pollini and D. Simoni, *Tetrahedron Lett.*, 1991, **32**, 683.

253   Y. Shigemasa, M. Yasui, S. Ohrai, M. Sasaki, H. Sashiwa and H. Saimoto, *J. Org. Chem.*, 1991, **56**, 910.

254   K. Iidri, *Tetrahedron*, 1985, **41**, 3049.

255   K. M. Chen, J. E. Semple and M. M. Joullie, *J. Org. Chem.*, 1985, **50**, 3997.

256   S. Hiroyuki, K. Yukari and H. Tamejiro, *Tetrahedron Lett.*, 1986, **27**, 1607.

257   V. Snieckus, *Chem. Rev.*, 1990, **90**, 879.

258   K. Mori, *Tetrahedron Lett.*, 1983, **24**, 1547.

259   A. Fürstner and T. Gastner, *Org. Lett.*, 2000, **2**, 2467.

260   D. Xue, J. Li, Z.-T. Zhang and J.-G. Deng, *J. Org. Chem.*, 2007, **72**, 5443.

261   M. Aldeghi, S. Malhotra, D. L. Selwood and A. W. E. Chan, *Chem. Biol. Drug Des.*, 2014, **83**, 450.

262   D. E. Pearson and C. A. Buehler, *Synthesis (Stuttg).*, 1972, **1972**, 533.

263   E. Buncel, J. M. Dust and F. Terrier, *Chem. Rev.*, 1995, **95**, 2261.

264   H. H. Wenk, M. Winkler and W. Sander, *Angew. Chem. Int. Ed. Engl.*, 2003, **42**, 502.

265   J. Hassan, M. Sévignon, C. Gozzi, E. Schulz and M. Lemaire, *Chem. Rev.*, 2002, **102**, 1359.

266   K. C. Nicolaou, S. A. Snyder, T. Montagnon and G. Vassilikogiannakis, *Angew. Chemie Int. Ed.*, 2002, **41**, 1668.

267   S. Suzuki, Y. Segawa, K. Itami and J. Yamaguchi, *Nat. Chem.*, 2015, **7**, 227.

268   A. V. Vorogushin, W. D. Wulff and H.-J. Hansen, *J. Am. Chem. Soc.*, 2002, **124**, 6512.

269   R. L. Danheiser, R. G. Brisbois, J. J. Kowalczyk and R. F. Miller, *J. Am. Chem. Soc.*, 1990, **112**, 3093.

270   Z. Xi, K. Sato, Y. Gao, J. Lu and T. Takahashi, *J. Am. Chem. Soc.*, 2003, **125**, 9568.

271   S. Saito and Y. Yamamoto, *Chem. Rev.*, 2000, **100**, 2901.

272   L. V. R. Boñaga, H.-C. Zhang, A. F. Moretto, H. Ye, D. A. Gauthier, J. Li, G. C. Leo and B. E. Maryanoff, *J. Am. Chem. Soc.*, 2005, **127**, 3473.

273   N. Asao, H. Aikawa and Y. Yamamoto, *J. Am. Chem. Soc.*, 2004, **126**, 7458.

274   N. Asao, K. Takahashi, S. Lee, T. Kasahara and Y. Yamamoto, *J. Am. Chem. Soc.*, 2002, **124**, 12650.

275   N. Asao, T. Nogami, S. Lee and Y. Yamamoto, *J. Am. Chem. Soc.*, 2003, **125**, 10921.

276   P. Langer and G. Bose, *Angew. Chem. Int. Ed. Engl.*, 2003, **42**, 4033.

277   A. R. Katritzky, J. Li and L. Xie, *Tetrahedron*, 1999, **55**, 8263.

278   P. Turnbull and H. W. Moore, *J. Org. Chem.*, 1995, **60**, 644.

279   S. Serra, C. Fuganti and A. Moro, *J. Org. Chem.*, 2001, **66**, 7883.

280   O. Barun, S. Nandi, K. Panda, H. Ila and H. Junjappa, *J. Org. Chem.*, 2002, **67**, 5398.

281   X. Bi, D. Dong, Q. Liu, W. Pan, L. Zhao and B. Li, *J. Am. Chem. Soc.*, 2005, **127**, 4578.

282   R. Ballini, L. Barboni, D. Fiorini, G. Giarlo and A. Palmieri, *Chem. Commun. (Camb).*, 2005, 2633.

283   M. J. Lee, K. Y. Lee, S. Gowrisankar and J. N. Kim, *Tetrahedron Lett.*, 2006, **47**, 1355.

284   H. Saimoto and T. Hiyama, *Tetrahedron Lett.*, 1986, **27**, 597.

285   A. O. King, N. Okukado and E. Negishi, *J. Chem. Soc. Chem. Commun.*, 1977, 683.

286   K. Tamao, K. Sumitani and M. Kumada, *J. Am. Chem. Soc.*, 1972, **94**, 4374.

287   Y. Hatanaka and T. Hiyama, *J. Org. Chem.*, 1988, **53**, 918.

288   A. Publication, *Org. Synth.*, 1990, **68**, 116.

289   N. Miyaura, K. Yamada and A. Suzuki, *Tetrahedron Lett.*, 1979, **20**, 3437.

290   N. Miyaura and A. Suzuki, *Chemistry*, 1995, **95**, 2457.

291   T. N. Glasnov and C. O. Kappe, *Adv. Synth. Catal.*, 2010, **352**, 3089.

292   C. D. Roy and H. C. Brown, *J. Organomet. Chem.*, 2007, **692**, 784.

293   M. Utsugi, Y. Kamada, H. Miyamoto and M. Nakada, *Tetrahedron Lett.*, 2007, **48**, 6868.

294   G. A. Molander and B. Canturk, *Angew. Chem. Int. Ed. Engl.*, 2009, **48**, 9240.

295   S. J. Lee, K. C. Gray, J. S. Paek and M. D. Burke, *J. Am. Chem. Soc.*, 2008, **130**, 466.

296   H. Ihara, M. Koyanagi and M. Suginome, *Org. Lett.*, 2011, **13**, 2662.

297   E. P. Gillis and M. D. Burke, *J. Am. Chem. Soc.*, 2007, **129**, 6716.

298   B. Basu, K. Biswas, S. Kundu and S. Ghosh, *Green Chem.*, 2010, **12**, 1734.

299   J. P. Simeone and J. R. Sowa, *Tetrahedron*, 2007, **63**, 12646.

300   F.-S. Han, *Chem. Soc. Rev.*, 2013, **42**, 5270.

301   K. Takenaka, M. Minakawa and Y. Uozumi, *J. Am. Chem. Soc.*, 2005, **127**, 12273.

302   R. Martin and S. L. Buchwald, *Acc. Chem. Res.*, 2008, **41**, 1461.

303   M. N. Hopkinson, C. Richter, M. Schedler and F. Glorius, *Nature*, 2014, **510**, 485.

304   C. C. C. Johansson Seechurn, M. O. Kitching, T. J. Colacot and V. Snieckus, *Angew. Chem. Int. Ed. Engl.*, 2012, **51**, 5062.

305   J. Smidt, W. Hafner, R. Jira, J. Sedlmeier, R. Sieber, R. Rüttinger and H. Kojer, *Angew. Chemie*, 1959, **71**, 176.

306   J. Smidt and W. Hafner, *Angew. Chemie*, 1959, **71**, 284.

307   R. F. Heck, *J. Am. Chem. Soc.*, 1968, **90**, 5546.

308   R. F. Heck, *J. Am. Chem. Soc.*, 1968, **90**, 5542.

309   R. F. Heck, *J. Am. Chem. Soc.*, 1968, **90**, 5538.

310   R. F. Heck, *J. Am. Chem. Soc.*, 1968, **90**, 5535.

311   R. F. Heck, *J. Am. Chem. Soc.*, 1968, **90**, 5531.

312   R. F. Heck, *J. Am. Chem. Soc.*, 1968, **90**, 5526.

313   R. F. Heck, *J. Am. Chem. Soc.*, 1968, **90**, 5518.

314   K. Sonogashira, Y. Tohda and N. Hagihara, *Tetrahedron Lett.*, 1975, **16**, 4467.

315   D. Milstein and J. K. Stille, *J. Am. Chem. Soc.*, 1978, **100**, 3636.

316   J. K. Stille, *Angew. Chemie*, 1986, **98**, 504.

317   C. Amatore, G. Le Duc and A. Jutand, *Chemistry*, 2013, **19**, 10082.

318   N. Miyaura, T. Yanagi and A. Suzuki, *Synth. Commun.*, 1981, **11**, 513.

319   B. H. Lipshutz, T. B. Petersen and A. R. Abela, *Org. Lett.*, 2008, **10**, 1333.

320   N. Miyaura, K. Yamada, H. Suginome and A. Suzuki, *J. Am. Chem. Soc.*, 1985, **107**, 972.

321   G. B. Smith, G. C. Dezeny, D. L. Hughes, A. O. King and T. R. Verhoeven, *J. Org. Chem.*, 1994, **59**, 8151.

322   K. Matos and J. A. Soderquist, *J. Org. Chem.*, 1998, **63**, 461.

323   J. Jover, N. Fey, M. Purdie, G. C. Lloyd-Jones and J. N. Harvey, *J. Mol. Catal. A Chem.*, 2010, **324**, 39.

324   A. A. C. Braga, N. H. Morgon, G. Ujaque, A. Lledós and F. Maseras, *J. Organomet. Chem.*, 2006, **691**, 4459.

325   R. Glaser and N. Knotts, *J. Phys. Chem. A*, 2006, **110**, 1295.

326   C. Amatore, A. Jutand and G. Le Duc, *Angew. Chem. Int. Ed. Engl.*, 2012, **51**, 1379–
.

327   C. Amatore, A. Jutand and G. Le Duc, *Chemistry*, 2012, **18**, 6616.

328   C. Amatore, A. Jutand and G. Le Duc, *Chemistry*, 2011, **17**, 2492.

329   K. Köhler, W. Kleist and S. S. Pröckl, *Inorg. Chem.*, 2007, **46**, 1876.

330   L. D. Pachón and G. Rothenberg, *Appl. Organomet. Chem.*, 2008, **22**, 288.

331   D. Astruc, *Inorg. Chem.*, 2007, **46**, 1884.

332   M. Weck and C. W. Jones, *Inorg. Chem.*, 2007, **46**, 1865.

333   N. T. S. Phan, M. Van Der Sluys and C. W. Jones, *Adv. Synth. Catal.*, 2006, **348**, 609.

334   M. B. Thathagar, P. J. Kooyman, R. Boerleider, E. Jansen, C. J. Elsevier and G. Rothenberg, *Adv. Synth. Catal.*, 2005, **347**, 1965.

335   A. F. Lee, P. J. Ellis, I. J. S. Fairlamb and K. Wilson, *Dalt. Trans.*, 2010, **39**, 10473.

336   A. K. Diallo, C. Ornelas, L. Salmon, J. Ruiz Aranzaes and D. Astruc, *Angew. Chem. Int. Ed. Engl.*, 2007, **46**, 8644.

337   P.-P. Fang, A. Jutand, Z.-Q. Tian and C. Amatore, *Angew. Chem. Int. Ed. Engl.*, 2011, **50**, 12184.

338   J. J. Davis, C. B. Bagshaw, K. L. Busuttil, Y. Hanyu and K. S. Coleman, *J. Am. Chem. Soc.*, 2006, **128**, 14135.

339   J. J. Davis and Y. Hanyu, *Nanotechnology*, 2010, **21**, 265302.

340   P. J. Ellis, I. J. S. Fairlamb, S. F. J. Hackett, K. Wilson and A. F. Lee, *Angew. Chem.*

Int. Ed. Engl., 2010, **49**, 1820.

341 A. V Gaikwad, A. Holuigue, M. B. Thathagar, J. E. ten Elshof and G. Rothenberg, *Chemistry*, 2007, **13**, 6908.

342 M. Pérez-Lorenzo, *J. Phys. Chem. Lett.*, 2012, **3**, 167.

343 N. Miyaura, M. Satoh and A. Suzuki, *Tetrahedron Lett.*, 1986, **27**, 3745.

344 L. W. Deady and D. M. Werden, *J. Org. Chem.*, 1987, **52**, 3930.

345 D.-H. Lee and M.-J. Jin, *Org. Lett.,* 2011, **13**, 252.

346 J. H. Kirchhoff, M. R. Netherton, I. D. Hills and G. C. Fu, *J. Am. Chem. Soc.*, 2002, **124**, 13662.

347 B. Saito and G. C. Fu, *J. Am. Chem. Soc.*, 2007, **129**, 9602.

348 M. Foà, R. Santi and F. Garavalia, *J. Organomet. Chem.*, 1981, **206**, C29.

349 K. M. Bjerglund, T. Skrydstrup and G. A. Molander, *Org. Lett.*, 2014, **16**, 1888.

350 N. Rodríguez and L. J. Goossen, *Chem. Soc. Rev.*, 2011, **40**, 5030.

351 Z. Lu, A. Wilsily and G. C. Fu, *J. Am. Chem. Soc.*, 2011, **133**, 8154.

352 G. A. Molander, S. L. J. Trice and S. M. Kennedy, *J. Org. Chem.*, 2012, **77**, 8678.

353 Q. Liang, P. Xing, Z. Huang, J. Dong, K. B. Sharpless, X. Li and B. Jiang, *Org. Lett.*, 2015, **17**, 1942.

354 T. Nishikata, A. R. Abela, S. Huang and B. H. Lipshutz, *J. Am. Chem. Soc.*, 2010, **132**, 4978.

355 E. P. Gillis and M. D. Burke, *J. Am. Chem. Soc.*, 2008, **130**, 14084.

356 J. Yang, P. Li and L. Wang, *Synthesis (Stuttg).*, 2011, **2011**, 1295.

357 X. Zhang, P. Li, Y. Ji, L. Zhang and L. Wang, *Synthesis (Stuttg).*, 2011, **2011**, 2975.

358 D. C. Gerbino, S. D. Mandolesi, H. G. Schmalz and J. C. Podestá, *European J. Org. Chem.*, 2009, **2009**, 3964.

359 G. A. Molander and N. Ellis, *Acc. Chem. Res.*, 2007, **40**, 275.

360 M. R. Dintzner, K. M. Morse, K. M. McClelland and D. M. Coligado, *Tetrahedron Lett.*, 2004, **45**, 79.

361 W. G. Dauben, J. M. Cogen and V. Behar, *Tetrahedron Lett.*, 1990, **31**, 3241.

362 L. Claisen, *Berichte der Dtsch. Chem. Gesellschaft*, 1912, **45**, 3157–3166.

363 S. Osuna, S. Kim, G. Bollot and K. N. Houk, *European J. Org. Chem.*, 2013, **2013**, 2823.

364 D. B. Smith, T. R. Elworthy, D. J. Morgans, J. T. Nelson, J. W. Patterson, A. Vasquez and A. M. Waltos, *Tetrahedron Lett.*, 1996, **37**, 21.

365 F. X. Talamás, D. B. Smith, A. Cervantes, F. Franco, S. T. Cutler, D. G. Loughhead, D. J. Morgans and R. J. Weikert, *Tetrahedron Lett.*, 1997, **38**, 4725.

366 K. Fries and G. Finck, *Berichte der Dtsch. Chem. Gesellschaft*, 1908, **41**, 4271.

367 K. Fries and W. Pfaffendorf, *Berichte der Dtsch. Chem. Gesellschaft*, 1910, **43**, 212.

368 T. Bach and J. P. Hehn, *Angew. Chemie Int. Ed.*, 2011, **50**, 1000.

369 S. Horne and R. Rodrigo, *J. Chem. Soc. Chem. Commun.*, 1992, 164.

370 C. Friedel and J. M. Crafts, *J. Chem. Soc.*, 1877, **32**, 725.

371 E. V. A. Schindlbeck, V. M. Chari and W. Germany, *Tetrahedron*, 1982, **38**, 133.

372 U. Hidemitsu, N. Yoshinori and M. Kazuhiro, *Tetrahedron*, 1984, **40**, 4741.

373 I. Thomsen and K. B. G. Torrssell, *Acta Chem. Scand.*, 1991, **45**, 539.

374 H. Gilman and R. L. Bebb, *J. Am. Chem. Soc.*, 1939, **61**, 109.

375 G. Wittig and G. Fuhrmann, *Berichte der Dtsch. Chem. Gesellschaft (A B Ser.*, 1940, **73**, 1197.

376 R. E. Ludt, J. S. Griffiths, K. N. McGrath and C. R. Hauser, *J. Org. Chem.*, 1973, **38**, 1668.

377 W. H. Puterbaugh and C. R. Hauser, *J. Org. Chem.*, 1964, **29**, 853.

378 H. W. Gschwend and H. R. Rodriguez, *Org. React.*, 1979, **26,** 772.

379 M. Morton, L. J. Fetters and E. E. Bostick, *J. Polym. Sci. Part C Polym. Symp.*, 2007, **1**, 311.

380 G. W. Klumpp and M. J. Sinnige, *Tetrahedron Lett.*, 1986, **27**, 2247.

381 C. D. Broaddus, *J. Org. Chem.*, 1970, **35**, 10–15.

382 D. A. Shirley, T. E. Harmon and C. Chun Fong, *J. Organomet. Chem.*, 1974, **69**, 327.

383 D. A. Shirley and J. P. Hendrix, *J. Organomet. Chem.*, 1968, **11**, 217.

384 R. R. Fraser, M. Bresse and T. S. Mansour, *J. Am. Chem. Soc.*, 1983, **105**, 7790.

385 A. Pross, L. Radom and R. W. Taft, *Prog. Phys. Org. Chem*, 1981, **13**, 176.

386 D. W. Slocum and B. P. Koonsvitsky, *J. Org. Chem.*, 1973, **38**, 1675.

387 R. D. Thomas, R. M. Jensen and T. C. Young, *Organometallics*, 1987, **6**, 565.

388 H. L. Lewis and T. L. Brown, *J. Am. Chem. Soc.*, 1970, **92**, 4664.

389 J. F. McGarrity and C. A. Ogle, *J. Am. Chem. Soc.*, 1985, **107**, 1805.

390 H. J. Reich, *Chem. Rev.*, 2013, **113**, 7130.

391 M. Iwao, T. Iihama, K. K. Mahalanabis, H. Perrier and V. Snieckus, *J. Org. Chem.*, 1989, **54**, 24.

392 P. Beak and R. A. Brown, *J. Org. Chem.*, 1982, **47**, 34.

393 M. P. Sibi, M. A. J. Miah and V. Snieckus, *J. Org. Chem.*, 1984, **49**, 737.

394 R. J. Mills, N. J. Taylor and V. Snieckus, *J. Org. Chem.*, 1989, **54**, 4372.

395 R. J. Billedau, M. P. Sibi and V. Snieckus, *Tetrahedron Lett.*, 1983, **24**, 4515.

396 Y. Wang, P. G. Goekjian, D. M. Ryckman and Y. Kishi, *J. Org. Chem.*, 1988, **53**, 4151.

397 J.-C. Cuevas, P. Patil and V. Snieckus, *Tetrahedron Lett.*, 1989, **30**, 5841.

398 K. A. Parker and K. A. Koziski, *J. Org. Chem.*, 1987, **52**, 674.

399 J. N. Reed and V. Snieckus, *Tetrahedron Lett.*, 1983, **24**, 3795.

400 M. Iwao, J. N. Reed and V. Snieckus, *J. Am. Chem. Soc.*, 1982, **104**, 5531.

401   S. O. de Silva, J. N. Reed and V. Snieckus, *Tetrahedron Lett.*, 1978, **19**, 5099.

402   M. WATANABE, M. DATE, M. TSUKAZAKI and S. FURUKAWA, *Chem. Pharm. Bull. (Tokyo).*, 1989, **37**, 36.

403   W. Bauer and D. Seebach, *Helv. Chim. Acta*, 1984, **67**, 1972.

404   A. I. Shatenshtein, *Tetrahedron*, 1962, **18**, 95.

405   R. J. Mills, R. F. Horvath, M. P. Sibi and V. Snieckus, *Tetrahedron Lett.*, 1985, **26**, 1145.

406   F. Marsais and G. Queguiner, *Tetrahedron*, 1983, **39**, 2009.

407   A. Godard, Y. Robin and G. Queguiner, *J. Organomet. Chem.*, 1987, **336**, 1.

408   R. Clark, *J. Org. Chem.*, 1987, **52**, 5378.

409   M. Reuman and A. I. Meyers, *Tetrahedron*, 1985, **41**, 837.

410   C. W. Chen and P. Beak, *J. Org. Chem.*, 1986, **51**, 3325.

411   J.-C. Cuevas and V. Snieckus, *Tetrahedron Lett.*, 1989, **30**, 5837.

412   M. Watanabe and V. Snieckus, *J. Am. Chem. Soc.*, 1980, **102**, 1457.

413   T. K. Macklin and V. Snieckus, *Org. Lett.*, 2005, **7**, 2519.

414   M. Alessi, A. L. Larkin, K. A. Ogilvie, L. A. Green, S. Lai, S. Lopez and V. Snieckus, *J. Org. Chem.*, 2007, **72**, 1588.

415   C. Schneider, E. Broda and V. Snieckus, *Org. Lett.*, 2011, **13**, 3588.

416   Y. Zhao and V. Snieckus, *J. Am. Chem. Soc.*, 2014, **136**, 11224.

417   M. Giannerini, M. Fañanás-Mastral and B. L. Feringa, *Nat. Chem.*, 2013, **5**, 667.

418   T. W. Green and P. G. M. Wuts, *Protective Groups in Organic Synthesis*, Wiley-Interscience, New York, 2006.

419   C. Ramesh, N. Ravindranath and B. Das, *J. Org. Chem.*, 2003, **68**, 7101.

420   P. S. Mukund and V. Snieckus, *J. Org. Chem.*, 1983, 1935.

421   M. G. Banwell and S. Chand, *Org. Prep. Proceed. Int.*, 2005, **37**, 275.

422   J. P. Deville and V. Behar, *J. Org. Chem.*, 2001, **66**, 4097.

423   *Marvin was used for drawing, displaying and characterizing chemical structures, substructures and reactions and calculator Plugins were used for structure property prediction and calculation, Marvin 6.1, 2015, ChemAxon (http://www.chemaxon.com),* .

424   C. Nihei, Y. Fukai and K. Kita, *Biochim. Biophys. Acta*, 2002, **1587**, 234.